VOLUME 34 | SUPPLEMENT 2 | MARCH 2021

MODERN PATHOLOGY

ABSTRACTS

GENITOURINARY PATHOLOGY (INCLUDING RENAL TUMORS) (422-531)

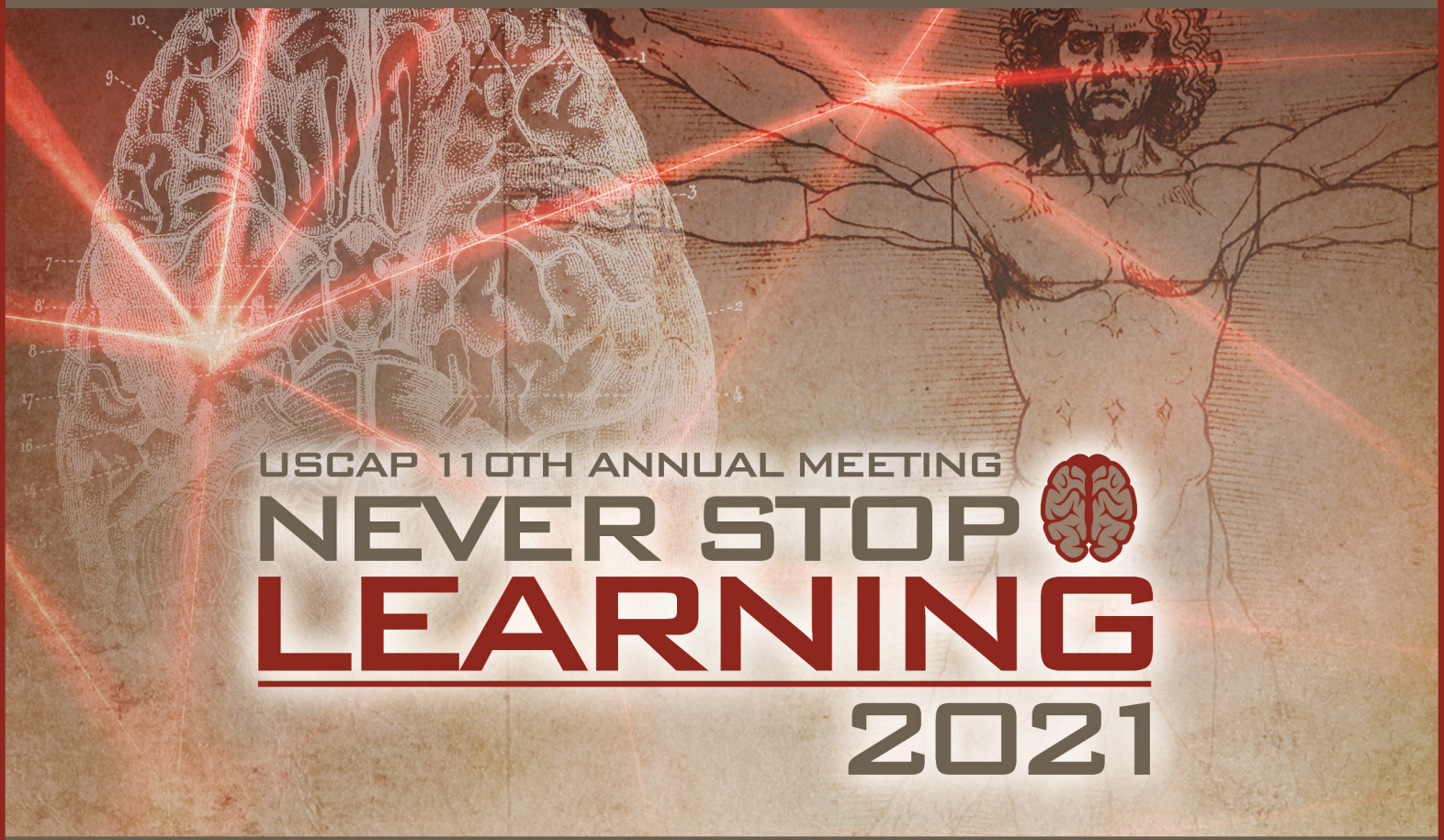

MARCH 13-18, 2021 | VIRTUAL AND INTERACTIVE

Published by
SPRINGER NATURE
www.ModernPathology.org

USCAP
Creating a Better Pathologist
AN OFFICIAL JOURNAL OF THE UNITED STATES AND CANADIAN ACADEMY OF PATHOLOGY

EDUCATION COMMITTEE

Jason L. Hornick
Chair

Rhonda K. Yantiss, Chair
Abstract Review Board and Assignment Committee

Kristin C. Jensen
Chair, CME Subcommittee

Laura C. Collins
Interactive Microscopy Subcommittee

Raja R. Seethala
Short Course Coordinator

Ilan Weinreb
Subcommittee for Unique Live Course Offerings

David B. Kaminsky
(Ex-Officio)
Zubair W. Baloch
Daniel J. Brat
Sarah M. Dry
William C. Faquin
Yuri Fedoriw
Karen Fritchie
Jennifer B. Gordetsky
Melinda Lerwill
Anna Marie Mulligan
Liron Pantanowitz
David Papke,
Pathologist-in-Training
Carlos Parra-Herran
Rajiv M. Patel
Deepa T. Patil
Charles Matthew Quick
Lynette M. Sholl
Olga K. Weinberg
Maria Westerhoff
Nicholas A. Zoumberos,
Pathologist-in-Training

ABSTRACT REVIEW BOARD

Benjamin Adam
Rouba Ali-Fehmi
Daniela Allende
Ghassan Allo
Isabel Alvarado-Cabrero
Catalina Amador
Tatjana Antic
Roberto Barrios
Rohit Bhargava
Luiz Blanco
Jennifer Boland
Alain Borczuk
Elena Brachtel
Marilyn Bui
Eric Burks
Shelley Caltharp
Wenqing (Wendy) Cao
Barbara Centeno
Joanna Chan
Jennifer Chapman
Yunn-Yi Chen
Hui Chen
Wei Chen
Sarah Chiang
Nicole Cipriani
Beth Clark
Alejandro Contreras
Claudiu Cotta
Jennifer Cotter
Sonika Dahiya
Farbod Darvishian
Jessica Davis
Heather Dawson
Elizabeth Demicco
Katie Dennis
Anand Dighe
Suzanne Dintzis
Michelle Downes
Charles Eberhart
Andrew Evans
Julie Fanburg-Smith
Michael Feely
Dennis Firchau
Gregory Fishbein
Andrew Folpe
Larissa Furtado
Billie Fyfe-Kirschner
Giovanna Giannico
Christopher Giffith
Anthony Gill
Paula Ginter
Tamar Giorgadze
Purva Gopal
Abha Goyal
Rondell Graham
Alejandro Gru
Nilesh Gupta
Mamta Gupta
Gillian Hale
Suntrea Hammer
Malini Harigopal
Douglas Hartman
Kammi Henriksen
John Higgins
Mai Hoang
Aaron Huber
Doina Ivan
Wei Jiang
Vickie Jo
Dan Jones
Kirk Jones
Neerja Kambham
Dipti Karamchandani
Nora Katabi
Darcy Kerr
Francesca Khani
Joseph Khoury
Rebecca King
Veronica Klepeis
Christian Kunder
Steven Lagana
Keith Lai
Michael Lee
Cheng-Han Lee
Madelyn Lew
Faqian Li
Ying Li
Haiyan Liu
Xiuli Liu
Lesley Lomo
Tamara Lotan
Sebastian Lucas
Anthony Magliocco
Kruti Maniar
Brock Martin
Emily Mason
David McClintock
Anne Mills
Richard Mitchell
Neda Moatamed
Sara Monaco
Atis Muehlenbachs
Bita Naini
Dianna Ng
Tony Ng
Michiya Nishino
Scott Owens
Jacqueline Parai
Avani Pendse
Peter Pytel
Stephen Raab
Stanley Radio
Emad Rakha
Robyn Reed
Michelle Reid
Natasha Rekhtman
Jordan Reynolds
Andres Roma
Lisa Rooper
Avi Rosenberg
Esther (Diana) Rossi
Souzan Sanati
Gabriel Sica
Alexa Siddon
Deepika Sirohi
Kalliopi Siziopikou
Maxwell Smith
Adrian Suarez
Sara Szabo
Julie Teruya-Feldstein
Khin Thway
Rashmi Tondon
Jose Torrealba
Gary Tozbikian
Andrew Turk
Evi Vakiani
Christopher VandenBussche
Paul VanderLaan
Hannah Wen
Sara Wobker
Kristy Wolniak
Shaofeng Yan
Huihui Ye
Yunshin Yeh
Anjana Yeldandi
Gloria Young
Lei Zhao
Minghao Zhong
Yaolin Zhou
Hongfa Zhu

To cite abstracts in this publication, please use the following format: **Author A, Author B, Author C, et al. Abstract title (abs#). In "File Title."** ***Modern Pathology*** **2021; 34 (suppl 2): page#**

422 Novel Prognostic Quantitation of PAX8 Expression and Tumor-Nuclear-Size by Digital Image Analysis in Renal Cell Carcinomas; Decreased PAX8 Expression and Higher-Tumor-Nuclear-Size are Associated with Tumors of larger Size, Higher Grade and Stage, and Risk of Metastasis

Ibrahim Abukhiran[1], Robert Humble[1], Nicholas Caldwell[1], Ilham Farhat[1], Anand Rajan KD[1], Andrew Bellizzi[1], Sarag Boukhar[1]
[1]*University of Iowa Hospitals & Clinics, Iowa City, IA*

Disclosures: Ibrahim Abukhiran: None; Robert Humble: None; Nicholas Caldwell: None; Ilham Farhat: None; Anand Rajan KD: None; Andrew Bellizzi: None; Sarag Boukhar: None

Background: PAX8 immunohistochemical stain (IHC) is a sensitive marker for renal cell carcinoma (RCC), though its prognostic value not identified. RCC grading (WHO/ISUP) relies on the presence of prominent nucleoli and nuclear pleomorphism, therefore subjected to observer variability and intra-tumoral heterogeneity. Herein, we utilized digital image analysis (DIA) to investigate the prognostic value of the qualitative/quantitative PAX8 expression and tumor cells average nuclear size (TCANS).

Design: PAX8 IHC was performed on tissue microarrays (TMAs) from 386 RCC cases between 2015 and 2019 (371 patients; 245 male and 126 female). Slides were digitally scanned, annotated, and Halo (Indica labs, NM) DIA was utilized to determine PAX8 positivity (using nuclear algorithm) and calculation of TCANS (in μm²). Fisher's exact, Mann-Whitney tests, and one-way ANOVA were used with $p<0.05$ considered significant.

Results: PAX8 was positive in 94% (364 of 386) of cases. PAX8 negative cases (22; 6%) were 44% grade III, 38% grade II, and 19% grade IV, but none was grade I. Compared to positive cases, PAX8-negative cases had a higher average size (8.7 vs 5.3) p= <0.0001, and associated with increase (odds ratio 3.0) risk of distant metastasis (p= 0.0272), with statistically significant association with higher stage. On the other hand, higher TCANS had a statistically significant directly proportional correlation with RCC grade (p=<0.0001), and furthermore, higher TCANS in CC-RCC is associated with presence of distant metastasis (p=0.02), and had a directly proportional correlation with pathologic T stage (p=0.004). See table-1 for further details.

Category	Sub-category	PAX8 + n (%)	P	Average Nucleus Area (μm²)	P
Histologic Type	MTSCC	5 (100)	**0.0022**	34.7	**<0.0001**
	Clear Cell Papillary	9 (100)		21.6	
	Others	9 (100)		30.2	
	Unclassified	8 (89)		26.0	
	Papillary	60 (98)		32.1	
	Chromophobe	18 (75)		29.2	
	Clear Cell	255 (95)		25.3	
Metastasis (CC-RCC)	Yes	49 (87)	**0.027**	25.7	**0.02**
	No	315 (95)		24.6	
WHO/ISUP Grade	1	15 (100)	0.5772	24	**<0.0001**
	2	148 (96)		24.53	
	3	146 (95)		26.14	
	4	34 (92)		26.38	
p Stage	pT1	229 (98)	**<0.0001**	25.07	**0.0046**
	pT2	32 (91)		24.43	
	pT3	85 (86)		25.94	
	pT4	6 (100)		28.17	
Focality	Multifocal	32 (97)	0.7081	25.7	0.4482
	Unifocal	327 (94)		25.9	

Conclusions:

1. PAX8 negativity is associated with increased risk of metastasis and is more frequent in tumors with larger size and higher pathologic stage.
2. TCANS is an unrecognized prognostic parameter that can be more objective than WHO grading, higher TCANS is associated with higher tumor stage, grade, and risk of metastasis.

423 Tumors of the Specialized Prostatic Stroma Harbor a Wide Range of Genomic Variants, Including Gene Fusions Seen in Uterine Sarcomas

Andres Acosta[1], Lynette Sholl[2], Brendan Dickson[3], Jesse McKenney[4], Jennifer Gordetsky[5], Michael Pins[6], Adrian Marino-Enriquez[2], Fei Dong[2], Christopher Fletcher[2]
[1]Brigham and Women's Hospital, Harvard Medical School, Boston, MA, [2]Brigham and Women's Hospital, Boston, MA, [3]Mount Sinai Health System, Toronto, Canada, [4]Cleveland Clinic, Cleveland, OH, [5]Vanderbilt University Medical Center, Nashville, TN, [6]Chicago Medical School, Park Ridge, IL

Disclosures: Andres Acosta: None; Lynette Sholl: *Grant or Research Support*, Genentech; Brendan Dickson: *Grant or Research Support*, Illumina; Jesse McKenney: None; Jennifer Gordetsky: None; Michael Pins: None; Adrian Marino-Enriquez: None; Fei Dong: None; Christopher Fletcher: None

Background: As defined in the latest WHO/ISUP classification (2016), tumors of the specialized prostatic stroma (PSTs) represent a category that comprises both sarcomas and stromal neoplasms of uncertain malignant potential. Microscopically, PSTs show variations of “phyllodes-like” or solid growth patterns, and histologic features classically associated with an aggressive biologic behavior are used to infer their malignant potential. Currently, it is unclear whether PSTs harbor distinctive molecular features or if they comprise homogeneous molecular subcategories. The objective of this research is to investigate the genomic alterations that underlie PSTs.

Design: Seventeen PSTs from 4 institutions were sequenced using our institutional solid tumor hybrid capture cancer gene panel.

Results: The histopathologic and molecular findings of the cases are presented in Table 1 and Figure 1, respectively. Four cases (4/17) showed “phyllodes-like” morphology and 13/17 cases showed solid spindle cell morphology, including 2 cases with a striking resemblance to low grade endometrial stromal sarcoma. Fifteen (15/17) cases underwent successful sequencing. Structural variants were identified in 7/15 cases (*JAZF1-SUZ12*, *NAB2-STAT6*, *TPM3-NTRK1*, *RGPD2-FOXO1*, as well as *P53*, *PALB2* and *BCOR* rearrangements with unidentified partners). Mutations/indels were detected in 10/15 cases, including 4/7 cases with concurrent structural variants (see Figure 1). One case (1/17) harbored a deep (homozygous) deletion of exons 6 and 7 of *CHEK2* and another case (1/17) did not harbor any genetic variants. Recurrently mutated genes were *ATRX* (2 cases) and *TP53* (3 cases). The 2 cases with *ATRX* mutations had concurrent biallelic inactivation of *TP53* and numerous copy number changes. Overall, copy number variants were more numerous in cases with mutations/indels and than in cases with structural variants, including a case with biallelic *PTEN* and *RASA1* inactivation and a near-haploid copy number profile (case 12).

Table 1 - Histologic Features of 17 Tumors of the Specialized Prostatic Stroma

CASE	AGE	ARCHITECTURE	MTCs	MITOSES	HYPERCELLULARITY	PLEOMORPHISM	NECROSIS
1	66	Solid (ESS-like)	no	15	+++	--	no
2	78	Solid (ESS-like)	no	<1	+++	--	no
3	21	Solid, SC/ET	no	25	+++	--	no
4	74	Phyllodes-like	no	<1	++	+	yes
5	30	Solid, SC/ET	no	22	+++	--	no
6	65	Solid, SC/ET	yes	<1	+	++	no
7	57	Solid, SC/ET	yes	<1	+	+	yes
8	57	Solid, SC/ET	no	14	++	++	yes
9	76	Solid, SC/ET	yes	11	+++	++	yes

10	64	Phyllodes-like	yes	<1	+	++	no
11	58	Phyllodes-like	yes	<1	+	++	no
12	60	Solid, SC/ET	no	6	+	--	no
13	64	Phyllodes-like	yes	<1	++	+	no
14	32	Solid, SC/ET	no	22	+++	--	no
15	69	Solid, SC/ET	no	<1	+	--	no
16	17	Solid, SC/ET	no	23	++	--	no
17	71	Solid, SC/ET	no	<1	+	--	no

Abbreviations: CNVs = copy number variants, ESS = endometrial stromal sarcoma, LG = low grade, MTCs = Multinucleated tumor cells, SC/ET = spindle cells with or without focal epithelioid components.

Figure 1 - 423

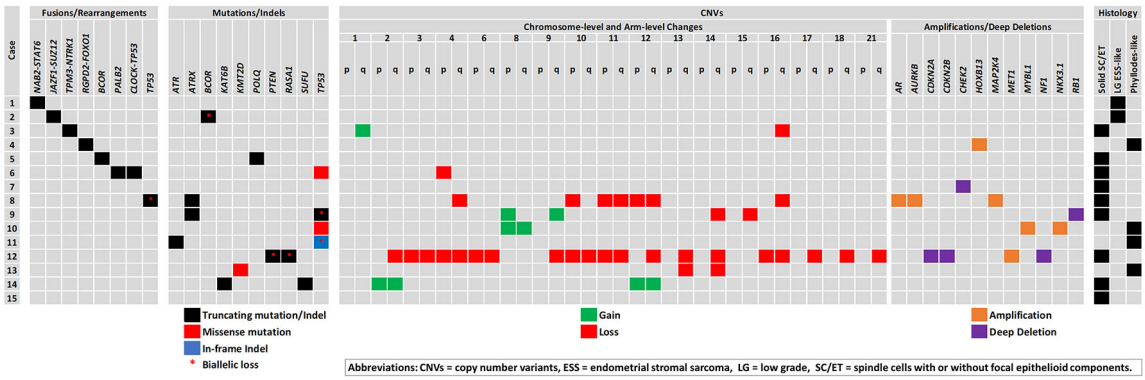

Conclusions: In conclusion, PSTs represent a heterogeneous category from a molecular perspective, with two subgroups of tumors: one driven by oncogenic gene fusions and another harboring mutations in cancer-related genes as well as numerous copy number events. Although recurrent fusions were not identified, the range of genes involved in structural variants is somewhat similar to that seen in endometrial sarcomas. Analysis of additional cases and RNA sequencing are ongoing.

424 Molecular Characterization of Primary Adenocarcinoma of the Bladder Demonstrates the Presence of Distinct Subgroups

Andres Acosta[1], Guru Sonpavde[2], Michelle Hirsch[3], Lynette Sholl[3]
[1]Brigham and Women's Hospital, Harvard Medical School, Boston, MA, [2]Dana-Farber Cancer Institute, Boston, MA, [3]Brigham and Women's Hospital, Boston, MA

Disclosures: Andres Acosta: None; Guru Sonpavde: None; Michelle Hirsch: None; Lynette Sholl: *Grant or Research Support*, Genentech

Background: Primary adenocarcinoma of the bladder (bAC) is rare, representing 0.5-2% of bladder malignancies overall. The spectrum of bAC includes both urachal and non-urachal adenocarcinomas with different phenotypes. The molecular features and the histologic correlates of the genetic alterations present in these tumors are still largely unexplored. A few small cohorts have demonstrated frequent mutations in *TP53*, *KRAS*, *PIK3CA*, *CTNNB1*, *APC*, *BRCA2*, *ARID1B*, *AURKB* and *KMT2B*, with some variation between the different phenotypes. The objective of this study is to explore the genetic alterations present in a series of bAC.

Design: Primary bAC collected as part of 2 institutional consented protocols underwent next-generation sequencing using an established solid tumor panel.

Results: Thirty bAC were sequenced and yielded interpretable results. The genetic variants of definite pathogenic significance identified in this cohort are illustrated in the Figure. The most frequently altered genes were (in order of frequency): *TP53* (53%), *ARID1A* (20%), FGFR3 (17%), KDM6A (17%), RB1 (13%), *ERBB2* (10%), *SMAD4* (10%) and *NF1* (10%). Two cases harbored pathogenic gene fusions involving *FGFR3* and *NRG1*, respectively. Analysis

of the distribution of the different variants demonstrates that there are two groups of bAC: one driven by activation of receptor tyrosine kinases pathways (*FGFR3*, *ERBB2*, *NRG1*, *HRAS*, *KRAS*; 11/30 cases, 36.7%) and another driven by inactivation of tumor suppressors and chromatin remodeling genes (*ARID1A*, *NF1*, *SMAD4*, *APC*; 11/30 cases, 36.7%). These two subgroups of bAC appear mutually exclusive, with only 1 case harboring both *ERBB2* and *ARID1A* variants. Co-mutations in *TP53*, *RB1*, *PTEN*, *KMT2D*, *KDM6A* and *FBXW7* were seen in both subgroups. Of the remaining 8 cases, 4 cases harbored *TP53* mutations, 1 case harbored a *TERT* promoter mutation, 1 case had *CCND1* amplification, and 2 did not have any pathogenic variants. Correlation with clinical and histologic features is ongoing.

Figure 1 - 424

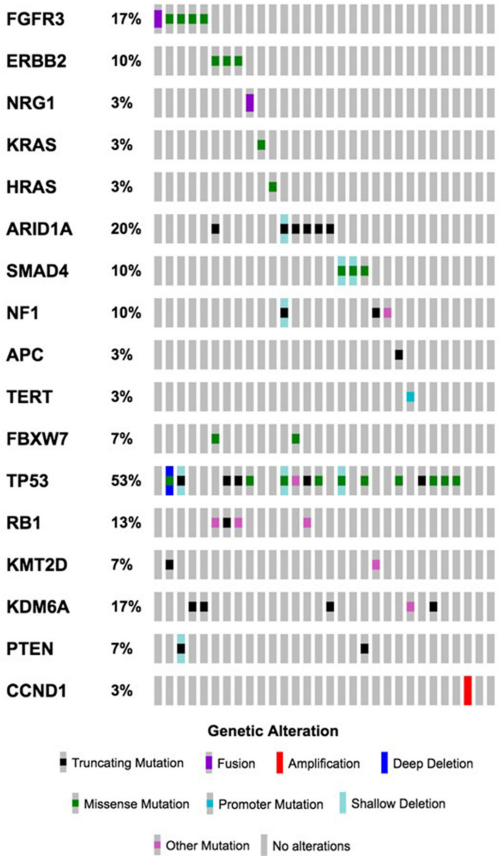

Conclusions: The present cohort suggests that there are 2 distinct and similarly frequent subgroups of bAC, driven by activation of receptor tyrosine kinase pathways and inactivation of tumor suppressors or chromatin remodeling genes, respectively, with a subset showing substantial genetic overlap with conventional urothelial carcinoma. A third subgroup of cases that does not fall into the above categories remains poorly defined and includes cases without clear driver alterations detected by next-generation sequencing.

425 Utility Of GATA3 Expression In Clear Cell Adenocarcinoma Of The Urinary Bladder

Mahmut Akgul[1], Niharika Pattnaik[2], Sourav Mishra[3], Nada Shaker[4], Shivani Sharma[5], Seema Kaushal[6], Manas Baisakh[7], Ankur Sangoi[8], Bonnie Balzer[9], Anil Parwani[10], Sambit Mohanty[11]
[1]Albany Medical Center, Albany, NY, [2]All India Institute of Medical Sciences, Bhubaneswar, India, [3]AMRI, Bhubaneswar, India, [4]University of California, San Diego, San Diego, CA, [5]Core Diagnostics, Gurgaon, India, [6]All India Institute of Medical Sciences, New Delhi, India, [7]Apollo Hospitals, Bhubaneswar, India, [8]El Camino Hospital, Mountain View, CA, [9]Cedars-Sinai Medical Center, Los Angeles, CA, [10]The Ohio State University, Columbus, OH, [11]AMRI Hospital, Chandigarh, India

Disclosures: Mahmut Akgul: None; Niharika Pattnaik: None; Sourav Mishra: None; Nada Shaker: None; Shivani Sharma: None; Seema Kaushal: None; Manas Baisakh: None; Ankur Sangoi: None; Bonnie Balzer: None; Anil Parwani: None; Sambit Mohanty: None

Background: Clear cell adenocarcinoma (CCAC) rarely occurs in the urinary bladder with distinct high-grade nuclei and tubulocystic, papillary, nephrogenic adenoma (NA)-like, or diffuse growth patterns and deep invasion. Florid cystitis cystica or glandularis, conventional or nested urothelial carcinoma (UCa), NA, and secondary involvement of the urinary bladder by CCAC of other tissue origins are in the differential diagnosis. The expression profile of GATA3, despite its wide utilization in the urinary tract, is not well documented in CCAC.

Design: Multi-institutional archival queries for CCAC of the urinary bladder and gynecologic tract were performed. Cases with any secondary malignancies were excluded. Patients" gender, age at the diagnosis, type of the procedure, and tumor size were recorded. All hematoxylin eosin and immunohistochemically stained slides were reviewed. Biomarker expression extent and intensity were graded as follows: diffuse and strong/moderate (+++); diffuse weak or focal moderate/strong (++); focal weak (+); and negative (-). P53 expression were interpreted as "mutant pattern" if diffusely positive or negative, and was considered non-mutant otherwise.

Results: 23 patients with CCAC of the urinary bladder and 7 with CCAC of the female genital tract were identified (Table1). Male-to-female ratio was 11:12 in CCAC of the urinary bladder with a median age at 59 years at the diagnosis for both CCAC of the urinary bladder (range: 20-92 years) and female genital tract (range 31-76), respectively.

Most tumors in the urinary bladder were located at the trigone or posterior wall (18/23). All CCAC in the urinary bladder had high grade cytology and predominantly more than one pattern (16/23, Figure 1A). PAX8 (23/23, Figure 1B), CK7 (21/21), AMACR (19/22), napsin A (15/22, Figure 1C) were mostly positive whereas WT1 (21/21), ER (19/19), and p63 (20/23) were consistently negative. Mutant p53 expression was seen in 4 cases (2 diffuse positive, 2 negative). In performed cases (21/23), MIB1 labeled more than 30%. GATA3 was expressed in 15/23 (65%) CCC (Figure 1D-1F), with moderate/strong intensity in all positive cases with diffuse/strong in 4 cases.

Similar heterogenous morphologic patterns and biomarker expression profiles were seen in CCC of the female genital tract (Table 1), although GATA3 was negative in all cases.

Table 1. Patient and Tumor Characteristics Of Clear Cell Adenocarcinoma of the Urinary and Female Genital Tracts

Site	Case Number	Age, Gender	Procedure Type	Location, size (cm)	Predominant Morphology	Immunohistochemical Profile	GATA3
Urinary Bladder	1	75M	Cystoprostatectomy	Trigone, 1.7	Tubulocystic/NA like	PAX8+++, CK7+++, CA125+, Napsin A+, AMACR+++, MIB1 70%, p63-, p53 nm, WT1-, ER-, CK20-	Diffuse and strong
Urinary Bladder	2	20F	TURBT	Right lateral, 4.5*	Tubulocystic/Papillary	PAX8+++, CK7+++, CA125++, Napsin A++, AMACR+++, MIB1 45%, p63-, p53 nm, WT1-, ER-, CK20-	Multifocal, moderate to strong
Urinary Bladder	3	69M	Cystoprostatectomy	Posterior, 5.2	Papillary/Diffuse	PAX8+++, CK7+++, CA125+, Napsin A-, AMACR++, MIB1 75%, p63-, p53m, WT1-, ER-, CK20-	Negative
Urinary Bladder	4	23F	TURBT	Trigone, 7.0*	Tubulocystic	PAX8+++, CK7+++, CA125++, Napsin A++, AMACR++, MIB1 50%, p63+, p53 nm, WT1-, ER-, CK20-	Multifocal, moderate to strong
Urinary Bladder	5	47M	Cystoprostatectomy	Trigone, 6.0	Tubulocystic/Papillary	PAX8+++, CK7+++, CA125++, Napsin A+++, AMACR+, MIB1 50%, p63-, p53 nm, WT1-, ER-, CK20-	Negative
Urinary Bladder	6	65M	Cystoprostatectomy	Right lateral, 3.5	Tubulocystic/Papillary	PAX8+++, CK7+++, CA125+, Napsin A-, AMACR+, MIB1 35%, p63-, p53 nm, WT1-, ER-, CK20	Negative
Urinary Bladder	7	71F	Cystectomy	Trigone, 2.5	Tubulocystic/NA like	PAX8+++,CK7+++,CA125-,Napsin A++, AMACR+++, MIB1 50%, p63-, p53 m, WT1-, ER-, CK20-	Diffuse and strong
Urinary Bladder	8	48M	Cystoprostatectomy	Posterior, 4.0	Tubulocystic/NA like	PAX8+++, CK7+++, CA125++, Napsin A++, AMACR+, MIB1 75%, p63-, p53 nm, WT1-, ER-, CK20-	Diffuse and strong
Urinary Bladder	9	73M	TURBT	Left lateral, 7.0*	Tubulocystic/Papillary	PAX8+++, CK7+++, CA125++, Napsin A-, AMACR++, MIB1 40%, p63+, p53 nm, WT1-, ER-, CK20-	Focal and strong
Urinary Bladder	10	39F	Cystectomy	Trigone, 2.9	Tubulocystic/Papillary	PAX8+++, CK7+++, CA125++, Napsin A++, AMACR++, MIB1 65%, p63-, p53 m, WT1-, ER-, CK20-	Multifocal and moderate
Urinary Bladder	11	68M	TURBT	Trigone, 4.7*	Tubulocystic	PAX8+++,CK7+++,CA125++,Napsin A++, AMACR++, MIB1 40%, p63-, p53 nm, WT1-, ER-, CK20-	Diffuse and strong
Urinary Bladder	12	50F	Cystectomy	Posterior, 3.0	Tubulocystic	PAX8+++,CK7+++,CA125-,Napsin A-,AMACR++,MIB1 60%, p63-, p53 nm, WT1-, ER-, CK20-	Negative
Urinary Bladder	13	61M	Cystoprostatectomy	Left lateral, 9.0	Diffuse	PAX8+++,CK7+++,CA125++,Napsin A+, AMACR+, MIB1 35%, p63-, p53 nm, WT1-, ER-, CK20-	Negative
Urinary Bladder	14	49F	Cystectomy	Trigone, 2.0	Papillary	PAX8+++, CK7+++, CA125-, Napsin A-, AMACR++, MIB1 70%, p63+, p53 nm, WT1-, ER-, CK20-	Focal and strong
Urinary Bladder	15	62M	Cystoprostatectomy	Trigone, 7.0	NA like	PAX8+++, CK7+++, CA125++, Napsin A++, AMACR++, MIB1 45%, p63-, p53 nm, WT1-, ER-, CK20-	Focal and strong
Urinary Bladder	16	43F	Cystectomy	Trigone, 6.1	Tubulocystic/NA like	PAX8+++,CK7+++,CA125++,Napsin A-, AMACR++, MIB1 55%, p63-, p53 nm, WT1-, ER-, CK20-	Focal and strong
Urinary Bladder	17	59F	Cystectomy	Posterior, 5.0	NA like	PAX8+++, CK7+++, CA125++, Napsin A-, AMACR++, MIB1 80%, p63-, p53 nm, WT1-, ER-, CK20-	Multifocal and moderate
Urinary Bladder	18	41M	Cystoprostatectomy	Trigone, 4.0	Tubulocystic/Papillary	PAX8+++,CK7+++,CA125+++,Napsin A++, AMACR++, MIB1 30%, p63-, p53 m, WT1-, ER-, CK20	Multifocal and moderate to strong

Urinary Bladder	19	73F	TURBT	Posterior, 2.5*	Papillary/Tubulocystic	PAX8+++, Napsin A++, p63-, p53 nm, ER-, PR-	Multifocal and strong
Urinary Bladder	20	68M	TURBT	Trigone, 4.0*	Papillary/Tubulocystic	PAX8+++, CK7+++, CA125+, Napsin A+, MIB1 55%, AMACR+, p63-, WT1-, CK20-	Negative
Urinary Bladder	21	49F	Cystectomy	Posterior, 6.5	Papillary/Solid	PAX8+++, CK7+++, Napsin A+++, MIB1 30%, AMACR-, p63-, WT1-, CK20-	Multifocal and strong
Urinary Bladder	22	41F	Cystectomy	Left lateral, 3.0	Tubulocystic/NA like	PAX8+++, CK7+++, CA125++, Napsin A+, MIB1 80%, AMACR++, p63-, WT1-, CK20+	Negative
Urinary Bladder	23	92F	TURBT	Trigone/Urethra	Tubulocystic/Papillary	PAX8+++, p63-	Negative
Female Genital Tract	24	76F	H-BSO	Uterus, 3.8	Tubular/Papillary	PAX8+++, CK7+++, CA125++, NapsinA++, MIB1 30%, AMACR-, p63-, WT1-, CK20-	Negative
Female Genital Tract	25	50F	H-BSO	Right ovary, 11.0	Tubular/Papillary	PAX8+++, CK7+++, CA125++, NapsinA+++, MIB1 70%, AMACR++, p63-, WT1-, CK20-	Negative
Female Genital Tract	26	65F	H-BSO	Left ovary , 15	Tubular/Papillary	PAX8+++, CK7++, CA125++, NapsinA++, MIB1 35%, AMACR++, p63-, p53 nm, WT1-, CK20-	Negative
Female Genital Tract	27	40F	H-BSO	Right ovary, 9.0	Tubular/Papillary	PAX8+++, CK7+++, CA125+++, NapsinA++, MIB1 60%, AMACR++, p63-, p53 nm, WT1-, CK20-	Negative
Female Genital Tract	28	72F	H-BSO	Uterus, 5.5	Papillary	PAX8+++, CK7+, CA125++, NapsinA+++, MIB1 45%, AMACR++, p63-, WT1-, p53 nm, CK20-	Negative
Female Genital Tract	29	59F	H-BSO	Uterus, 5.0	Papillary	PAX8+++, CK7+++, CA125-, NapsinA++, MIB1 30%, AMACR-, p63-, p53 nm, WT1-, CK20-	Negative
Female Genital Tract	30	31F	H-BSO	Left ovary, 8.5	Papillary	PAX8+++, CK7+++, CA125++, NapsinA+++, MIB1 55%, AMACR-, p63-, p53 nm, WT1-, CK20-	Negative

*size per cystoscopic evaluation; +++ diffuse and strong/moderate; ++diffuse weak, focal moderate/strong; +focal weak; - negative; H-BSO: hysterectomy and bilateral salpingo-oophorectomy; NA: nephrogenic adenoma; nm: non-mutant; m: mutant

Figure 1 - 425

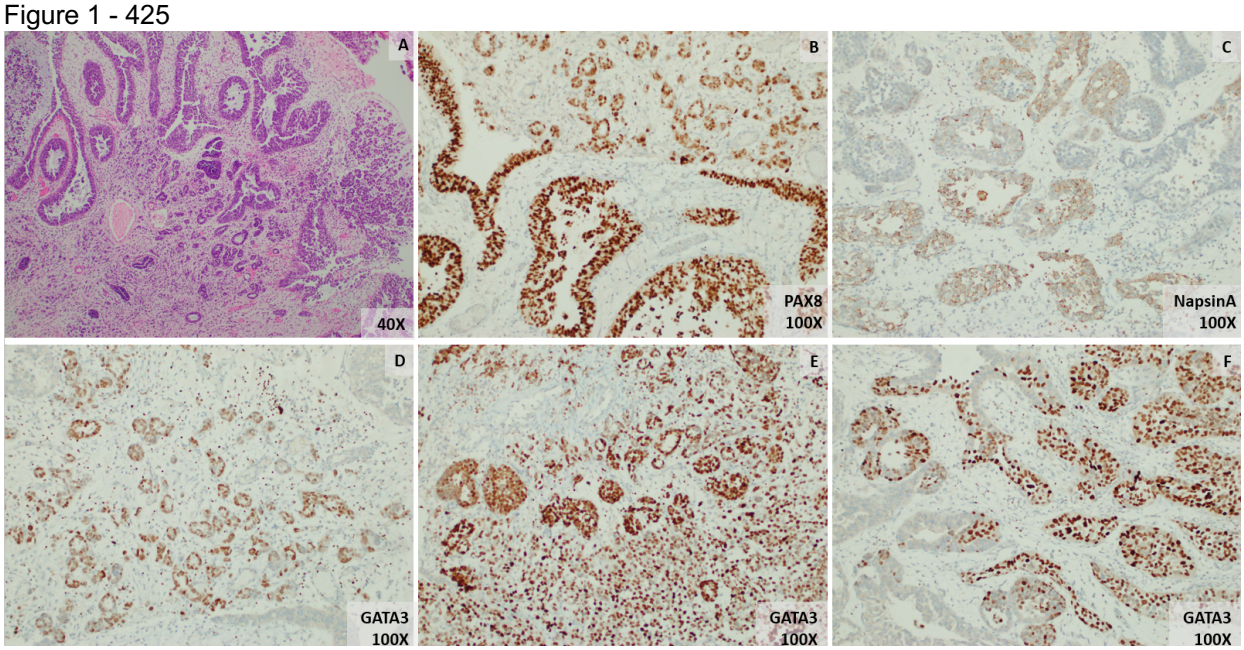

Conclusions:

- CCAC predominantly demonstrates more than one architectural pattern, this increases the number of entities in the differential diagnosis and the need of ancillary work-up with a panel of biomarkers.
- CCAC of the urinary bladder frequently expresses GATA3, which may be helpful in distinguishing CCAC of the female genital tract.
- There is a risk of misdiagnosing CCAC as a UCa or benign urothelial lesion if GATA3 is solely utilized to determine the tissue origin.

426 IRF2, A Potential Biomarker for Urothelial Carcinoma Progression

Mohammad Al-Attar[1], Kenneth Rock[1], Xiaoqin Zhu[2], Jian Zou[3], Karen Dresser[4], Zhong Jiang[1]
[1]UMass Medical School, Worcester, MA, [2]UMass Medical School, UMass Memorial Medical Center, Worcester, MA, [3]Worcester Polytechnic Institute, Worcester, MA, [4]UMass Memorial Health Care, Worcester, MA

Disclosures: Mohammad Al-Attar: None; Kenneth Rock: None; Xiaoqin Zhu: None; Jian Zou: None; Karen Dresser: None; Zhong Jiang: None

Background: Bacillus Calmette and Guérin (BCG) as an immunotherapy has been used for superficial high-grade urothelial carcinoma (UC) for a long time. Recently, programmed death-ligand 1 (PD-L1) has revolutionized the treatment of metastatic UC, with five approved agents for treatment of platinum-refractory UC. Therefore, it is crucial to know how different UCs respond to different types of immunotherapeutic agents.

Interferon regulating factor 2 (IRF2) is a transcription factor that has been shown to positively regulate the MHC-1 pathway and to negatively regulate PD-L1 expression. Many cancers undergo immune evasion by downregulating IRF2 expression, leading to reduced antigen presentation and increasing PD-L1 expression, culminating in making tumor cells harder to be detected by the host's immune system and thus less susceptible to being eliminated by CD8+ T-cells. Therefore, IRF2 downregulation could have important implications in cancer progression and immunotherapy.

In this study, we investigated whether IRF2 can serve as a biomarker for urothelial carcinoma progression, which can be a potential factor for immunotherapy response.

Design: A total of 67 UC cases, including 18 cases with low-grade non-invasive (LGNI) UC, 19 cases with high-grade non-invasive (HGNI), 18 cases with high-grade invasive (HGI), and 12 cases with metastatic urothelial carcinoma were examined by using immunohistochemistry for IRF2. The resulting IRF2 staining pattern was then divided into two categories: Diffuse positive staining (60-100% of cells showing nuclear positive staining) which also included normal internal control, and focal positive staining (<30% of cells showing nuclear positive staining) indicating significant loss of IRF2 expression. Fisher's exact test was used for statistical analysis.

Results: Of the 68 cases studied, we found that IRF2 expression is significantly reduced with increasingly aggressive behavior of UCs (Table 1), as evidenced by the decreasing staining pattern mainly observed in the HGI and metastatic groups (Figure 1). Statistical analysis resulted in a p-value equal to 0.024 (<0.05), indicating a statistically significant difference of IRF2 staining among the 4 groups.

Urothelial carcinoma category	Number of cases with significantly reduced IRF2 expression/ total number of cases	Percentage of significantly reduced IRF2 expression
Low-grade non-invasive (LGNI)	0/18	0%
High-grade non-invasive (HGNI)	2/19	11%
High-grade invasive (HGI)	5/18	28%
Metastatic	4/12	33%

Figure 1 - 426

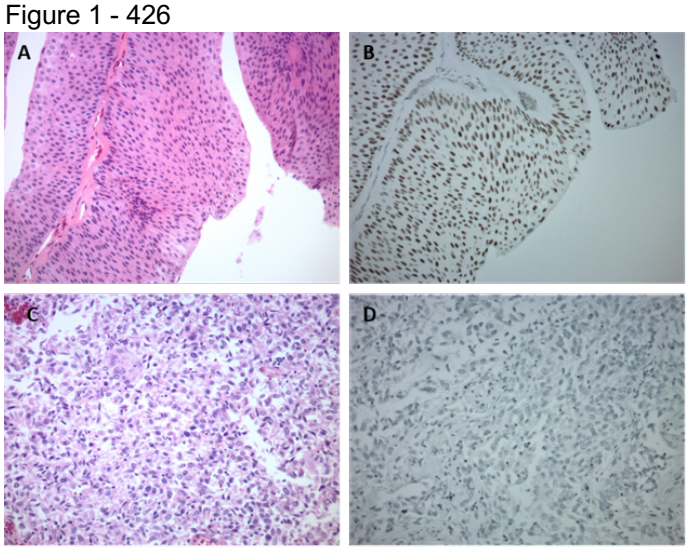

Figure 1. (A) Low-grade UC, H&E stain. (B) Low-grade UC, IRF2 stain showing diffuse positive nuclear staining. (C) High-grade invasive UC, H&E stain. (D) High-grade UC, IRF2 stain showing negative staining of neoplastic cells. (original magnification, A-D: 200x).

Conclusions: Our results show the significant reduction of IRF2 expression that occurs with increasingly aggressive behavior of urothelial carcinoma. More importantly, the findings suggest that the reduction or loss of IRF2 expression could potentially be used as a marker for high-grade and metastatic urothelial carcinoma, and this might also contribute to the role of IRF2 in urothelial carcinoma immunotherapy, including both BCG and PD-L1 immunotherapy.

427 OCT3/4 is a Sensitive and Specific Marker for Renal Medullary Carcinoma: An Immunohistochemical Analysis of 173 Renal Epithelial Tumors

Khaleel Al-Obaidy[1], Asma Abu-Salah[1], Liang Cheng[2], Muhammad Idrees[1]
[1]Indiana University School of Medicine, Indianapolis, IN, [2]Indiana University, Indianapolis, IN

Disclosures: Khaleel Al-Obaidy: None; Asma Abu-Salah: None; Liang Cheng: None; Muhammad Idrees: None

Background: Renal medullary carcinoma is a rare, aggressive tumor. It typically affects young black patients with sickle cell trait. Tumors are located in the renal medulla; demonstrate high-grade architecture exhibiting poorly formed glands, nests, and sheets with a background of desmoplasia and frequent infiltrating neutrophils. Sickle cells are usually visible within the vessels and in extravasation at light microscopy. OCT3/4, a vital transcription factor with a critical role in regulating cell pluripotency and self-renewal, is pivotal in testicular germ cell tumors work up. We recently encountered a high grade renal epithelial tumor centered in the renal medulla with aggressive clinicopathologic features. The patient was a 78-year-old male without a history of hemoglobinopathy. OCT3/4 showed diffuse expression, while INI1 expression was lost. Despite OCT3/4 being often positive in most renal medullary carcinoma, the data is scarce about its expression in other common and rare renal epithelial tumors. We, therefore, studied OCT3/4 expression in an expanded group of renal epithelial tumors.

Design: Four renal medullary carcinoma cases were identified on a retrospective search of the electronic database between 1990 and 2020. An additional cohort of diverse 169 renal tumors was included in the analysis. Hematoxylin and eosin-stained slides were reviewed to confirm the diagnosis. OCT3/4 immunohistochemistry was performed on 4 µm sections on Dako automated platform along with appropriate controls.

Results: The cohort included 4 cases of renal medullary carcinoma with ages ranging from 16-78 years, and tumor size ranged from 5-7.5 cm. Three patients had known hemoglobinopathy (sickle cell trait). The fourth and oldest patient presented with metastatic disease. Three patients succumbed to the disease in a period ranged from 5 months to 6 years, and 1 is alive with stable metastatic disease. All cases showed variable proportions of glandular, tubulopapillary and solid growth patterns in a desmoplastic stroma. All 4 cases showed loss of SMARCB1 (INI1) immunostaining, 2 had positive OCT3/4 nuclear staining (1 diffuse and 1 focal), and 2 were nonimmunoreactive for OCT3/4. Additional renal epithelial tumors, included: clear cell renal cell carcinoma (n=30), papillary RCC (n=30), chromophobe RCC (n=29), renal oncocytoma (n=28), Xp11 (TFE3) translocation RCC (n=15), clear cell papillary RCC (n=10), acquired cystic disease-associate RCC (n=7) mucinous and tubular spindle cell RCC (n=6), renal cell carcinoma with leiomyomatous Stroma (n=5), collecting duct carcinoma (n=4), tubulocystic carcinoma (n=4), and succinate dehydrogenase deficient RCC (n=1). None of these tumors exhibited OCT3/4 immunoreactivity.

Conclusions: Our results indicate that OCT3/4 is a reliable marker of renal medullary carcinoma and helps distinguish it from other renal epithelial tumors, especially its mimicker, collective duct carcinoma.

428 The Effect of Intraductal Carcinoma of the Prostate on the Revision of the Gleason Grading System

Afnan Al-Saleh[1], Meghan Forest[2], Arthur Plante[1], Véronique Ouellet[1], Yanxin Hu[1], Vincent Quoc-Huy Trinh[3], Feryel Azzi[4], Babak Mansoori[1], Nazim Benzerdjeb[1], Assia Ait Slimane[1], Jennifer Sirois[5], Andrée-Anne Grosset[4], Ségolène Chagnon-Monarque[6], Nathalie Delvoye[1], Fred Saad[2], Dominique Trudel[6]
[1]Centre de recherche du Centre hospitalier de l'Université de Montréal (CRCHUM) and Institut du cancer de Montréal, Montreal, Canada, [2]Centre Hospitalier de l'Université de Montréal (CHUM), Montreal, Canada, [3]Vanderbilt University Medical Center, Nashville, TN, [4]Centre de recherche du Centre hospitalier de l'Université de Montréal (CRCHUM), Montreal, Canada, [5]Hôpital Pierre-Le Gardeur, Terrebonne, Canada, [6]Centre Hospitalier de l'Université de Montréal (CHUM), Montréal, Canada

Disclosures: Afnan Al-Saleh: None; Meghan Forest: None; Arthur Plante: None; Véronique Ouellet: None; Vincent Quoc-Huy Trinh: None; Feryel Azzi: None; Nazim Benzerdjeb: None; Jennifer Sirois: None; Andrée-Anne Grosset: None; Ségolène Chagnon-Monarque: None; Dominique Trudel: None

Background: Intraductal carcinoma of the prostate (IDC-P) is associated with poor prognosis. Discussions are ongoing about the inclusion or exclusion of IDC-P in cancer grading. The aim of this study was to determine the differences in grade from the 2005 grading system, which did not necessarily exclude IDC-P, from the 2014 grading system excluding the status of IDC-P, in a cohort of radical prostatectomies (RPs) and to compare the grade modifications in RPs according to the IDC-P status.

Design: Eligible patients were men who underwent first-line RP for prostate cancer between 1993 and 2011 at Centre hospitalier de l'Université de Montréal (CHUM) and were included in the CHUM biobank. The exclusion criteria were set to missing data or Hematoxylin & Eosin slides, unconfirmed IDC-P status, or refusal to participate in research. Data from original pathology reports were compared to the reviewed grading following re-examination of RPs. Reviewed data included grade group (GG), pathologic stage (pT), presence or absence of IDC-P, seminal vesicle invasion (SVI), lymph node invasion (LNI), and surgical margins status (SM). Kruskal-Wallis tests were performed on pre- and post-revision data to describe the variation of grade caused by the evaluation of IDC-P.

Results: 313 were included in the cohort, 130 were positive for IDC-P (42%) and 162 had BCR (52%). In the updated data, the most frequent GG in presence of IDC-P was 2 (40%), then GG 3 (38%), 4-5 (18%) and 1 (3%). In the absence of IDC-P, the most frequent GG was 2 (48%), 1 (36%), 3 (11%) and 4-5 (5%). Reviewed GG were increased compared to original grading, the main modification being an increase from Gleason score (GS) 3+4 =7 to GG 3 for IDC-P(+) men and from GS 6 to GG2 for IDC-P(-) men. From the 313 RPs, 146 (47%) were reclassified: half of GS 6 were reclassified as GG2 (50%); most of GS 7 and higher remained the same (GS 3+4 =7, 66%; GS 4+3 =7, 78% and GS 9-10, 59%) and some GS 8 were reclassified as GG3 (39%).

Conclusions: As the differences in the grading systems encompass more than the inclusion of IDC-P in the grading, the increase from 3+4=7 to GG3 in IDC-P (+) men paralleled the increase from GS 6 to GG2 in IDC-P (-) men.

429 Malignant Mesothelioma of the Tunica Vaginalis: A Clinical and Pathological Study of 27 Cases

Ahmad Alkashash[1], Khaleel Al-Obaidy[2], Muhammad Idrees[2]
[1]Indiana University, Indianapolis, IN, [2]Indiana University School of Medicine, Indianapolis, IN

Disclosures: Ahmad Alkashash: None; Khaleel Al-Obaidy: None; Muhammad Idrees: None

Background: Malignant mesothelioma arising from the serosal membranes of the tunica vaginalis is rare. Most examples in the published medical literature are individual case reports. This study presents the clinicopathological findings of mesothelioma of the tunica vaginalis in one of the largest series to date. Individuals with mesothelioma of the tunica vaginalis were identified from our institution database, and their clinicopathological features were recorded.

Design: A retrospective search of the pathology electronic medical record was performed for paratesticular malignant mesothelioma diagnosed between 1990 and 2020. A total of 27 cases were identified. The morphologic and immunohistochemical features were reviewed. Follow-up information was obtained from physicians' notes.

Results: The median age was 58 years (range, 16-85 years). Nine presented with hydrocele, 4 with testicular mass and one with testicular pain. The latter was incidentally diagnosed on microscopic examination and no grossly identified tumor. All patients were diagnosed on orchiectomy, except one who was diagnosed on a hydrocelectomy specimen. The clinical presentation of the remaining is unknown—most but one patient presented with unilateral tumors, predominantly right-sided (n=18). Follow-up data were available for 13 patients (range 2 mon-15 years), 6 had no evidence of disease, 4 died of disease and 3 are alive with metastatic disease. Tumor size was available for 11. The median size was 6.5 cm (range, 1-13 cm). Microscopically, tumors were predominantly epithelioid (n=18) with papillary, tubulopapillary, solid, or tubular architectures. The cells had moderate amounts of pale to eosinophilic cytoplasm with moderate to marked nuclear pleomorphism. The remaining showed a mixed biphasic

morphology with epithelioid and sarcomatoid (spindle cell) components (n=9). No purely sarcomatoid tumors were identified. Immunohistochemically, tumors were consistently positive for calretinin, WT1, and podoplanin, while are negative for MOC31, BER-EP4 and OCT3/4. L1CAM was negative, all except one (1/8).

Conclusions: Malignant mesothelioma of the tunica vaginalis is a rare malignant tumor with poor survival and a high propensity for metastasis. Tumors arising within the testis and metastasis to the testis should be excluded to establish an accurate diagnosis, and careful evaluation of clinicopathologic and immunohistochemical features are required.

430 A Molecular Comparison of Fumarate Hydratase-Deficient Renal Cell Carcinomas with Partial Versus Complete Loss of FH Expression

William Anderson[1], Harrison Tsai[2], Lynette Sholl[2], Michelle Hirsch[2]
[1]Brigham and Women's Hospital, Harvard Medical School, Boston, MA, [2]Brigham and Women's Hospital, Boston, MA

Disclosures: William Anderson: None; Harrison Tsai: None; Lynette Sholl: *Grant or Research Support*, Genentech; Michelle Hirsch: None

Background: Fumarate hydratase-deficient renal cell carcinoma (FH-def RCC) is a rare aggressive renal malignancy with poor prognosis that typically arises in the setting of hereditary leiomyomatosis and RCC syndrome (HLRCC). FH deficiency drives oncogenesis and results in the accumulation of the oncometabolite 2-succino-cysteine (2SC). Immunohistochemistry (IHC) for FH is a useful diagnostic biomarker, in that loss of expression is often observed in tumors with biallelic inactivation of *FH*. However, occasional tumors with otherwise characteristic features of FH-def RCC show only partial/patchy FH loss for unclear reasons, making diagnosis challenging. We aimed to investigate the *FH* mutational status of RCCs with partial versus complete FH loss, to characterize any additional genetic drivers, and to evaluate the role of 2SC IHC in these cases.

Design: FH-def RCCs with partial FH loss (n=2) or complete loss (n=4) were retrieved from departmental and consultation files. IHC for 2SC was performed. Targeted next-generation sequencing, using a clinically-validated platform covering the coding regions of 447 cancer-associated genes, was performed on all cases. This assay does not discriminate between somatic and germline variants.

Results: All 6 patients were male. The median patient age was 40 (range 26-74) years. None had a history of HLRCC or additional known clinical features suggestive of this syndrome. All tumors had histologic features within the morphologic spectrum described for FH-def RCC. The IHC and molecular findings are summarized in Figure 1 (VUS: variant of uncertain significance; TMB/Mb: tumor mutational burden per megabase). By IHC, all 6 cases were positive for 2SC. Both cases with partial FH loss harbored *FH* missense variants (p.G326E and p.N340K) within Domain 2 of the protein, and both had concomitant copy neutral loss of heterozygosity (CNLOH). These variants have been reported as a variant of unknown significance and pathogenic for HLRCC, respectively, in germline databases. In cases with complete loss, *FH* alterations included a splice variants (n=2), gene deletions (n=3), and CNLOH with a detectable deleterious alteration (n=1). Other non-recurrent alterations included biallelic alterations of *TP53*, *NF2*, *SMAD4* and activation of *PIK3CA*.

Figure 1 - 430

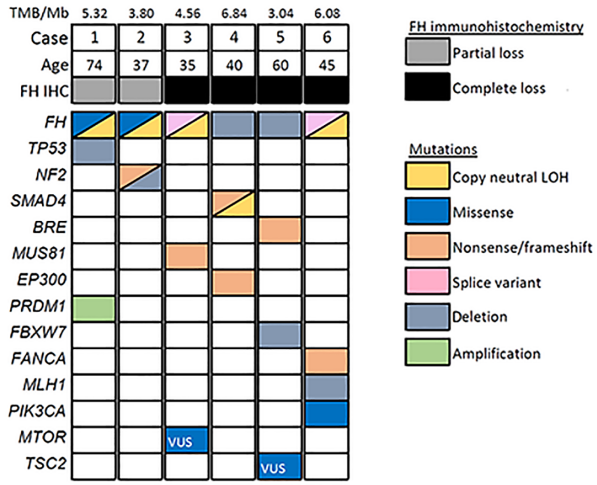

Conclusions: Partial loss of FH expression is an uncommon staining pattern that is important to recognize as it is still compatible with a diagnosis of FH-def RCC. In this context, IHC for 2SC and molecular testing are both useful in supporting the diagnosis of FH-def RCC. Targeted NGS is useful for the detection of most, but not all, of the molecular mechanisms leading to loss of FH protein expression. We observed that tumors with missense mutations showed partial FH loss. This patchy staining pattern may be attributable to coding alterations that interfere with protein function yet retain a relatively intact epitope.

431 Malignant Mesothelioma of the Tunica Vaginalis: A Clinicopathologic and Molecular Study of 11 Cases

William Anderson[1], Stephanie Schulte[2], Li Juan Wang[3], Lynette Sholl[4], Michelle Hirsch[4]
[1]Brigham and Women's Hospital, Harvard Medical School, Boston, MA, [2]Brigham and Women's Faulkner Hospital, Boston, MA, [3]Alpert Medical School of Brown University, Providence, RI, [4]Brigham and Women's Hospital, Boston, MA

Disclosures: William Anderson: None; Stephanie Schulte: None; Li Juan Wang: None; Lynette Sholl: *Grant or Research Support*, Genentech; Michelle Hirsch: None

Background: Malignant mesothelioma (MM) of the paratesticular region is an uncommon neoplasm thought to arise from the tunica vaginalis. Despite being the second most common paratesticular malignancy, few case series have been reported to date and, in contrast with mesotheliomas at other sites, there are very limited data on their molecular features. We therefore sought to characterize the clinicopathologic features and mutational landscape of paratesticular MM and mesothelial neoplasms of uncertain malignant potential.

Design: Primary paratesticular MM and atypical mesothelial neoplasms (AMN) were retrieved from departmental and consultation files. Original slides were reviewed to confirm diagnoses and clinical follow-up data were sought. Immunohistochemistry (IHC) was performed for MTAP, BAP1, and a novel mesothelial biomarker, SOX6, in a subset of cases. Targeted next-generation sequencing, using a clinically-validated platform covering the coding regions of 447 cancer-associated genes, was performed on 5 cases (3 additional cases are pending). In 2/5, a second region of the primary tumor was also sequenced to evaluate mutational heterogeneity.

Results: 11 cases were identified, including 9 MM and 2 AMN; one AMN was favored to be malignant at the time of diagnosis. The median patient age was 54 years (range 34 - 85). The histologic subtypes were epithelioid (6/11) and biphasic (5/11); there were no pure sarcomatoid cases. By IHC, BAP1 expression was lost in 2/7 cases and MTAP was lost in 2/6 cases. SOX6 was positive in all MM tested (5/5) and negative in 1 AMN tested. Molecular findings are summarized in Figure 1. The most frequently altered genes were *CDKN2A* (4/5) and *NF2* (3/5). Non-recurrent events were identified in *BAP1*, *PTCH1*, *TSC1*, and *TRAF7*. Minimal tumor heterogeneity (cases 1 and 5) was seen. Clinical follow-up was available in 7 cases (median: 16 months; range: 7 - 50 months). There were no

local recurrences. Three patients (including case 1 in Figure 1) developed distant metastases and died of their disease; one additional patient (case 2 in Figure 1) developed lung metastases and is still living 2 years after orchiectomy.

Figure 1 - 431

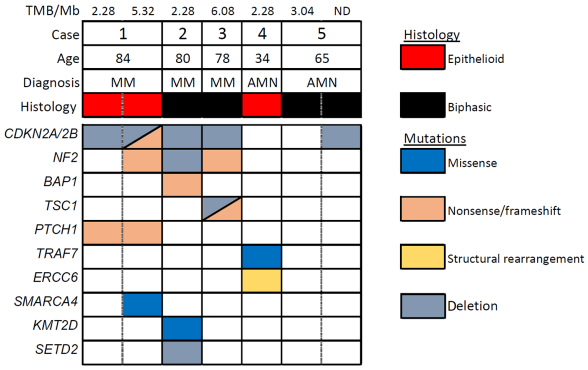

Conclusions: Both MTAP and BAP1 appear less sensitive for the diagnosis of paratesticular MM compared to other sites. In contrast, SOX6 is highly sensitive. Paratesticular MMs harbor mutations in genes known to be recurrently mutated in pleural/peritoneal MM (*CDKN2A*, *NF2*, *BAP1)* and thereby exhibit a broadly similar mutational profile. In addition, 2 cases were identified with inactivation of tumor suppressor genes unusual for MM at other sites (*PTCH1* and *TSC1)*.

432 Pathologic Predictors of Higher Clinical Stage at Presentation in Testicular Germ Cell Tumors

Alessa Aragao[1], Charisse Liz Treece[2], Krishna Irrinki[3], Maria Picken[1], Vikas Mehta[4]
[1]Loyola University Medical Center, Maywood, IL, [2]University of Illinois at Chicago, Chicago, IL, [3]Mount Sinai Hospital, Chicago, IL, [4]University of Illinois at Chicago Hospital and Medical Center, Chicago, IL

Disclosures: Alessa Aragao: None; Charisse Liz Treece: None; Krishna Irrinki: None; Maria Picken: None; Vikas Mehta: None

Background: Testicular Germ cell tumors (TGCTs) account for 1% of all male malignancies with over 8500 new diagnoses every year. Approximately 75% of patients with TGCTs are diagnosed without evidence of metastatic disease (clinical stage I); whereas up to 30% of nonseminomatous germ cell tumors (NSGCT) and 5% of the pure seminomas (PS) present with metastatic disease (clinical stages II and III). Risk stratification has been accomplished using clinical variables, such as serum tumor markers (β-HCG, AFP, and LDH), as well as pathologic findings on orchiectomy. We investigated the pathologic predictors of advanced clinical stage at presentation in a cohort of 168 consecutive TGCTs.

Design: In this multi-institutional retrospective study, a total of 168 consecutive GCTs diagnosed between 2009 and 2019 were reviewed by three pathologists. The following clinical and pathologic features were evaluated: age, tumor size, coagulative necrosis, vascular invasion, rete testis invasion and tumor extension into tunica vaginalis, hilar soft tissue, epididymis, or spermatic cord. Studied parameters were correlated with the clinical stage at presentation.

Results: Of the 168 patients with GCTs, 66 (39%) were PS, 102 (61%) were NSGCTs. 96 (57%) were clinical stage I, 27 (16%) were stage II, and 45 (27%) were stage III at presentation. 67% (44) of PS were clinical stage I, 23% (15) were stage II and 10% (7) were stage III at presentation. 51% (52) of NSGCT were clinical stage I, 12% (12) were stage II and 37% (38) were stage III at presentation. Mean patient age was 34 years (range, 16-83) with PS patients 6-years older than NSGCTs (34.6 vs 40.5 years). Mean tumor size was 4.4 cm (range, 0.2-20). Advanced clinical stage at presentation was associated with vascular invasion (VI) (P<0.001), hilar soft tissue

invasion (HSTI) (P<.001), rete testis invasion (only stromal invasion; cases with pagetoid spread only were excluded) (RTI) (P<0.010) and coagulative necrosis (CN) (P=0.005) by univariate analysis while VI (P=0.003), RTI (P<.03) and HSTI (P<.001) demonstrated significant association on multivariate analysis. Pathologic parameters like size of tumor, dominant tumor type and epididymis involvement were not significant.

Conclusions: We conclude that pathologic parameters like vascular invasion, tumor invasion into the hilum (rete testis or hilar soft tissue) as well as presence of coagulative necrosis strongly correlate with advanced clinical stage at presentation not only in NSGCT but also in PS. These findings are consistent with prior studies on NSGCT by Yilmaz et al (Modern Pathology (2013) 26, 579–586) and also validate the changes in the eighth edition of the AJCC Cancer Staging Manual.

We propose that rete testis invasion (excluding pagetoid spread only) should also be stage as pT2 in testicular GCTs.

433 Optimized Multi-Disciplinary Biobanking Protocol for Localized Prostate Cancer

Muhammad Asad[1], Peter Cai[2], Francesca Khani[3], Michael Augello[1], Maria Laura Martin[4], Christopher Louie[1], Spyridon Basourakos[2], Christopher Gaffney[2], Jonathan Shoag[2], Douglas Scherr[5], Juan Miguel Mosquera[3], Christopher Barbieri[5], Brian Robinson[3]
[1]Weill Cornell Medical Center, New York, NY, [2]New York-Presbyterian/Weill Cornell Medicine, New York, NY, [3]Weill Cornell Medicine, New York, NY, [4]Englander Institute for Precision Medicine, New York, NY, [5]Weill Cornell Medical College, New York, NY

Disclosures: Muhammad Asad: None; Francesca Khani: None; Maria Laura Martin: None; Christopher Louie: None; Spyridon Basourakos: None; Juan Miguel Mosquera: None; Christopher Barbieri: None; Brian Robinson: None

Background: Biobanking of a localized prostate cancer (PCa) tissue representing high purity tumor has been an uphill task. We aimed to integrate pre-operative variables with on-site adequacy evaluation using cytology into the radical prostatectomy (RP) biobanking protocol from our SPORE PCa program to improve the fidelity of biobanked PCa tissue—a critical need for cancer genomics research.

Design: We conducted a pilot study evaluating RP from patients enrolled under an IRB-approved protocol. Genitourinary pathologists and urologists correlated pre-operative MRI findings, positive biopsy locations, and gross examination of sliced RP as part of a next-generation protocol (NGP). Fresh tissue was evaluated by on-site cytology smear preparation (*Anticancer Res* 2017). Positive areas were cored and submitted for patient-derived tumor organoids (PTDO), and mirror tissue slices were frozen for biobanking (Figure 1). We evaluated the pathologic concordance of biobanked tissue comparing our standard protocol (SP; Diag Mol Path 2012) vs this novel (NGP).

Results: Baseline demographics (age, BMI, prostate weight, race) and clinico-pathologic characteristics (pre-operative PSA, pathologic Grade Group, pathologic stage) from were similar between the two groups (51 SP vs 10 NGP). The NGP cases had higher concordance between the biobanked tissue and the prostatectomy index lesion (100.0% vs. 68.6%, p=0.039) (Figure 2). On multivariable analysis, tumor volume (OR 11.00 [95% CI 1.30 – 93.26], p=0.028) and pathologic T stage (OR 9.86 [95% CI 1.27 – 76.29], p=0.028] were associated with higher odds of pathologic concordance. Attempts to establish localized PCa PDTOs are ongoing for a robust pre-clinical model of localized PCa.

Figure 1 - 433

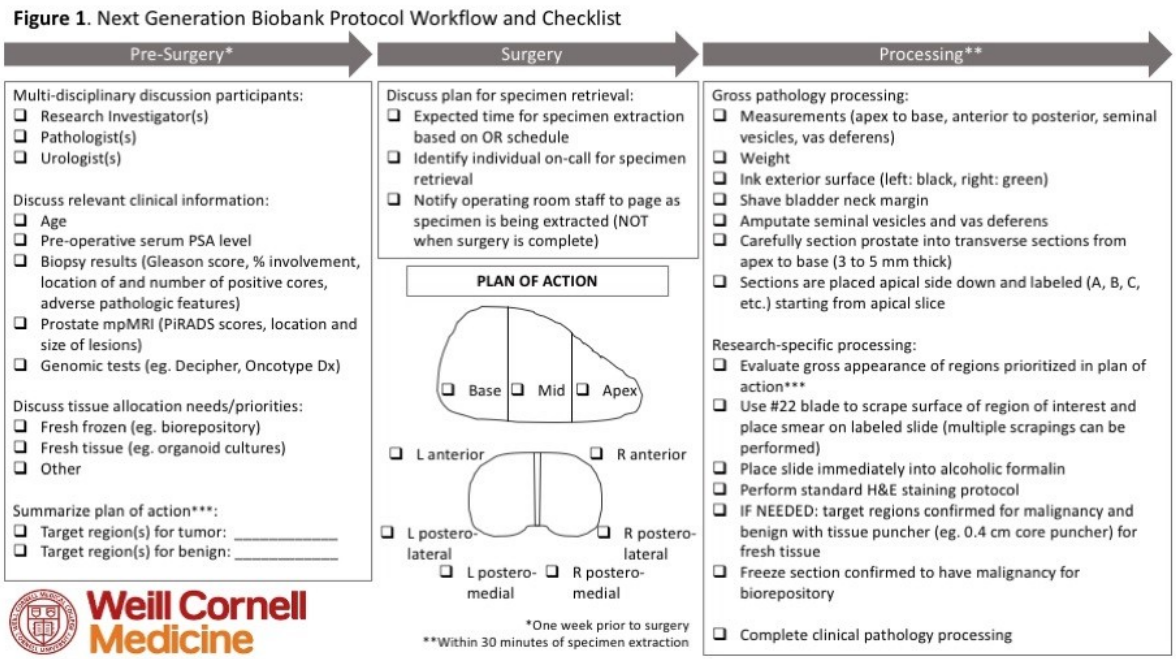

Figure 2 - 433

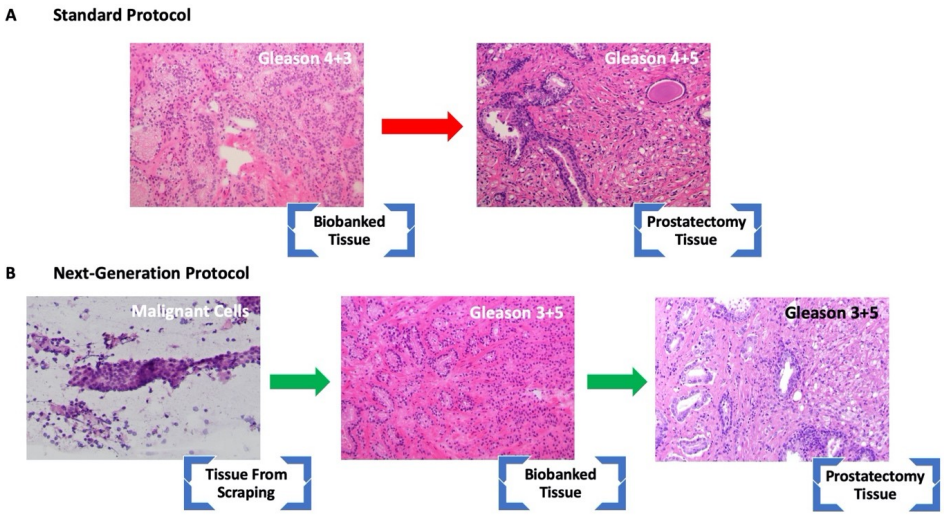

Conclusions: Our pilot study supports the use of this NGP as an improved multi-disciplinary approach for improving the fidelity of biobanked primary PCa tissue for future studies. Optimizing the fidelity of biobanked tissue is an important step forward to improve the multi-omics data generated from banked tissue and the establishment of *in vitro* patient models (e.g. organoids) as we move towards precision medicine.

434 mTORC1 Paradoxically Drives MiT/TFE Activity and Lysosomal Biogenesis in Tuberous Sclerosis Complex

Kaushal Asrani[1], Daniela Salles[1], Juhyung Woo[2], Thiago Vidotto[1], Sanjana Murali[2], Adrianna Mendes[1], Tamara Lotan[2]
[1]Johns Hopkins Medical Institutions, Baltimore, MD, [2]Johns Hopkins University School of Medicine, Baltimore, MD

Disclosures: Kaushal Asrani: None; Daniela Salles: None; Juhyung Woo: None; Thiago Vidotto: None; Sanjana Murali: None; Adrianna Mendes: None; Tamara Lotan: *Grant or Research Support*, Roche; *Grant or Research Support*, Myriad Genetics; *Grant or Research Support*, DeepBio

Background: Tuberous Sclerosis Complex (TSC) is characterized by *TSC1/2* loss, dysregulated mTORC1 signaling & renal tumors (angiomyolipomas (AML) & renal cell carcinoma (RCC)). The MiT/TFE transcription factors (*MITF*/*TFE3*/*TFEB*/*TFEC*) drive autophagy/ lysosomal biogenesis & are negatively regulated by mTORC1. However, this model raises a paradox in cancer, where elevated lysosomal activity must persist with mTORC1 activity. We recently showed that epidermal *Tsc1* loss paradoxically increases MiT/TFE-activity. Intriguingly, *TFE3*/*TFEB* gene rearrangements/amplifications and TSC1/2 loss are mutually exclusive driver alterations in PEComas and RCC. This raises the possibility that *TSC1/2* loss & *TFE3*/*TFEB* gene rearrangements have overlapping cellular consequences. Here, we address the hypothesis that MiT/TFE-driven lysosomal biogenesis is a key driver of tumorigenesis in TSC.

Design: We used HEK293T cells +/- CRISPR deletion (KO) of *TSC1*, *2* or both, to examine: a) Lysosomal gene enrichment by RNA-seq/GSEA, b) Expression of MiT/TFE & lysosomal markers (immunoblotting, qRT-PCR & IF), c) MiT/TFE localization (IF & nuclear fraction immunoblots), d) MiT/TFE activity (4X-CLEAR luciferase assays, qRT-PCR, cathepsin processing, autophagic flux, LC3 puncta). We analysed spontaneous renal tumors in *Tsc2* +/- mice for MIT/TFE protein/gene expression (IHC, IF & qRT-PCR analyses of laser capture micro-dissected (LCM) renal tumors). We examined MIT/TFE proteins/ lysosomal markers in FFPE samples of renal PEComas & eosinophilic solid & cystic (ESC) RCC & normal kidney.

Results: RNA-seq/GSEA showed enrichment of lysosomal gene sets in *TSC1/2* KO cells compared to controls. *TSC2* KO cells had increased expression of lysosomal transcripts & proteins in cellular lysates & lysosomal fractions, compared to controls. *TSC1, 2 & 1/2* KO cells showed increased nuclear TFEB/TFE3 (IF/nuclear-fraction immunoblots), compared to controls. MiT/TFE activity in 4X-CLEAR luciferase reporter assays was increased in *TSC2* KO cells compared to controls. Treatment of *TSC2* KO cells with chloroquine increased lipidated LC3-II, indicating increased autophagic flux. *TSC2* KO cells also showed increased LC3-labelled puncta by IF. We analyzed renal tumors in *Tsc2* +/- mice, where elevated mTORC1 signaling was confirmed by p-S6 IHC. Expression of lysosomal proteins (LAMP1, Lamtor 1, Rag C, Cathepsin B) & nuclear localization of TFE3 & TFEB was increased in these lesions by IF/IHC, compared to normal kidney. We performed LCM on renal tumors from *Tsc2* +/- mice & found levels of MiT/TFE transcriptional targets to be significantly enriched in tumors compared to normal kidney. We analyzed TFE3 expression in 10 cases of ESC- RCC with sporadic bi-allelic *TSC1/2* mutations & 2 cases of TSC-associated RCC; 8/10 cases showed elevated nuclear TFE3.

Conclusions: Elevated MiT/TFE levels & activity may represent oncogenic drivers in human & murine renal tumors in TSC

435 Significance and Followup of Atypical Intraductal Proliferations (AIPs) in Prostate Core Needle Biopsies with an Emphasis on AIP Alone and AIP with Low-Intermediate Grade Prostatic Adenocarcinoma (PCa)

Aaron Belknap[1], Rajal Shah[2], Angela Wu[3], Lakshmi Kunju[4]
[1]Michigan Medicine, Ann Arbor, MI, [2]UTSouthwestern Medical Center, Dallas, TX, [3]Michigan Medicine, University of Michigan, Ann Arbor, MI, [4]University of Michigan, Ann Arbor, MI

Disclosures: Aaron Belknap: None; Rajal Shah: None; Angela Wu: None; Lakshmi Kunju: None

Background: Atypical intraductal proliferations (AIP) of the prostate in the absence of intraductal carcinoma (IDC-P) on prostate biopsy is a rare lesion, and the significance of AIP on core biopsy is not well delineated.

Design: We identified 112 patients between 2013 and 2019 with either AIP alone or AIP with PCa. Cases with concurrent IDC-P were excluded. Slides were reviewed and the diagnosis of AIP (defined as atypical glands with either: loose cribriform architecture lacking sufficient nuclear atypia/necrosis for IDC-P or significant nuclear atypia but without sufficient architectural features for IDC-P) was confirmed. Clinical and pathologic parameters were recorded including followup biopsy results and adverse prognostic factors on radical prostatectomy (RP). PTEN staining of these cases is in progress.

Results: After exclusions, 90 patients were included. 13 patients had AIP alone, 6 had grade group (GG) 1 PCa, 36 had GG2 PCa, and 35 had >=GG3 PCa. Median follow up time was 1.7 years. Of the 13 patients with AIP only, 4 underwent a subsequent biopsy with the following diagnoses: Benign (1), AIP alone (1), GG1 PCa (1), GG2 PCa (1). One was lost to follow up, 9 patients are being followed, 1 received androgen deprivation therapy (ADT) and radiation therapy (RT), and 2 patients had GG2 and 3 PCa on prior/subsequent biopsies and underwent RT. Of the 6 patients with GG1 PCa, 4 underwent subsequent biopsy with the following results: Benign (1), GG1 PCa (2), GG2 PCa (1). 1 was lost to follow up, 1 is on active surveillance (AS), 4 had radical prostatectomy (RP). Of the 36 patients with GG2 PCa, 8 were lost to follow up, 9 are on AS, 8 had RP, 19 received RT with/without ADT. Of the 35 patients with > or = to GG3 PCa, 8 were lost to follow up, 9 had RP, 23 received ADT and/or RT. Please see table for number of cases with adverse prognostic factors on RP.

Number of cases with adverse prognostic factors on RP

RP results	Overall cases with pathology available	GG increase	EPE	SV	+ margin	IDC
AIP w/o PCa	0	0	0	0	0	0
AIP w/ GG1 PCa	3	2 (one GG2, one GG3)	1	0	0	0
AIP w/ GG2 PCa	5	2 (one GG3, one GG4)	5	0	3	2

Conclusions: AIP in the absence of IDC-P is a rare but potentially clinically significant lesion. AIP alone is associated with PCa on subsequent biopsies. AIP with low to intermediate PCa is associated with GG upgrades, EPE and positive margins in RP. While the study is small, it lends support to the fact that AIP alone and AIP associated with GG 1 should be considered for at a minimum an immediate rebiopsy.

436 Cancer Extent and Stromal Gaps on a Conservatively Treated Cohort of 998 Men with Prostate Cancer

Luis Beltran[1], Kier Finnegan[2], Henrik Moller[3], Jack Cuzick[1], Daniel Berney[1]
[1]Queen Mary University of London, London, United Kingdom, [2]Centre for Molecular Oncology, Barts Cancer Institute, Queen Mary University of London, London, United Kingdom, [3]King's College, London, United Kingdom

Disclosures: Luis Beltran: None; Kier Finnegan: None; Henrik Moller: None; Jack Cuzick: *Consultant*, Myriad Genetics; Daniel Berney: None

Background: Several measures of cancer extent (CE) in prostate biopsies (PB) may be used in pathology reports including variability in including stromal gaps (SG) to measure cancer length (CL). There are very few studies into the prognostic value of CE that use prostate cancer death (PCD) as end point. We here assess frequently employed measures of CE as predictors of PCD including the utility of inclusion or exclusion of SGs

Design: PB from 998 men with clinically localized PC diagnosed and managed conservatively between 2000 and 2003 were centrally reviewed by two uropathologists. Follow up was through cancer registries up until 2012. Deaths were divided into those from PC and those from other causes according to WHO criteria. For every case, the number of positive cores (NPC), the maximum CL (MCL), the total CL (TCL) and the percentage of positive cores (%PC) was calculated and univariate and multivariate analysis using PSA, T-stage and Gleason were performed. In addition, the presence of SG was recorded and where present. CL was assessed both including and excluding this. Univariate models were run on the patients where SG made a difference to the MCL.

Results: All variables of CE showed a significant association with PCD in the univariate models. In the multivariate models, incorporating PSA, T-stage and Gleason score , only %PC is a significant predictor of PCD with a 10% increase in %PC resulting in an hazard ratio (HR) of 1.07 (**LRT p > X^2 =** 0.01). There were 120 patients where SG made a difference to the MCL and a total of 20 events in this group. Including SG, the median MCL was 10 mm and HR was 1.16 (p=0.007), not including SG the median MCL was 6 mm and HR was 1.23 ($p=6.3x10^{-4}$). Inclusion or exclusion of SG made no significant difference to TCL as a predictor of PCD.

	Median (min-max)	HR (95% CI)	p-value	Harrell's c-statistic
Max cancer length (including SG)	10 (2, 20)	1.16 (1.04-1.30)	0.007	0.656
Max cancer length (excluding SG)	6 (1, 19)	1.23 (1.09-1.38)	$6.3x10^{-4}$	0.698

Conclusions: CE is a strong predictor of PCD but only %PC adds to the multivariate model. Expressed as a fraction of NPC/total number of cores, this the simplest method of CE assessment which we favour over more complicated methods in non-targeted PB. There is suggestion that MCL is a marginally better predictor when SG are not included but there is insufficient evidence for a dogmatic approach and where SG make a significant difference to MCL the assessment method employed should be specified.

437 Is Length As Well As The Percentage of Gleason Pattern 4 of Significance In Predicting Outcome in Grade Group 2 and 3 Prostate Cancer? A Study on 510 Conservatively Treated Cases

Luis Beltran[1], Kier Finnegan[2], Henrik Moller[3], Jack Cuzick[1], Daniel Berney[1]
[1]Queen Mary University of London, London, United Kingdom, [2]Centre for Molecular Oncology, Barts Cancer Institute, Queen Mary University of London, London, United Kingdom, [3]King's College, London, United Kingdom

Disclosures: Luis Beltran: None; Kier Finnegan: None; Henrik Moller: None; Jack Cuzick: *Consultant*, Myriad Genetics; Daniel Berney: None

Background: The percentage of Gleason pattern 4 (%G4) on biopsies is an established predictor of prostate cancer death (PCD). However, its value has been questioned in cases where disease burden is small as there is more interobserver variability and some of these tumours may be undersampled. There are few studies focusing on the association of %G4 as a predictor of mortality and cancer extent in biopsies and comparing these with grade group (GG) This may assist active surveillance criteria when the amounts of tumour present are small.

Design: Core biopsies from 998 men with clinically localized PC diagnosed and treated conservatively in the United Kingdom, mostly between 200 and 2003 were centrally reviewed by two uropathologists. Follow up was through cancer registries up until 2012. Deaths were divided into those from PC and those from other causes according to WHO criteria. Only men with a Gleason score of 3+4=7 or 4+3=7 were included in this study. The maximum length of pattern 4 (ML4) in a single core as well as the total length in all cores (TL4) model were compared with %G4 and GGs as a predictors of mortality. All new variates were compared with the known clinical variates, PSA and clinical T stage.

Results: 510 men were included, 301 with GG2 and 209 with GG3. On univariate anaysis all parameters were highly predictive of death from prostate cancer (See table). Using a multivariable model comparing the four methods of pattern assessment (GG, %G4, ML4 and TL4) it was demonstrated that TL4 and GG were the optimal model. For the models incorporating clinical factors (serum PSA and T stage) neither ML4 and TL4 added any information. However, although a model including clinical data and GG was optimal, similar strong models could be constructed using T stage and ML4 or TL4 and GG. After further modelling, it was shown that %G4 and total cancer length resulted in the best model and %G4 is a very strong predictor whatever the overall cancer length.

Table1: Univariate model results

Variable	Median (IQR)[min,max]	HR (95% CI)	p-value	Harrell's c-statistic[a]
Log (1 + PSA)*	16.9 (9.6, 35.7) [0.4, 100]	1.54 (1.22, 1.96)	$3.6x10^{-4}$	0.609
Clinical T-stage	2 (2, 2) [1, 3]	1.98 (1.39, 2.81)	$1.5x10^{-4}$	0.586
4+3 versus 3+4	N/A	1.95 (1.34, 2.84)	$4.9x10^{-4}$	0.597
Max length pattern 4 in core (mm)	3.4 (1.6, 6.3) [0.04, 15]	1.10 (1.05, 1.16)	$0.9x10^{-5}$	0.628
Total length pattern 4 across all cores (mm)	6.0 (2.1, 14.4) [0.04, 90.3]	1.03 (1.01, 1.04)	$3.4x10^{-5}$	0.621
Percentage pattern 4 across all cores (mm)**	35.8 (20, 60.8) [0.9, 97.5]	1.12 (1.04, 1.20)	$3.2x10^{-3}$	0.599
* Median based on PSA not log (1 + PSA) ** For 10% increase in pattern 4				

Conclusions: Although calculations of the total and length of pattern 4 are highly prognostic in univariate analysis of PCD, it appears that simpler measures, including standard clinical parameters, GG and the percentage of pattern 4 are sufficient for prediction of prognosis, regardless of total cancer length. We would encourage pathologists to attempt to quantify the percentage of pattern 4 disease even on small foci, and to avoid complex calculations on biopsy series.

438 NF-κB p65 Nuclear Expression in Intraductal Carcinoma of the Prostate: A Biomarker of Aggressive Prostate Cancer

Farouk Benadada[1], Frederique Rouleau-gagne[1], Teodora Boblea[1], Andrée-Anne Grosset[2], Véronique Ouellet[1], Christine Caron[1], Gabriela Fragoso[1], Véronique Barrès[1], Theodorus Van Der Kwast[3], Anne-Marie Mes-Masson[4], Fred Saad[5], Dominique Trudel[6]

[1]Centre de recherche du Centre hospitalier de l'Université de Montréal (CRCHUM) and Institut du cancer de Montréal, Montreal, Canada, [2]Centre de recherche du Centre hospitalier de l'Université de Montréal (CRCHUM), Montreal, Canada, [3]University Health Network, Toronto, Canada, [4]Centre de recherche du Centre hospitalier de l'Université de Montréal (CRCHUM), Montréal, Canada, [5]Centre Hospitalier de l'Université de Montréal (CHUM), Montreal, Canada, [6]Centre Hospitalier de l'Université de Montréal (CHUM), Montréal, Canada

Disclosures: Farouk Benadada: None; Frederique Rouleau-gagne: None; Andrée-Anne Grosset: None; Véronique Ouellet: None; Véronique Barrès: None; Theodorus Van Der Kwast: None; Anne-Marie Mes-Masson: None; Dominique Trudel: None

Background: Intraductal carcinoma of the prostate (IDC-P), an aggressive variant of prostate cancer (PC), is associated with recurrence, metastasis and cancer-specific death. The discovery of new biomarkers is necessary to improve the identification of IDC-P. In addition, the evaluation of the molecular content of IDC-P will allow a better understanding of signaling pathways associated with high-risk PC. In recent years, we have identified nuclear factor-kappa B (NF-kB) p65 as a predictor of bone metastasis and PC-specific mortality (Grosset *et al.*, PLoS Med 2019). In the present study, we evaluated the nuclear expression of NF-kB p65 in IDC-P and adjacent PC.

Design: We used tissue microarrays (TMAs) from the Canadian Prostate Cancer Biomarker Network (CPCBN). The Validation-TMA series, a large pan-Canadian cohort, includes radical prostatectomy specimens from 1262 PC patients. The presence of IDC-P on each core was assessed by three observers (AAG, FB and TB) and a genitourinary pathologist (DT). Following immunostaining of NF-kB p65, two independent observers then quantified the frequency of the nuclear expression (Figure 1; arrows for IDC-P and arrowheads for adjacent PC). For the scoring of invasive PC, the interclass correlation between observers was 0.88 (Grosset *et al.*, PLoS Med 2019). For statistical analyses, the average of NF-kB p65 frequency in IDC-P, adjacent PC or non-IDC-P tumors for each patient was used.

Results: We identified 67 patients with at least one core with IDC-P of which 37 patients also had adjacent PC to the IDC-P lesion. A total of 1156 patients were identified with only invasive PC without IDC-P. The frequency of nuclear expression of NF-kB p65 was higher in IDC-P than in non-IDC-P tumors ($p<0.001$). In contrast, the nuclear expression of NF-kB p65 in IDC-P and in adjacent PC was comparable ($p=0.101$).

Figure 1 - 438

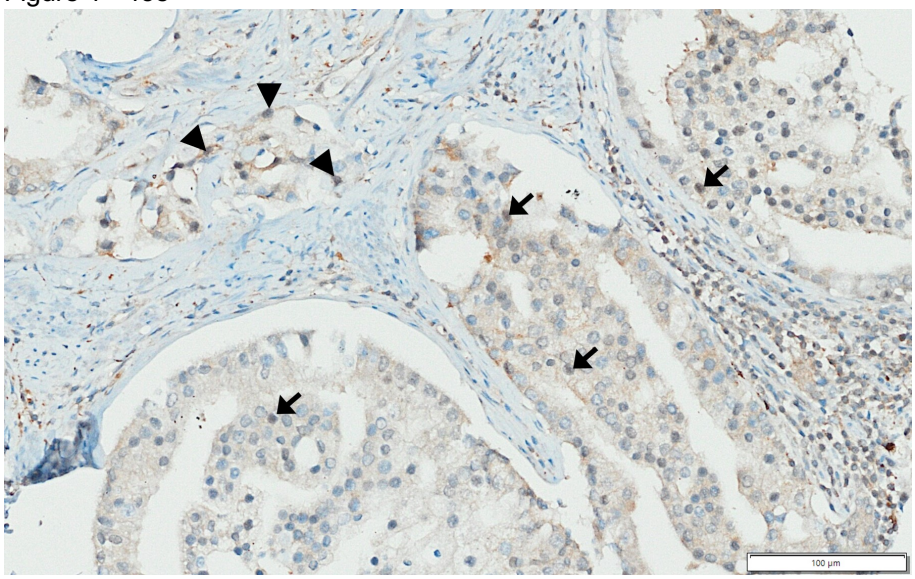

Conclusions: The NF-kB signaling pathway is a potential molecular mechanism of IDC-P. Our findings are also in line with previous studies showing that IDC-P shares genetic and molecular features with adjacent PC. A larger cohort will be necessary to validate NF-kB p65 as a diagnostic biomarker in IDC-P.

439 CCP Score Compared with Ki-67 for the Prediction of Death in Localised Conservatively Treated Prostate Cancer

Daniel Berney[1], Luis Beltran[1], Steve Stone[2], Henrik Moller[3], Solene-Florence Kammerer-Jacquet[4], Kier Finnegan[5], Jack Cuzick[6]

[1]Queen Mary University of London, London, United Kingdom, [2]Myriad Genetics, Inc., [3]King's College, London, United Kingdom, [4]University Hospital, Rouen, France, [5]Centre for Molecular Oncology, Barts Cancer Institute, Queen Mary University of London, London, United Kingdom, [6]Queen Mary University, London, United Kingdom

Disclosures: Daniel Berney: None; Luis Beltran: None; Henrik Moller: None; Solene-Florence Kammerer-Jacquet: None; Kier Finnegan: None; Jack Cuzick: *Consultant*, Myriad Genetics

Background: The natural history of prostate cancer (PC) is highly variable, making advice on treatment options challenging. The development of an expression signature composed of genes involved in cell cycle progression (CCP: Prolaris) has been shown to be highly prognostic in numerous cohorts. However other studies have shown that immunochemistry for Ki-67 is also a robust predictor of outcome. We wished to compare the prognostic power of CCP score (Prolaris) and Ki-67 index in a large cohort of prostate cancers with outcome data and compare them with established prognostic markers

Design: The cohort investigated was of 981 patients, with clinically localized PC diagnosed by needle biopsy and managed conservatively in the United Kingdom, between 2000 and 2003. The primary end point was prostate cancer death. Follow-up to 31 December 2012 was conducted through the cancer registries. Clinical variables included centrally reviewed Gleason score, baseline PSA, clinical stage, and cancer extent. CCP score was calculated using RNA from 31 cell cycle progression and 15 housekeeper genes. Ki-67 index was pathologically assessed by two expert pathologists. Univariate and multivariate modelling was performed

Results: 755 patients had a CCP score available and 752 had Ki-67 data. 668 patients had data on both. On univariate analysis of the available dataset, both high CCP score (HR=1.97 (95%CI 1.71,2.26) X^2= 70.82 p=3.9x10^{-17}) and raised Ki67 (HR=1.42 (95%CI 1.31,1.55 X^2 =47.08 p=6.8x10^{-12}) were highly significant predictors of PC death whether calculated as continuous data or using a variety of cut-offs, but CCP was clearly superior based on the magnitude of delta X^2. The 2 variables were highly positively correlated (Spearman's rank= 0.504). The four clinical variables were also highly associated with outcome. A number of multivariate models were assessed using the known clinico-pathological predictors. Adding CCP or Ki-67 to the clinical model removed the significance of baseline PSA. The most information comes from adding CCP score and a quadratic term derived from the CCP score. Ki67 added hardly any further information.

Table 1: Adding CCP^2, Ki67 and Log(1+Ki67) to a clinical variables + CCP model

	Hazard Ratios (95%CI)			
	Base MV Model	**Base MV + CCP^2**	**Base MV + Ki67**	**Base MV + log(1+Ki67)**
Base MV Model variables:				
Log(1+PSA)	1.24 (0.98, 1.57)	1.19 (0.94, 1.51)	1.23 (0.97, 1.55)	1.23 (0.97, 1.55)
Gleason score	1.29 (1.07, 1.57)	1.30 (1.07, 1.57)	1.29 (1.06, 1.57)	1.29 (1.06, 1.57)
% Cancerous cores*	1.11 (1.04, 1.20)	1.12 (1.04, 1.20)	1.11 (1.03, 1.19)	1.11 (1.03, 1.19)
Clinical T-stage	1.46 (1.03, 2.07)	1.36 (0.96, 1.93)	1.52 (1.07, 2.16)	1.48 (1.05, 2.09)
CCP	1.49 (1.24, 1.78)	2.26 (1.50 3.41)	1.35 (1.07, 1.70)	1.37 (1.12, 1.69)
Variable added:				
CCP^2		0.86 (0.75, 0.99)		
Ki67**			1.09 (0.95, 1.25)	
log(1+Ki67)				1.24 (0.92, 1.67)
c-statistic	0.765	0.764	0.767	0.768
X2	127.47***	5.66	1.62	2.04
Df	5	1	1	1
p-value	8.2x10^{-26}	0.017	0.202	0.153

Base MV Model = Log(1 + baseline PSA) + Gleason + Perc. Cancerous cores + T-stage + CCP
* Per 10% Increase in Percentage of Cancerous Cores (PCC)
** Per 5% Increase in Ki67
*** Compared to null model

Figure 1 - 439

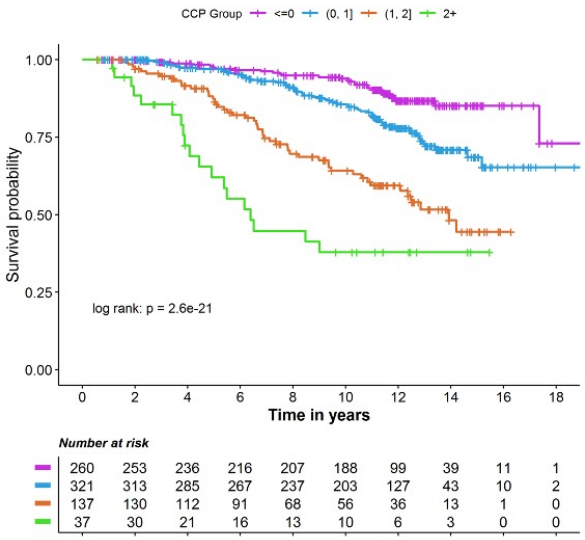

Figure 2 - 439

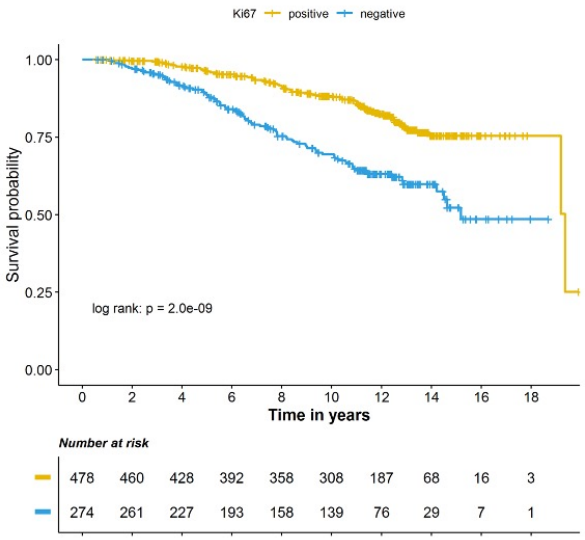

Conclusions: CCP was a very strong predictor of PC death. Ki-67 was also prognostic, but was much weaker than CCP, and added no independent prognostic information to models that included CCP and established clinico-pathologic features. These data support the power of CCP score in precision PC prognostic assessments.

440 Comparing the 5-Year Biochemical Recurrence Risk for Neurovascular Structure-Adjacent Frozen-Section Examination (NeuroSAFE) and Standard Prostatectomies While Adjusting for Histopathological Variables

Khawaja Bilal[1], Swati Bhardwaj[1], George Haines III[2], Qiusheng Si[1]
[1]Icahn School of Medicine at Mount Sinai, New York, NY, [2]Mount Sinai Hospital, New York, NY

Disclosures: Khawaja Bilal: None; Swati Bhardwaj: None; Qiusheng Si: None

Background: It is believed that nerve-sparing procedures convey higher risk of biochemical recurrence (BCR) when compared to conventional radical prostatectomies. NeuroSAFE Radical Prostatectomy (NSRP) is a form of nerve sparing prostatectomy utilizing extensive intraoperative assessment of surgical margins for improved patient outcomes. This study compares the five-year BCR risk for patients undergoing NSRP compared to those undergoing standard radical prostatectomy (StRP), while accounting for histopathological characteristics such as TNM stage, Gleason Grade group, tumor burden, extraprostatic extension (EPE), and positive surgical margins.

Design: Retrospective cohort study of 327 patients, who had undergone either NSRP or StRP between 11/01/2014 to 12/30/2015. Patient's pathology reports were analyzed for further stratification of sample, based on histopathological variables. Electronic medical records of the patients were then queried to assess the 5-year BCR.

Results: Overall, 13.15 % (43/327) of patients had a biochemical recurrence by 5 years post-operatively. Higher TNM stage, higher Gleason Grade group, presence of extraprostatic extension, positive surgical margins, and calculated tumor burden greater than 10g were strongly related to higher BCR risk, for both NSRP and StRP patients. Overall BCR risk for NSRP patients was 11.83 % (31/262) compared to 18.46% (12/65) for StRP patients ($p > 0.05$). BCR increased with T stage, with a trend toward lower BCR in NSRP patients. For pT2 tumors, NSRP patients had 4.12% risk of BCR compared to 5.77% for StRP patients (p=0.71). For pT3 tumors, NSRP patients had 34% risk of BCR compared to 69.23% for StRP patients (p=0.061). BCR increased with Gleason Grade group. NSRP patients with Gleason grade group 1&2 tumors had 3.21% risk of BCR compared to 11.36% for StRP patients (p=0.156). Patients with Grade Group 3-5 tumors, had an equal risk of BCR of 33.4% in both NSRP and StRP groups. NSRP patients with EPE had 32.20% risk of BCR compared to 63.64% for StRP patients (p=0.07). NSRP patients without EPE had a 5.91% risk of BCR compared to 9.26% for StRP patients (p=0.34). No statistically significant difference were found in BCR risk for patients undergoing NSRP and StRP, with tumor burden less than 10g. Patients with tumor burden greater than 10g, had a significantly lower risk of BCR when undergoing NSRP compared to StRP patients (26.19% vs 88.89%, $p<0.0001$).

Tumor Characteristic	Surgical Protocol	Number of Cases	Number of cases with BCR (%)
Overall	NSRP	262	31 (11.83%)
	StRP	65	12 (18.46%)
pT2	NSRP	194	8 (4.12%)
	StRP	52	3 (5.77%)
pT3a	NSRP	37	9 (24.32%)
	StRP	9	5 (55.56%)
pT3b	NSRP	24	12 (50%)
	StRP	4	4 (100%)
Gleason Grade Group			
Group 1 & 2	NSRP	187	6 (3.21%)
	StRP	44	5 (11.36%)
Group 3, 4 & 5	NSRP	75	25 (33.34%)
	StRP	21	7 (33.34%)
Extraprostatic Extension (EPE)			
EPE Present	NSRP	59	19 (32.2%)
	StRP	11	7 (63.64%)
EPE not present	NSRP	203	12 (5.91%)
	StRP	54	5 (9.26%)

Positive Surgical Margins (PSM)			
PSM present	NSRP	19	4 (21.05%)
	StRP	17	5 (29.41%)
PSM not present	NSRP	243	27 (11.12%)
	StRP	48	7 (14.58%)
Tumor burden (grams)			
Tumor Burden			
<10g	NSRP	219	19 (8.68%)
	StRP	56	4 (7.14%)
Greater than >10g	NSRP	42	11 (26.19%)
	StRP	9	8 (88.8%)

Figure 1 - 440

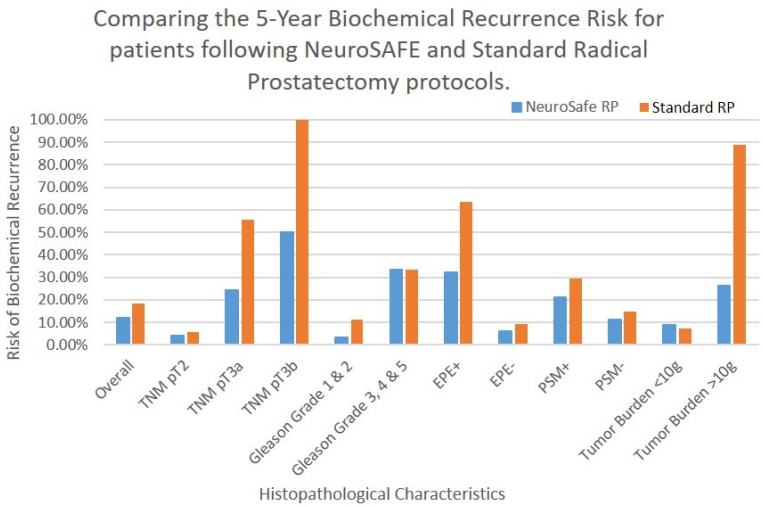

Conclusions: NSRP in patients with a tumor burden > 10g had a significantly lower rate of BCR compared to standard radical prostatectomy procedures. There was a trend toward lower BCR rates with NSRP regardless of the pT stage and in cases with low grade prostate cancers. No difference in outcome was seen in patients with high grade (Grade Group 3-5) tumors. Further analysis on a larger number of cases will be needed to further characterize the Grade Group 3-5 tumors.

441 An Alternative Multisite 3D Gross Sampling for Grading Angiogenetic and Immune Signatures in Renal Cell Carcinoma

Matteo Brunelli[1], Anna Calio'[1], Stefano Gobbo[2], Diego Segala[3], Jose Lopez[4], Enrico Munari[5], Guido Martignoni[6]

[1]University of Verona, Verona, Italy, [2]Ospedale Pederzoli, Peschiera del Garda, Italy, [3]ASST Spedali Civili di Brescia, Brescia, Italy, [4]Hospital de Cruces-Osakidetza, Barakaldo, Spain, [5]University of Brescia, Brescia, Italy, [6]University of Verona, Ospedale Pederzoli, Peschiera del Garda, Italy

Disclosures: Matteo Brunelli: None; Anna Calio': None; Stefano Gobbo: None; Diego Segala: None; Jose Lopez: None; Enrico Munari: None; Guido Martignoni: None

Background: Grading angiogenetic versus immune signatures in clear cell in renal cell carcinoma (RCC) is an unmeet need at tissue based level.

Design: We sampled advanced staged RCCs in toto. Multisite tumor sampling was performed to analyse the whole tumours. We investigated the TCGA public platforms for angiogenesis and immunity molecular signatures. CD31 and CD34 were used to evaluate the absolute count (manual and digital) and density (spots/mm^2) of the vessels. PD-L1 (E1L3N and sp263 clones) expression in neoplastic cells were also assessed again on whole tumours.

Results: 2383 tissue cores after wholly inclusion of RCCs from 100 radical nephrectomies were evaluated. Through a preliminary investigation of mRNA levels based on a large RCC cohort from TCGA, we demonstrated strong correlation between CD31 and CD34 and sparse upregulation of CD274. The digital vessels count of the entire series showed a mean of 90, median of 60, SD of 86 and CV of 0.97 for CD31 and a mean of 114, median of 93, SD of 93 and CV of 0.82 for CD34. The microscopic evaluation of combined CD31 and CD34 produced respectively a mean of 102 and 99, median of 82 and 68, SD of 81 and 96 and CV of 0.80 and 0.95. Mean CD31-microvascular density (vessels/mm^2) was 321, median was 207, SD was 310 and CV was 0.96. Mean CD34-microvascular density was 352, median was 243, SD was 336 and CV was 0.95.

Only 18% of cores displayed homogeneous pattern of neoangiogenesis (CV < 0.2) with two distinct pattern: homogeneous high level of angiogenesis (pattern A) (10% of cases) or homogeneous low level of angiogenesis (pattern B) (8% of cases). Cases characterized by the heterogeneous profile showed back to back high level of angiogenesis zones with zones with low density of angiogenesis (82%) (pattern C). PD-L1 diffuse expression (≥50% of neoplastic cells) was seen in a minority of clear cell RCC (7%), a low level of PD-L1 expression (1-49% of cells) was observed in 33% of cases whereas absence of expression (<1%) in 60% of cases, after in toto 3D tumor inclusion. After comparison in between grading of neoangiogenesis versus immune signatures we observed that cases with scarce immunoexpression for PD-L1 (grade 0 or 1) usually expressed high density of angiogenesis (grade 3).

Conclusions: Grading of angiogenetic (pattern A, B and C) versus immunity (grade 0, 1 and 2) signatures in clear cell RCCs may be performed, by a simple easy to perform 3D gross sampling method to avoid at minimum the bias of heterogeneity.

442 Prognosis of Mixed-Grade, Non-Muscle Invasive, Papillary Carcinoma of the Bladder: A Survival Analysis

Meagan Chambers[1], Jonathan L Wright[1], Michael Haffner[2], Nicholas Reder[1], Maria Tretiakova[1], Funda Vakar-Lopez[1], Lawrence True[3]
[1]University of Washington, Seattle, WA, [2]Fred Hutchinson Cancer Research Center, Seattle, WA, [3]University of Washington Medical Center, Seattle, WA

Disclosures: Meagan Chambers: None; Jonathan L Wright: *Primary Investigator*, Merck; *Primary Investigator*, altor biosciences; *Primary Investigator*, Nucleix; *Consultant*, UpToDate; *Consultant*, Sanofi Genzyme; Michael Haffner: None; Nicholas Reder: None; Maria Tretiakova: None; Funda Vakar-Lopez: None; Lawrence True: None

Background: Though most papillary carcinomas of the bladder are graded as either low- or high-grade, a minority are mixed-grade being composed of a predominantly low-grade cancer with a minor high-grade component. These cancers are commonly treated as high-grade cancers. However, limited outcome studies of these cancers suggest that their course is comparable to low-grade lesions, leading to their overtreatment. Herein, we present the largest cohort of mixed-grade papillary carcinomas to date with corresponding recurrence-free and progression-free survival analysis.

Design: Pathology records, (between 2009 and 2020) of our hospital were searched for diagnoses of stage Ta/T1 papillary carcinoma of the bladder wherein the majority of cells were low grade. Predominantly low-grade cancers with <10% of a high-grade component, > 2 months follow-up and at least one surveillance cystoscopy were included. Exclusion criteria included a prior or concurrent high-grade diagnosis, a subsequent diagnosis of high-grade cancers on immediate repeat resection (within 2-4 weeks), and patients on clinical trials.

Results: 52 cancers met inclusion criteria; 43 men and 9 women (M:F = 4.7:1), average age 71.1 years, with median follow-up 18.1 months (SD = 20.1 months, range = 2.0 – 93.6 months). The majority of cancers were solitary mixed grade tumors; 9 (17%) had a concurrent low-grade cancer, 6 (12%) had multifocal mixed grade cancers, and one (1.9%) had concurrent carcinoma in situ. Four cancers (7.7%) invaded the lamina propria. 27 cancers recurred (52%); 20 (37%) recurred as low or mixed-grade while 7 (13%) recurred as high-grade cancers. One high-grade recurrence had progressed to T2 (1.9%). Recurrence-free survival suggests a high rate of recurrence (90% at 80 months, CI: 70%-100%) but a lower rate of progression to high grade 15% at 80 months, CI: 73% - 98%).

Figure 1 - 442

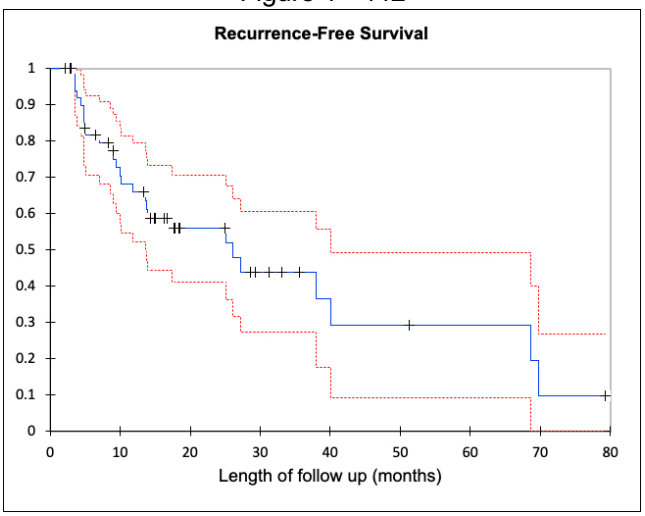

Figure 2 - 442

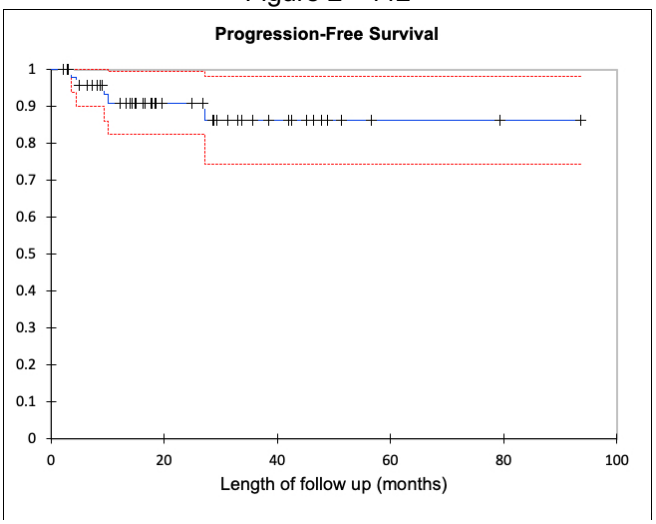

Conclusions: In this series, mixed-grade non-muscle invasive cancers had recurrence rates comparable to low and high-grade cancers. Stage-progression was a rare event comparable to low-grade cancers.

443 Clinicopathologic, Immunohistochemical, and Molecular Characterization of Aggressive Chromophobe Renal Cell Carcinomas

Constance Chen[1], Nicole Croom[1], Bradley Stohr[1], Emily Chan[1]
[1]University of California, San Francisco, San Francisco, CA

Disclosures: Constance Chen: None; Nicole Croom: None; Bradley Stohr: None; Emily Chan: None

Background: Chromophobe renal cell carcinoma (ChRCC) is a relatively rare subtype of RCC and has a characteristic histologic appearance. Most chRCCs are indolent, but sarcomatoid differentiation and metastases can occur, indicative of aggressive behavior and poor prognosis. There are currently no established markers to predict when chRCCs will behave poorly prior to sarcomatoid change or metastases. In this study, we characterize a series of aggressive chRCCs.

Design: We retrospectively examined ten cases of chRCC with aggressive components, identified in our pathology archives. Each case was subject to IHC (CK7, CD117, and CA IX) and capture-based next-generation DNA sequencing of 479 cancer-related genes on available formalin-fixed paraffin-embedded tissue blocks. Differential profiling of the conventional and aggressive components was performed.

Results: On histology, all ten cases showed a conventional chRCC component. Of these, three cases had sarcomatoid change, four cases had metastases, and three cases had both. In the conventional components, a typical IHC pattern for chRCC (CK7+, CD117+ and CAIX-) was observed in 8/10 cases; 2 cases had reduced CK7 staining to only rare+ cells. In the aggressive components, CD117 and/or CK7 was lost in 7/10 cases; 3 of these showed loss of both markers. Surprisingly, 2/10 cases showed significant CAIX+ in the aggressive component. On molecular analysis, all 7 cases in which molecular profiling was performed showed chRCC characteristic pattern of chromosomal losses as well as TP53 mutations (TP53m). Interestingly, the conventional and aggressive components had no shared TP53m: TP53m was present in the aggressive component only in 2 cases, in the conventional component only in 1 case, and in the remaining 4 cases the two components demonstrated different TP53m. Overall, of the 21 different pathogenic alterations identified across the 7 tumors, only one (a PTEN splicing alteration) was shared between both components in one case.

Conclusions: ChRCCs can have IHC staining patterns that differ between their conventional and aggressive components, and evaluation of metastases or small biopsies can be misleading. Rather than a linear model of progression from conventional to more aggressive phenotype, the lack of shared pathogenic mutations between the

two components supports a model in which aggressive chRCCs frequently contain convergent subclones, each with a different TP53 alteration.

444 Primary Urothelial Carcinoma of the Urethra Without Concurrent Renal Pelvic, Ureteral or Bladder Carcinoma: A Contemporary Clinicopathologic Analysis

Fengming Chen[1], Shreyas Joshi[1], Bradley Carthon[1], Adeboye O. Osunkoya[1]
[1]*Emory University, Atlanta, GA*

Disclosures: Fengming Chen: None; Shreyas Joshi: None; Bradley Carthon: None; Adeboye O. Osunkoya: None

Background: Primary urothelial carcinoma (UCa) of the urethra is relatively uncommon, and the underlying pathogenesis has not been well characterized, especially when there is no concurrent UCa at other sites.

Design: A search for cases of primary UCa of the urethra was conducted through the Urologic Pathology and expert consultation files of the senior author. Patients with concurrent UCa of the renal pelvis, ureter or bladder at the time of diagnosis were excluded. Clinicopathologic and follow-up data was obtained.

Results: Thirty-five cases from 29 patients (25 male and 4 female) were included in the study. Mean age at initial diagnosis was 72 years (range: 41-90 years). The specimens included urethra biopsies 16/35 (46%), urethrectomies 11/35 (31%), prostatic urethral biopsies 4/35 (11%), transurethral resection of prostate 2/35 (6%), and penectomies 2/35 (6%). Twenty six of the 35 cases (74%) were composed of high grade UCa, 4/35 (11%) low grade UCa, and 5/35 (14%) UCa in situ (CIS). Five cases (5/35=14%) showed divergent differentiation including 3 squamous, 1 mixed mucinous and neuroendocrine, and 1 case had an inverted growth pattern. Invasion was present in 14/26 (54%) cases of high grade UCa. Pathological staging was documented in 13 patients, among which 7 (54%) were categorized as high stage (6: pT2 and 1: pT3) and 6 (46%) were categorized as low stage (2: pTis and 4: pTa). Clinical history and follow-up were available in 28 patients with a mean duration of 21.2 months (range: 0.2 to 97.5 months). Interestingly, 20/28 (71%) patients had a previous history of high grade papillary UCa (19) or CIS (1) of the bladder. Six of 19 (32%) cases of the previous high grade UCa of the bladder showed divergent differentiation or variant morphology (2: micropapillary, 1: signet ring cells, 1: sarcomatoid, 1: squamous and 1: squamous and glandular. In contrast, no patients subsequently developed UCa at other sites after diagnosis of UCa of the urethra. Three patients (10%) died of this disease.

Conclusions: This is one of the largest studies to date of primary UCa of the urethra without concurrent UCa of the renal pelvis, ureter or bladder. Previous history of UCa of the bladder, especially with divergent differentiation or variant morphology is conceivably an important risk factor for developing subsequent UCa of the urethra. These findings are critical for the development of surveillance protocols.

445 Immunohistochemistry-Based Assessment of RB1 Status in Correlation with Genomic Sequencing and p16 Expression in High-Risk Localized and Metastatic Castration-Resistant Prostate Cancer

Jie-Fu Chen[1], Jatin Gandhi[1], Jason Chang[1], Sounak Gupta[2], Wassim Abida[1], Judy Sarungbam[1], S. Joseph Sirintrapun[1], Ying-Bei Chen[1], Hikmat Al-Ahmadie[1], Samson Fine[1], Satish Tickoo[1], Howard Scher[1], Victor Reuter[1], Anuradha Gopalan[1]
[1]*Memorial Sloan Kettering Cancer Center, New York, NY,* [2]*Mayo Clinic, Rochester, MN*

Disclosures: Jie-Fu Chen: None; Jatin Gandhi: None; Jason Chang: None; Sounak Gupta: None; Wassim Abida: *Consultant*, Clovis Oncology; *Consultant*, Daiichi; *Consultant*, MORE Health; *Consultant*, ORIC Pharma; *Primary Investigator*, Clovis Oncology, AstraZeneca, Zenith Epigenetics, GSK, Epizyme, ORIC pharma; Judy Sarungbam: None; S. Joseph Sirintrapun: None; Ying-Bei Chen: None; Hikmat Al-Ahmadie: None; Samson Fine: None; Satish Tickoo: None; Howard Scher: None; Victor Reuter: None; Anuradha Gopalan: None

Background: Alteration of *RB1* gene emerged as the strongest factor associated with survival and time on treatment with first-line androgen receptor signaling inhibitors (ARSIs) in a recent study of metastatic castration-resistant prostate cancer (mCRPC) patients, including conventional adenocarcinoma and neuroendocrine (NE)

carcinoma. *RB1* loss has been reported in up to 56% of mCRPC and 35% of localized, intermediate risk prostate cancer, raising the possibility of subclonal *RB1* loss at early stage of disease evolution. RB1 immunohistochemistry (IHC) correlated with the total number of genomic aberrations in one pilot study. Here we investigated the concordance rate between RB1 expression by IHC and *RB1* alterations detected by next-generation sequencing (NGS). Considering the potential role of p16 as a surrogate to RB1 alterations, we also evaluated p16 IHC in conjunction with RB1 IHC in detecting *RB1* alterations.

Design: RB1 IHC was performed on 30 mCRPC tumors with known *RB1* status by NGS (27 previously reported; 29 metastatic biopsies and 1 prostatectomy; all adenocarcinoma but 1 with distinct NE component). RB1 and p16 IHC was also performed on 14 prostatectomy samples from high-risk localized prostate cancer (HRPC) patients receiving neoadjuvant ARSI (GS 7-9, GG 3-5; 4 not graded due to therapy-related changes). Results were compared to NGS profiling focusing on *RB1* status. IHC were evaluated by H-score, as defined by: (% negative) x 0 + (% weak positivity) x 1 + (% moderate positivity) x 2 + (% strong positivity) x 3, for a total of 1-300.

Results: Concordance between RB1 IHC and NGS was observed in 27 (90%) mCRPC tumors and in 11 (79%) HRPC tumors (**Table 1**). RB1 IHC exhibited substantial intra-tumoral staining heterogeneity (H-score: 82-200 in mCRPC; 90-245 in HRPC), which may indicate subclonal *RB1* alterations and contribute to the discrepancies between NGS and IHC. Overexpression of p16 occurred in one HRPC tumor with *RB1* loss and negative RB1 IHC, which had large residual adenocarcinoma with NE differentiation after neoadjuvant ARSI. There was no correlation between p16 and RB1 IHC in the other cases.

	NGS	RB1 IHC	p16 IHC
mCRPC (n=30)	10 *RB1* alteration detected (7 copy number loss, 2 small in/del, 1 missense mutation)	8 loss (H-score: 5-70)	Not performed
		2 retained (H-score: 173 and 160)	
	20 *RB1* wild type	1 loss (H-score: 5)	
		19 retained (H-score: 82-200)	
HRPC (n=14)	3 *RB1* alteration detected (3 copy number loss)	1 loss (H-score: 3)	1 overexpressed (H-score: 297)
		2 retained (H-score: 90 and 175)	2 diffusely positive (H-score: 150 and 160)
	11 *RB1* wild type	1 loss (H-score: 32)	1 focally positive (H-score: 45)
		10 retained (H-score: 90-245)	1 negative (H-score: 12)
			9 focally to diffusely positive (H-score: 57-200)

Conclusions: *RB1* alteration is frequent in metastatic castration-resistant prostate cancer (37%), and can be detected in high-risk localized prostate cancer (29%). RB1 IHC detects majority of cases with *RB1* alterations; discrepancies between NGS and RB1 IHC were noted in a small subset of cases which require further investigation. Intra-tumoral heterogeneity is observed with RB1 IHC, which may indicate subclonal *RB1* alterations. p16 IHC did not correlate with *RB1* status in majority of cases. Further analysis and correlation with clinical outcomes in a larger cohort is required.

446 Renal Cell Carcinoma with Fibromyomatous Stroma Associated with TSC/MTOR Alterations and ELOC (TCEB1) Mutations Differ in mTOR Activation Status Assessed by Immunohistochemistry

Jie-Fu Chen[1], Liwei Jia[2], Jatin Gandhi[1], Judy Sarungbam[1], S. Joseph Sirintrapun[1], Anuradha Gopalan[1], Hikmat Al-Ahmadie[1], Samson Fine[1], A. Hakimi[1], Satish Tickoo[1], Victor Reuter[1], Ying-Bei Chen[1]
[1]Memorial Sloan Kettering Cancer Center, New York, NY, [2]UTSouthwestern Medical Center, Dallas, TX

Disclosures: Jie-Fu Chen: None; Liwei Jia: None; Jatin Gandhi: None; Judy Sarungbam: None; S. Joseph Sirintrapun: None; Anuradha Gopalan: None; Hikmat Al-Ahmadie: None; Samson Fine: None; A. Hakimi: None; Satish Tickoo: None; Victor Reuter: None; Ying-Bei Chen: None

Background: Renal cell carcinoma with fibromyomatous stroma (RCC-FMS) is an emerging/provisional entity in the 2016 WHO classification and encompasses a group of RCCs with clear cells and prominent smooth muscle and fibromatous stroma. Recent studies identified subsets of RCC-FMS with recurrent mutations (mt) involving *TSC1/2*, *mTOR*, or *ELOC* (*TCEB1*) genes, in the absence of *VHL* and chromosome 3p alterations. Questions remain whether *TSC/MTOR*-mt RCC-FMS and *ELOC*-mt RCC-FMS should be merged as one distinct entity. Here we report the clinicopathologic features of a cohort of RCC-FMS, and explore the utility of immunohistochemistry (IHC) for phosphorylated-ribosomal protein S6 (pS6) and phosphorylated-4E-BP1 (p4EBP1) to differentiate *TSC/MTOR*-mt RCC-FMS from *ELOC*-mt RCC-FMS.

Design: We retrospectively identified 25 RCC-FMS with clinical follow-up and genomic profiling (4 *TSC1*-mt, 5 *MTOR*-mt, 16 *ELOC*-mt); IHC for pS6 and p4EBP1 were performed on 15 and 17 cases with available material, respectively. H-score [intensity (0-3+) x % of positive cells] was used to assess IHC results. Comparison was made between *TSC/MTOR*-mt and *ELOC*-mt cases.

Results: Median age of 9 patients (7 female, 2 male) with *TSC/MTOR*-mt RCC-FMS was 45 years (range: 25-66); during a median follow-up period of 48 months (range: 12-218) after resection (pT1a to pT3b), one patient had distant lymph node metastasis. Median age of 16 patients (1 female, 15 male) with *ELOC*-mt RCC-FMS was 60 years (range: 42-77); 15 had nephrectomy (pT1a to pT3b) and 2 had pleural metastasis at the diagnosis. During a median follow-up of 51 months (range: 8-116), 1 succumbed to disease, 1 had no recurrence post-systemic therapy, and the others remained disease-free. Tumors in both groups were multinodular with various growth patterns including acinar/alveolar, pseudopapillary/papillary, solid, and predominantly composed of tumor cells with clear and voluminous cytoplasm. Pseudocapsule and septa with fibrous and smooth muscle components were seen in all cases. The tumors showed patchy to diffuse membranous staining of CA IX, CK7, and CD10; TFE3, TFEB, HMB45, and AMACR were negative. The average H-scores for pS6 and p4EBP1 IHC were both significantly higher in *TSC/MTOR*-mt RCC-FMS than those in *ELOC*-mt RCC-FMS (p=0.016 for pS6 and 0.005 for p4EBP1; **Figure 1**).

Figure 1 - 446

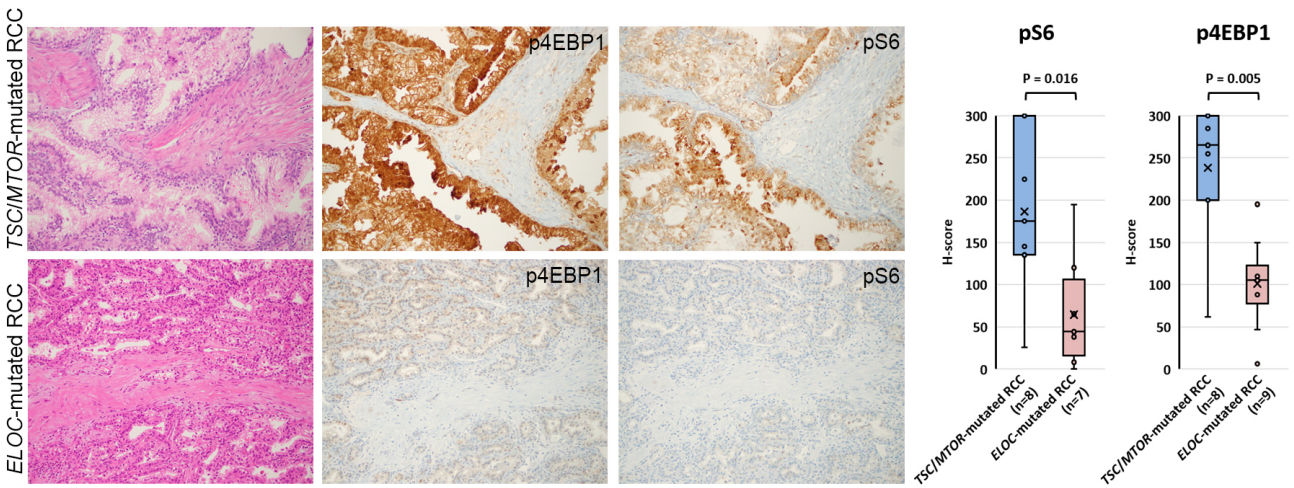

Conclusions: *ELOC*-mt RCC occurred predominantly in male patients whereas *TSC*/*MTOR*-mt RCC-FMS more in females. Despite overlapping morphologic features, these two groups differ significantly in immunoreactivity for pS6 and p4EBP1, which supports a different role of the mTOR complex 1 activation in the tumor pathogenesis.

447 Variant Histology Predicts Poor Clinical Outcome in Patients with Upper Tract Urothelial Carcinoma: A Single Institution Experience

Zhengshan (Allen) Chen[1], Alireza Ghoreifi[2], Hooman Djaladat[2], Andy Sherrod[2], Guang-Qian Xiao[2], Manju Aron[2]
[1]LAC+USC Medical Center, Los Angeles, CA, [2]Keck School of Medicine of USC, Los Angeles, CA

Disclosures: Zhengshan (Allen) Chen: None; Alireza Ghoreifi: None; Hooman Djaladat: None; Andy Sherrod: None; Guang-Qian Xiao: None; Manju Aron: None

Background: Upper tract urothelial carcinoma (UTUC) accounts for 5-7% of all urothelial carcinomas. Limited data exists regarding the incidence of variant histology in UTUC, and its association with adverse pathological features and oncologic outcomes. In this study, we report the incidence of variant histology in a contemporary series of UTUC from a single institutional cohort and analyze its association with adverse pathological features and oncologic outcomes.

Design: All cases of resected UTUC diagnosed at our institution from 2014-2020 were retrieved from our prospectively maintained UTUC database. A total of 203 cases were identified. The slides of all these cases were reviewed to identify the presence of variant histology and to document the presence of additional pathological parameters as listed in Table 1. The pathological, demographic and clinical variables including oncologic outcomes were compared between conventional UTUC (cUTUC) and UTUC with variant histology(vUTUC).

Results: 44 out of 203 (21.7%) were vUTUC, however 12 (27.2%) of these cases were missed on initial diagnosis. Of these 36 (81.8%) had only one histological variant, 6 (13.6%) had two variants, and 2 (4.5%) had three variants. Squamous differentiation was the most common variant (15.8%), followed by glandular (3.4%), nested (2.0%), sarcomatoid (1.5%), giant cell (1.5%), micropapillary (1.0%), and 0.5% each of small cell, trophoblastic and microcystic variant. There was no age or gender differences between cUTUC and vUTUC (Table 1). However, vUTUC was significantly associated with all analyzed pathologic parameters including higher pT stage ($p < 0.0001$), positive surgical margins ($p < 0.0001$), lymphovascular invasion ($p < 0.0001$), lymph node metastasis ($p < 0.0001$), necrosis ($p = 0.0001$), multifocality ($p = 0.0045$) and carcinoma in situ ($p = 0.0239$). The period of clinical follow up ranged from 1-76.4 months (median: 14.9 months, IQR: 5.6-31.4 months). 10% of cUTUC (16/159) and 15.9% of vUTUC (7/44) received neoadjuvant chemotherapy. vUTUC predicted shorter recurrence free survival ($p = 0.0002$; Figure 1) and shorter overall survival ($p = 0.0029$; Figure 2) compared to cUTUC.

Table 1. Clinicopathological features of conventional UTUC compared with UTUC with variant histology

	Conventional UTUC (n=159)	UTUC with variant histology (n=44)	p value
Age (mean ± SD, y)	73.2 ± 10.2	71.3 ± 9.9	0.26
Gender			0.15
Male	104	34	
Female	55	10	
Pathological stage			<0.0001
≤ T1	102	5	
≥ T2	57	39	
Surgical margins			<0.0001
Positive	13	16	
Negative	146	28	
LVI			<0.0001
Present	24	24	
Absent	135	20	
LNM			<0.0001
Present	15	12	
Absent	144	32	
Necrosis			0.0001

Present	10	13	
Absent	149	31	
Carcinoma in situ			0.0239
Present	56	24	
Absent	103	20	
Multifocality			0.0045
Present	15	12	
Absent	144	32	

UTUC: upper tract urothelial carcinoma; SD: standard deviation; LVI: lymphovascular invasion; LNM: lymph node metastasis

Figure 1 - 447

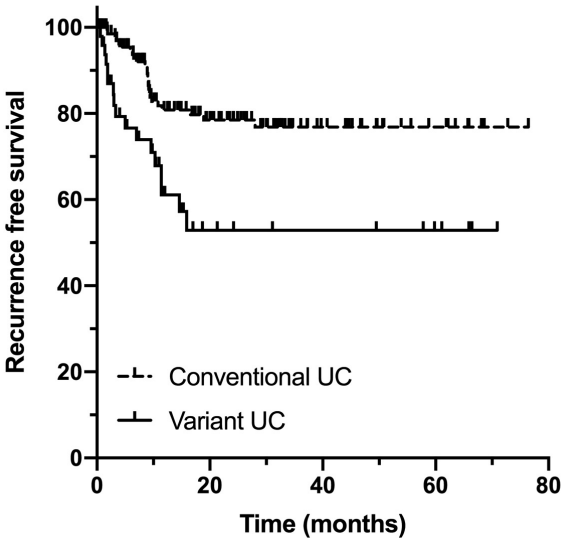

Figure 2 - 447

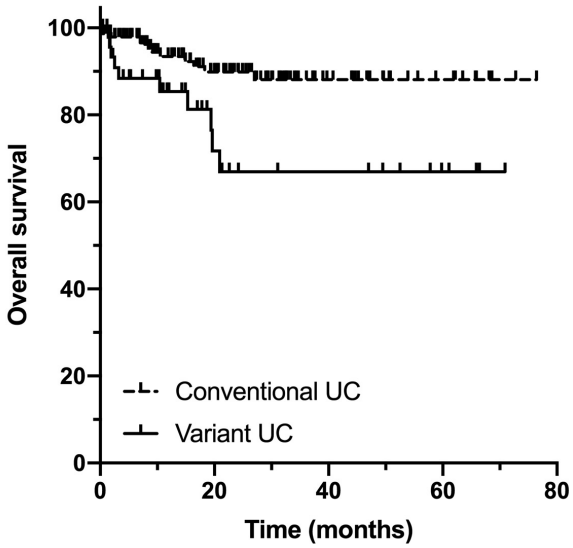

Conclusions: Variant histology is seen in about 20% of UTUC but may be underreported in about a quarter of the cases. Squamous differentiation is the most common . vUTUC is significantly associated with adverse pathological features and is associated with poor recurrence free and overall survival. Our findings further underscore the importance of recognizing and reporting variant histology in UTUC.

448 Fine Tuning of Deep Neural Networks(DNN) Trained on Prostate Needle Biopsies to Diagnose Transurethral Resection of Prostate Images

Joonyoung Cho[1], Minsun Jung[2], Cheol Lee[2], Han Suk Ryu[3], Tae-Yeong Kwak[4], Sun Woo Kim[1], Hyeyoon Chang[1]

[1]Deep Bio Inc., Seoul, South Korea, [2]Seoul National University Hospital, Seoul, South Korea, [3]Seoul National University College of Medicine/Hospital, Seoul, South Korea, [4]Deep Bio Inc., Guro-gu, South Korea

Disclosures: Joonyoung Cho: *Employee*, Deep Bio Inc.; Minsun Jung: None; Cheol Lee: None; Han Suk Ryu: None; Tae-Yeong Kwak: *Employee*, Deep Bio Inc.; Sun Woo Kim: *Stock Ownership*, Deep Bio Inc.; Hyeyoon Chang: *Employee*, DeepBio Inc.

Background: Transurethral resection of the prostate(TURP) is a surgery for treatment of benign prostatic hyperplasia. Incidental prostate cancer is reported in 4.1-16.7% in TURP cases. In our previous study, we reported an automatic diagnosis of TURP whole slide images (WSIs) by translationally applying a DNN model which was developed for the diagnosis of prostate needle biopsy. It showed low specificity, 0.469 compared to high sensitivity, 0.978. False positive signals were detected in tissue with cauterization and squeezing artifacts. In this study, we performed a fine tuning of DNNs using benign TURP and transurethral resection of bladder (TURB) WSIs to advance our model's performance.

Design: We used additional 216 benign TURP and 22 TURB slides for training and tested its performance in 565 cases (3682 glass slides) of TURP. All slides were scanned using Aperio AT2 digital slide scanner (Leica Biosystems Imaging, Inc., Vista, CA, United States) An experienced pathologist reviewed all the glass slides. If there is a disagreement between the original hospital diagnosis and the pathologist's review, immunohistochemical staining for high molecular weight cytokeratin was done to determine the diagnosis. Urothelial carcinoma cases and slides consisting of only other tissues were excluded. Finally, a total of 55 prostate cancer and 510 benign cases were included in this study. The accuracy, sensitivity and specificity were measured.

Results: The model's detection accuracy, sensitivity, and specificity were 0.943, 0.945, and 0.943 respectively. The confusion matrix and results are shown in Table. 1. False negative cases often showed cancers with gleason pattern 3 with very small cancer areas. False positive signals were detected in other organs, such as an urothelium. The representative images of the model's analyses are shown in Fig 1, with true positive case(Fig. 1), false positive case(Fig. 2A and B), and false negative case(Fig. 2C).

		Diagnosis		
		Cancer	Benign	Total
AI	Cancer	52	29	81
	Benign	3	481	484
	Total	55	510	565
Accuracy		0.943		
Sensitivity		0.945		
Specificity		0.943		

Figure 1 - 448

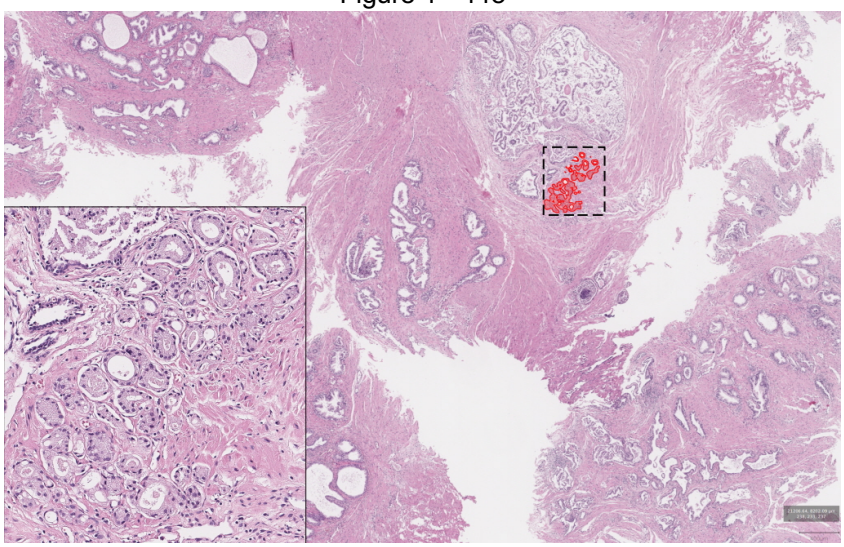

Figure 2 - 448

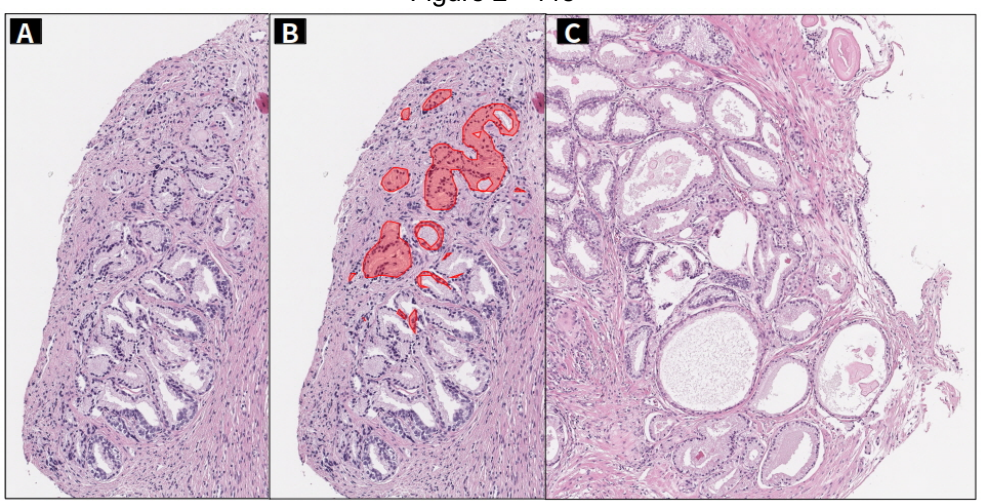

Conclusions: In this study, we focused on the weaknesses of the previous model which showed false positive detections for cauterization and squeezing artifacts of tissue periphery. Adding benign tissues in training, the performance of the model was improved.

449 Primary Malignancy After Urologic Reconstruction Procedures: A Multicenter Case Series

Chelsea Cornell[1], Francesca Khani[2], Adeboye O. Osunkoya[3], Andres Matoso[4], Hiroshi Miyamoto[5], Jennifer Gordetsky[1], Safia Salaria[1], Giovanna Giannico[1]
[1]Vanderbilt University Medical Center, Nashville, TN, [2]Weill Cornell Medicine, New York, NY, [3]Emory University, Atlanta, GA, [4]Johns Hopkins Medical Institutions, Baltimore, MD, [5]University of Rochester Medical Center, Rochester, NY

Disclosures: Chelsea Cornell: None; Francesca Khani: None; Adeboye O. Osunkoya: None; Andres Matoso: None; Hiroshi Miyamoto: None; Jennifer Gordetsky: None; Safia Salaria: None; Giovanna Giannico: None

Background: Juxtaposition of urinary and intestinal mucosa is used for reconstructive urologic surgery, such as urinary diversion and reconstruction cystoplasty. Increased incidence of primary malignancies in intestinal mucosa within these reconstructive procedures is well-known and estimated around 0.18% to 15% of patients undergoing urinary diversion, more frequently ureterosigmoidostomies and cystoplasties. However, data regarding clinicopathologic features of these malignancies are scant. The aim of this study is to describe the clinicopathological features of primary tumors arising after different urologic reconstruction procedures.

Design: A search was conducted in the pathology files of the collaborating academic institutions. Cases of primary malignancy were included. Cases with recurrence of urothelial carcinoma if this was the primary diagnosis for reconstruction were excluded. Clinicopathologic data were collected and staging was assigned based on the gastrointestinal segment included in the reconstruction. Immunohistochemical stains for CK7, CK20, CK903, GATA-3, SATB2, CDX2, and beta-catenin was performed on a representative tumor slide in 9/10 adenocarcinomas, and were scored on a scale from 0-3+. Focal expression was defined as <50% of tumor expression.

Results: A total of 11 cases were identified, including 7 ileal conduits, 2 gastrocystoplasties, 1 augmentation cystoplasty NOS, and 1 Indiana pouch (Table). The mean age was 51.7 years (range: 29-70). The male to female ratio was 8:3. Reconstruction was for benign disease in 8/10 patients and malignancy in 2/10. Median time from reconstruction to malignancy was 36 years (range: 2-58). Primary malignancy was adenocarcinoma in 10 patients and squamous cell carcinoma in 1. In 9 patients with adenocarcinoma, subtypes were intestinal in 6, gastric in 2, and signet ring cell in 1. Immunohistochemical analysis showed the following expression: CK7 (4/9, 45%), CK20 (8/9, 89%, 4 focal), CK903 (7/9, 78%, all focal), CDX2 (8/9, 89%, 2 focal), SATB2 (6/9, 67%, 3 focal), beta-catenin (9/9, 100%, 7 membranous, 2 membranous and cytoplasmic). GATA-3 was negative in all cases. Stage was advanced in 8/10 cases and lymph node or distant metastasis was present in 8/10. Treatment included surgery, chemotherapy, and radiation. Follow-up was available for 10/11 cases (mean follow-up time 27.4 months, range: 7-82). Four patients were alive without evidence of disease, three were alive with disease, two were deceased, and two entered hospice at the last known follow-up.

Case	Age/ Gender	Reconstruction	Primary disease	Time to disease (years)	Specimen type	Histology	Stage	Treatment	Follow-up (months)	Outcome
1	60/M	Ileal conduit	Bladder exstrophy	40	Resection	Adenocarcinoma gastric type	pT4N1	Surgery	7	AWOD
2	53/F	Ileal conduit	Vesicoureteral reflux	48	Resection	Adenocarcinoma intestinal/ villous type	pT1Nx	Surgery	48	AWOD
3	58/F	Ileal conduit	Urothelial carcinoma	2	Resection	Treatment effect	T3Nx	Chemotherapy Radiation	82	AWOD
4	59/M	Ileal conduit	Bladder exstrophy	58	Resection	Squamous cell carcinoma	pT2N2b	Surgery	7	DOU
5	38/M	Ileal conduit	Obstructive uropathy s/p kidney transplant	36	Resection	Adenocarcinoma with signet ring features	pT2N2	Surgery Chemotherapy	9.5	LTF
6	36/M	Gastrocystoplasty	Reflux nephropathy s/p kidney transplant	24	Resection	Adenocarcinoma intestinal type	pT3aN2	Surgery Chemotherapy	8.5	DOD
7	29/M	Gastrocystoplasty	Renal dysplasia	26	TURBT	Adenocarcinoma gastric type	pT2N3M1	Surgery Chemotherapy	18	AWD

Case	Age/ Gender	Reconstruction	Primary disease	Time to disease (years)	Specimen type	Histology	Stage	Treatment	Follow-up (months)	Outcome
8	50/F	Colocystoplasty converted to ileal conduit	End-stage bladder s/p chemotherapy	44	Biopsy	Adenocarcinoma intestinal/ villous type	pT1NxM1	Radiation Immunotherapy	7	AWD
9	59/M	Ileal conduit	Diabetes insipidus and bladder dysfunction	Childhood	Biopsy	Adenocarcinoma intestinal/ villous type	NA	Chemotherapy	2	AWD
10	70/M	Indiana pouch	Leiomyosarcoma bladder	6	Resection	Adenocarcinoma intestinal/ villous type	pT2N1a	Surgery Chemotherapy	24	LTF
11	57/M	Augmentation cystoplasty	NA	Childhood	Resection	Adenocarcinoma intestinal/ villous type	pT1Nx	Surgery	63	AWOD

Abbreviations: AWOD = alive without disease; AWD = alive with disease; DOU = died of unknown cause; DOD = died of disease; LTF = lost to follow-up.

Conclusions: Primary malignancy arising after surgical reconstruction is rare. Adenocarcinoma is the most frequent histologic pattern, and often presents at an advanced stage.

450 Whole Slide Microvascular Density (MVD) Evaluation in Metastatic Clear Cell Renal Cell Carcinoma (mccRCC): Association With ISUP/WHO Grade, PD-L1 Expression, and Mast Cell Infiltration.

Thomas Denize[1], Alessia Cimadamore[1], Emily Walton[2], Maura Sticco-Ivins[2], David Braun[3], Maxine Sun[4], Evelyn Wang[5], Toni Choueiri[6], Sabina Signoretti[2]
[1]Brigham and Women's Hospital, Harvard Medical School, Boston, MA, [2]Brigham and Women's Hospital, Boston, MA, [3]Dana-Farber Cancer Institute, Harvard Cancer Center, Boston, MA, [4]Dana-Farber Cancer Institute, Boston, MA, [5]Exelexis, Alameda, CA, [6]Dana-Farber Cancer Institute, Harvard Medical School, Boston, MA

Disclosures: Thomas Denize: None; Alessia Cimadamore: None; Emily Walton: None; Maura Sticco-Ivins: None; David Braun: *Consultant*, Bristol-Myers Squibb; *Speaker*, LM Education and Exchange Services; *Consultant*, Schlesinger; Maxine Sun: None; Evelyn Wang: *Employee*, Exelixis, Inc; *Employee*, Exelixis, Inc; Toni Choueiri: *Consultant*, BMS, Roche, Exelixis, Merck, AZ; *Grant or Research Support*, BMS, Roche, Exelixis, Merck, AZ; Sabina Signoretti: *Grant or Research Support*, Bristol-Myers Squibb, AstraZeneca, Exelixis, Novartis; *Consultant*, Bristol-Myers Squibb, AstraZeneca, Merck, CRISPR Therapeutics AG, AACR, and NCI; *Consultant*, Biogenex

Background: Anti-angiogenic tyrosine kinase inhibitors (TKIs) targeting the VEGF pathway are approved for mccRCC either alone or in combination with anti-PD-1/PD-L1 agents; however, the relationship between tumor vascularity, PD-L1 status, and pathological features remains unclear. It has been suggested that in some tumor types, tumor-infiltrating mast cells (MC) promote angiogenesis through VEGF-dependent and -independent pathways and modulate response to anti-angiogenic therapy, but their role in mccRCC is unknown. Here, we studied the relationship between MVD and i) MC density (MCD), ii) tumor cell (TC) PD-L1 expression, iii) WHO/ISUP nuclear grade, in pretreatment tumors from patients with mccRCC enrolled in the phase III METEOR trial of cabozantinib versus everolimus

Design: Tumor samples from 446 patients were collected and underwent pathology review. Each sample was double immunostained with anti-CD31 and anti-Tryptase antibodies. Tumor area on whole scanned slides was annotated and analyzed with the HALO colocalization algorithm v1.3 and a random forest classifier (Indica Lab) was trained in each case to exclude CD31-positive macrophages and necrotic areas. MVD (vessels/mm2) and MC density (MCD) (MCs/mm^2) were assessed using an object quantification algorithm (Indica Lab). Results were independently validated by 2 pathologists. TC PD-L1 expression data was available for a subset of the patients (n=269). Wilcoxon test was used to analyze continuous variable with dichotomous predictor; Spearman correlation was used for the comparison of two continuous variables

Results: Mean MVD was 241, 177, and 125 vessels/mm^2 for grade 2, 3, and 4 tumors, respectively. Grade 4 tumors had lower MVD than grade 3 (p=0.00095) and grade 2 (p<0.005) tumors. Similarly, grade 3 tumors

had lower MVD than grade 2 ones (p<0.005). MCD (median 7 MC/mm^2, range 0-72.8 MC/mm^2) was positively correlated to MVD, with a Spearman correlation coefficient of 0.41 (p<0.005). TC PL-L1 positivity (cutoff >=1%) was detected in 83/269 (31%) cases. MVD was lower in PD-L1 positive versus PD-L1 negative tumors (mean MVD was 141 vs 196 vessel/mm^2 respectively, p<0.005), but the result was not independent from the WHO/ISUP grade since no difference in MVD was observed between PD-L1 positive and negative tumors when the analysis was stratified by the grade.

Figure 1 - 450

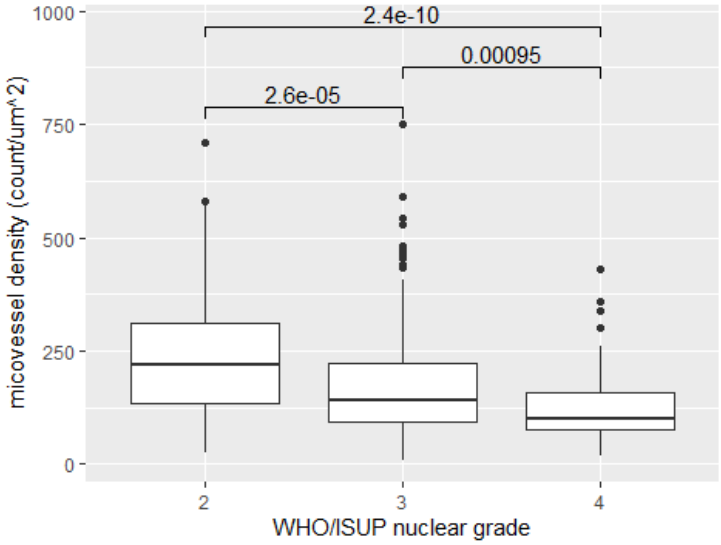

Figure 2 - 450

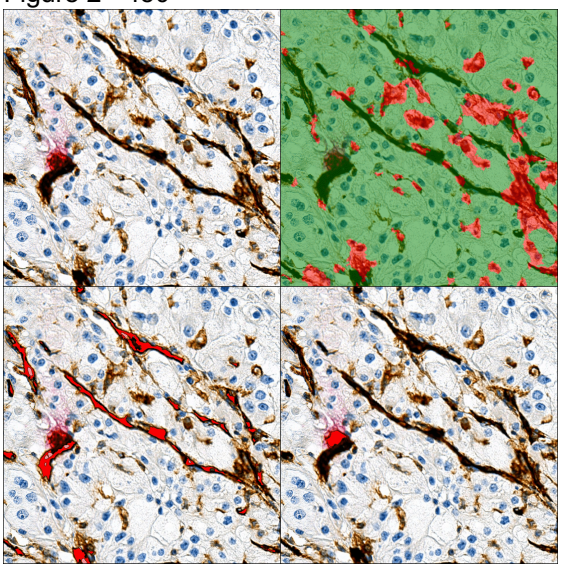

Conclusions: Our results indicate that in mccRCC, MVD is inversely correlated with features of tumor aggressiveness (nuclear grade and TC PD-L1 expression). The positive correlation between MVD and MCD supports mast cell effects on tumor angiogenesis. Correlation of results with clinical data to assess the role of MVD and MCD in predicting outcome to systemic anti-VEGF therapy is ongoing

451 Clinicopathologic Analysis of an ISUP Grade 2, Lymph Node Positive Radical Prostatectomy Series

Michelle Downes[1], Hilda de Barros[2], Pim van Leeuwen[2], Henk G. van der Poel[2], Theodorus Van Der Kwast[3]

[1]Sunnybrook Health Sciences Centre, Toronto, Canada, [2]Netherlands Cancer Institute, Amsterdam, Netherlands, [3]University Health Network, Toronto, Canada

Disclosures: Michelle Downes: None; Hilda de Barros: None; Pim van Leeuwen: None; Henk G. van der Poel: None; Theodorus Van Der Kwast: None

Background: Radical prostatectomy with positive lymph nodes (pN+) may be identified in up to 15% of cases with an associated pelvic lymph node dissection (PLND). Most of these pN+ are in the setting of a high ISUP grade/Gleason score. ISUP grade 2/Gleason score 7/10 (3+4) prostatectomies rarely have synchronous nodal metastases. We investigated the frequency of ISUP grade 2, pN+ disease at prostatectomy along with the clinicopathologic features of these cases at three academic institutions.

Design: The laboratory information system at each institution was searched to identify all prostatectomy cases with a final diagnosis of ISUP grade 2 or Gleason score 7/10 (3+4) prostatic adenocarcinoma. Cases that were pN+ were retrieved for review to confirm the grade, stage, margins and nodal status. Each case was additionally reviewed for the presence of cribriform pattern 4 (CC), intraductal carcinoma (IDC) and tertiary/minor grade 5.

Results: The search identified 2834 cases with the specified criteria. Overall, 67/2834 (2.36%) were pN+. Of these 67 cases, 63 reports contained information on CC and IDC and/or slides were available for retrospective review.

The mean patient age was 63 years and the median pre-operative PSA was 8.8ng/ml (range 3.4- 32.2). The mean tumour volume (%) was 27% gland involvement (range 5-85%). The breakdown of pT stage was: 13 pT2 (20.6%), 28 pT3a (44.5%), 21 pT3b (33.3%) and 1 pT4 (1.6%). Margin positivity was noted in 28 cases (43.8%). A tertiary/minor pattern 5 component was seen in 11 cases (17.2%). A cribriform architecture (CC and/or IDC) was identified in 56/63 cases (88.9%). The mean nodal yield in extended PLND was 18.1 (range 4-44 nodes) and the mean yield in standard PLND was 9.9 nodes (range 2-29 nodes). 20/67 (29.9%) had > 1 positive lymph node. The rate of pN1 was significantly higher in the extended PLND group (37/261, 14.1%) as was the frequency of pT2 disease (12/37, 32.4%).

Conclusions: ISUP grade 2 pN+ cases are infrequent at radical prostatectomy and have a strong association with CC and/or IDC, extent of PLND and ≥ pT3 disease.

452 Relationship of STAG2 Expression with Intrinsic Molecular Subtypes and Recurrence/Progression Status in Non-Muscle-Invasive Bladder Cancer

Zeynep Betul Erdem[1], Caglar Cakir[2], Alper Otunctemur[2]
[1]*Cemil Tascioglu City Hospital, Istanbul, Turkey,* [2]*Istanbul, Turkey*

Disclosures: Zeynep Betul Erdem: None; Caglar Cakir: None; Alper Otunctemur: None

Background: STAG2 gene is located on X chromosome and is a subunit of the cohesin complex. It is now identified as one of the most commonly mutated genes along with FGFR3 and p53 in bladder cancers. Literature data shows differences among the outcomes of patients with STAG2 mutations. Aim of this study is to determine the role of STAG2 expression and intrinsic molecular subtypes in the prediction of reccurence/progression risk of non-muscle-invasive bladder cancer (NMIBC). It is intended to provide foresight about disease prognosis and to decrease the follow-up costs of these cancers with highest-cost follow-up protocols.

Design: A total of 102 patients diagnosed as NMIBC (pTa, pT1) with TUR operation material in the Prof. Dr. Cemil Tascioglu City Hospital Pathology Department from January 1, 2011 to May 1, 2016, with a follow-up time of at least 36 months were included in the study. Only the initial biopsies were included. GATA 3, CK 20, CK 5/6, p53 and STAG 2 immunohistochemistry was performed on chosen whole tissue blocks from each patient. Association of intrinsic molecular subtypes and STAG2 expression with prognostic parameters were analysed.

Results: GATA 3 positivity was seen in 99% of the cases. By using CK 20 and CK 5/6 as surrogate markers for molecular subtyping, 4 subtypes were defined; 46.1% was luminal, 16.7% was basal, 13.7% was mixed and 23.5% was null. Luminal subtype was correlated with high grade morphology (p=0.024). Statistically significant association between basal subtype, low grade morphology and loss of STAG 2 expression was revealed (p=0.040). Loss of STAG2 expression was highly correlated with female gender, lower grade and stage (p=0.001). p53 positivity had no correlation with intrinsic molecular subtypes. No significant association between intrinsic molecular subtypes, STAG2 expression and recurrence/progression was found.

Figure 1 - 452

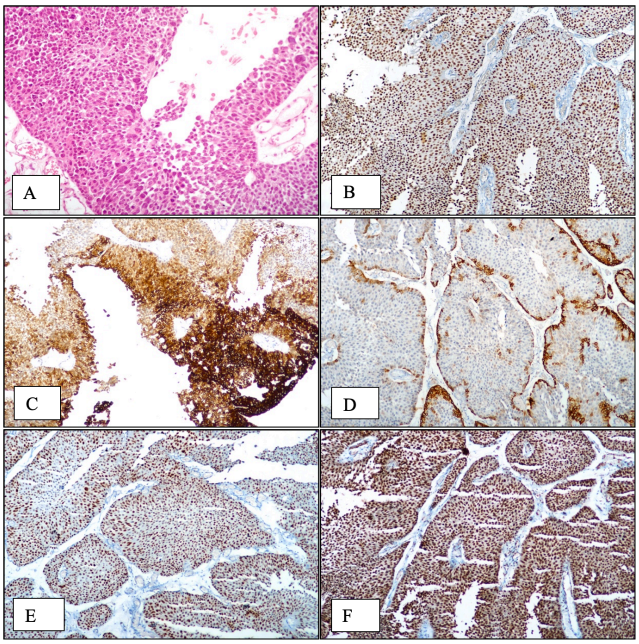

Figure 2 - 452

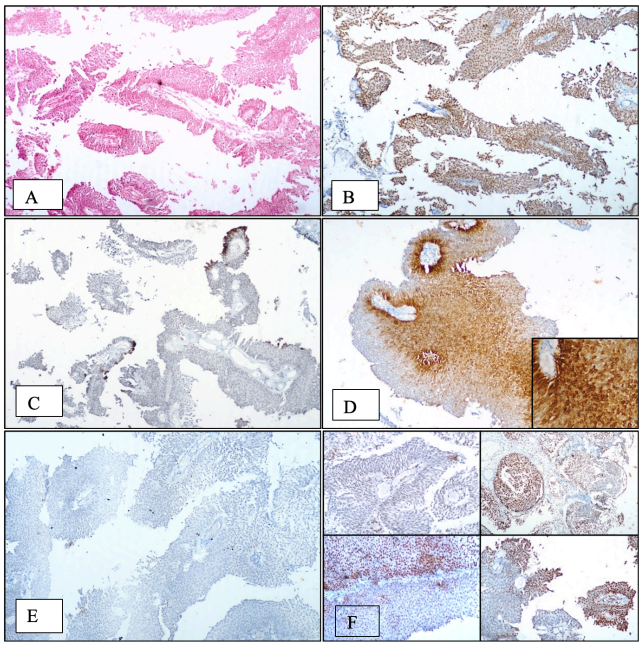

Figure footnotes:

Figure 1: A case with Luminal Fenotype. A) High grade papillary urothelial carcinoma (H&E, 200x). B) GATA3 expression (100x). C) CK 20 expression (100x). D) CK 5/6 expression limited to the basal layer, normal pattern (100x). E) p53 expression, mutated (100x). F) Diffuse strong expression of STAG2 (100x)

Figure 2: A case with Basal Fenotype. A) Low grade papillary urothelial carcinoma (H&E, 100x). B) GATA3 expression (100x). C) CK 20 expression limited to the superficial (umbrella) cells, normal pattern (100x). D) CK 5/6 expression (100x). E) p53 negativity (100x). F) Expression of STAG2 with mosaic pattern (200x)

Conclusions: GATA 3 is not an useful marker for subgrouping of NMIBCs. In contrast to the data obtained from muscle invasive bladder cancers, luminal subtype is associated with high grade morphology, while basal subtype is associated with low grade morphology in NMIBCs. Based on our results no significant relationship was found with recurrence/progression rates. Treatment modalities of the cases included in the study were heterogenous. Significant results can be achieved with larger population based studies where the treatment status is homogeneous and known clearly.

453 Renal Mass Core Needle Biopsy Is High Yield and Has Significant Impact on Patient Management: Pathological, Radiological and Clinical Correlation of 260 Cases

Haijuan Gao[1], Behdokht Nowroozizadeh[2], Joaquin Ponce-Zepeda[1], Di Lu[1], Ted Farzaneh[1], Cary Johnson[2], Hirad Hosseini[1], Min Han[1]
[1]University of California, Irvine, Orange, CA, [2]University of California, Irvine, Irvine, CA

Disclosures: Haijuan Gao: None; Behdokht Nowroozizadeh: None; Joaquin Ponce-Zepeda: None; Di Lu: None; Ted Farzaneh: None; Cary Johnson: None; Hirad Hosseini: None; Min Han: None

Background: With increased imaging, benign findings among resected renal masses have significantly increased, suggesting a need for better preoperative diagnosis. Renal core needle biopsy (CNB) has not been widely accepted in this regard, however, due to perceived low yield and concern for complications.

Design: 260 consecutive CNBs from 250 patients who underwent percutaneous image-guided CNB from January 2015 to December 2019 were retrieved from a tertiary academic center and formed the basis of this study. The rapid on-site evaluation was performed by cytology staff in all cases.

Results: The age range was 28-87 years (median 63). 91 (35%) procedures were performed under ultrasound guidance and 169 (65%) were done under CT guidance. The size of the renal masses ranged from 1 to 17 cm and 68.9% of cases were 4 cm or less. The median number of cores acquired was 3 (range 1-12) in diagnostic cases and 4 (range 2-7) in non-diagnostic cases (p=0.003). Of 260 CNBs, 216 (83.1%) were diagnostic, constituting 175 (70%) renal cell carcinomas (RCCs), 11 (4.4%) malignant neoplasm non-RCC and 30 (12%) benign processes. 13 (5%) CNBs were indeterminant and 31 were negative (Table 1). Of 31 patients with initial negative results, 9 underwent repeat CNB. 8 turned positive and 1 remained negative. Subsequently, 105 (42.0%) patients underwent partial or total nephrectomy, revealing 103 RCCs (95 RCCs, 4 indeterminant and 4 negatives on CNB), 1 angiomyolipoma (negative CNB), and 1 oncocytoma (concordant CNB). In addition, 54 (21.6%) tumors, mostly RCC (n=42) underwent ablation, 51 (20.4%) patients, including 29 of 30 benign neoplasms, underwent active surveillance, and 21 (8.4%) patients received chemoradiation therapy for advanced-stage RCC, metastatic carcinoma or lymphoma. RCC subtypes were reported in 89 of 95 (93.7%) RCCs and WHO/ISUP (formerly Fuhrman) nuclear grade was provided in 65 of 72 (92.3%) CCRCCs on CNB (Figure 1). The concordance rate was 97.8% and 72.3% respectively. Complications were documented in a subset of patients but were non-severe in all cases.

Table 1: Correlation of 260 Renal Mass Core Needle Biopsy Diagnoses with Resection Diagnoses for Tumor Typing and Subtyping

Biopsy Dx	Subtypes_Bx	No. of CNB (% Total)	No. of Resection (% resected)	Concordance	Resection Dx_Discordant only
RCC		**175 (67.3%)**	**95 (54.3%)**	**100%**	**-**
	Clear Cell	120 (46.2%)	72 (60%)	97.2%	1 Papillary RCC, 1 Chromophobe RCC
	Papillary	22 (8.5%)	8 (36.4%)	100%	-
	Chromophobe	14 (5.4%)	7 (50%)	100%	-
	Rare variant	5 (1.9%)	2 (40%)	100%	-
	Un-subclassified	14 (53.8%)	6 (42.9%)	-	5 Clear Cell RCC, 1 Chromophobe RCC
Malignant, non-RCC		**11 (4.2%)**	**0**	**-**	**-**
Indeterminant		**13 (5%)**	**4 (30.8%)**	**0**	
	Neoplasm, UMP	5 (1.9%)	1 (20%)	0	1 Clear Cell RCC
	Atypical/Suspicious	8 (3.1%)	3 (37.5%)	0	3 Clear Cell RCC
Benign		**30 (11.5%)**	**1 (3.3%)**	**100%**	
	Oncocytoma	19 (7.3%)	1 (5.3%)	100%	
	Angiomyolipoma	6 (2.3%)	0	0	0
	Inflammatory process	4 (1.5%)	0	0	0
	Hemangioma	1 (0.4%)	0	0	0
Negative		**31 (11.9%)**	**5 (16.1%)**	**0**	3 Clear Cell RCC, 1 Papillary RCC 1 AML
Total		**260**	**105 (42%)**		

Dx: Diagnosis, RCC: renal cell carcinoma, UMP: unknown malignant potential, AML: Angiomyolipoma

Conclusions: Renal mass CNB provided definitive diagnoses in 83.1% of cases. Tumor subtyping proved to be highly accurate, and nuclear grading for CCRCC was accurate in most but not all cases. CNB was also able to identify a significant number of non-surgical conditions (15.7%), potentially preventing unnecessary nephrectomy. Regarding non-diagnostic cases, repeat CNB would likely increase diagnostic yield.

454 PDL1 Expression in Squamous Cell Carcinoma and Urothelial Carcinoma with Squamous Differentiation of the Urinary Bladder

Jennifer Gordetsky[1], Jonathon Craig[1], Giovanna Giannico[1], Prabin Thapa[2], Stephen Boorjian[2], Igor Frank[2], John Cheville[2]
[1]*Vanderbilt University Medical Center, Nashville, TN,* [2]*Mayo Clinic, Rochester, MN*

Disclosures: Jennifer Gordetsky: None; Jonathon Craig: None; Giovanna Giannico: None; Prabin Thapa: None; Stephen Boorjian: *Consultant*, Ferring; *Consultant*, FerGene; *Consultant*, ArTara; Igor Frank: None; John Cheville: None

Background: Bladder cancer may show divergent differentiation. Urothelial carcinoma with squamous differentiation (USD) and pure squamous cell carcinoma (SCC) of the urinary bladder are two of the more common divergent histologic subtypes encountered. The immunophenotypic properties of different histologic subtypes are critical for treatment response Patients who are positive for programmed cell death-ligand 1 (PD-L1) may be eligible for immunotherapy. We explored the clinical, pathologic, and PD-L1 immunophenotypic characteristics of patients who underwent radical cystectomy for UCD and SCC.

Design: After IRB approval, a retrospective review was performed for patients who underwent radical cystectomy between 1980 and 2015. Patients who had a diagnosis of SCC or USD were included. All cases were re-reviewed for pathologic features by a urologic pathologist, and clinical data including outcome information were obtained. Criteria of inclusion were presence of both urothelial and squamous components for diagnosis of USD and absence of any urothelial component for diagnosis of SCC. Immunohistochemistry for PD-L1 (SP263, SP142, 22C3) was performed on all patients utilizing a tissue microarray. A standardized h score was utilized, ranging from 0 (no staining) to 300 (100% positively staining cells in membrane pattern at highest intensity). The h score used the following formula ([1 x (% cells 1+) + 2 x (% cells 2+) + 3 x (%cells 3+). Cancer specific survival was evaluated with PDL1 expression. Multivariate Cox regression was used to identify prognostic factors. Kaplan-Meier curves were plotted to a

Results: We identified 217 patients with USD and 135 with SCC. Overall, the mean age was 68.1±11.4 years. More female patients were present in the SCC cohort (35.6% vs 21.7%, p=0.004). There was no statistically significant difference in age, ECOG performance status, BMI, lymphovascular invasion, smoking history, stage, margin status, lymph node status, or length of follow-up between the groups. 95% of patients had ≥pT2 disease at the time of radical cystectomy. For all three PD-L1 clones (22C3, SP263, and SP142), we found a statistically significant difference in the PD-L1 h score based on histologic subtype, with the mean h score being significantly higher in SCC compared to UCSD. The mean h scores were as follows: clone 22C3 (SCC-35.7, UCSD-13.2, p<0.0001), clone SP263 (SCC-86.9, UCSD-53.5, p<0.0001), and clone SP142 (SCC-14.8, UCSD-8.9, p=0.022). There was a statistically significant difference (p=0.02) in CSS for SCC based on PD-L1_22C3 expression, with a cutoff of ≥70 predicting improved CSS (Figure 1). PD-L1_SP142 expression also showed improved CSS for SCC (p=0.046), with a cutoff of ≥60 predicting i

Conclusions: PD-L1 expression is present in USD and SCC of the bladder but variable based on histologic subtype. PD-L1 expression may predict cancer-specific survival for patients with SCC of the bladder.

455 Molecular Risk Classifier Score and Biochemical Recurrence Risk Are Associated with Cribriform Pattern Type in Gleason 3+4=7 Prostate Cancer

Nancy Greenland[1], Anthony Wong[1], Jeffry Simko[1], Bradley Stohr[1]
[1]*University of California, San Francisco, San Francisco, CA*

Disclosures: Nancy Greenland: None; Anthony Wong: None; Jeffry Simko: None; Bradley Stohr: None

Background: Cribriform patterns have been associated with worse outcomes in prostate cancer. We hypothesized that the expansile cribriform pattern at prostatectomy would be associated with increased scores with a molecular risk classifier and worse biochemical recurrence (BCR) risk.

Design: We included patients who had the Decipher molecular assay, which predicts metastatic risk, performed from January 2016 to March 2020. The prostatectomy slide on which Decipher testing was performed was re-

reviewed in a blinded manner for Gleason score and presence of simple cribriform and expansile cribriform, with expansile cribriform defined as large cribriform acini with greater than 12 lumen spaces and a diameter at least twice that of adjacent normal glands. BCR was defined as two consecutive PSA levels of 0.2 ng/mL or more starting 8 weeks after prostatectomy. Differences in Decipher score were analyzed in a generalized linear model controlling for T and N stage. A multivariable Cox proportional hazards model was performed for BCR-free survival.

Results: Of 337 cases, 118 were Gleason score 3+4=7. The mean Decipher scores in the 3+4=7 cases without cribriform, with simple cribriform, and with expansile cribriform were 0.41, 0.54, and 0.62, respectively (Figure 1). In a multivariable model controlling for T and N stage, compared to cases without cribriform, simple cribriform was associated with a 0.10 increase in Decipher score (p=0.016) and 4.7-fold hazard ratio of BCR (CI 0.47-47.5, p=0.19) and expansile cribriform was associated with a 0.17 increase in Decipher score (p<0.001) and 15.9-fold hazard ratio of BCR (CI 1.9-130.7, p=0.01) (Figure 2).

Figure 1 - 455

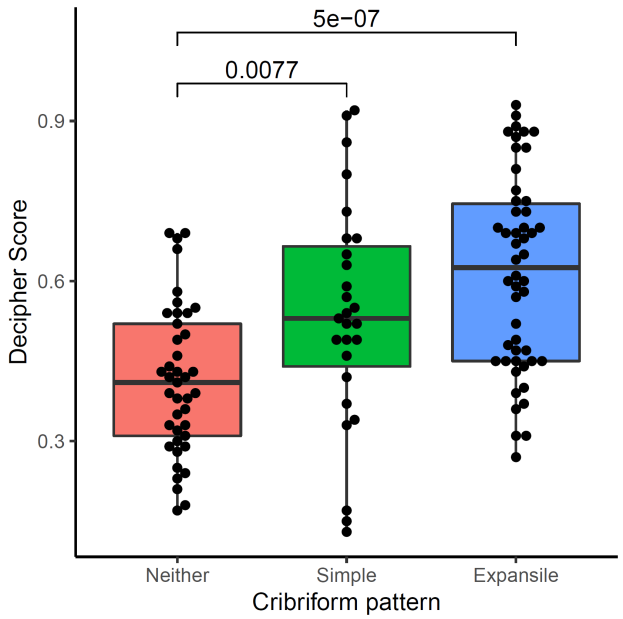

Figure 2 - 455

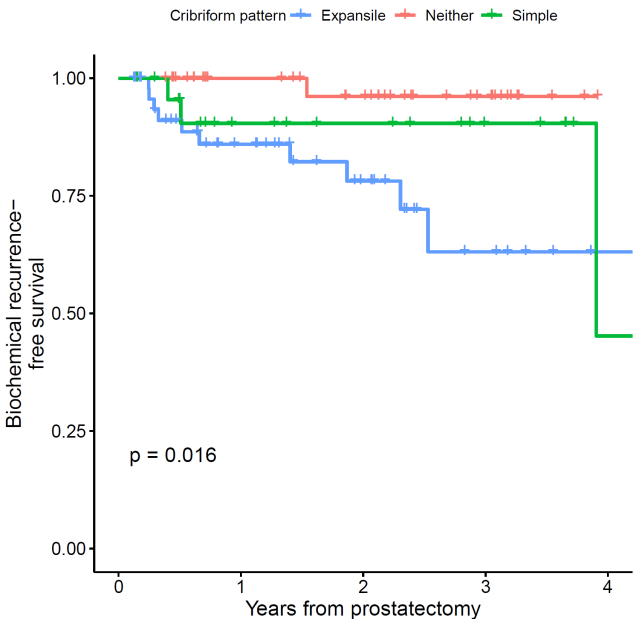

Conclusions: The progression in Decipher score and BCR risk observed with simple versus expansile cribriform patterns supports the theory that expansile cribriform is an aggressive subtype of Gleason pattern 4.

456 Genomic Signatures for Post-Operative Radiation Therapy and Androgen Deprivation Therapy Response in Prostate Cancer: A Precision Medicine Initiative

Abhinav Grover[1], Sheldon Greenfield[2]
[1]Medical College of Wisconsin Affiliated Hospitals, Milwaukee, WI, [2]University of California, Irvine, Irvine, CA

Disclosures: Abhinav Grover: None; Sheldon Greenfield: None

Background: Post-operative radiation therapy (PORT) and androgen deprivation therapy (ADT) combination has been shown to improve outcomes in prostate cancer patients with biochemical recurrence after radical prostatectomy. However, these treatments may be associated with significant detriments in patient-reported quality of life. Currently, there is no routine method to determine which patients may benefit from combining ADT with PORT. Therefore, the aim of this study was to identify demographic, clinical and genetic predictors of PORT and ADT response to help optimize clinical outcomes.

Design: A total of 209 prostate cancer patients were analyzed for factors predicting GRID (genome resource information database) gene expression scores for PORT and ADT response (score = 1-100) using linear

regression. Factors included in the analysis were age, race, stress, comorbidity measured by TIBI-CaP (Total Illness Burden Index–Carcinoma Prostate), androgen receptor signaling and tumor proliferation signaling gene signatures, PSA (prostate specific antigen) levels, and Gleason grade.

Results: African American men had PORT and ADT response scores of 38.8 ± 27.2 and 30.5 ± 25.9 whereas Whites had scores of 31.1 ± 26.9 and 35.3 ± 27.8, respectively based on GRID gene signatures. In a regression analysis, however, decreasing androgen receptor signaling (β = -0.25, p =0.003) and increasing tumor proliferation signaling gene signatures (β =0.25, p =0.002) were significant predictors of genetics of PORT response. Androgen receptor signaling gene signature (β =0.25, p =0.007) was the only significant predictor of genetics of ADT response.

Conclusions: Optimization of PORT and ADT response requires consideration of patient's race, androgen receptor signaling and tumor proliferation signaling gene signatures. The molecular signature for PORT and ADT responses could aid precision medicine initiatives by improving clinical outcomes in prostate cancer patients.

457 Gene Methylation Patterns of Aggressive Chromophobe Renal Cell Carcinoma

Tao Guo[1], Jun Li[1], Khalida Wani[1], Paari Murugan[2], Fadi Brimo[3], Alexander Lazar[1], Pheroze Tamboli[1], Jianhua Zhang[1], Krishna Bhat[1], Kanishka Sircar[1]
[1]The University of Texas MD Anderson Cancer Center, Houston, TX, [2]University of Minnesota, Minneapolis, MN, [3]McGill University, Montréal, Canada

Disclosures: Tao Guo: None; Jun Li: None; Khalida Wani: None; Paari Murugan: None; Fadi Brimo: None; Alexander Lazar: None; Pheroze Tamboli: None; Jianhua Zhang: None; Krishna Bhat: None; Kanishka Sircar: None

Background: The majority of chromophobe renal cell carcinomas (ChRCC) are indolent with a small subset of tumors that are potentially lethal. Determining the behavior of ChRCC is challenging due to the absence of a validated pathologic grading system and the lack of reliable prognostic biomarkers in this tumor type. The Cancer Genome Atlas (TCGA) study on ChRCC suggested that gene methylation patterns may hold promise in predicting the behavior of ChRCC; however, follow up epigenetic studies have not been conducted on aggressive ChRCC. The aim of this study was to characterize the genome wide methylation features of aggressive ChRCC in a clinical setting.

Design: We defined aggressive ChRCC as showing recurrence, metastasis or sarcomatoid features and indolent ChRCC as lacking these attributes. TCGA methylation data from 12 aggressive and 54 indolent ChRCC (Infinium 450K) was examined *in silico* as a discovery cohort. We extracted DNA from FFPE tissues of a multi-institutional validation cohort of 19 aggressive ChRCC cases. Paired tumor and normal samples were subjected to genome wide methylation (Infinium Methylation Epic, Illumina, San Diego, CA). Gene expression analysis of RNA-seq data from TCGA ChRCC cases was also performed.

Results: Among the TCGA discovery cohort, 40824 mapped genes were differentially methylated in aggressive ChRCC whereas the validation cohort showed 9257 differentially methylated genes. In total, 835 genes were shared between the cohorts of which 130 genes also showed differential gene expression among indolent and aggressive ChRCC cases from TCGA. Gene set enrichment analysis showed "hemophilic cell adhesion via plasma membrane adhesion molecules" as the most enriched pathway in aggressive ChRCC based purely on methylation(P=4.8E-31) and the combination of methylation and gene expression (P=7.8E-4). Among aggressive ChRCC, the following candidate genes were identified that were significantly hypermethylated (P< 0.05), resided in promoter regions and showed significantly lower gene expression (P< 0.05): FRAT1, PON3, TMEM171, ZSCAN18, ELAVL3, CYYR1, NEFH, SLC7A14, GLB1L3.

Conclusions: The epigenetic features of ChRCC suggest the deregulation of cell adhesion as a principal pathway to the development of aggressive disease. Using methylation and expression data derived from clinical grade samples, we have identified potential prognostic biomarkers and therapeutic targets for aggressive ChRCC.

458 Loss of MHC Class 1 Expression is Associated with Shorter Progression-Free Survival in Patients with Advanced Urothelial Carcinoma Treated with Immune Checkpoint Inhibitors

Akriti Gupta[1], Stephen Culp[1], Elizabeth Gaughan[2], Anne Mills[1], Helen Cathro[2]
[1]University of Virginia, Charlottesville, VA, [2]The University of Virginia Health System, Charlottesville, VA

Disclosures: Akriti Gupta: None; Stephen Culp: None; Elizabeth Gaughan: None; Anne Mills: None; Helen Cathro: None

Background: Major histocompatibility complex (MHC) class I antigen expression may affect tumor response to immune checkpoint inhibitor (ICI) therapy. Immunoproteasome subunits of MHC class I are down regulated in urothelial carcinoma (UCA), altering tumor recognition by naïve T-cells. Mouse models and rare human studies suggest that MHC class I modulation may play a role in ICI resistance. We set out to examine the relationship between MHC class I/PD-L1 immunohistochemical expression (IHC) and ICI therapy response in advanced UCA patients.

Design: Sequential cases of advanced UCA treated with PD-1 and PD-L1 inhibitors from 2016-2020 were identified through the University of Virginia Cancer Center. IHC for MHC class I (Abcam EMR8-5) and PD-L1 (SP142) was scored as follows: MHC expression, present >80%; incompletely lost 10-80%; and lost <10% nuclear staining. PD-L1 was scored as 1=<5%, 2=5-25%, 3=>25% in both tumor and tumor infiltrating cells (TIC). Progression-free survival (PFS) was defined as increasing size of or new metastasis (MET) on CT or PET imaging within 6 months of ICI therapy.

Results: Of 41 patients, primary material was available in 19, only MET in 11 and both in 11. All but two of 36 patients with evaluable tissue had high-grade UCA. Most were treated with either pembrolizumab or atezolizumab, with three receiving both. Twenty-seven of 36 patients with long-term follow-up have died. Of nine living patients, six have stable advanced disease and three have disease progression. While on CPI treatment, 9 patients had stable disease. There was no significant correlation between MHC class I expression and PD-L1 tumor or TIL expression, in primary or metastatic tissue. Including those patients who died before imaging (n=5), there was no significant difference in PFS with loss of MHC class I expression. In contrast, of those with available imaging (n=36), there was a significant decrease in PFS with incomplete (HR 3.69, p=0.013), but not with complete MHC loss (HR 2.01, p=0.226). (Figure 1).

Figure 1 - 458

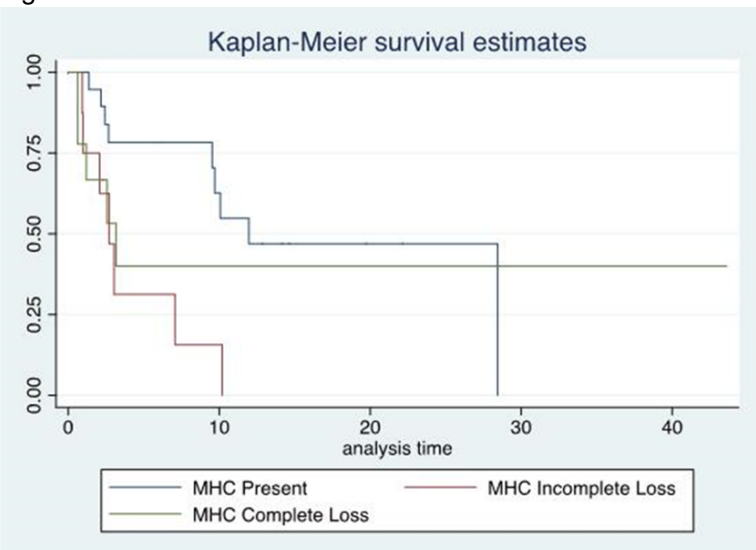

Progression-free survival in patients with available imaging according to MHC Class 1 expression profile. Incomplete Loss – HR 3.69 (1.32, 10.30) p=0.013; Complete Loss – HR 2.01 (0.65, 6.20) p=0.226.

Conclusions: We conclude that incomplete loss, and perhaps also complete loss of MHC class I expression is associated with worse PFS in patients with advanced urothelial carcinoma. No association was found between

MCH class I and PD-L1 expression in either the tumor or TIC. In addition, there was no association between PD-L1 expression in either tumor or TIC, and PFS. The study is limited by small case numbers and single center design, which will be addressed in a larger study.

459 Primary Urothelial Carcinoma of the Ureter without Concomitant Renal Pelvic or Bladder Carcinoma: A Contemporary Clinicopathologic Analysis

Christina Gutierrez[1], Bradley Carthon[2], Shreyas Joshi[2], Adeboye O. Osunkoya[2]
[1]Emory University School of Medicine, Atlanta, GA, [2]Emory University, Atlanta, GA

Disclosures: Christina Gutierrez: None; Bradley Carthon: None; Shreyas Joshi: None; Adeboye O. Osunkoya: None

Background: Primary ureteral urothelial carcinoma (UCa) is relatively uncommon, comprising less than 10% of all urinary tract tumors. However, the majority of cases of ureteral UCa are found concomitantly with other urinary tract tumors. Only small case series and case reports have analyzed the clinicopathological features of primary ureteral UCa without concomitant UCa of the renal pelvis and/or bladder.

Design: A search for cases of primary ureteral UCa without concomitant UCa of the renal pelvis or bladder was made through our urologic pathology files and the senior author's expert consult cases. Clinicopathologic parameters including extent of invasion, lymphovascular invasion (LVI), variant histology, presence of UCa in situ, inverted growth pattern, and clinical follow-up information was obtained.

Results: The study included ninety-seven cases. Mean patient age was 70 years (range: 38-90 years). The preponderance of cases was from males (77%; 75/97). Thirty-nine cases (40%; 39/97) had invasion which consisted of 15 cases with lamina propria invasion (15%; 15/97), 9 with muscularis propria invasion (9%; 9/97), 14 showed periureteral soft tissue invasion (14%; 14/97), and 1 invaded through soft tissue into the seminal vesicle (1%; 1/97). LVI was present in 17 cases (18%; 17/97). Ten cases (10%, 10/97) showed variant histology including 2 cases with micropapillary UCa. UCa in situ was present in 18 cases (19%; 18/97). Nine cases (9%; 9/97) had an inverted growth pattern. Clinical follow-up data was available for 80 patients, mean 35 months (range: 1-206 months). Metastatic UCa developed in 28 patients (35%; 28/80), 20 of which had invasive disease at presentation (71%; 20/28). Of the 17 patients who died of disease (21%; 17/80), 12 of them initially presented with invasive UCa (71%; 12/17).

Conclusions: This is one of the largest studies to date of primary ureteral UCa without concomitant UCa of the renal pelvis or bladder. Although more patients had non-invasive UCa, the likelihood of poor outcomes in patients with invasive disease is higher than typically seen at other sites of the urinary tract. These findings further emphasize the importance of early recognition of these tumors, in view of the relatively high preponderance of advanced disease and mortality in a subset of these patients.

460 Disparities in Tumor Microenvironment : A Detailed Morphologic and Molecular Evaluation of Prostate Cancer in Men of African Descent

Kareem Hosny[1], Sahar Farahani[2], Yan Xiang[3], Abhishek Shah[3], Timothy Rebbeck[4], Shivanshu Awasthi[5], Kosj Yamoah[5], Anders Berglund[5], Kevin Trowell[3], Brittney Imblum[3], Priti Lal[6]
[1]Pennsylvania Hospital of the University of Pennsylvania Health System, Philadelphia, PA, [2]Renaissance School of Medicine at Stony Brook University, Stony Brook, NY, [3]Hospital of the University of Pennsylvania, Philadelphia, PA, [4]Dana-Farber Cancer Institute, Harvard Cancer Center, Boston, MA, [5]H. Lee Moffitt Cancer Center & Research Institute, Tampa, FL, [6]University of Pennsylvania, Philadelphia, PA

Disclosures: Kareem Hosny: None; Sahar Farahani: None; Yan Xiang: None; Abhishek Shah: None; Timothy Rebbeck: None; Shivanshu Awasthi: None; Kosj Yamoah: None; Anders Berglund: None; Kevin Trowell: None; Brittney Imblum: None; Priti Lal: None

Background: Tumor microenvironment (TME) plays an important role in the outcomes of many cancers and directs the selection of immune based treatments. Pre-existing, adaptive or post treatment immune response are not included in any of the algorithms, for determination of treatment or for calculating prognosis. Amongst GU

cancers, prostate cancer is considered pauci immune and TME of prostate cancer is not fully understood. Furthermore, it is now well documented that not only presence or absence, but also spatial & contextual arrangement of tumor infiltrating lymphocytes (TILs) are important determinants of outcome. We sought to acquire an in-depth understanding of TME in prostate cancer, along with racial differences and morphologic associations. The ultimate goal of the study is to use this immune signature to identify patients who may be candidates for newer treatment modalities.

Design: A total of 132 stage matched prostate cancer patients were evaluated of which 50 were African American (AA) and 82 were of European origin (EAM). A single most representative slide was scanned using Aperio software, and then reviewed for presence of tertiary lymphoid structures (TLS) in the peritumoral (PTTLS) and intratumoral (ITTLS) compartments using Q-Path software tools. Additionally, for AA subgroup, TLS, small cribriform, large cribriform, intraductal and ductal components was correlated with Affymetrix based expression analysis of select immune markers including CD3, CD4, CD8, IFNA1, IFNA2, IFNG, PDCD1, CD274, cTLA4, TCF7, LAG3, HAVCR2, IFITM3.

Results: AA cases revealed an average of 1.72 PTTLS (STDV 2.2), EAM cases revealed 0.93 PTTLS (STDV 1.49). This difference was statistically significant using both 1 tailed T test as well as 2 tailed T test with p values of 0.01 and 0.03 respectively. AA cases revealed an average of 5.92 ITTLS (STDV 7.084), while EAM cases revealed an average of 9.12 ITTLS aggregates (STDV 10.5). This difference was statistically significant using both 1 and 2 tailed T test with p values of 0.02 and 0.04 respectively.

Neither aggregated surface area of ITTLS, nor the aggregated number of lymphocytes, reveal statistically significant difference is size.

Different morphologic features of prostate cancer were associated with varying immunologic profiles as obtained from the affymetrix data (Table 1)

Comparison of TLS characteristic EAM vs AA	T test pValue
PTTLS number of clusters	0.01
PTTLS size	0.04
ITTLS number of clusters	0.02
ITTLS size	0.23
AA Morphologic characteristics and Immune signature	
Poorly formed glands associated with CD4	0.02
Small cribriform associated with CD3E and IFITM3	0.04 &0.03
Large cribriform (present absent) associated with IFNG	0.02
Intraductal (present absent) associated with CD3E	0.03
Ductal (present absent)	Did not reach statistical significance
Tertiary pattern 5(present absent)associated with IFITM3	0.02

Conclusions: 1) A subset of prostate cancer reveal brisk lymphocytic infiltrates, with TLS formation.

2) The distribution of TILs reveals significant differences in AA and EAM men within stage matched prostate cancer cohort

3) Morphologic characteristics of prostate cancer influence the TME, and need to be studied in depth

4) Consideration of TME together with morphology may help develop a future model for patient management with newer treatment modalities, such and immune based therapy.

461 Improving the Quality Fresh Tissue Procurement and FFPE Tissue: Patient-Specific 3D Molds with MRI Co-Registered Slicing Guides

Wei Huang[1], David Rutkowski[1], Alejandro Roldán-Alzate[1], Shane Wells[2], Brian Johnson[1], David Jarrard[1], Lang Joshua[2], Steve Cho[2], Christo Kyriakopoulos[2]
[1]University of Wisconsin, Madison, WI, [2]University of Wisconsin School of Medicine and Public Health, Madison, WI

Disclosures: Wei Huang: None; Shane Wells: None; Steve Cho: *Consultant*, Progenics Pharmaceuticals; *Consultant*, Blue Earth Diagnostics; *Grant or Research Support*, GE HealthCare; *Consultant*, Radmetrixs; *Grant or Research Support*, Advanced Accelerator Applications

Background: Radiology-pathology correlation studies demand prostate slicing co-registered with axial oblique MRI imaging planes. Current grossing techniques fail to meet this requirement and do not provide quality fresh prostate tissue procurement for personalized medicine. Moreover, the prostate is often inadequately fixed due to turn-around-time pressure. Therefore, the quality of formalin-fixed, paraffin-embedded (FFPE) tissues often is suboptimal, leading to poor histology and artificial variability in downstream biomarker analysis. A patient-specific device providing stability and accuracy for cutting fresh prostates is needed.

Design: 3D mold design and fabrication: 18F-DCFPyL prostates specific membrane antigen (PSMA) positron emission tomography (PET)/MRI was performed on patients before and after therapy. The axial oblique T2-weighted prostate MRI sequences were contoured by an experienced abdominal radiologist. Slicing guides at 2.5mm increments, precisely co-registered to axial oblique T2-weighted MRI slices were incorporated into patient-specific 3D models that were fabricated with a photopolymer resin in a steriolothography additive manufacturing machine (Figure 1A-C). The estimated cost for making a patient-specific mold was $120.

Cutting fresh prostate with a 3D mold: The mold was sterilized with a quick dipping in 75% alcohol and followed by 30-minute UV light radiation in a biosafety hood. After the prostate was weighed, measured and inked, the apex and bladder neck margins were removed. The prostate was then placed in the in the 3D mold with appropriate alignment and cut with a tissue slicer blade along the slots of the mold (Figure 1D).

Results: Using 3D molds, we cut fresh prostates into 2.5 mm slices, ranging from 10-18 slices co-registering with MRI imaging planes (Figure 2A). Odd numbered slices, the last slice and the seminal vesicles were retained, laid on dry paper towels (Figure 2B) between two porous polyethylene plates and secured, and then immersed in 10% neutral formalin (Figure 2C) for fixation. Even numbered slices were used for research. Evenly well fixed whole mount tissue blocks and quality tissue sections (Figure 2D) were produced for microscopic examination.

Figure 1 - 461

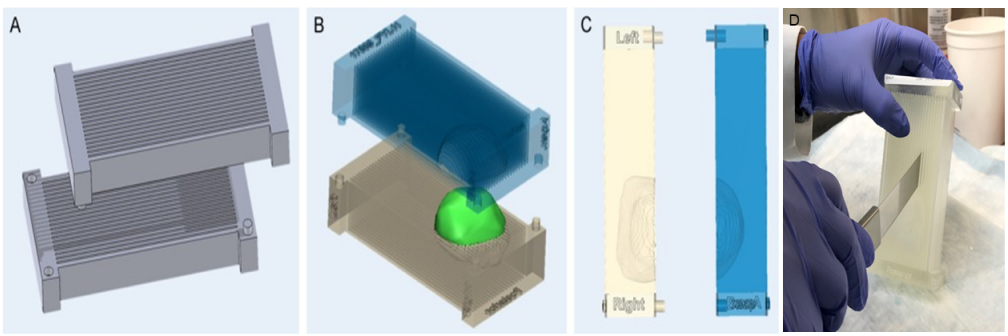

Figure 1. 3D mold design (A, B and C) and application (D)

Figure 2 - 461

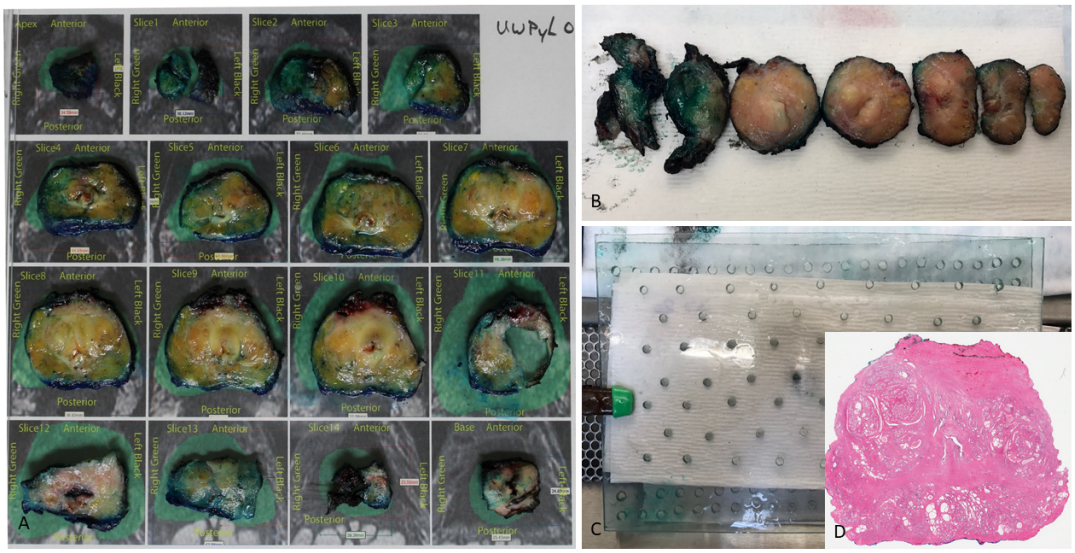

Figure 2. Fresh prostate slices produced using a 3D mold, co-registering with MRI imaging planes (A) and prepared for fixation (B and C), A prostate whole mount H&E section (D).

Conclusions: 3D molds enable pathologists to cut prostate fresh procuring quality tissue for PCa research and shorten fixation time while improving the quality of FFPE tissue for histology and downstream biomarker analysis, especially for pathology-radiology correlation studies.

462 SATB2 Expression in Renal Cell Carcinoma (RCC) is Infrequent and Specific for Proximal Tubular Origin

Robert Humble[1], Nicholas Caldwell[1], Ibrahim Abukhiran[1], Anand Rajan KD[1], Sarag Boukhar[1]
[1]*University of Iowa Hospitals & Clinics, Iowa City, IA*

Disclosures: Robert Humble: None; Nicholas Caldwell: None; Ibrahim Abukhiran: None; Anand Rajan KD: None; Sarag Boukhar: None

Background: SATB2 (special AT-rich sequence-binding protein 2) immunohistochemistry (IHC) is currently used as a marker of colorectal origin. However, low levels of RNA expression have been demonstrated in kidney tissue, primarily in proximal tubules. Few prior studies have demonstrated decreased SATB2 expression by RT-PCR, Western blot, and IHC in clear cell renal cell carcinoma (ccRCC). Here we utilize digital image analysis (DIA) to investigate SATB2 IHC expression in a large RCC cohort of multiple histologic subtypes. Ki-67 proliferation index and p53 expression were also assessed.

Design: SATB2, Ki-67, and p53 IHC were performed on tissue microarrays (TMAs) from 386 RCC cases between 2015 and 2019 (371 patients; 245 male and 126 female). Slides were digitally scanned and Halo (Indica labs, NM) DIA was utilized to determine IHC positivity. H-score was calculated according to the following formula: H-Score= [(strong ITC% X 3) + (moderate ITC% X 2) + (weak ITC%)]. Fisher's exact, Mann-Whitney tests, and one-way ANOVA were used with $p<0.05$ considered significant.

Results: SATB2 was positive in 5.2% (20 of 386) of renal cell carcinomas (RCC) included. The 20 SATB2 positive cases (4 F, 16 M) were 55% papillary, 40% clear cell, and 5% other, with significant correlation between SATB2 positivity and histologic subtypes ($p<0.001$). SATB2 positivity was not significantly associated with tumor grade, stage, size, focality, or presence of metastases in our cohort. There was a significant correlation between Ki-67 H-score and histologic subtype ($p<0.0001$) with chromophobe RCC demonstrating the highest mean H-score. In addition, there were significant associations with Ki-67 H-score with WHO/ISUP Grade ($p<0.001$) and presence of metastatic disease ($p = 0.0014$). p-53 H-score was only significantly associated with histologic type ($p<0.0001$).

Expression of SATB2, Ki-67, and p53 in relation to clinicopathologic variables

Category	Sub-category (n)	SATB2+ n (%)	p	SATB2+ H-Score (SD)	p	Ki-67 H-Score (SD)	p	p53 H-Score (SD)	p
Histologic Type	Chromophobe (24)	0 (0)	<0.0001	NA	0.5611	19 (26)	<0.0001	2 (5)	<0.0001
	Clear Cell (269)	8 (3)		10 (6)		8 (10)		2 (6)	
	Clear Cell Papillary (9)	0 (0)		NA		2 (1)		1 (1)	
	Mucinous tubular and spindle cell carcinoma (5)	0 (0)		NA		1 (0)		5 (8)	
	Papillary (61)	11 (18)		18 (22)		7 (9)		8 (9)	
	Other* (18)	1 (6)		5 (0)		7 (11)		3 (4)	
WHO/ISUP Grade	1 (15)	1 (7)	0.8489	7 (0)	0.2031	6 (9)	<0.0001	1 (1)	0.1489
	2 (154)	10 (6)		13 (17)		5 (6)		3 (5)	
	3 (153)	8 (5)		18 (18)		8 (11)		4 (8)	
	4 (36)	1 (3)		5 (0)		13 (14)		5 (13)	
p Stage	pT1 (234)	15 (6)	0.589	16 (19)	0.8012	7 (10)	0.1336	3 (6)	0.5441
	pT2 (35)	2 (6)		9 (1)		5 (7)		3 (6)	
	pT3 (99)	3 (3)		8 (4)		11 (16)		4 (9)	
	pT4 (6)	0 (0)		NA		22 (24)		0 (0)	
Focality	Multifocal (34)	3 (9)	0.404	44 (31)	0.0719	8 (15)	0.1816	3 (7)	0.1029
	Unifocal (352)	17 (5)		9 (5)		8 (11)		3 (7)	
Metastases	Present (56)	1 (7)	0.3102	5 (0)	NA	12 (16)	0.0014	3 (7)	0.5685
	Not present (330)	19 (6)		15 (17)		7 (10)		3 (6)	

*Includes tubulocystic RCC, tuberous sclerosis-associated RCC, Xp11 translocation RCC, RCC unclassfied, and mixed RCC.

Conclusions:

1. Low expression of SATB2 can be seen in RCC but is strictly seen in clear cell and papillary renal cell carcinoma.
2. High Ki-67 H-score is significantly associated with RCC histologic subtype (highest in chromophobe RCC), higher WHO/ISUP grade, and presence of metastatic disease.

463 PRAME is Preferentially Expressed by Seminoma Among Testicular Germ Cell Tumors

Robert Humble[1], Matthew Gosse[1], Andrew Bellizzi[1]
[1]*University of Iowa Hospitals & Clinics, Iowa City, IA*

Disclosures: Robert Humble: None; Matthew Gosse: None; Andrew Bellizzi: None

Background: PRAME (PReferentially expressed Antigen in MElanoma) is a cancer/testis (CT) antigen expressed by cutaneous and ocular melanomas, with expression in normal tissues largely limited to testis. CT antigens are highly immunogenic and represent attractive immunotherapy targets. PRAME immunohistochemistry (IHC) has recently emerged as a positive melanoma marker in the differential diagnosis with challenging melanocytic nevi and nodal nevi. There are limited data on PRAME expression in testicular germ cell tumors, with one study reporting preferential staining of seminomas in a cohort of 69 seminomas and 33 embryonal carcinomas (PMID: 2771500). We sought to further characterize PRAME expression in testicular germ cell tumors with potential pathogenetic, diagnostic, and therapeutic implications.

Design: PRAME IHC (clone EPR20330) was performed on tissue microarrays (TMAs) constructed from 198 orchiectomies with the following histologies represented: normal testis (n=12), germ cell neoplasia in situ (GCNIS; 15), seminoma (92), embryonal carcinoma (53), yolk sac tumor (25, including 4 pediatric), immature teratoma (9), mature teratoma (11), and choriocarcinoma (10). TMAs were also constructed from 27 melanomas. IHC was assessed for intensity (0-3+) and extent (0-100%) of staining, and an H-score was calculated (0-300). Two-tail Fisher's exact, Mann Whitney, and Kruskal-Wallis tests were used with $p<0.05$ considered significant.

Results: PRAME was strongly expressed by 100% of normal germ cell and GCNIS cases. Among tumors, PRAME was nearly always (92%) positive in seminoma, typically at least moderately strongly so. It was often (52%), though weakly, expressed by yolk sac tumor, and only rarely, weakly expressed by other tumor types. Median H-scores were different for normal germ cell, GCNIS, and seminoma case (p=0.015). Although the frequency of positivity was similar in melanoma and seminoma (p=1), melanomas were more strongly expressing (p=0.0009). One outlier strongly expressing yolk sac tumor (H=167) occurred in a 1-year-old. Detailed data are presented in the Table.

Relative expression of PRAME in normal testis, germ cell tumors, and melanoma

	n	% PRAME-positive	Mean (Median) H-score (if positive)
Normal testis	12	100	240 (248)
GCNIS	15	100	224 (230)
Seminoma	92	92	167 (165)
Embryonal carcinoma	53	13	11 (5)
Yolk sac tumor	25	52	50 (43)
Immature teratoma	9	22	9 (9)
Mature teratoma	11	9	13 (13)
Choriocarcinoma	10	30	22 (15)
Melanoma	27	93	236 (255)

Conclusions: Although PRAME is highly expressed by melanoma it is not specific and should not be used to support a diagnosis of melanoma in the context of a high-grade tumor of uncertain lineage. PRAME expression by normal testis, GCNIS, and seminoma supports a developmental link between these 3 tissues. Downregulation of PRAME is associated with germ cell and somatic differentiation.

464 Grade Variation in Radical Prostatectomy (RP) with Assessment of Each Tumor Nodule (TN) Versus Global Grading

Oleksii Iakymenko[1], Isabella Lugo[2], Ivan Nemov[3], Oleksandr Kryvenko[3]
[1]Jackson Memorial Hospital, Miami, FL, [2]University of Miami, Davie, FL, [3]University of Miami Miller School of Medicine, Miami, FL

Disclosures: Oleksii Iakymenko: None; Isabella Lugo: None; Ivan Nemov: None; Oleksandr Kryvenko: None

Background: Prostate cancer (PC) at RP can be graded globally per case or individual TN can be graded. We assessed grade change in multifocal PC in RP when case grade was assigned based on a TN with the highest Grade Group (GG) vs global grade derived from a sum of all TNs graded together.

Design: From 1,629 entirely submitted and centrally reviewed RPs we culled all treatment naïve multifocal PCs. We determined tumor volume in cm³ and recorded percent of Gleason pattern 4 and 5 (GP4% and GP5%) in each TN. Gleason score (GS) and GG were assigned to each separate TN. Global GS was generated by combination of Gleason pattern volumes as if all available patterns constituted a single tumor. We documented the presence of extraprostatic extension (EPE), seminal vesicle invasion (SV+), positive surgical margins (SM+) for each TN and positive lymph nodes (LN+) for a case. Statistical assessment was performed in R 4.0.2 and included chi-square and binomial regression analysis.

Results: We selected 776 men with multifocal PC including 402 GG2, 193 GG3, 31 GG4, 150 GG5 in the highest-grade TN. The global grade model generated 471 GG2, 152 GG3, 58 GG4, and 95 GG5 PC. We observed GP4% <5% in 67/313 men with original GG2 (GP4%>=5) and one original GG3 (GP4%=70) which could be recorded as GG1 PC with tertiary pattern 4 according to some guidelines; GP5% <5% in 4/10 original GG4 (358) and 10/150 GG5 cases. 32% (118/374) of GG3-5 were globally downgraded by 1 GG, 7% (13/181) of GG4-5 changed globally by 2 GG, and 2% (3/150) GG5 were downgraded as GS347 (GG2) with tertiary pattern 5. The risk of GG change inversely correlated with the highest grade TN volume (OR=0.5, p<0.0001). Although globally graded groups demonstrated increased EPE, SV+, SM+, LN+ comparatively to corresponding GGs, the difference lacked

statistical significance (all p>0.05). One global GS347 with tertiary pattern 5 from original GG5 (459) demonstrated LN+ and none of the original GG2 cases had LN+.

Conclusions: Global grading leads to a lower grade per case compared to individual TN grading. Tumor volume of the highest grade TN inversely correlates with the risk of downgrading. Although both approaches demonstrate similar incidence of associated adverse surgical outcomes for corresponding GS, this grade diversity likely introduces inconsistency in multi-institutional databases diminishing reproducibility and interchangeability of the research and clinical data.

465 Morphologic Variation of Large Cribriform Glands Stratifies the Likelihood of Intraductal Prostatic Carcinoma vs Invasive Cancer

Oleksii Iakymenko[1], Sabrina Oneto[2], Laurence Briski[3], Merce Jorda[2], Oleksandr Kryvenko[2]
[1]Jackson Memorial Hospital, Miami, FL, [2]University of Miami Miller School of Medicine, Miami, FL, [3]University of Miami Health System

Disclosures: Oleksii Iakymenko: None; Merce Jorda: None; Oleksandr Kryvenko: None

Background: Immunohistochemical (IHC) work up to differentiate intraductal prostatic carcinoma (IDC) from invasive prostate cancer (PC) featuring large cribriform morphology is recommended when the result could change the grade. We assess morphologic features of large cribriform glands to differentiate IDC from invasive PC and to narrow down indications for IHC.

Design: We prospectively selected all prostate cancers (PC) featuring large cribriform glands. The latter defined by the presence of >=12 lumina and size that exceeds at least two times a normal gland. We distinguished large glomeruloid morphology by the presence of a central cribriform nest encased into dilated cytologically malignant gland and attached to its wall in 1 or 2 places. We excluded prostatic ductal carcinoma, fused glands, glands with perineural invasion, mucinous fibroplasia, and extraprostatic extension. We analyzed each gland for the presence of 1) pushing borders, 2) comedonecrosis, 3) fine intratumoral blood vessels, 4) circumferential retraction artifact, 5) extraglandular mucin, 6) stromal desmoplasia, and 7) glomeruloid architecture. PIN4 IHC cocktail was performed for each case.

Results: We analyzed 826 individual large cribriform glands from 77 specimens (64 radical prostatectomies and 13 biopsies) with Grade Group 2-5 PC. All large cribriform glands with glomeruloid architecture (403) and large cribriform glands with circumferential retraction artifact (18) were invasive PC. Combinations of fine intratumoral blood vessels with retraction artifact (53), extraglandular mucin (12), comedonecrosis (1), and stromal desmoplasia (1) around large cribriform glands were all invasive PC. Ninety-two percent of large cribriform glands with fine intratumoral blood vessels (167/182) were invasive. Large cribriform glands with pushing borders were IDC in 82% (121/147) of cases. All large cribriform glands with comedonecrosis (9) represented IDC.

Conclusions: All large cribriform glands with glomeruloid architecture, circumferential retraction artifact, and combinations of fine intratumoral blood vessels with retraction artifact, extraglandular mucin, comedonecrosis, and desmoplasia represent invasive PC. A majority of large cribriform glands with fine intratumoral vessels represents invasive PC. Large cribriform glands demonstrating a pushing border with or without comedonecrosis are IDC in majority of cases. These observations have important implications for appropriate grading as well as selective usage of IHC in PC.

466 Growth and Differentiation Factor 15 (GDF15) and NFκB Expression in Benign Prostatic Biopsies Are Associated With Risk of Subsequent Prostate Cancer Detection

Kenneth Iczkowski[1], Benjamin Rybicki[2], Sudha Sadasivan[3], Yalei Chen[3], Watchareepohn Palangmonthip[4], Nilesh Gupta[3], Sean Williamson[5], Dhananjay Chitale[2], Oleksandr Kravtsov[6], Kanika Arora[3], Kevin Bobbitt[3], Deliang Tang[7], Andrew Rundle[8]
[1]Medical College of Wisconsin, Milwaukee, WI, [2]Henry Ford Hospital, Detroit, MI, [3]Henry Ford Health System, Detroit, MI, [4]Chiang Mai University, Muang, Thailand, [5]Cleveland Clinic, Cleveland, OH, [6]Indiana University, Indianapolis, IN, [7]Columbia University Mailman School of Public Health, New York, NY, [8]Columbia University Irving Medical Center, New York, NY

Disclosures: Kenneth Iczkowski: None; Benjamin Rybicki: None; Sudha Sadasivan: None; Yalei Chen: None; Watchareepohn Palangmonthip: None; Nilesh Gupta: None; Sean Williamson: None; Dhananjay Chitale: None; Oleksandr Kravtsov: None; Kanika Arora: None; Kevin Bobbitt: None; Deliang Tang: None; Andrew Rundle: None

Background: Growth and differentiation factor 15 (GDF-15), also known as macrophage inhibitory cytokine 1 (MIC-1), may act as both a tumor suppressor and promotor in prostate cancer and, by regulating NFκB and macrophage signaling, serve as a promoter of early carcinogenesis.

Design: Benign biopsies with 508 cases (subsequent cancer dx.) versus 508 control pairs were matched on date, age, and race, nested within a historical cohort of 10,478 men. To determine how the expression of these two inflammation-related cytokines affects prostate cancer susceptibility, dual immunostaining of benign prostatic biopsies for GDF15 and NFκB was done [**Figure 1**]. Whole slide scanning of NFκB and GDF15 stained matched slides was performed on a platform. Glandular regions were annotated and the annotated regions were then processed using a customized script developed to estimate the intensity and percent of reactivity based on positively-stained pixels.

Results: GDF15 and NFκB expression were positively correlated (r=0.39; p<0.0001); both were significantly lower in African American (AA) compared with white men.In models that adjusted for each marker and other prostate cancer risk factors, the odds ratio (OR) for NFκB expression in white men was statistically significant for decreased risk, OR=0.86; p=0.02; 95% confidence interval (CI) = 0.75 - 0.98, while GDF15 expression was associated with a nominally increased risk, OR=1.08; p=0.11; 95% CI = 0.98 - 1.20. When modeling expression levels by quartiles, the highest quartile of NFκB expression was associated with about a 40% reduction in prostate cancer risk (OR=0.57; p=0.06; 95% CI = 0.32-1.02). In stratified models, NFκB had the strongest negative association with subsequent cancer in non-aggressive cases (p=0.05), older men (p=0.03) and in case-control pairs with longer follow-up (p=0.04). GDF15 expression had the strongest positive association with prostate cancer risk in older men (p=0.01).

Among less-aggressive cases in AA men, NFκB and GDF15 inverse associations with prostate cancer were most stark – the OR for a linear trend in NFκB association was 0.60 whereas the comparable OR for GDF15 was 1.20.

In prostatic biopsies with chronic inflammation, GDF15 expression was significantly lower than in biopsies with no inflammation (p=0.001). Examining grade and extent of chronic inflammation, GDF15 expression showed an inverse linear trend with worsening inflammation (p=0.002). There was no suggestion of a modifying effect of inflammation on cancer risk associated with either marker.

Figure 1 - 466

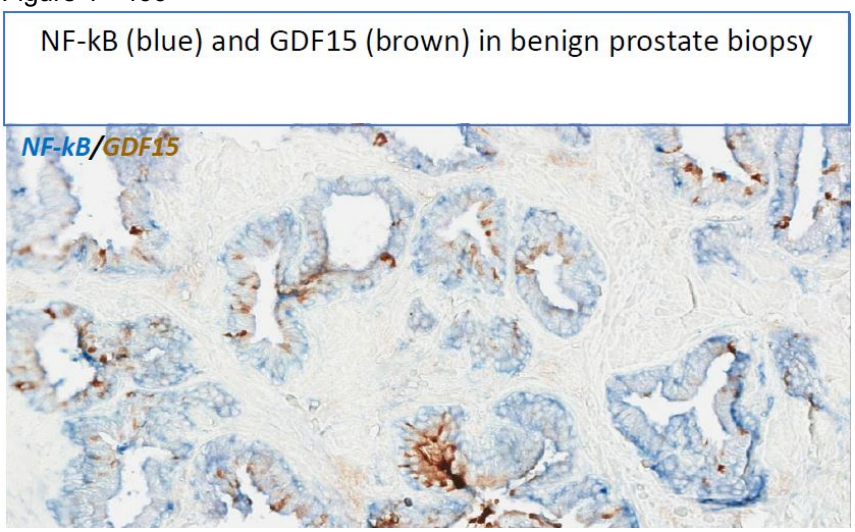

Conclusions: Although NFκB and GDF15 expression are positively correlated in benign prostatic biopsies, these 2 cytokines appear to exert opposite effects on prostate tumor development, especially in older AA men and AA men

with less aggressive prostate cancer. GDF15 may repress chronic inflammation in the benign prostate, extending our prior finding [PMID:25327758] though this did not modify cancer risk.

467 In Gleason 3+4 Prostate Cancer, Is Cribriform Growth More Influential Than Percent Gleason 4?

Kenneth Iczkowski[1], Rebecca Czaja[1], Sergey Tarima[1], Ruizhe Wu[2]
[1]Medical College of Wisconsin, Milwaukee, WI, [2]Medical College of Wisconsin, Milwaukee, WA

Disclosures: Kenneth Iczkowski: None; Rebecca Czaja: None; Sergey Tarima: None; Ruizhe Wu: None

Background: The International Society of Urological Pathology (ISUP) grading consensus conference of 2019 endorsed specifying the presence of cribriform (C) architecture in reporting Gleason (G4) prostate cancer [PMID:32459716] because of abundant evidence supporting C's aggressive nature.

The relative effect of C presence versus the percentage of G4 within Gleason 3+4, Grade group (GG)2 is uncertain. A prior study was done in GG2, but it combined intraductal cancer with C architecture [PMID:28530220].

Design: Database search (11/2013 to 10/2017) included 194 men's biopsies with GG2 with or without C (glomeruloid not counted as C) and GG3 (only) without C.

Clinicopathologic features were assessed on chart review and slide review. 173 cases had follow-up including 147 GG2 (15/147 or 10% had C) and 26 GG3. Effects of total tumor specimen involvement (TSI), %GP4, and growth patterns like C were assessed by Cox proportional hazards model stratified on prostatectomy (n=90), radiotherapy (n=61) and watching waiting (n=22).

Results: Median follow-up duration was 3.32 years (range 1.90-6.18), and biochemical failures in the above 3 cohorts numbered 9 (9/90; 10%), 5 (5/61; 8%), and 13 (13/22; 59%) respectively. In GG2, the comparison of C to non-C (including glomeruloid) conferred a hazard ratio (HR) of 1.51 (p = 0.48). If glomeruloid were excluded from non-cribriform, hazard ratio was 1.38. When evaluating the cohort followed with watchful waiting only, the absence of C conferred a HR of 0.38 (p = 0.086). Among all cases (GG2+ GG3, n=173), the HR for C pattern was .97; and the remainder of the comparisons based on age, TSI, and fraction of cores were not significant.

Comparison	Hazard Ratio (95% CI)	P
All cases (Events/Total N = 29/173, 17%)		
% Gleason 4	1.01 (1.00-1.03)	0.16
GG2, C vs. non-C (including G)	1.51 (0.48-4.79)	0.48
GG2, C vs. non-C only	1.38 (0.43-4.49)	0.32
GG2 or 3, C vs. non-C (including G)	0.75 (0.34-1.64)	0.46
GG2 or 3, C vs. non-C only	0.61 (0.29-1.29)	0.19
Watchful waiting (Events/N = 13/22, 59%)		
% Gleason 4	1.01 (0.98-1.04)	0.41
GG2 or 3, C vs. non-C (including G)	0.61 (0.19-2.00)	0.42
GG2 or 3, C vs. non-C only	0.38 (0.13-1.15)	0.086

Abbreviations: C – cribriform pattern; G – glomeruloid pattern; GG – Grade Group

Conclusions: The HRs for all groups comparing C with non-C (including glomeruloid) showed no significant difference in rate of biochemical failure, but it neared significance within the watchful waiting subset.

It is probably not feasible to detect differences based on C versus %G4 in GG2 because their current outcomes are so favorable (only 22 failures among 147). Also, C is inherently less frequent in GG2 (it was just 10% in this study). Prior studies, including our own, have had much higher-grade mixtures of cases with more Gleason 4 and 5 thus more failures and more C; many such studies also were enriched for failures (1:1 match with non-failures). An added limitation of the current study was use of biopsy tissue, not prostatectomy; biopsy samples introduce sampling variation, but they hold special relevance since they are the basis of treatment decisions.

468 PUNLMP and Low-Grade Noninvasive Papillary Urothelial Carcinoma Are Indistinguishable by Prognosis and Molecular Subtype

Chelsea Jackson[1], Lina Chen[2], Celine Hardy[2], Gottfrid Sjödahl[3], D. Siemens[2], David Berman[2]
[1]Queen's University, Kingston Health Sciences Centre, Kingston, Canada, [2]Queen's University, Kingston, Canada, [3]Lund University, Lund, Sweden

Disclosures: Chelsea Jackson: None; Lina Chen: None; Celine Hardy: None; Gottfrid Sjödahl: None; D. Siemens: None; David Berman: None

Background: Papillary urothelial neoplasm of low malignant potential (PUNLMP) is a controversial diagnostic category with papillary architecture and increased urothelial thickness but without nuclear atypia or architectural disorder. Low-grade noninvasive papillary urothelial carcinomas (TaLGs) are similar papillary lesions with mild but noticeable architectural and/or cytologic atypia. However, recent publications argue that the diagnostic distinction between PUNLMP and TaLG is subjective, unreliable, and lacks clinical relevance. Furthermore, there is considerable controversy regarding potential molecular and prognostic differences between PUNLMP and TaLG. Molecular subtyping yields important insights into the pathogenesis of bladder cancers and their precursors, but has not been previously explored in PUNLMP lesions. We recently validated a three-antibody clinical grade immunohistochemistry (IHC) assay for non-muscle invasive bladder cancer that identified 3 molecular subtypes: Urothelial (URO), KRT5+ Uro, and Genomically Unstable (GU). Here we use molecular subtypes to investigate whether PUNLMPs and TaLG cancers represent similar or different pathways in urothelial carcinogenesis. Furthermore, we compare clinical outcomes of PUNLMP and TaLG patients.

Design: GATA3, KRT5 and p16 IHC was conducted on tissue microarrays representing 54 PUNLMPs and 184 TaLGs, sampled in duplicate. Staining intensity, localization and prevalence was scored using visual and digital image analysis.

Results: PUNLMPs and TaLGs showed similar recurrence-free survival (Figure 1, p-value = 0.41). Unsupervised hierarchical clustering of a validated IHC algorithm revealed the same three molecular subtypes in similar proportions (Figure 2, Table 1). When stratified by molecular subtypes, PUNLMP and TaLGs demonstrated similar recurrence-free survival and remained relatively stable over multiple recurrences.

Table 1: Summary of PUNLMP and TaLG samples by molecular subtype

Subtype	PUNLMP (n=54) (%)	TaLG (n=184) (%)	Total (n=238) (%)
URO	12 (22)	74 (40)	86 (36)
URO-KRT5+	33 (61)	71 (39)	104 (44)
GU	9 (17)	39 (21)	48 (20)

Figure 1 - 468

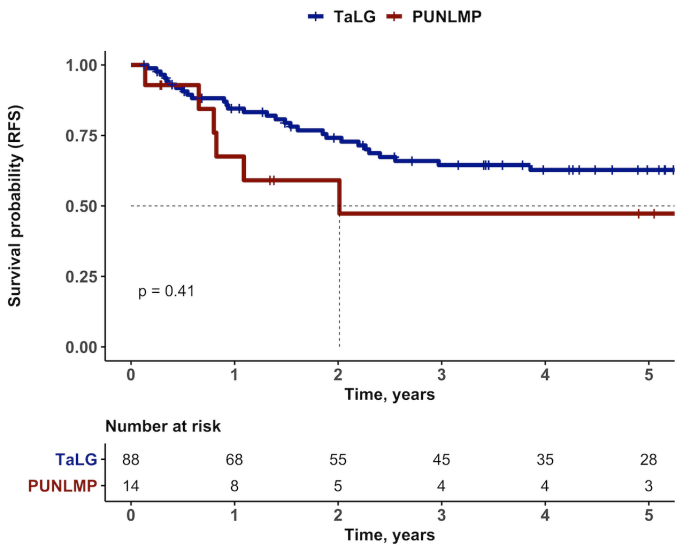

Figure 2 - 468

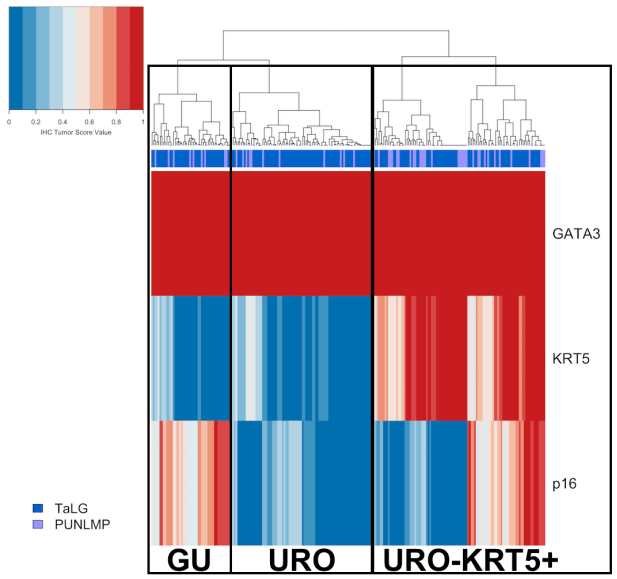

Conclusions: As we found no prognostic or molecular differences between PUNLMP and TaLG cancers, we join previous investigators who have proposed that these two diagnostic categories be merged.

469 Post-Chemotherapy Metastatic Testicular Germ Cell Tumors (mTGCTs): A Clinicopathological, Immunohistochemical (IHC) and Molecular Characterization of 54 Cases

Liwei Jia[1], Rajal Shah[1]
[1]*UTSouthwestern Medical Center, Dallas, TX*

Disclosures: Liwei Jia: None; Rajal Shah: None

Background: Due to their exquisite chemosensitivity, resection of post-chemotherapy residual mTGCTs comprises an integral part of the multimodality management in patients with advanced TGCTs. Evaluation and reporting of these post-chemotherapy masses may pose significant diagnostic challenges due to its rarity and broad morphological diversity that may suggest chemosensitivity or resistance.

Design: All post-chemotherapy surgical resections from TGCTs patients were retrospectively identified (2011-2020). Clinical and morphological features and selective IHC markers were evaluated. In a small subset of cases with viable residual tumors molecular alterations were investigated using a next-generation sequencing (NGS) platform.

Results: A total of 54 patients with 80 resection specimens were identified and comprised the study. The median age was 26 years (range, 15-47) at initial presentation. Nineteen (35%) patients were staged pT1, 23 (41%) pT2, 6 (11%) pT3, and ypT0 (3). Morphological spectrum of primary TGCT included mixed GCT (37), pure seminoma (6), embryonic carcinoma (EC, 5), teratoma (2) and choriocarcinoma (1). Primary or salvage chemotherapy was given in all patients, including pre-orchiectomy chemotherapy in 7 patients for clinical metastases. One patient had persistent elevation of serum markers during median follow up of 16 months (range 1-252 months), who deceased for undocumented reason. The specimens included: retroperitoneal lymph node dissection (RPLNs, 50), kidney (9), lung (9), colon/small intestine (4), adrenal gland (4), liver (3), and non-RPLNs (1). Morphological spectrum in post-chemotherapy resections included: complete response with no viable tumor (35, 43%), viable teratoma only (39, 49%) and viable non-teratomatous component (6, 8%), comprising of yolk sac tumor (YST, 4), EC (3), seminoma (3), and choriocarcinoma (1). Findings suggestive of treatment effects included fibrosis (43), ischemic necrosis (34), xanthomatous inflammation (33), and chronic inflammation (15). Atypical features within teratoma exhibited cells with marked cytological atypia in stroma or cyst lining, mimicking viable non-teratomatous tumor, particularly YST

or cystic trophoblastic tumor. Thirteen of them prompted IHC work up, including SALL4 and glypican 3, only 4 of which aided to identify YST or choriocarcinoma element. Molecular study of a subset of cases (n=5) with residual viable tumor demonstrated loss of function mutations in two cases (one residual EC and YST harboring mutations of *MAP3K1, DDX3X* and *KMT2D*, one teratoma harboring *TP53* mutation).

Conclusions: The majority of mTGCT demonstrated morphological features suggesting chemosensitivity. Residual viable tumors were identified in a small subset, with teratoma being the most common chemo-resistant component, which can display a variety of atypical features, mimicking non-teratoma. LOF mutations are common in chemo-resistant tumors.

470 Autosomal Dominant Polycystic Kidney Disease Associated Renal Neoplasia

Derek Jones[1], Leili Mirsadraei[2], Kimon Argyropoulos[3], Jonathan Melamed[4], Fangming Deng[5], Kyung Park[6], Qinghu Ren[6]

[1]New York University Langone Medical Center, New York, NY, [2]NYU Langone Health/NYU Winthrop Hospital, Mineola, NY, [3]NYU Langone Medical Center, New York, NY, [4]New York University, New York, NY, [5]New York University Medical Center, New York, NY, [6]NYU Langone Health, New York, NY

Disclosures: Derek Jones: None; Leili Mirsadraei: None; Kimon Argyropoulos: None; Jonathan Melamed: None; Fangming Deng: None; Kyung Park: None; Qinghu Ren: None

Background: Autosomal dominant polycystic kidney disease (ADPKD) is caused by mutations in the genes encoding polycystin 1 and polycystin 2 (*PKD1* and *PKD2*, respectively), leading to florid cystic change of the renal parenchyma. The incidence of carcinoma associated with ADPKD remains unclear although there are studies to suggest that the incidence may be higher.

Design: We queried our department pathology database for surgical specimens with ADPKD from 1990 to 2020. We evaluated these cases for the presence of associated malignant or benign neoplasia, as well as pathological and clinical parameters.

Results: The majority of the surgical specimens are kidney explants with a clinical diagnosis of ADPKD and the status of end stage kidney diseases. All specimens showed radiological, gross and microscopic features of ADPKD. Eight of 33 ADPKD patients with kidney resection specimens examined contained a malignant neoplasm, including 2 patients with bilateral malignancy. The types of renal cell carcinoma (RCC) associated with the following types: four cases of clear cell RCC, two cases of papillary RCC, type 2, two cases of unclassified high grade RCC, one case of unclassified low grade, as well as one case of *TFE3* translocated RCC. Associated carcinomas ranged in size from less than 1 cm to 12 cm. One case with a concurrent oncocytoma and several cases with associated papillary adenoma were also reported.

Conclusions: In this cohort, a wide distribution of renal cell carcinoma subtypes were observed, with clear cell RCC being the most common type. The incidence of associated malignancy (24%) is higher than previously reported by Jilg et al. 2013 (5%), possibly due to differences in patient management or patient populations between the institutions. This case series highlights the high occurrence of carcinoma in APKD nephrectomies suggesting a clinical risk of malignancy in patients with ADPKD. Additionally this case series reports the first case of a *TFE3* translocated renal cell carcinoma arising synchronously with a contralateral clear cell renal cell carcinoma in a patient with ADPKD. The heterogeneity of renal carcinoma subtypes within the group (and within contralateral kidneys in one patient with bilateral involvement) suggests that stimuli for tumorigenesis arise at the kidney microenvironment level rather than on the basis of gene mutation alone. Accrual of an expanded cohort of patients is planned to enable confirmation of differences between carcinomas arising in the setting of ADPKD versus those arising in end stage renal disease due to other causes, and in the sporadic setting. Furthermore a role for molecular studies is suggested to evaluate if any of the ADPKD causing mutations (*PKD1*, *PKD2*, or other) is associated with the development of carcinoma.

471 Features of Fibrous Epithelial Cellular Components (FECC) within Renal Oncocytoma

Derek Jones[1], Fangming Deng[2], Jonathan Melamed[3]
[1]New York University Langone Medical Center, New York, NY, [2]New York University Medical Center, New York, NY, [3]New York University, New York, NY

Disclosures: Derek Jones: None; Fangming Deng: None; Jonathan Melamed: None

Background: Entrapped cells or tubules within the fibrous stroma/central scar (fibrous epithelial cellular component = FECC) of oncocytoma have been previously reported although not to date studied in detail. While benign, the varied features of these cells may at times pose a diagnostic challenge. Although these have been attributed as entrapped tubules of oncocytoma, the underlying nature and differentiation of the fibrous epithelial cellular component (FECC) remains unexplored.

Design: We evaluated cases of renal oncocytoma for cellular components in the fibrous stroma ("entrapped tubules") and describe their morphologic variation and immunohistochemical features in comparison to the surrounding oncocytoma.

Results: We examined twelve oncocytoma cases with fibrous stroma ("central scar") containing FECC which were evaluated further by immunohistochemical studies, including CD117 and CK7. In select cases, additional immunohistochemical stains were performed depending on the renal tumor differential diagnosis. These included carbonic anhydrase IX (CA-9), 34Be12 and AE1/AE3 in select cases. The fibrous stroma of the oncocytoma ("central scar") was noted to represent from 10% to 50% of the tumor area and while predominantly central also extended peripherally as short septa. FECC was predominantly in the stroma immediately subjacent to the usual oncocytoma component. The architecture varied as tubular, trabecular, to diminutive acini with adjacent single cells and showed mixed pattern in majority. Cytologically the FECC had cleared cytoplasm, and slightly larger and vesicular nuclei than oncocytoma cells. Some cases demonstrated an area of transition between oncocytoma and the fibrous cellular component with trabecular bands containing scattered oncocytic intermingled with clear cells. Immunohistochemical studies showed FECC positive for CK7 and CA-9 and negative for CD117 (CK7 +/ CA-9 +/CD117 -), whereas oncocytoma cells showed the reverse pattern (CK7 -/ CA-9 -/CD117 +). Immunostains for 34betaE12 and AE1/AE3 performed in a subset of cases showed positive staining of in contrast to the non-reactivity in the oncocytoma.

Figure 1 - 471

Oncocytoma Component							Entrapped Cell Component						
Case	CD117	CK7	CA9	AE1/AE3	34BE12	CK20	Case	CD117	CK7	CA9	AE1/AE3	34BE12	CK20
1	P						1		P				
2	P	FP	N				2						
3	P	FP	N		N		3	N	P	FP		P	
4	FP	N	N			N	4	N	P	P			
5	P	FP	N				5						
6	P	N	N		N		6		P	P		P	
7	P	N				N	7	N	P				N
8	P	N					8	N	P				
9	P	N					9	P	N				
10	P	FP	N	N			10	N	P	P	P		
11		N					11		P				
12		FP					12		FP				

Figure 1. **The immunohistochemical findings of the oncocytoma and entrapped cell components.**
Legend: P = positive, FP = focally positive, and N = negative

Figure 2 - 471

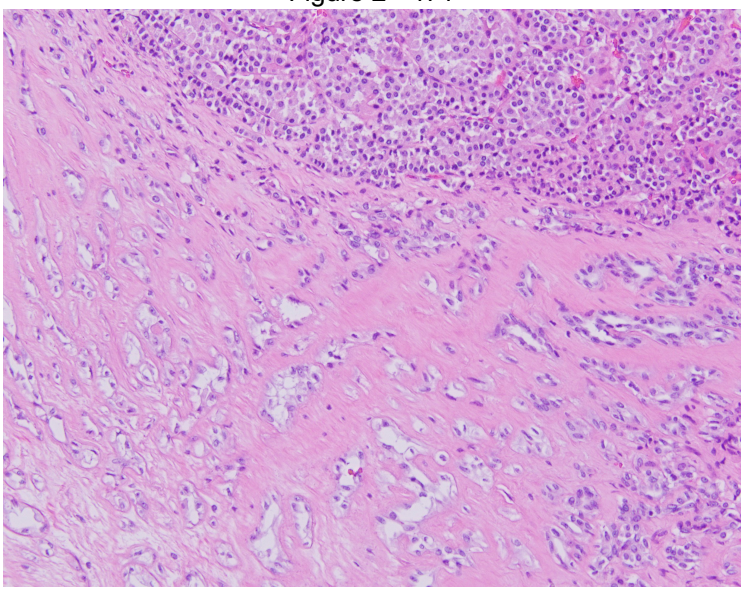

Conclusions: FECC or "entrapped tubules" likely represents a fibrous stromal component of oncocytoma with different microscopic appearance and immunohistochemical profile. It is important to be aware of the variant histological pattern and immunohistochemical profile of oncocytoma as may pose diagnostic difficulty in limited sampling by core needle biopsy. The clear appearance and narrowed trabecular/ tubular pattern is suggestive of an atrophic/ entrapped tumor component, however its varied immunoprofile also raises question as to whether this represents a different differentiation of tumor in an altered microenvironment.

472 Differentially Expressed Genes Associated with Lymphatic Dissemination in TMPRSS2-ERG Molecular Subtype of Prostate Cancer

Dmitry Kalinin[1], Anastasiya Kobelyatskaya[2], Elena Pudova[2], George Krasnov[2], Maria Fedorova[2], Vladislav Pavlov[2], Anastasiya Snezhkina[2], Anna Kudryavtseva[2]
[1]A.V. Vishnevsky National Medical Research Center of Surgery of the Russian Ministry of Healthcare, Moscow, Russia, [2]Engelhardt Institute of Molecular Biology, Russian Academy of Sciences, Moscow, Russia

Disclosures: Dmitry Kalinin: None; Anastasiya Kobelyatskaya: None; Elena Pudova: None; George Krasnov: None; Maria Fedorova: None; Vladislav Pavlov: None; Anastasiya Snezhkina: None; Anna Kudryavtseva: None

Background: Prostate cancer (PC) is one of the most important socially significant oncological diseases in men. In relation to PC seven molecular subtypes were found out, the most common one is TMPRSS2-ERG (approximately 45% of PC cases). One of the most actual clinical problem is to correct assessment of the aggressiveness of the tumor process. Lymphatic dissemination is one of the manifestations of tumor aggressiveness, which is characterized as the spread of the tumor process to regional lymph nodes. The exploration of essential molecular genetic changes associated with lymphatic dissemination can be used to identify perspective prognostic markers for PC. Our research is aimed at identification of differentially expressed genes associated with lymphatic dissemination in TMPRSS2-ERG molecular subtype of PC.

Design: The study included RNA-Seq data of 104 TMPRSS2-ERG-positive locally advanced PC (LAPC) samples based on The Cancer Genome Atlas (TCGA-PRAD). The cohort was divided into two groups: tumors with lymphatic dissemination (N1 group, n=22) and tumors without lymphatic dissemination (N0 group, n=82). Differential expression analysis was performed in statistical environment R with using the edgeR package. Trimmed mean of M-values (TMM) method of counts matrix normalization, quasi-likelihood F-test (QLF) and Mann-Whitney test were applied for identification differentially expressed genes. Differentially expressed genes had to pass QLF p-value<0.05 and Mann-Whitney p-value<0.05.

Results: During the differential expression analysis 150 genes were identified, 15 of which had the most striking change (Fig. 1). Among detected genes two were upregulated (*GPR158, PTPRT*) and 13 – downregulated (*ACOX2, CEACAM1, FAM3D, JPH4, MYBPC1, PTGDS, PYGM, RBM24, SLC22A3, SLC2A4, SRD5A2, ST6GAL1, TENT5B*).

Figure 1 - 472

Gene name	LogFC	LogCPM	QLF p-value	Mann-Whitney p-value
ACOX2	-1,09	3,00	2,47E-04	2,71E-04
CEACAM1	-1,00	5,54	6,59E-05	5,18E-05
FAM3D	-1,18	5,64	1,19E-03	2,32E-04
GPR158	2,23	3,28	3,02E-07	3,68E-04
JPH4	-1,63	3,83	4,88E-05	4,68E-05
MYBPC1	-1,25	7,12	5,15E-04	9,15E-05
PTGDS	-1,08	7,34	7,40E-04	5,44E-04
PTPRT	1,28	5,14	4,28E-03	4,37E-05
PYGM	-1,24	3,88	5,49E-04	8,86E-05
RBM24	-1,40	3,49	2,87E-05	3,31E-05
SLC22A3	-1,36	6,43	1,30E-05	1,02E-05
SLC2A4	-1,29	3,39	1,03E-04	5,18E-05
SRD5A2	-1,46	4,24	1,09E-04	3,68E-05
ST6GAL1	-1,15	8,78	8,55E-05	3,31E-05
TENT5B	-1,26	3,37	1,13E-03	7,02E-05

Conclusions: Thus, in this study were identified 15 genes associated with lymphatic dissemination in TMPRSS2-ERG molecular subtype of PC, which could be considered as potential prognostic markers.

This work was founded by the Russian Science Foundation, grant 18-75-10127.

473 Homologous Recombination Deficiency (HRD) Score in Germline BRCA2- Versus ATM-Altered Prostate Cancer

Harsimar Kaur[1], Daniela Salles[2], Sanjana Murali[3], Jerry Lanchbury[4], William Isaacs[3], Robert Brown[5], Andrea Richardson[6], Olivier Cussenot[7], Geraldine Cancel-Tassin[8], Kirsten Timms[4], Emmanuel Antonarakis[3], Tamara Lotan[3]

[1]Johns Hopkins University, Baltimore, MD, [2]Johns Hopkins Medical Institutions, Baltimore, MD, [3]Johns Hopkins University School of Medicine, Baltimore, MD, [4]Myriad Genetics, Inc., Salt Lake City, UT, [5]Imperial College London, London, United Kingdom, [6]Johns Hopkins Medicine, Baltimore, MD, [7]Sorbonne University, Assistance Publique Hôpitaux de Paris, Paris, France, [8]Paris, France

Disclosures: Harsimar Kaur: None; Daniela Salles: None; Sanjana Murali: None; William Isaacs: None; Robert Brown: None; Andrea Richardson: *Primary Investigator*, Myriad Genetics; Geraldine Cancel-Tassin: None; Kirsten Timms: *Employee*, Myriad Genetics Inc; *Stock Ownership*, Myriad Genetics Inc; Emmanuel Antonarakis: None; Tamara Lotan: *Grant or Research Support*, Roche; *Grant or Research Support*, Myriad Genetics; *Grant or Research Support*, DeepBio

Background: The homologous recombination deficiency (HRD) score integrates three DNA-based measures of genomic instability and is understudied in prostate cancer. Given the recent FDA-approval of PARP inhibitors for prostate cancer, HRD score analysis could help refine treatment selection.

Design: HRD score, defined as the sum of loss-of-heterozygosity, telomeric allelic imbalance, and large-scale state transitions, was assessed in three cohorts of primary prostate cancer, including a Johns Hopkins University (JHU)

cohort with mutations in *BRCA2*, *ATM* or *CHEK2* (n=64), the TCGA cohort (n=391), and the PROGENE cohort (n=102).

Results: In the JHU cohort, tumors with germline *BRCA2* mutations had a higher HRD score (median=27) than those with germline *ATM* or *CHEK2* mutations (median=16.5 [p=0.029] and 9 [p<0.001], respectively). For TCGA tumors without underlying HR pathway mutations, the median HRD score was 11, significantly lower than ovarian carcinoma lacking *BRCA1/2* mutations (median=28). In the absence of HR gene mutations, the median HRD score was higher among prostate cancers with *TP53* mutations versus those without (17 vs 11; p=0.015); this finding was confirmed in the PROGENE cohort (24 vs 16; p=0.001). Preliminarily, among 8 *BRCA2*-altered patients who received olaparib, progression-free survival trended longer in those with HRD scores above versus below the median (14.9 vs 9.9 months).

Conclusions: HRD scores are low in primary prostate cancer and higher in cases with germline *BRCA2* or somatic *TP53* mutations. Germline *BRCA2*-altered cases have significantly higher scores than germline *ATM*-altered or *CHEK2*-altered cases, consistent with the lower efficacy of PARP inhibitors among the latter.

474 Prognostic Stratification of Molecular Subtypes and Their Correlation with PDL1 Expression and Tumor Infiltrating Lymphocytes in Muscle Invasive Bladder Cancer: Implications for Therapeutic Benefits in the Immunotherapy Era

Seema Kaushal[1], Hena Khandakar[1], Hemlata Jangir[1], Amlesh Seth[1], Ranjit Sahoo[1], Amit Dinda[1]
[1]All India Institute of Medical Sciences, New Delhi, India

Disclosures: Seema Kaushal: None; Hena Khandakar: None; Hemlata Jangir: *Employee*, AIIMS, new Delhi

Background: Little is known about differential expression of PDL1 and TIL profiling in molecular subtypes of MIBCs. We analyzed the expression of PD-L1 and examined its relationship with TIL status in molecular subtypes. We also investigated the relation of PD-L1 and TIL expression with clinicopathological factors including prognostic value of various subtypes.

Design: CK5/6, GATA3, p53 and claudin-3 immunoexpression was evaluated in 100 formalin-fixed paraffinembedded MIBCs. Tumors were classified into luminal, basal/squamous and double negative/ non-specified. Luminal category was classified into 'Urothelial-like' and 'Genomically unstable-like' based on the pattern of CK5/6 expression.

PD-L1 (clone E1L3N), CD4 and CD8 immunoexpression status was examined in these subtypes. The determination results of PD-L1in tumor cells and immune cells was defined by tumor proportion score (TPS) and Immune cell Score (ICS). We considered TPS≧1% as positive. Tumor was considered PD-L1 positive for immune cells if they had an ICS ≥5 %

For evaluation of CD4+ and CD8+ TIL density, we counted the number of 3 non-contiguous areas of highest lymphocyte density located in the tumor and averaged over three high-power fields for each case.

Results: 42% tumors were luminal and 49% were basal while 9% were double negative The luminal subtype was subdivided into 28% urothelial-like tumors, and 14% genomically unstable-like.

- PD-L1 positivity rates in the tumor cells was 46% (TCS>1%)
- PD-L1 positivity in the immune cells (ICS≥5%) was seen in 24% cases.
- Basalsubtype showed the highest proportion of PD-L1 positive tumor cells, followed by the double negative subtype (p=0.025), urothelial-like subtype showed the least.
- The double negative and genomically unstable subtypes showed higher proportion of PD-L1 positive immune cells than the other subtypes (p=0.014).
- The urothelial-like subtype showed the least total T cell infiltration (p=0.027), in addition to showing lowest CD4 and CD8 counts.
- Tumors with high CD8 T cell infiltration was seen in greater proportion in the double negative subtype (77.8%), while the GU-like (57.%) and basal subtype (51%) showed comparable values (p=0.085).

- Highest proportion of diffuse strong P53 immunopositivity was seen in the genomically unstable-like subtype and in the basal subtype (p=0.019).

Clinical Parameters	Urothelial-like (N=28)	Genomically unstable-like (N=14)	Basal/ squamous (N=49)	Double Negative/ NS (N=9)	P value
Mean Age	59±10years	57.3±8.4years	54.8±10years	59±7.9years	
Stage II at diagnosis	2 (7%)	5 (36%)	2 (4%)	2 (22%)	0.02
Stage III at diagnosis	23 (82%)	7 (50%)	38 (78%)	7(78%)	
Stage IV at diagnosis	3 (11%)	2 (14%)	9 (18%)	0	
Stage II at end of follow-up	2 (7%)	3 (21%)	1 (2%)	1(11%)	0.03
Stage III at end of follow-up	16 (57%)	4 (29%)	28 (57%)	1 (11%)	
Stage IV at end of follow-up	10 (36.7%)	7 (50%)	20 (41%)	7 (78%)	
Stage progression following CT	6/24 (25%)	4/11 (36.4%)	12/43 (27.9%)	5/6 (83.3%)	0.042
Visceral Metastasis	8 (28.6%)	4 (28.6%)	13 (26.5%)	5(55.6%)	0.145
Nodal metastasis	2 (7.1%)	2 (14.3%)	6 (12.2%)	2 (22.2%)	
Recurrence (local)	4/28 (14.3%)	3/14 (21.4%)	3/49 (6.1%)	1/9 (11.1%)	0.383

Figure 1 - 474

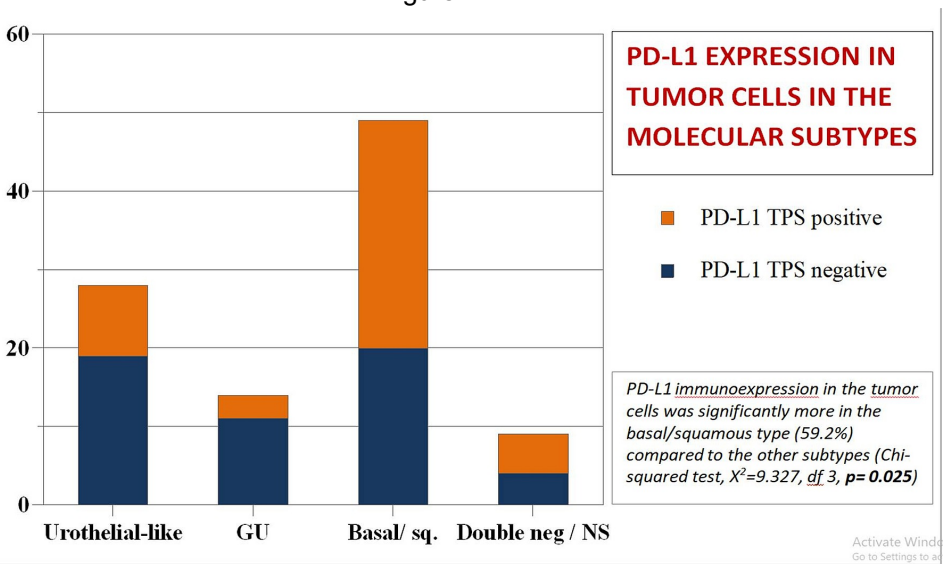

Figure 2 - 474

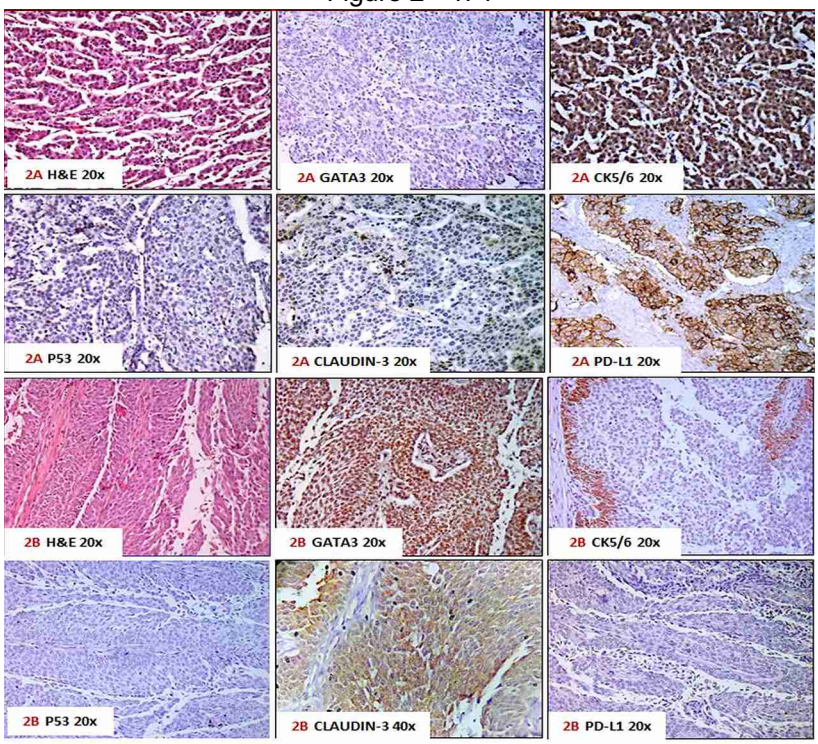

2A Basal/squamous molecular subtype, 2B Urothelial-like subtype

Conclusions:

- There is a significant difference in survival of molecular subtypes (p=0.018) with double negative subtype having the shortest OS, followed by basal subtype; between luminal tumors, GU-like tumors behave worse than urothelial-like tumors.
- There is a significant difference in PD-L1 tumor cell and immune cell positivity rates in the molecular subtypes (p=0.025 and 0.014 respectively).
- Our results suggest that immune system and PD-L1 are differentially expressed in the molecular subtypes and have different prognostic and therapeutic implications.

475 Precancerous Lesions of the Prostate and the Risk of Upgrading in Men on Active Surveillance Undergoing MRI-Ultrasound Fusion Biopsy

Ghazal Khajir[1], Kamyar Ghabili[2], Olayemi Olubowale[3], Michael Leapman[2], Angelique Levi[4], Peter Humphrey[2], Preston Sprenkle[2]
[1]Yale School of Medicine, Yale New Haven Hospital, New Haven, CT, [2]Yale School of Medicine, New Haven, CT, [3]Tulane School of Medicine, New Orleans, LA, [4]Yale University, New Haven, CT

Disclosures: Ghazal Khajir: None; Kamyar Ghabili: None; Olayemi Olubowale: None; Michael Leapman: None; Angelique Levi: None; Peter Humphrey: None; Preston Sprenkle: None

Background: The study of precancerous lesions of the prostate is crucial for understanding prostatic carcinogenesis and for developing potential chemopreventive measures for prostate cancer. Little is known about the role of high-grade prostatic intraepithelial neoplasia (HGPIN), atypical small acinar proliferation (ASAP), or perineural invasion (PNI) on the risk of upgrading in subsequent MRI-ultrasound fusion biopsies. We aimed to determine if the presence of those pathological characteristics on prostate biopsy increases the risk of upgrading on subsequent MRI-ultrasound fusion biopsy for active surveillance (AS).

Design: We retrospectively queried an IRB-approved institutional MRI-ultrasound fusion prostate biopsy database to identify men in AS for grade group (GG) 1 prostate cancer. Upgrading in AS cohort was defined as increase from

GG1 on initial biopsy to GG≥2 on subsequent biopsy between January 2013 and February 2019. Binary logistic regression was performed to identify clinical, radiological, and biopsy pathological features (HGPIN, ASAP, or PNI) associated with the presence of upgrading on surveillance biopsy.

Results: Our AS cohort included 127 men; 16 men (12.6%) had at least one of the studied pathological features (HGPIN, PNI or ASAP) on their first biopsy. 101 (79.5%) and 93 (73.2%) had region(s) of interest on initial and subsequent prostate MRIs, respectively, and therefore underwent MRI-ultrasound fusion biopsy. Among men on AS, 31 (24.4%) showed upgrading on subsequent biopsy and of those, 9 (29.0%) men had HGPIN, ASAP or PNI on initial biopsy. Although HGPIN was associated with upgrading among patients on AS in univariate analysis (p=0.01), there was no independent significance in multivariable analysis (OR 3.84, 95%CI 0.60-24.63, p=0.15). Age (OR 1.07, 95%CI 1.001-1.15, p=0.04) and PI-RADS (4-5 versus ≤3, OR 2.89, 95%CI 1.14-7.35, p=0.02) remained significantly associated with an increased risk of upgrading on subsequent biopsy in men on AS (Table 1).

Table 1. Univariate and multivariate logistic regression models for the prediction of upgrading on subsequent biopsy in men on active surveillance

	Univariable			Multivariable		
	OR	95%CI	P value	OR	95%CI	P value
ASAP	5.03	0.80-31.65	0.08	3.42	0.26-44.55	0.34
HGPIN	9.03	1.65-49.29	0.01	3.84	0.60-24.63	0.15
PNI	2.69	0.67-10.75	0.16			
More than 2 of above pathologic features	2.13	0.34-13.42	0.41			
Age	1.07	1.01-1.14	0.02	1.07	1.001-1.15	0.04
PI-RADS 4-5	3.27	1.36-7.86	0.008	2.89	1.14-7.35	0.02
PSA density (per 0.1 unit)	1.85	1.08-3.15	0.02	1.70	0.93-3.09	0.08

Conclusions: No association was found between any of the studied pathological features (HGPIN, ASAP, or PNI) and upgrading on subsequent biopsy in AS cohort. Therefore, the presence of HGPIN, ASAP, or PNI on biopsy should not influence the management of men undergoing AS in the MRI-ultrasound fusion biopsy era.

476 Unique Histologic Subtypes of Post-transplant Renal Cancer

Takeda Kotaro[1], Aisha Kousar[1], Kimbely Briley[1], Lorita Rebellato[1]
[1]*East Carolina University, Greenville, NC*

Disclosures: Takeda Kotaro: None; Aisha Kousar: None; Kimbely Briley: None; Lorita Rebellato: None

Background: Kidney transplantation has been improved the quality of life of patients with end-stage renal disease on dialysis. One drawback is an increased risk of malignancy after kidney transplantation. Both end-stage renal disease and dialysis are the significant risks for renal cancer, thus kidney transplant recipients are facing even higher risk for that due to necessity of immunosuppression. We analyzed post-transplant renal cancer incidence and histologic subtypes.

Design: Adult Caucasians and African Americans with primary renal transplants performed at Vidant Medical Center between 2009 and 2015 were included in this study. Renal cancer diagnosis through 2019 was determined through medical record review. The study evaluated the renal cancer incidence, time interval until kidney cancer diagnosis, histologic subtypes, tumor size and focality, pathologic staging, treatments and prognosis.

Results: 447 kidney transplant recipients (Caucasians 130; African Americans 317) were analyzed. 8 recipients (1.8 %) developed post-transplant renal cancer (Caucasians 2; African Americans 6). African Americans had slightly higher incidence than Caucasians (1.9 % vs 1.5 %). The average time interval to the cancer diagnosis was 1832 days. Seven cancers (87.5 %) were developed in the native kidneys. Histologic subtypes were variable

including acquired cystic disease-associated renal cell carcinoma (RCC) (2), unclassified RCC (2), clear cell RCC (1), papillary RCC (1), and highly suspected case of RCC (1). All were unifocal with an average size of 3.4 cm and confined in the kidney without lymph node or distant metastasis (Stage I), thus all patients received nephrectomy with complete cure. In contrast, one patient developed cancer in donor kidney. He had donor-derived high grade neuroendocrine carcinoma with liver metastasis (Stage IV), required transplant nephrectomy as well as chemotherapy. The neuroendocrine carcinoma was positive for TTF-1, suggesting the donor had undetected lung neuroendocrine carcinoma. No death due to the kidney cancers was observed in this study.

Conclusions: This study found post-transplant renal cancer incidence of 1.8 %, which was 45 times higher than that of general population (approximately 0.04 %). Majority of renal carcinoma was developed in recipient's native kidney and found in an early stage, thus treated accordingly with good prognosis. Clear cell RCC, the most common subtype in general population, appeared uncommon in post-transplant kidney cancer. Donor-derived cancer transmission was a rare event, although it was found at late stage, indicating requirement of more thorough donor screening.

477 AI-Based Solution for Cancer Diagnosis in Prostate Core Needle Biopsies: A Prospective Blinded Multi-Site Clinical Study

Daphna Laifenfeld[1], Manuela Vecsler[1], Delphine Raoux[2], Anat Albrecht Shach[3], Judith Sandbank[4], Lilach Bien[1], Yuval Globerson[1], Chaim Linhart[1], Mahul Amin[5]
[1]Ibex Medical Analytics, Tel Aviv, Israel, [2]Medipath, Toulon, France, [3]Assuta Ashdod Hospital, Ashdod, Israel, [4]Maccabi Health Services, [5]Methodist University Hospital, Memphis, TN

Disclosures: Daphna Laifenfeld: *Employee*, Ibex Medical Analytics; Manuela Vecsler: *Employee*, Ibex Medical Analytics; Delphine Raoux: None; Anat Albrecht Shach: *Employee*, Ibex Medical Analytics; Judith Sandbank: None; Lilach Bien: *Employee*, Ibex Medical Analytics; Yuval Globerson: *Employee*, Ibex Medical Analytics; Chaim Linhart: None; Mahul Amin: *Advisory Board Member*, Cell Max; *Consultant*, Urogen; *Consultant*, Advanced Clinical; *Advisory Board Member*, Core Diagnostics; *Advisory Board Member*, Precipio Diagnostics

Background: Computer-assisted diagnostic solutions to evaluate prostate core needle biopsies (CNBs) have shown great promise to increase efficiency and accuracy in diagnosis. Despite several publications in the field, rigorous multi-site clinical studies using pre-determined success criteria and multi-pathologist Ground Truth have not been published. In the context of supporting clinical decisions, the need for an AI-based solution that combines high accuracy levels validated on large independent cohorts that incorporates clinically meaningful features, such as Gleason grading, is still unmet.

Objective: To clinically validate the performance of the AI-based algorithm on detection and grading of prostate adenocarcinoma against rigorous ground truth (GT) established by multiple blinded pathologists.

Design: The study was conducted as a prospective performance study using 100 consecutive retrospective prostate CNBs (870 H&E slides) from 2 established medical institutions in different geographies. Two certified and experienced pathologists (blinded to the original diagnosis report) reviewed the cases and reported the endpoints on a slide basis. In case of discrepancies between them, a third assessment was performed by a specialist blinded uropathologist, to achieve majority agreement, thus establishing GT. The algorithm was run in a blinded manner on the scanned slides. GT data from the participating sites and, separately, algorithmic output were sent to an external bio-statistician for analysis. The study endpoints were detection of adenocarcinoma, intermediate/high-grade cancer (benign/G6 vs G7+), differentiating between G6 and G7+ and perineural invasion.

Results: The algorithm demonstrated high performance when compared with the GT, specifically, it showed a specificity of 95.65% and a sensitivity of 98.62% with an AUC of 0.997. Additionally, the algorithm achieved an AUCs of 0.991 and 0.935 for detecting G7+ and differentiating between G6 vs. G7+, respectively and an AUC of 0.978 for detection of perineural invasion. The concordance between the original GT pathologists was 98.4% on cancer detection and only 82.7% and 79.8% on Gleason 7+ and perineural invasion detection, respectively.

Conclusions: This study reports the successful clinical validation of an AI-based algorithm in detecting, grading and automatically imparting clinically relevant diagnostic parameters regarding prostate adenocarcinoma, offering an important tool for computer-aided diagnosis in routine pathology practice.

478 New Panel of Molecular/Cellular Markers of Prostate Cancer for Risk Stratification

Kirk Lin[1], Anil Prasad[2]
[1]Arizona Urology Specialists, Phoenix, AZ, [2]Northwest Medical Center, Tucson, AZ

Disclosures: Kirk Lin: None

Background: We have previously demonstrated that PTEN/ERG/Ki67 tests could provide comparable results for prostate cancer risk stratification as other genomic test modalities (PTEN/ERG/Ki67 provide comparable results as other genomic tests in risk stratification of prostate cancer. Mod Pathol. 2020; 33 (Suppl 2):S83). More recently, we have incorporated P27, MUC1, and P53 into the test menu to assess gene mutation/deletion/fusion, cell proliferation, migration, and metastasis. This study provides our most recent data to further define our testing protocol for future prognostic applications.

Design: Prostate cancer diagnosed with biopsies with Gleason Score 6 and 7 were tested for PTEN and ERG using fluorescence in-situ hybridization technique while Ki67, P27, MUC1 and p53 were tested using immunohistochemical stains. Validations and the cut-off levels were established at our Laboratory. The risk profiles were classified as very low/low, moderate, high/very high. For the convenience of comparison, the current panel is designated as PTEN Plus versus previous PTEN/ERG/Ki67.

Results: From January to October 2020, a total of 210 cases of newly diagnosed prostate cancer had been tested with PTEN Plus. The age of the patients ranged from 52 to 85 with mean PSA of 6.98 (ranging from 1.0 to 15.5ng/ml). Fifty percent (50%, 105 men) were very low/low risk group, 35% (73 men) were moderate risk, 15% (32 men) were high/very high risk. As compared to previous tests of 585 men with PTEN/ERG/Ki67 (data from Mod Pathol. 2020;33(Suppl 2):S83), the number of low risk patients was down from 59.4% to 50% with PTEN Plus tests. Since most patients in the low risk group would be placed in surveillance program, the PTEN Plus would provide more patient safety at active surveillance. For comparison purpose, the data from previous presentation is listed again in the table below.

	Cases tested	Mean Age	Mean PSA	Very Low Or Low	Moderate	High or Very High
PTEN Plus	210 (new)	69.5	6.98	50%	35%	15%
PTEN/ERG/Ki67	585	70.0	7.15	59.4%	32.8%	7.8%
Prolaris	127	68.7	7.21	56.6%	30.2%	13.2%
OncoType Dx	129	69.1	7.05	51.4%	28.8%	14.0%

Conclusions: The new panel of PTEN/ERG/Ki67/P27/MUC1/P53 (PTEN Plus) is an improved test protocol in the evaluation of prostate cancer prognosis. Compared to other genomic test modalities, PTEN Plus could potentially provide better and more cost effective results in cancer risk stratification and reliably categorize patients for active surveillance.

479 Variable Expression of Nectin-4 in Bladder Urothelial Carcinoma with Divergent Differentiation

Kara Lombardo[1], Woonyoung Choi[2], Bridget McGuire[2], Vamsi Parimi (Parini)[3], Sonia Kamanda[4], Andres Matoso[1]
[1]Johns Hopkins Medical Institutions, Baltimore, MD, [2]Greenberg Bladder Cancer Institute, Johns Hopkins University School of Medicine, Baltimore, MD, [3]Johns Hopkins University School of Medicine, Baltimore, MD, [4]James Buchanan Brady Urological Institutions, Johns Hopkins Hospital, Johns Hopkins Medical Institutions, Baltimore, MD

Disclosures: Kara Lombardo: None; Woonyoung Choi: None; Bridget McGuire: None; Vamsi Parimi (Parini): None; Sonia Kamanda: None; Andres Matoso: None

Background: The antibody-drug conjugate (ADC) enfortumab vedotin (EV) is poised to change the bladder cancer treatment landscape by targeting nectin-4, a protein that is nearly ubiquitously expressed in conventional urothelial cancer (UC). However, the expression of nectin-4 in tumors with divergent differentiations has not been reported and could have potential implications in therapeutic responses.

Design: Immunohistochemistry (IHC) for nectin-4 was performed on 71 specimens of conventional and variant urothelial carcinoma using 2 commercially available antibodies, one rabbit monoclonal and one rabbit polyclonal. Membranous and cytoplasmic staining was scored for intensity (0-3) and extent (% positive cells) using the H-score system, where >15 was considered positive. Whole transcriptome RNA sequencing was performed using Ion Torrent's AmpliseqRNA platform on an S5XL sequencer.

Results: Fourteen of 17 (82.3%) cases of conventional UC were positive when assessed using a polyclonal antibody versus 3/8 (37.5%) with a monoclonal antibody (p=0.06). Expression in pure squamous cell carcinoma was seen in 5/6 (83.3%) cases with a polyclonal antibody and in 3/6 (50%) with a monoclonal. Expression in micropapillary carcinoma was positive in 6/11 (55%) with a polyclonal antibody and in 3/11 (27.3%) with a monoclonal antibody. Plasmacytoid variant was positive in 7/8 (87.5%) with a polyclonal antibody and in 5/8 (62.5%) with a monoclonal antibody. Glandular and nested variants were positive in 1/3 (33%) cases of each with both antibodies. Strikingly, none of the small cell carcinoma cases (n=15) or sarcomatoid carcinoma cases (n=8) were positive (0%) with either antibody. Whole transcriptome RNA sequencing showed that compared to conventional urothelial carcinomas, sarcomatoid and small cell carcinomas expressed very low levels of nectin-4 mRNA. Conversely, some cases with low nectin-4 expression had high expression of Trop2 and ERBB2, which are the molecular targets of two other ADCs - sacituzumab gavitecan (trop-2) or trastuzumab deruxtecan (ERBB2/HER2).

Conclusions: Our study demonstrates that despite variation in monoclonal and polyclonal IHC, there is overall heterogeneity of expression of nectin-4 in urothelial carcinoma with variant morphology but consistent low-level expression in small cell and sarcomatoid carcinomas by both IHC and RNAseq. These results have important implications for the use of EV in bladder cancer patients whose tumors have small cell and sarcomatoid differentiation. Increased expression of trop2 and ERBB2 in some tumors with low nectin-4 expression suggests these patients may benefit from other targeted therapies.

480 Histopathological Characterization of Prostate Cancer from a Contemporary Cohort of Nigerian Patients: A Retrospective Review

Jenaye Mack[1], Kayode Adebamiji Adeniji[2], Folakemi Odedina[3], Romonia Reams[4], Srikar Chamala[3], Sara Falzarano[1]
[1]University of Florida College of Medicine, Gainesville, FL, [2]University of Ilorin Teaching Hospital, Ilorin, Nigeria, [3]University of Florida, Gainesville, FL, [4]Tallahassee, FL

Disclosures: Jenaye Mack: None; Kayode Adebamiji Adeniji: None; Folakemi Odedina: None; Romonia Reams: None; Sara Falzarano: None

Background: Nigeria is the world's seventh biggest country, and prostate cancer (PCa) represents the most prevalent male cancer. Moreover, a disproportion of aggressive disease that rapidly progresses towards castration-resistance is a common occurrence among PCa patients in Nigeria. Recent studies have shown that specific pathological features, particularly the presence of invasive cribriform and intraductal carcinoma of the prostate (CR/IDC), are associated with adverse outcome in PCa and could have predictive value for response to therapy and development of castration-resistance. To our knowledge, histopathological features-focused studies on PCa samples from Nigerian patients are currently lacking. We herein will review histopathological features of prostate cancer in archived biopsy tissue samples obtained from a contemporary cohort of Nigerian patients, with particular emphasis on presence of CR/IDC.

Design: Archived tissue samples from a cohort of Nigerian men who underwent prostate biopsy between 2015 and 2018 were obtained and reviewed by a subspecialty-trained genitourinary pathologist. Available clinical data and

histopathological features (including Grade Group/Gleason score, presence of CR/IDC, and cancer volume, in terms of percentage of tissue involvement and/or linear length of cancer, if applicable) were annotated.

Results: 73 prostate biopsy specimens were evaluated. Mean age of patients at presentation was 70 years (range 50-88). GG was 1 in 1 (1%), 2 in 10 (14%), 3 in 15 (20%), 4 in 18 (25%) and 5 in 29 (40%) cases. IDC/CR was identified in 36 (49%) cases, 2 (5%) of which were GG2, 6 (17%) GG3 and 28 (78%) GG4-5. Of the tissue available for review, the mean highest percentaqe of core involvement was 93% (range 25-100). The mean max length of core involvement was 6 mm (range 1-12).

Conclusions: Nigerian men in this cohort presented with high-grade prostate cancer in the majority of cases. There is a high incidence of IDC/CR in any given Grade Group.

481 Can Palpation Guided Needle Biopsy at the Time of Prostatectomy Provide Adequate and Representative Fresh Tissue for Future Study?

Ciera Mangone[1], Lauren Schwartz[2], Daniel Lee[3], Raju Chelluri[3]
[1]University of Pennsylvania Health System, Philadelphia, PA, [2]Perelman School of Medicine at the University of Pennsylvania, Philadelphia, PA, [3]Hospital of the University of Pennsylvania, Philadelphia, PA

Disclosures: Ciera Mangone: None; Lauren Schwartz: None

Background: Harvesting fresh tissue from prostatectomy (PRx) specimens is critical for the future of prostate cancer related research. Routine, reproducible protocols for procuring fresh tissue from PRx specimens have not been clearly established. Common existing harvesting methods involve sectioning the fresh prostate. This can hinder histologic examination of margin status and assignment of Grade Group (GG). In this study we attempted to determine if palpation guided needle core biopsies (NCBxs) taken after removal of the prostate could recover tissue that accurately represents the tumor without hindering histologic examination.

Design: 19 PRx cases being performed for biopsy proven prostatic carcinoma by one surgeon at our institution were prospectively identified. Following PRx and prior to fixation, 3-7 NCBx were procured in the pathology lab by the surgeon from the PRx based on palpation. The NCBx and remainder of the PRx were then fixed for 12-24 hours and subsequently entirely submitted to histology as per institutional standards. The PRx and NCBx were histologically evaluated, a composite final report rendered, and the pathologic findings compared. Data points included size of dominant nodule based on microscopy, percentage of PRx involved by carcinoma (%PRx), overall dominant GG of the carcinoma within the PRx, proportion of NCBx with carcinoma and GG of the carcinoma present in the NCBx.

Results: Of the 19 patients in the study, 11 were found to have carcinoma present in at least one of the retrieved NCBx, with the NCBx GG being equivalent to the PRx GG in 4 of these 11 patients. In 2 NCBx the GG was greater than in the PRx and in 4 the GG was less than in the PRx. One case with carcinoma in the NCBx was unable to be compared due to treatment effect in the PRx. Presence of carcinoma in the NCBx was directly related to %PRx. When carcinoma was identified in the NCBx it tended to present in the majority of cores (ranging from 1/4 cores to 6/6 cores).

Conclusions: In summary, tumor tissue was procured through NCBx in 11/19 cases (58%) with 4/11 showing GG concordance. For the PRx demonstrating a high risk GG (>3), carcinoma was identified in 67% of the retrieved NCBx, excluding one case with no identifiable dominant nodule. In the cases with %PRx>50, 100% of the retrieved cores contained carcinoma. These findings suggest that palpation guided NCBx can be done in cases with large tumor burdens but is not an ideal way to collect fresh tissue from PRx where GG concordance is crucial. Of note, despite mismatch of GG between the NCBx and PRx we did not investigate correlation on a molecular level. Further study is needed to refine this procurement technique, perhaps with the assistance of portable imaging, to ensure more reproducible results.

482 Genomic Characterization of Acquired Cystic Disease-Associated Renal Cell Carcinoma (ACD-RCC): Insights Into Tumor Biology

Rahul Mannan[1], Christopher Przybycin[2], Pankaj Vats[3], Yuping Zhang[4], Pushpinder S. Bawa[1], Xiaoming (Mindy) Wang[3], Fengyun Su[3], Rui Wang[3], Todd Morgan[3], Daniel Spratt[3], Xuhong Cao[3], Jesse McKenney[2], Arul Chinnaiyan[3], Saravana Dhanasekaran[3], Rohit Mehra[3]

[1]Michigan Medicine, University of Michigan, Ann Arbor, MI, [2]Cleveland Clinic, Cleveland, OH, [3]University of Michigan, Ann Arbor, MI, [4]Michigan Center for Translational Pathology, Ann Arbor, MI

Disclosures: Rahul Mannan: None; Christopher Przybycin: None; Pankaj Vats: None; Yuping Zhang: None; Pushpinder S. Bawa: None; Xiaoming (Mindy) Wang: None; Fengyun Su: None; Rui Wang: None; Todd Morgan: None; Daniel Spratt: None; Xuhong Cao: None; Jesse McKenney: None; Arul Chinnaiyan: None; Saravana Dhanasekaran: None; Rohit Mehra: None

Background: Acquired cystic disease associated renal cell carcinoma (ACD-RCC) is a distinct renal tumor subtype arising in individuals with acquired cystic kidney disease (ACKD) and a background of dialysis dependent end stage renal disease (ESRD). Since its original description, few case series have described the various clinical-pathological correlates associated with ACD-RCC. Morphologically, these tumors may demonstrate acinar, solid or papillary architecture and are enriched for cytoplasmic lumina and calcium oxalate crystals. However, details on genomic aberrations or additional biomarkers associated with this disease are relatively limited. Herein, by means of next generation sequencing (NGS) methodology, we describe the molecular aberrations identified in a cohort of ACD-RCC.

Design: Six ACD-RCC patients with ESRD whose clinical attributes are described (Table-1) were selected to generate a mutation profile associated with the disease. NGS data was generated from all the patients using standard in-house protocol and processed through standard analysis pipelines to estimate germline/somatic mutations and copy number events.

Results: Integrative NGS profiling and analysis of ACD-RCC revealed a high frequency whole chromosomal gains of 7 (observed in 3/6 (50%) of cases) and 16 (seen in 4/6 (67%) cases); 19p loss was observed in (2/6) 33% of the cases. Few other notable mutations observed in some functionally important genes included a missense mutation in *KEAP1*, somatic loss of function in *FLCN* and a frameshift mutation in *KMT2C* genes. A summary of the molecular findings from our cohort is presented in Table 1.

Table-1 Patient Demographic and Respective Molecular Aberration Summary

Case #	Age	Sex	Tumor Size (cm)	Mutational Aberrations	CNV* whole chromosome gain	CNV* chromosome loss
Case #1	52	M	0.4	PRDM15: p.R88fs	**7, 12, 16**	5p partial
Case #2	64	M	4.5	**FLCN** two somatic hits: p.D80fs and p.P404fs	**7, 16**	NS**
Case #3	64	M	2.5	NS**	**5, 7, 8p, partial 8q, 16, 17q, 21**	18, 19p
Case #4	51	M	1	DICER subclonal	**NS****	NS**
Case #5	72	M	0.6	**KEAP1 missense**: p.I128N and copy loss	**16**	1p partial, 1q partial, 19, 12p partial
Case #6	66	F	3	**KMT2C** two somatic hits: p.K1665fs and p.N3747fs	**5q**	NS**

CNV* Copy number variation; NS None significant; Age in years**

Conclusions: This study identifies somatic mutational diversity in ACD-RCC including *KEAP1* missense mutation, *FLCN* (also noted as a germline event in Birt-Hogg-Dubé syndrome) and *KMT2C* gene, a potential cancer driver. Several major kidney cancer subtypes show signature whole chromosomal and or arm level CNV patterns and now our study has exposed yet another interesting CNV pattern that might be more prevalent and perhaps a signature of ACD-RCC. The recurrent whole chromosomal gains in chromosomes 7 and 16, may constitute this pattern and warrants future investigation in a larger cohort. Identification of potential diagnostic and prognostic

biomarkers associated with ACD-RCC, is currently under progress and may be amenable to immunohistochemical and/or RNA *in situ* hybridization technologies.

483 Comparative Analysis of LINC01187 and CD117 Expression in Chromophobe Renal Cell Carcinoma and Related Oncocytic Neoplasms

Rahul Mannan[1], Xiaoming (Mindy) Wang[2], Pushpinder S. Bawa[1], Stephanie Skala[2], Nikita Daniel[2], Yuping Zhang[3], Sylvia Zelenka-Wang[3], Lisa McMurry[3], Xuhong Cao[2], Daniel Spratt[2], Todd Morgan[2], Arul Chinnaiyan[2], Saravana Dhanasekaran[2], Rohit Mehra[2]
[1]Michigan Medicine, University of Michigan, Ann Arbor, MI, [2]University of Michigan, Ann Arbor, MI, [3]Michigan Center for Translational Pathology, Ann Arbor, MI

Disclosures: Rahul Mannan: None; Xiaoming (Mindy) Wang: None; Pushpinder S. Bawa: None; Stephanie Skala: None; Nikita Daniel: None; Yuping Zhang: None; Sylvia Zelenka-Wang: None; Lisa McMurry: None; Xuhong Cao: None; Daniel Spratt: None; Todd Morgan: None; Arul Chinnaiyan: None; Saravana Dhanasekaran: None; Rohit Mehra: None

Background: Chromophobe renal cell carcinoma (RCC) is the third most common RCC subtype and can be diagnosed and sub-classified based on morphology and immunohistochemical (IHC) studies. Our recent work using transcriptome profiling and experimental validation has proposed a long non-coding RNA (*LINC01187*) as a sensitive and specific biomarker for the diagnosis of chromophobe RCC and related oncocytic neoplasms. Herein we compared the performance of *LINC01187* RNA *in situ* hybridization (RNA-ISH) and CD117 IHC (commonly used IHC based marker in genitourinary service line) on a cohort of chromophobe RCC and related oncocytic tumors.

Design: We generated a cohort of 60 oncocytic tumors (Table-1) and performed CD117 IHC and *LINC01187* RNA-ISH on formalin fixed paraffin embedded (FFPE) sections. A product score (out of 300) was calculated for CD117 membranous expression by IHC based on staining intensity and percentage positivity noted in the tumor cells. For RNA-ISH based *LINC01187* assessment, individual chromogenic mRNA transcripts were recorded in the tumor cells and a final H-score (out of 400) was calculated. In addition, we recorded the bio-characterization profile of both biomarkers in terms of heterogeneity, edge effect and distribution (peripheral vs central) of staining within the tumors.

Results: CD117 expression showed greater range of variability in terms of staining (average score of 185.81 and a range of 2 to 288). In contrast, *LINC01187* expression was noted to be more homogeneous and exhibit less variability (average score of 353.7 and a range of 122 to 400). Upon comparing the staining score of two biomarkers, the R^2 value observed was 0.16. Besides, 27% of renal tumors showed prominent differential peripheral to central expression of CD117, 16 % had edge effect and 38% of cases were noted to demonstrate heterogeneous staining of CD117. These effects, recognized as known confounders of immunohistochemical assessment, were observed to be significantly absent with *LINC01187* RNA ISH assessment. Similar findings were noted when we compared the two biomarkers in a single, individual patient having multiple metastatic sites, where CD117 expression demonstrated considerable variability and heterogeneity.

Table-1 Expression profiles of CD117 and LINC01187 biomarkers

		***LINC01187* RNA-ISH H-Score (400 Max)**			***LINC01187* Characterization**			**CD117 IHC Product Score (300 Max)**			**CD117 Characterization**		
	N	**Min**	**Max**	**Avg**	**FE**	**EE**	**Hetero**	**Min**	**Max**	**Avg.**	**FE**	**EE**	**Hetero**
Classic CHRCC[a]	13	247	394	363	0	0	0	46	275	188	4	2	5
Eo-CHRCC[b]	4	4	347	239	0	0	0	3	288	139	1	1	2
Sarco-CHRCC[c]	3	122	333	212	0	0	0	105	225	175.33	1	0	2
Oncocytoma	18	373	396	386.67	0	0	0	157	278	225.8	4	2	2
Oncocytic-U[d]	5	189	400	336	0	0	0	2	220	124.2	1	1	2
Met-CHRCC[e]	17	308	400	368.82	0	0	0	67	256	158.8	5	4	10

N= Total samples; Min=Minimum score; Max.=Maximum Score; Avg=Average score; FE=Differential peripheral to central expression; EE= Edge effect; Hetero=Heterogeneous effect

a-Classic chromophobe RCC; b-Eosinophilic variant of chromophobe RCC; c-Sarcomatoid chromophobe RCC; d-RCC-Unclassified (oncocytic); e-Metastatic Chromophobe RCC

Conclusions: *LINC01187* expression showed less variability in terms of total scores in comparison to the currently clinically utilized biomarker CD117 for the oncocytic group of tumors, in both primary and metastatic setting. *LINC01187* confers an additional benefit over CD117 in terms of uniform expression across the tissue samples, whereas ~40% of cases in this cohort showed heterogeneous expression of CD117, including edge and fixation related effects. Overall, these observations support *LINC01187* as a robust biomarker (tolerant to RNA degradation) owing to higher H-scores, more consistent, and easy to elucidate for chromophobe RCC and related oncocytic neoplasm in clinical practice.

484 Papillary Renal Neoplasm with Reverse Polarity. Expanding the Molecular and Immunohistochemical Features

Stefano Marletta[1], Anna Calio'[1], Lavinia Stefanizzi[2], Diego Segala[3], Matteo Brunelli[1], Guido Martignoni[4]
[1]University of Verona, Verona, Italy, [2]Ospedale Pederzoli, Peschiera del Garda, Italy, [3]ASST Spedali Civili di Brescia, Brescia, Italy, [4]University of Verona, Ospedale Pederzoli, Peschiera del Garda, Italy

Disclosures: Stefano Marletta: None; Anna Calio': None; Lavinia Stefanizzi: None; Diego Segala: None; Matteo Brunelli: None; Guido Martignoni: None

Background: Papillary renal neoplasm with reverse polarity (PRNRP) is a recently described renal tumor characterized by (i) papillary or tubulopapillary structures covered by a single layer of eosinophilic cells with finely granular cytoplasm and apically located round nuclei with inconspicuous nucleoli; ii) absence of mitotic figures and necrosis; iii) a high frequency of KRAS mutations (37/39 cases studied); iv) immunohistochemical expression of GATA3 and, variably, of α-methylacyl-CoA-racemase (AMACR) which suggest that these neoplasms differentiation toward distal nephron rather than the proximal tubules. Parvalbumin is a cytosolic calcium-binding protein expressed in the distal convoluted tubule of the renal nephron and commonly observed in chromophobe renal cell carcinomas and oncocytomas and there are no data available on its expression in PRNRP.

Design: Four unreported PRNRPs were retrieved from the files of the institution and immunohistochemically stained with AMACR (clone 13H7, dilution 1:25; Dako), cytokeratin 7 (clone RN7, dilution 1:100; Novocastra), parvalbumin (clone P19, dilution 1:500; Sigma, USA), GATA3 (clone L50-823, dilution 1:150; BD Pharmingen, USA) and S100A1 (clone M01, dilution 1:600; Abnova, Taiwan). Moreover, KRAS mutation status was analyzed (Idylla™ platform).

Results: All of the tumors tested were positive for parvalbumin, GATA 3, cytokeratin 7 and S100A1, while two of them expressed AMACR. KRAS mutations were found in all of the samples. The KRAS mutation types observed were G12V (2 cases), G12R (1 case), and the unreported mutation at codon 61 (Q61K) (1 case).

Conclusions: In our series we recorded a strong expression of parvalbumin in all PRNRPs, along with a new undescribed mutation of the KRAS gene. Hence our findings both strengthen the hypothesis of a distal nephron differentiation of PRNRPs and widen the current knowledge on the molecular biology of this newly discovered renal neoplasm.

485 Lymphovascular Invasion and Hilar Soft Tissue Invasion Predict Advanced Clinical Stage in Pure Seminomas

Vikas Mehta[1], Charisse Liz Treece[2], Alessa Aragao[3], Krishna Irrinki[4], Maria Picken[3]
[1]University of Illinois at Chicago Hospital and Medical Center, Chicago, IL, [2]University of Illinois at Chicago, Chicago, IL, [3]Loyola University Medical Center, Maywood, IL, [4]Mount Sinai Hospital, Chicago, IL

Disclosures: Vikas Mehta: None; Charisse Liz Treece: None; Alessa Aragao: None; Krishna Irrinki: None; Maria Picken: None

Background: Testicular Germ cell tumors (GCTs) account for 1% of all male malignancies with over 8500 new diagnoses every year. Approximately 40% of these tumors in postpubertal males are pure seminomas (PS).

Majority of these PS diagnosed without evidence of metastatic disease (clinical stage I) and up to 5% present with metastatic disease (clinical stages II and III). Risk stratification has been accomplished using clinical variables, such as serum tumor markers (β-HCG, AFP, and LDH), as well as pathologic findings on orchiectomy. We investigated the pathologic predictors of advanced clinical stage at presentation in a cohort of 66 consecutive PS.

Design: In this multi-institutional retrospective study, a total of 66 consecutive PS diagnosed between 2009 and 2019 were reviewed by three pathologists. The following clinical and pathologic features were evaluated: age, tumor size, coagulative necrosis, vascular invasion, rete testis invasion and tumor extension into tunica vaginalis, hilar soft tissue, epididymis, or spermatic cord. Studied parameters were correlated with the clinical stage at presentation.

Results: Of the 66 patients with PS, 26 (39%) were left sided and 40 (61%) were right sided. Mean patient age was 40.5 years (range, 19-83). The tumor size ranged from 0.2 to 20 cm (Mean 4.9 cm). 40 (67%) cases presented as clinical stage I while 15 (23%) were clinical stage II and 7 (10%) were stage III. Among the pathologic parameters, pathologic stage distribution for pT1, pT2, pT3 and pT4 was 40 (61%), 18 (27%), 8 (12%) and 0 respectively. Lymphovascular invasion (LVI) was present in 29 (44%) of cases, Hilar soft tissue invasion (HSTI) in 22 (33%), Rete testes invasion (RTI), excluding pagetoid only spread in 22 (33%), epididymis involvement in 5 (7%) and spermatic cord involvement (SCI) in 14 (21%) of cases.

Advanced clinical stage at presentation was associated with LVI (P<0.001) and HSTI (P<.007) by univariate analysis. On multivariate analysis again LVI (P<0.001) and HSTI (P<.011) were the only statistically significant pathologic factors. Pathologic parameters like RTI, coagulative necrosis, size of tumor, dominant tumor type and epididymis involvement were not significant.

Conclusions: We conclude that pathologic parameters like vascular invasion, tumor invasion into the hilum (hilar soft tissue) strongly correlate with advanced clinical stage at presentation in pure seminomas.

In contrast to non-seminomatous germ cell tumors , the role of rete testis invasion in upstaging the pure seminomas is still not clear.

486 Molecular Correlates of Immune Infiltrate in Treatment Naïve Prostate Adenocarcinoma

Adrianna Mendes[1], Harsimar Kaur[2], Jiayun Lu[3], Corinne Joshu[3], Mohammed Alshalalfa[4], Edward Schaeffer[5], Tamara Lotan[6]
[1]Johns Hopkins Medical Institutions, Baltimore, MD, [2]Johns Hopkins University, Baltimore, MD, [3]Johns Hopkins Bloomberg School of Public Health, Baltimore, MD, [4]GenomeDx Biosciences Inc, Vancouver, Canada, [5]Northwestern University Feinberg School of Medicine, Chicago, IL, [6]Johns Hopkins University School of Medicine, Baltimore, MD

Disclosures: Adrianna Mendes: None; Harsimar Kaur: None; Jiayun Lu: None; Corinne Joshu: None; Mohammed Alshalalfa: None; Tamara Lotan: *Grant or Research Support*, Roche; *Grant or Research Support*, Myriad Genetics; *Grant or Research Support*, DeepBio

Background: Although prostate cancer (PCa) is considered to be poorly immunogenic, some molecular subsets are associated with increased T-cell infiltrates. Previous gene expression studies suggest that treatment-naïve tumors with low androgen receptor activity (AR-A) are also more immunogenic. Here, we examined the molecular and oncologic outcome correlates of immunohistochemistry (IHC)-assessed immune infiltrate in untreated PCa.

Design: A retrospective cohort of 323 prostatectomy samples from patients with treatment-naïve intermediate and high risk PCa were scored for *ETS* and PTEN status using genetically validated *in situ* hybridization and/or IHC protocols. Tumors were classified as either AR-A low or AR-A normal using a previously validated weighted gene expression score and cutoff for 9 AR target genes. The density of macrophages, B-cells, T-cells and T-cell subsets were measured using digital quantification of IHC staining for CD163, CD79a, CD3, CD8, and FoxP3, respectively, per area of tissue sampled on tissue microarrays.

Results: Across this cohort, T- and B-cell densities were significantly correlated (rho=0.47, p<0.0001). *ETS*-positive tumors had significantly higher T-cell densities compared to *ETS*-negative tumors (p=0.005) and ERG-

positive tumors had lower macrophage densities (p=0.04), with no significant change in B-cells. FOXP3+ T-cells were significantly higher in tumors with PTEN loss compared to those with PTEN intact (p=0.005), though no significant difference in macrophages or B-cells. AR-A low tumors had significantly higher T-cell and B-cell densities compared to AR-A intact tumors (p=0.0081 and 0.002, respectively). Clinical-pathologic variables were not significantly associated with immune cell densities. Univariate and multivariate analysis did not show significant associations of metastasis risk with immune infiltrate.

Conclusions: Molecular subclass may play an important role in the regulation of the anti-tumoral response. Consistent with prior studies in patients treated with neoadjuvant androgen deprivation therapy or gene expression studies in untreated populations, our data showed a significant increase in T- and B-cell density in treatment-naïve tumors with low AR-A, implying that reduced basal AR-A may also stimulate inflammatory infiltrate. Future studies may focus on the mechanisms of this interaction and how to modulate it through current and novel therapies.

487 Multiparametric Magnetic Resonance Imaging (mpMRI) for the Detection of Clinically Significant Prostate Cancer and Adverse Pathology: Direct Comparison with Final Pathology on Whole Mount Radical Prostatectomy

Christopher Metter[1], Qi Cai[1], Kenneth Goldberg[1], Daniel Costa[1], Rajal Shah[1]
[1]UTSouthwestern Medical Center, Dallas, TX

Disclosures: Christopher Metter: None; Qi Cai: None; Kenneth Goldberg: None; Daniel Costa: None; Rajal Shah: None

Background: The detection and accurate assessment of tumor aggressiveness are essential in diagnosing prostate cancer (PCa) and counseling patients for further treatment, for which mpMRI is increasingly utilized in practice. This study aims to determine the characteristics of detected and missed PCa foci on mpMRI with matched histopathological findings from radical prostatectomy (RP) specimen.

Design: A retrospective review of 51 men with biopsy-proven PCa who underwent RP was included. All patients had been examined using mpMRI following PI-RADS version 2 guidelines. Histopathological findings of the whole mount RP specimen were reviewed by dedicated genitourinary pathologists and compared with prospective clinical mpMRI interpretation (PI-RADS score and ADC value) for both index and non-index tumors. PI-RADS score ≤ 2 was considered a negative MRI. Clinically significant PCa was defined as grade group (GG) ≥ 2 and GG 1 with intraductal carcinoma (IDC-P) and adverse pathology as the presence of GG ≥ 3 and “cribriform architecture” (IDC-P and/or invasive cribriform pattern 4).

Results: At RP, 86 (48 index and 38 non-index) tumors with clinically significant PCa were identified. In all, 73 of these tumors were identified by mpMRI with an overall sensitivity of 85%. Three index tumors detected at mpMRI were GG1. Thirteen tumors missed by mpMRI had following characteristics: 1 index and 12 non-index tumors, median tumor size 1.5 cm (interquartile range, 2.5), 92% (n=12) GG2, 8% (n=1) GG3, and 62% (n=8) anteriorly located. Higher PI-RADS value significantly correlated with both higher GG and adverse pathology ($p < 0.05$). ADC value significantly correlated with detection of clinically significant PCa but did not correlate with adverse pathology ($p > 0.05$)

Conclusions: mpMRI offers high accuracy for the detection of a clinically significant tumor at the patient level, however, in the setting of multifocal tumors, smaller and anteriorly located non-index tumors may be missed. Our study also suggests that mpMRI has a similar level of high sensitivity for the detection of PCa with “cribriform architecture”.

488 Clinicopathologic Implications of Unifocal vs Multifocal Invasive Urothelial Carcinoma of the Bladder with Lamina Propria Invasion

Patrick Mullane[1], Shreyas Joshi[1], Mehmet Bilen[2], Adeboye O. Osunkoya[1]
[1]Emory University, Atlanta, GA, [2]Emory University School of Medicine, Atlanta, GA

Disclosures: Patrick Mullane: None; Mehmet Bilen: *Advisory Board Member*, Exelixis, Bayer, BMS, Eisai, Pfizer, AstraZeneca, Janssen, Genomic Health, Nektar, and Sanofi; *Grant or Research Support*, Xencor, Bayer, Bristol-Myers Squibb, Genentech/Roche, Seattle Genetics, Incyte, Nektar, AstraZeneca, Tricon Pharmaceuticals, Peleton Therapeutics, and Pfizer; Adeboye O. Osunkoya: None

Background: Patients diagnosed with urothelial carcinoma (UCa) with lamina propria (LP) invasion in bladder biopsies are at significant risk for disease recurrence and progression to UCa with muscularis propria (MP) invasion. The ability to identify patients at risk for recurrence and progression based on clinicopathologic features thus holds prognostic significance. Multifocal tumors are commonly found in patients with UCa with LP invasion, yet the implications of this finding remain uncertain. Here, we describe the clinicopathologic characteristics of unifocal vs. multifocal cases of UCa with LP invasion at a major academic institution.

Design: We searched our Urologic Pathology files and expert consult cases of the senior author for patients with a diagnosis of UCa with LP invasion. Patients with a prior diagnosis of UCa with MP invasion or upper tract UCa were excluded. Multifocality was defined as two or more discrete tumors present at time of transurethral resection or biopsies. Only cases in which tumor focality was explicitly documented were included in the study.

Results: Two hundred forty-two cases were identified: 112 unifocal and 130 multifocal. Patient demographics were similar for both groups, with 69% males and 31% females and a mean age of 73 years (range: 44-95 years) for unifocal cases, and 76% males and 24% females and a mean age of 72 years (range: 49-91 years) for multifocal cases. Although presence of MP was similar when comparing all cases (77% and 73% for unifocal and multifocal, respectively), biopsy naïve patients were less likely to have MP sampled if multifocal tumors were present (68% vs 86%). Biopsy naïve patients with multifocal tumors also had increased rates of recurrence on repeat biopsy (80% vs. 63%). Interestingly, while the rate of variant UCa subtypes was similar for unifocal and multifocal cases (33% and 25%, respectively), the variant subtypes differed. Most notably, the micropapillary (33% vs 11%) and nested (12% vs 3%) variants were more frequent in multifocal cases compared to unifocal cases, respectively.

Conclusions: In our cohort, Biopsy naïve patients with multifocal tumors were less likely to have MP sampled on initial biopsy, and had increased disease recurrence on repeat TURBT. Additionally, distribution of variant UCa subtypes differed between the two groups, with higher rates of micropapillary and nested variants observed in multifocal tumors. Our findings support multifocality as a risk factor for disease recurrence and provide evidence of aggressive clinical behavior in multifocal tumors.

489 INSM1: A Reliable Marker to Distinguish Small Cell Carcinoma of the Prostate from High-Grade Prostatic Acinar Adenocarcinoma

Meredith Nichols[1], Jesse McKenney[1], Jane Nguyen[1], Jordan Reynolds[1], Jonathan Myles[1], Christopher Przybycin[1], Roni Cox[1]
[1]Cleveland Clinic, Cleveland, OH

Disclosures: Meredith Nichols: None; Jesse McKenney: None; Jane Nguyen: None; Jordan Reynolds: None; Jonathan Myles: None; Christopher Przybycin: None; Roni Cox: None

Background: Small cell carcinoma (SCC) of the prostate may arise de novo or after androgen deprivation therapy. While SCC is often readily diagnosed by histologic features, some may have overlap with high-grade prostatic adenocarcinoma (HGPC). Synaptophysin and chromogranin are commonly used in this setting; however, they show variable staining patterns in SCC and may be expressed in otherwise typical HGPC. INSM1 is reported as a valuable marker of neuroendocrine differentiation at other sites, but its utility in the urologic tract is not fully explored. Therefore, we examined the expression of INSM1, in conjunction with Ki-67 proliferation index, in this differential diagnostic setting.

Design: A formalin-fixed paraffin-embedded block from 54 total cases was chosen for immunohistochemical staining with synaptophysin (Biogenix/Snp88), chromogranin (Agilend/DAK-A3), INSM1 (Santa Cruz Biotechnology/A-8), and Ki-67 (Ventana/30-9). Cases consisted of 36 HGPC (1 case GS7; 1 case GS7 with tertiary 5; 33 cases GS9; and 1 case GS10), 14 SCC, and 4 "HGPC with neuroendocrine differentiation." In SCC, 5 were 100% SCC, 8 were mixed SCC and HGPC, and 1 was SCC with sarcomatoid differentiation. Staining was graded semi-quantitatively (0: no staining, 1+: 1-25%, 2+: 26-50%, 3+:51-75%, 4+: >75% staining). Ki-67 was assessed by counting at least 500 cells within areas of highest staining.

Results: 13 of 14 cases of SCC had nuclear immunoreactivity for INSM1: 4+ (5 cases), 3+ (5 cases), and 2+ (3 cases). 12 cases had strong intensity and 1 had moderate intensity. Ki-67 was greater than 50% in 13 of 14 SCC cases, with the remaining case 44%. Synaptophysin had at least 2+ staining in all SCC cases, but chromogranin showed more variable staining. INSM1 was positive in 5 of 34 (15%) HGPC cases, all 5 with only 1+ staining. Ki-67 was less than 50% in all HGPC cases. Synaptophysin was positive in 10 of 34 HGPC cases (9 cases 1+; 1 case 2+) and chromogranin was positive in 9 of 34, all with 1+ staining. The 4 cases diagnosed as "HGPC with neuroendocrine differentiation" showed heterogenous staining: all were synaptophysin positive (2+ or greater) and 3 (75%) were chromogranin positive (1+=1, 3+=1, and 4+=1); Ki-67 was less than 50% in all 4 cases; and INSM1 staining varied from 1+ to 3+.

Conclusions: INSM1 and Ki-67 may have utility in the diagnosis of neuroendocrine carcinoma in the prostate, especially in the distinction between SCC and HGPC.

490 Metastatic Urothelial Carcinoma to the Brain, Spinal Cord and Spine: A Contemporary Multi-Institutional Clinicopathologic Analysis of 24 Cases

Oluwaseun Ogunbona[1], Andres Matoso[2], Liang Cheng[3], Steven Shen[4], Suzanne Powell[5], Adeboye O. Osunkoya[6]

[1]Emory University School of Medicine, Atlanta, GA, [2]Johns Hopkins Medical Institutions, Baltimore, MD, [3]Indiana University, Indianapolis, IN, [4]Houston Methodist Hospital, Houston, TX, [5]The Methodist Hospital, Houston, TX, [6]Emory University, Atlanta, GA

Disclosures: Oluwaseun Ogunbona: None; Andres Matoso: None; Liang Cheng: None; Steven Shen: None; Adeboye O. Osunkoya: None

Background: Metastatic urothelial carcinoma (UCa) to lymph nodes, liver, lung, and bone have been well documented in the literature, however, only case reports and small series of metastatic UCa to the central nervous system (CNS) or spine have been published.

Design: A search was made for cases of metastatic UCa to the brain, spinal cord, or spine from the Neuropathology and Urologic Pathology files of four major academic institutions in the United States.

Results: We identified 24 cases. The mean patient age was 63.5 years (range: 41 to 78 years) with a male to female ratio of 2:1. Nineteen (79%) cases involved the brain, 3 (13%) and 2 (8%) cases involved the spinal cord and spine, respectively. Most of the cases (79%) were a single mass with a mean size of 2.8 cm (range: 0.9 to 5.5 cm). Of the 19 cases involving the brain, 10 (53%) involved the supratentorial region only, 6 (32%) involved the cerebellum only, and 3 (16%) were multifocal disease including a case of carcinomatous meningitis, and 2 other cases involving both the supra- and infratentorial regions. The spinal cord and spine lesions involved the lumbar spinal cord and thoracic vertebrae, respectively. In two cases, sarcomatoid and micropapillary features were present in the metastatic tumors and were not identified in the primary tumors, and in 1 case both the primary and metastatic tumor had micropapillary features. Prior to CNS and spinal metastasis, there was a history of UCa involving only the bladder in 16 (67%) patients, ureter in 1 (4%) patient and kidney (renal pelvis) in 1 (4%) patient. In 1 additional patient (4%) each, the primary tumor involved both bladder and ureter, bladder and kidney, and ureter and kidney, respectively. Three (13%) patients had no known primary site. In two patients, the diagnosis of UCa of bladder was made concurrently as the CNS metastasis, and the time interval from primary UCa diagnosis to presentation of CNS metastasis ranged up to 30 years in other patients. Follow-up was available in 14 patients with a mean duration of 7 months (range: 0 to 23 months), and 4 patients died of disease.

Conclusions: This is the largest study to date of metastatic UCa to the brain, spinal cord, or spine. Metastatic UCa should be considered in the differential diagnosis of a solitary brain or spinal cord/spinal mass in patients with a prior history of invasive high grade UCa. Both clinicians and pathologists should be aware that late brain metastases may occur, even over a decade after the initial diagnosis of UCa.

491 Automated Classification of Transurethral Resection of Bladder Slides Using Deep Weakly Supervised Learning

Inyoung Paik[1], Minsun Jung[2], Han Suk Ryu[3], Tae-Yeong Kwak[4], Sun Woo Kim[1], Hyeyoon Chang[1]
[1]Deep Bio Inc., Seoul, South Korea, [2]Seoul National University Hospital, Seoul, South Korea, [3]Seoul National University College of Medicine/Hospital, Seoul, South Korea, [4]Deep Bio Inc., Guro-gu, South Korea

Disclosures: Inyoung Paik: *Employee*, Deepbio Inc.; Minsun Jung: None; Han Suk Ryu: None; Tae-Yeong Kwak: *Employee*, Deep Bio Inc.; Sun Woo Kim: *Stock Ownership*, Deep Bio Inc.; Hyeyoon Chang: *Employee*, Deepbio Inc.

Background: The pathological diagnosis is the most important determinant of treatment and prognosis for bladder cancer. But interobserver variation is observed, especially between low-grade cancer and precancerous lesion such as PUNLMP. Deep learning is a powerful tool for image recognition and classification. However, a large amount of labeled data is needed for deep learning training, but area annotation is time-consuming and expensive. Therefore weakly supervised learning frameworks that can be trained with a slide-level diagnosis are receiving great attention. We introduce a novel weakly supervised learning framework that can handle regions that are not directly related to slide-level diagnoses, such as blood, stroma, and inflammatory cells.

Design: The 1,428 transurethral resection of bladder(TURB) glass slides were collected and scanned using Aperio AT2 digital slide scanner (Leica Biosystems Imaging, Inc., Vista, CA, United States). The reference standard was constructed by a uropathologist with 10 years of experience and a general pathologist. In cases with discrepancies, the consensus was reached through a consensus meeting. Each slide was annotated by the existence of cancer(class 1~4, see Table 1), the proliferative lesion(5~7), and benign epithelium(8). Slides were mostly from the single institute, but PUNLMP and UPUMP slides were collected from 3 different institutes. The area of epithelium is annotated for only 50 benign slides. 199 and 200 slides are randomly sampled to form tuning and validation data.

We used a 4-model ensemble of MNasNet to perform patch-level 3-class(benign/proliferative/cancer) classification. The multi-resolution image patch(100x and 50x) was extracted and processed by the model simultaneously. We used a modified selective network, which allows the model to 'refuse' to answer, for the image patches that are not directly related to the slide-level diagnosis. We used hierarchical softmax and 'entropy minimization' techniques. We used attention MIL to make a final decision.

Results: The model's AUC for the presence of a proliferative lesion was 0.972, and of cancer was 0.928.

Figure 1 - 491

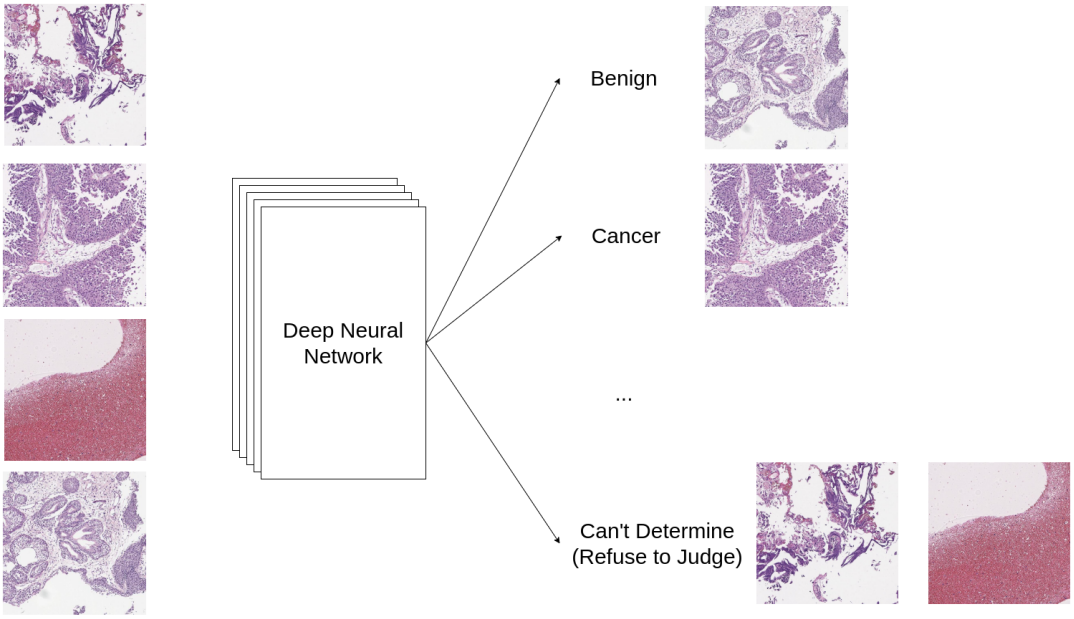

Figure 2 - 491

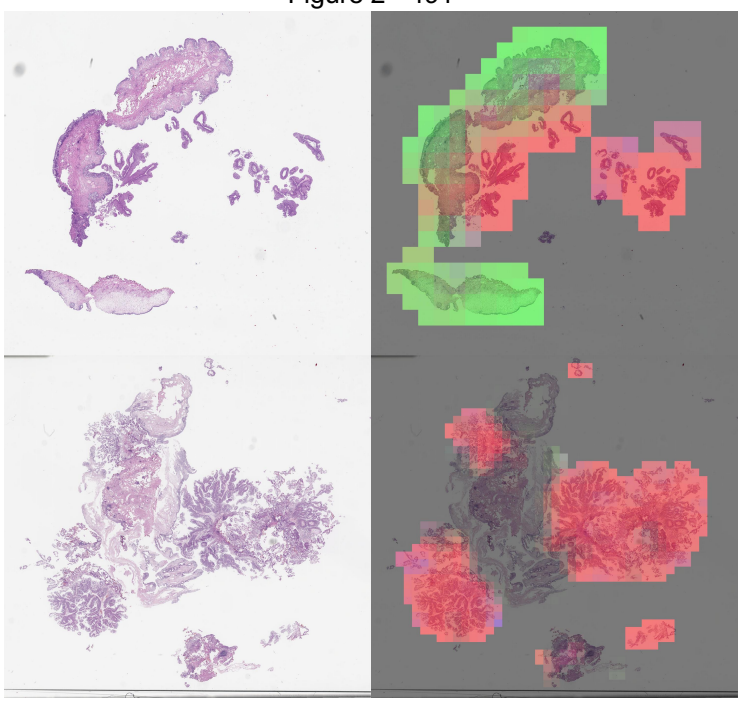

Conclusions: We found that the low performance of the cancer classifier was mostly due to carcinoma in situ(CIS) data. If we exclude the pure CIS slides, cancer-or-not AUC was increased up to 0.980. Further study is needed to make a better classifier that can detect lesions like CIS, which can be confused with benign.

492 Clinicopathological and Genomic Characterization of Prostate Cancer Post-Radiation Failure

Doreen Palsgrove[1], Jeffrey Gagan[1], Ganesh Raj[2], Raquibul Hannan[2], Rajal Shah[1]
[1]UTSouthwestern Medical Center, Dallas, TX, [2]The University of Texas at Southwestern, Dallas, TX

Disclosures: Doreen Palsgrove: None; Jeffrey Gagan: None; Rajal Shah: None

Background: Definitive radiation therapy (XRT) with androgen deprivation is a commonly utilized treatment regimen for patients with high-risk prostate cancer (PCa). Post-XRT PCa failures likely harbor a distinct morphological phenotype and molecular make up that may provide PCa with a survival advantage and exhibit clinically aggressive course.

Design: Fifty-four patients, status post radiation, and androgen deprivation therapy, who failed and subsequently underwent salvage prostatectomy (SP) comprised the study cohort. Morphological features of PCa were divided into three groups: tumor exhibiting treatment effect, partial effect, and no effect. Tumors without treatment effect were Gleason graded and analyzed based on the 2014 ISUP modified grading system. PCa with invasive cribriform pattern 4 and intraductal carcinoma (IDC-P) were collectively defined as “cribriform architecture”. Molecular features of 10 representative tumor samples with no treatment effect and enriched in “cribriform architecture” with matched benign prostate tissue were analyzed using a targeted next-generation sequencing panel with full exon coverage of 1,425 cancer-related genes.

Results: Of 54 PCa at SP, 36 (67%) exhibited no treatment effect with adverse pathological features: GG ≥ 3 (81%), invasive cribriform pattern (78%), IDC-P (64%), extra prostatic disease [pT3a (33%), pT3b (39%), pT4 (6)] and lymph node metastasis (14%). Clinicopathological and molecular features of 10 representative cases is shown in Table 1.

Case	Grade Group	% Cribriform or IDC-P	TNM	Genetic Alterations
1	4	70	ypT2N0	Alterations in SPOP and PALB2; gain of MYC; trisomy 7
2	5	40	ypT4N1	Alteration in TP53; high aneuploidy
3	5	95	ypT3bN1	Alterations in TP53 and KMT2D; MYC amplification; loss of chr 8
4	2	90	ypT2N0	ETV1 fusion; alterations in KMT2D and ARHGEF7; loss of chr 18q
5	4	50	ypT3aN0	Alterations in KMT2D, RNF43, and PIK3CA
6	5	100	ypT3bN0	TMPRSS2:ERG; gain of MYC; loss of chr 8p
7	5	95	ypT3bN0	TMPRSS2:ERG; alterations in PTEN, TP53, CTNNB1, and BRCA2/BRCA1; loss of chr 8p; gain of MYC
8	5	95	ypT3aN0	TMPRSS2:ERG; alterations in PTEN, BRCA1, MAP3K1; loss of chr 8p, gain of MYC
9	4	70	ypT3aN0	PRIM2:BRAF; TMPRSS2 amplification; alterations in TP53; loss of chr 8p
10	5	80	ypT3aN0	TMPRSS2:ERG; alterations in PTEN, TP53, FOXA1, STAT3, and PPP2RA; loss of chr 8p and 18q

Conclusions: XRT failure PCa exhibits several adverse pathological features including enrichment in “cribriform architecture”, and frequently harbor molecular features associated with aggressive PCa including *ETS* fusions, *PTEN* loss, defects in DNA repair pathway genes (*BRCA1/2* and *TP53* mutations), and increased genomic instability, characterized by frequent 8p loss and gain of *MYC*. Further analysis of these findings in the context of both pre- and post-treatment, will likely elucidate whether these tumors acquire resistance secondary to treatment or were inherently radioresistant and would therefore benefit from early exposure to XRT dose intensification or sensitizing adjuvant treatments such as PARP inhibitors.

493 Prostate Rapid Optical Examination for Cancer STATus (proSTAT): An AI-assisted, 3D Approach to Thoroughly Examine Numerous Levels of Prostate Tissue

Yu-Ching Peng[1], Teh-Ying Chou[2], Yu-Chieh Lin, Yung-An Chen[3], Yen-Yin Lin[4], Yu-Ling Hung, Margaret Chang[5]

[1]Taipei Veterans General Hospital, Taiwan, [2]Taipei Veterans General Hospital, Taipei, Taiwan, [3]JelloX, Taiwan, [4]Taiwan, [5]Hsinchu, Taiwan

Disclosures: Yu-Ching Peng: None; Teh-Ying Chou: None; Yu-Chieh Lin: *Employee*, JelloX Biotech Inc.; Yung-An Chen: None; Yen-Yin Lin: *Employee*, JelloX Biotech Inc.; Yu-Ling Hung: None; Margaret Chang: *Employee*, JelloX Biotech Inc.

Background: Intrinsic opacity and heterogeneity of human tissues have prevented efficient light penetration for signal detection by confocal microscopy. This hurdle has largely been overcome by tissue clearing technology that renders biological tissue transparent. Here we introduce a novel method termed proSTAT, which generates high-resolution 2D and 3D images on thick human prostate tissue without the need of paraffin processing and thin sectioning. Given that proSTAT can generate numerous optical levels by imaging the tissue intact, we further exploit an Artificial Intelligence (AI)-assisted system to localize prostate cancer throughout the z-stacks.

Design: Fifteen tissue cores measuring ~15x2x2 mm per core from five radical prostatectomies were used in this study. The specimens were fixed with 10% formalin, sliced into 100 µm, stained with universal nuclear and cell membrane fluorescence dyes, subjected to tissue clearing solution, and imaged with confocal microscopy. 3D reconstruction and visualization of tumor glands were achieved using the volume rendering function in Avizo software. Three optical slices were manually annotated from the 3D stack images which contained 100 slices. The AI model was trained from these three annotated slices and then inference applied to the rest of slices.

Results: Prostatic adenocarcinoma of various Gleason patterns could be readily identified in tissue cores using proSTAT. Open lumens in Gleason pattern 3 tumors were readily evaluated by tracing a single tumor gland through multiple optical images of the z-stacks (Fig. 1). 3D rendering further provided information on the complexity and heterogeneity of tumor glands. Furthermore, a semi-supervised AI model highlighted tumor areas and enabled calculation of tumor percentage throughout z-stacks (Fig. 2). Totally 79 optical levels were analyzed (3 levels with annotation and 76 with AI inference) and tumor percentage ranged from 14% to 36%, suggesting heterogeneity of tumor distribution along the depth. Calculation of individual cell size revealed significantly larger cells in tumor glands as compared to benign tissue (tumor: 75.8 μm^2 *vs.* benign: 70.0 μm^2).

Figure 1 - 493

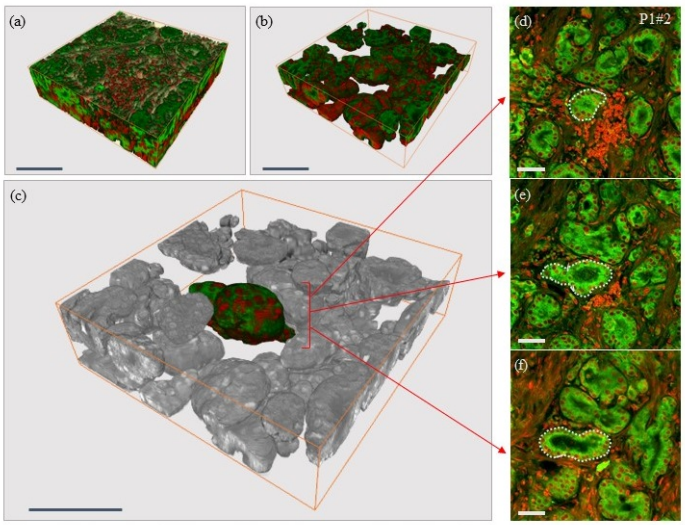

Figure 1 3D reconstructed images of prostate cancer and multiple optical images of the z-stacks. (a) gross view of tumor region, (b) epithelium segmentation of Fig. 1a, (c) single gland segmentation of Fig. 1b. Bar: 100 µm; Prostate cancer sectioned sample imaging along axial-axis with 15-µm interval in depth of (d) 23-µm, (e) 38-µm, (f) 53-µm. Scale bar: 50 µm, Green: cell membrane. Red: nuclei.

Figure 2 - 493

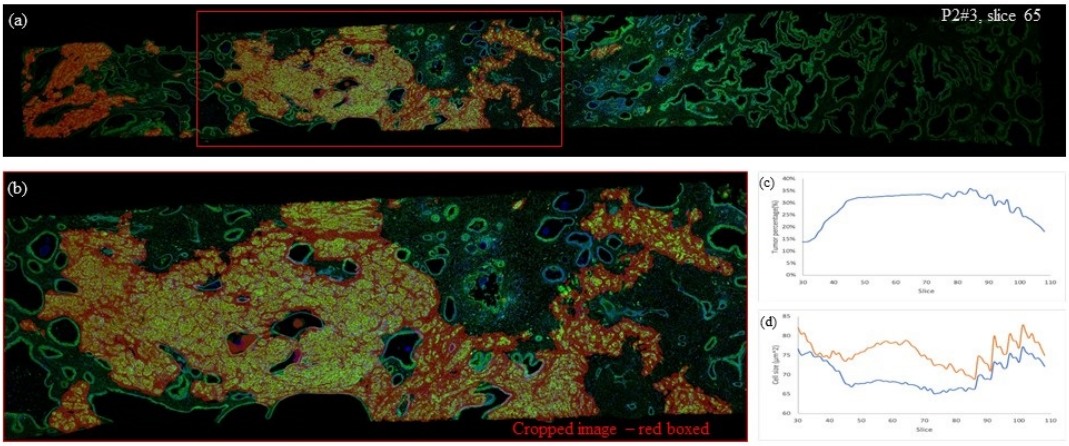

Figure 2 Semi-supervised tumor cell recognition. (a) Whole slide view of the specimen, (b) 2X zooming in (red boxed area in a), (c) pixel-wised tumor percentage with AI model-assisted tumor recognition along the z-stacks, (d) average cell size comparison between tumor/normal cells along the z-stacks. Red: tumor area, Green: cell membrane, Blue: nuclei.

Conclusions: proSTAT presents a rapid, nondestructive method for evaluation of prostate tissue with the advantage of 3D visualization. AI assistance further empowers pathologists to thoroughly examine the entire tissue, providing a potential niche to minimize the risk of missing a small focus of cancer.

494 LZTS2, a Novel and Independent Prognostic Biomarker for Clear Cell Renal Cell Carcinoma: Clinicopathologic Correlation and Immunohistochemical Study

Yue Peng[1], Bradley Stohr[1]
[1]*University of California, San Francisco, San Francisco, CA*

Disclosures: Yue Peng: None; Bradley Stohr: None

Background: Leucine zipper tumor suppressor 2 (*LZTS2*), a putative tumor suppressor gene, has been demonstrated as a negative regulator of microtubule severing during cytokinesis and a negative regulator of the Wnt signaling pathway. In a genetically modified mouse model, deletion of *Lzts2* altered normal ureteric bud branching morphogenesis and caused cystogenesis in mice (Peng, 2011). Cyst-lining cells demonstrated atypical features, closely resembling those observed in mouse models of human clear cell renal cell carcinoma (ccRCC), which were considered as preneoplastic lesions. Notably, high level expression of *LZTS2* is an unfavorable prognostic marker in ccRCC based on RNA sequencing (RNA-seq) data that are available in The Cancer Genome Atlas (TCGA) analyzed by The Human Protein Atlas Project. However, the functions of *LZTS2* in human ccRCC remain largely unknown. Therefore, the aim of this study is to establish an association between *LZTS2* expression and clinicopathologic features of ccRCCs.

Design: Gene expression data by RNA-seq for cohorts of 512 ccRCC cases that have clinical outcome data were extracted from TCGA through cBioPortal. Chi-squared tests, Kaplan-Meier curves and Cox regression models were used to investigate the possible relationship between *LZTS2* mRNA expression levels (z scores) and clinicopathological characteristics as well as patient survival. To examine its cellular localization, we performed LZTS2 antibody staining and scored expression levels (H score) in a pilot study of 35 ccRCCs.

Results: Our analysis of the TCGA data demonstrated that higher LZTS2 expression correlates with worse overall survival and disease specific survival ($p < 0.001$) (Figures 1A and 1B), as well as higher histologic grade ($p = 0.0223$) (Figure 1C). Multivariate Cox regression analysis revealed that high level of LZTS2 is an independent poor prognostic factor for overall survival (HR=5.521 $p = 0.004$) and disease-specific survival (HR=14.881 $p = 0.006$) in ccRCC. By immunohistochemistry, LZTS2 demonstrated predominantly cytoplasmic staining. Four staining patterns were observed as shown in Figure 2. High level cytoplasmic, but not membranous LZTS2 staining correlates with high nuclear grades ($p = 0.041$) in ccRCCs. Thus, LZTS2 IHC staining revealed a range of expression levels and a

diversity of staining patterns, suggesting that LZTS2 may function differently in ccRCCs of various histologic grades. Its role as a biomarker for centrosome amplification in ccRCC is being investigated.

Figure 1 - 494

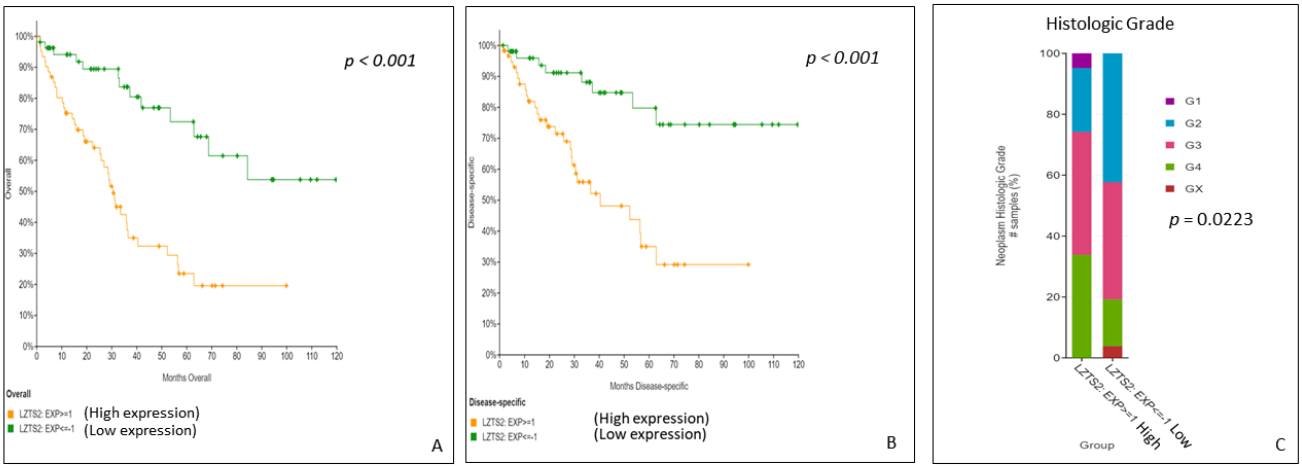

Figure 2 - 494

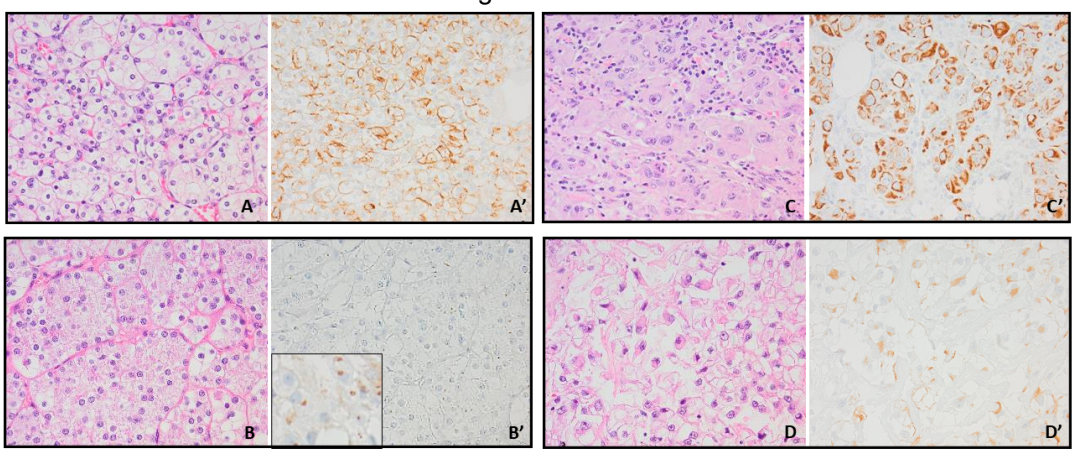

Representative CcRCC specimens (A, B, C, D) and corresponding LZTS2 immunostaining patterns. A and A') A nuclear grade 2 tumor with patchy membranous staining pattern. B and B') A nuclear grade 2-3 tumor with perinuclear dot-like centrosomal staining pattern. C and C') A nuclear grade 4 tumor with perinuclear accentuation staining pattern. D and D') A rhabdoid nuclear grade 4 tumor with perinuclear aggregation staining pattern. All photos were taken at 400X.

Conclusions: Our pilot IHC study demonstrated both differential expression levels and various expression patterns of LZTS2 in ccRCCs. A larger scale of study will be performed to understand how these two parameters correlate with tumor grades, clinical behavior, and tumorigenesis.

495 Implications of a Negative Confirmatory Biopsy Among Men on Active Surveillance for Prostate Cancer Along with PTEN/ERG as a Predictor of Pathologic Progression

Anil Prasad[1], Kirk Lin[2], Ashish Prasad[3], Zane Bartlett[4], Kenneth Belkoff[5], Jay Page[5], Michael Levine[5], Rajal Shah[6]
[1]Northwest Medical Center, Tucson, AZ, [2]Arizona Urology Specialists, Phoenix, AZ, [3]Nova Southeastern University, Fort Lauderdale, FL, [4]Burrell College of Osteopathic Medicine, Las Cruces, AZ, [5]Arizona Institute of Urology, Tucson, AZ, [6]UTSouthwestern Medical Center, Dallas, TX

Disclosures: Anil Prasad: None; Anil Prasad: None; Kirk Lin: None; Ashish Prasad: None; Zane Bartlett: None; Rajal Shah: None

Background: Active surveillance (AS) is increasingly used in managing very low-risk and low risk prostate cancer. To mitigate the risk of unsampled higher risk disease, most AS protocols call for a confirmatory prostate biopsy (B2) within 12-18 months following initial diagnostic biopsy. In this study, we investigate whether the results of confirmatory biopsy impact the outcomes of men on AS. We also assessed the role PTEN/ERG FISH Assay as a predictor of pathologic progression.

Design: We retrospectively reviewed all prostate biopsy results from men enrolled in AS between January 2017-December 2019. All AS patients had a serum prostate-specific antigen (PSA) level of ≤ 10 ng/ml, cT1 or T2 stage disease, Gleason grade 6, </=3 positive cores, and no core involved with >50% tumor. Results of PTEN/ERG FISH Assay performed on the initial positive biopsy were also recorded. Only patients with three or more consecutive biopsies were selected and then dichotomized based on presence or absence of cancer on B2, most of which were performed between 12 to 24 months of initial diagnosis. PSA levels were measured at the time of every serial biopsy.

Results: A total of 123 out of 499 men were enrolled in AS (24%). There were 105 fusion biopsies and 18 non fusion biopsies. 25 out of these 123 men (20%) had negative B2. Out of the remaining 98 positive B2, 87 had stable disease in terms of grade and volume whereas 11 had an upgrade of Gleason's score from 3+3 to 3+4. A third serial biopsy on all 25 negative B2 revealed no disease in 20 men. Five showed similar grade and volume of cancer to the first biopsy. PTEN/ERG FISH assay revealed no deletion or fusion in 113 of 123 men on AS. 10 had PTEN deletion and no ERG fusion. 4 of these 10 had stable disease on subsequent biopsies while 6 had an upgrade in Gleason's score &/tumor volume with increase in PSA levels.

Conclusions: Our study shows that negative B2 in men on AS is about 20% and these men have a reduced risk of pathologic progression in grade and tumor volume (>3 positive cores/>50% tumor in a single core), hence the intensity of their follow up can be reduced. Low risk PTEN/ERG profile is a reliable predictor of absence of disease progression and an indicator of low grade disease.

496 Molecular Profiling of Clear Cell Adenocarcinoma of the Urinary Tract

Rayan Rammal[1], Antoun Toubaji[2], Judy Sarungbam[1], S. Joseph Sirintrapun[1], Ying-Bei Chen[1], Anuradha Gopalan[1], Samson Fine[1], Satish Tickoo[1], Bernard Bochner[1], Eugene Pietzak[1], Jonathan Rosenberg[1], Dean Bajorin[1], Gopa Iyer[1], David Solit[1], Victor Reuter[1], Hikmat Al-Ahmadie[1]
[1]Memorial Sloan Kettering Cancer Center, New York, NY, [2]George Washington University Medical Faculty Associates, Washington, DC

Disclosures: Rayan Rammal: None; Antoun Toubaji: None; Judy Sarungbam: None; S. Joseph Sirintrapun: None; Ying-Bei Chen: None; Anuradha Gopalan: None; Samson Fine: None; Satish Tickoo: None; Bernard Bochner: None; Eugene Pietzak: None; Jonathan Rosenberg: None; Dean Bajorin: None; Gopa Iyer: *Consultant*, Mirati Therapeutics; *Grant or Research Support*, SeaGen, Inc; *Grant or Research Support*, Janssen; David Solit: *Consultant*, Pfizer; *Consultant*, Lilly Oncology; *Consultant*, BridgeBio; Victor Reuter: None; Hikmat Al-Ahmadie: None

Background: Clear cell adenocarcinoma (CCA) of the urinary tract is a rare tumor, commonly involving the urethra, occurs predominantly in females and histologically resembles clear cell carcinoma of the female genital tract. Molecular characteristics of CCA are not well-documented. The aim of this study is to investigate the pathologic and genomic features of primary CCA of the urinary tract.

Design: We performed a retrospective review of Memorial Sloan Kettering Cancer Center database from 2002-2020 to identify patients with CCA. Slides were reviewed and clinical data was collected. Targeted Next Generation Sequencing (NGS) was performed using MSK-IMPACT on tumors with available tissue.

Results: We identified 26 patients with primary CCA arising in: urethra (n=20), bladder (n=4) and ureter/renal pelvis (n=2). There were 21 females (81%) and 5 males (19%). The age range was 21-76 years (mean 52.3; median 59). The procedures performed included: radical cystectomy (n=15), TUR (n=5), partial excision/urethrectomy (n=3), nephroureterectomy (n=2) and urethral biopsy (n=1). The tumor was most commonly located in the urethra/periurethral gland (n=20). Other locations included bladder trigone or posterior wall (n=4), distal ureter (n=1) and renal pelvis (n=1). Association with urethral diverticulum was identified in 9 patients, all of whom were females. Invasive urothelial carcinoma with nested features was found in one case admixed with CCA and urothelial atypia bordering on urothelial carcinoma in situ was found in 2 additional cases. Tumor morphology consisted of tubulocystic, glandular, solid and nested patterns, with one tumor each additionally showing a sarcomatoid component and areas of marked nuclear pleomorphism.

NGS was performed on tumors from 16 patients. There were 82 mutations in 57 different genes (range: 0-24 mutations per sample; mean 5.5; median 4). The most common mutations were found in *ARID1A* (n=4), *TP53* (n=4), *KRAS* (n=3), *PPP2R1A* (n=2) and *SMARCA4* (n=2). Other putative driver mutations were found in one of each of *TSC1, PTEN, PIK3R1*, *SMAD4*, *FBXW7*, *ATM*, *ATR* and *ARID1B*. Only one tumor harbored a *TERT* promoter mutation and one tumor harbored *ERBB2* amplification. Copy number alterations were uncommon (range: 0-7 copy number alterations per sample; mean 1; median 0.5). Of note, one tumor each harbored amplification in *ERBB2*, *EGFR* and *CD274* and one tumor harbored *CDKN2A* deletion.

Conclusions:

- Clear cell adenocarcinoma (CCA) of the urinary tract primarily involves the urethra but can arise in the urinary bladder or rarely in the ureter.
- CCA most commonly affects females.
- The most frequently mutated genes are *ARID1A*, *TP53*, *KRAS* and *PPP2R1A.*
- Unlike urothelial carcinoma, *TERT* promoter mutation is rare.
- CCA may rarely harbor copy number alterations with potential therapeutic implications.
- The mutation profile of CCA is more similar to CCA of the female genital tract than to urothelial carcinoma.

497 Novel AI-Based Solution for Supporting Prostate Cancer Diagnosis Increases the Efficiency and Accuracy of Reporting in Clinical Routine

Delphine Raoux[1], Issar Yazbin[2], Shay Arbov[3], Gev Decktor[3], Stéphane Rossat[4], Vincent Rouleau[5], Claire Tingaud[4], Christian Boissy[4], Severine Carpentier[4], Frederic Neumann[6], Jean-Pierre Terrier[4], Manuela Vecsler[3], Daphna Laifenfeld[3], Chaim Linhart[3]
[1]Medipath, Toulon, France, [2]Ibex Medical Analytics, Israel, [3]Ibex Medical Analytics, Tel Aviv, Israel, [4]Medipath, Frejus, France, [5]Medipath Perpignan, Perpignan, France, [6]Medipath, Eguilles, France

Disclosures: Delphine Raoux: None; Issar Yazbin: *Employee*, Ibex Medical Analytics; Shay Arbov: *Employee*, Ibex Medical Analytics; Gev Decktor: None; Stéphane Rossat: None; Vincent Rouleau: None; Claire Tingaud: None; Christian Boissy: None; Severine Carpentier: None; Frederic Neumann: None; Jean-Pierre Terrier: None; Manuela Vecsler: *Employee*, Ibex Medical Analytics; Daphna Laifenfeld: *Employee*, Ibex Medical Analytics; Chaim Linhart: None

Background: There is a high demand to develop clinically useful computer-assisted diagnostic solutions to bring about significant efficiency improvements for pathologists, reduce turn-around times (TATs), decrease error rates, and provide objective, reproducible, and detailed diagnoses. Successful implementations of digital pathology in a variety of scenarios have started to demonstrate benefits for both research and routine diagnosis, encouraging adoption, however, implementation of AI as clinical support solution during diagnosis reporting is yet to be implemented. While several publications have demonstrated the feasibility of developing such algorithms and tools, this is the first report of a study in which pathologists perform the full diagnosis with the support of and artificial intelligence (AI)-based solution.

AIM: To demonstrate the impact of an AI-based tool used to support the pathologist as they review prostate core needle biopsies (PCNBs) on reporting efficiency and accuracy and on turnaround time in a large network of pathology laboratories.

Design: A two-arm study in which the standard of care arm (using a microscope) was compared with an arm in which pathologists conducted the reporting using an AI-based solution workflow. Eight pathologists from six different sites participated in the study, and reported on 1,231 slides from 160 PCNB cases (20 cases/ pathologist). Each case was reported twice, both with the microscope and with the AI-based solution randomized between pathologists. Detailed time measurements were taken for each step and compared between study arms, as was TAT. To assess the effect on the accuracy of reporting, discrepant reports were adjudicated and reviewed by a team of blinded uropathologists.

Results: The study endpoints included the accuracy of the AI-based algorithm on prostate cancer detection, grading and tumor quantitation, the efficiency of the pathologists reporting with the AI solution, TAT, and pathologists' satisfaction/feedback. The study demonstrated that reporting with the AI-based solution leads to >30% efficiency gains and a significant decrease in TAT.

Conclusions: This is the first report of an AI-based workflow supporting the diagnostic process in PCNBs. Significant efficiency gains are observed for the pathologist in addition to the potential of improving diagnosis accuracy and harmonization. Moreover, the overall user experience, as reported by pathologists, was markedly better with the AI solution compared to a microscope.

498 Pathology Data Based Risk Group Stratification is Equivalent to that Obtained by Oncotype DX Testing in Prostatic Adenocarcinoma

Pranav Renavikar[1], Subodh Lele[1]
[1]*University of Nebraska Medical Center, Omaha, NE*

Disclosures: Pranav Renavikar: None; Subodh Lele: None

Background: Prostate carcinoma cases diagnosed as Gleason score 3+3 (low risk/grade) or 3+4 (intermediate risk/grade) on needle biopsy of the prostate are frequently referred for gene expression studies such as Oncotype DX (Genomic Health, Redwood City, CA) to help confirm or validate the risk. Risk assessment helps in determining prognosis and therapeutic decision making (watchful waiting versus intervention). The goal of this study is to determine if addition of molecular testing is necessary (due to higher cost of testing), by evaluating its correlation with risk stratification provided by information in the pathology report (Gleason score, grade group, number of positive cores, percent involvement) on routine biopsy assessment and PSA level. To our knowledge, such a study in which the biopsy pathology data in more than 95% of cases was all assessed by one pathologist prior to molecular testing and subsequent follow-up data was also reviewed, has not been previously published.

Design: Our single institutional pathology database was searched for cases that had molecular testing (Oncotype DX) after prostate biopsy. The final risk category determined by molecular testing studies was recorded and compared to the risk stratification predicted by information in the surgical pathology report (Gleason score, grade group, number of positive cores, percent involvement) and PSA levels. Cases were classified as concordant if they fell under the same NCCN risk/recommended initial therapy group. Follow-up information (radical prostatectomy pathology findings or watchful waiting results) on discordant cases was obtained and used to determine if risk stratification by molecular testing was superior to that obtained from the pathology data and PSA level.

Results: A total of 4967 prostate biopsy cases (2015-2020) were reviewed. More than 95% of the carcinomas had been diagnosed and graded by one of the authors. 131 prostate carcinoma cases had Oncotype DX testing and 113 cases had follow-up information. There was direct risk stratification concordance in 83% of cases. All 17% of cases that were discordant had a follow-up course that matched the risk predicted by pathology biopsy data and PSA level.

Conclusions: Risk stratification provided by information in the pathology report (Gleason score, grade group, number of positive cores, percent involvement) on routine biopsy assessment coupled with PSA level is equivalent to that obtained by Oncotype DX testing.

499 Comparative Molecular Analysis Demonstrates the Presence of Three Genetic Subsets of Aggressive Leydig Cell Tumors

Natalie Rizzo[1], Lynette Sholl[1], Muhammad Idrees[2], John Cheville[3], Kristine Cornejo[4], Sounak Gupta[3], Hiroshi Miyamoto[5], Michelle Hirsch[1], Andres Acosta[6]
[1]Brigham and Women's Hospital, Boston, MA, [2]Indiana University School of Medicine, Indianapolis, IN, [3]Mayo Clinic, Rochester, MN, [4]Massachusetts General Hospital, Boston, MA, [5]University of Rochester Medical Center, Rochester, NY, [6]Brigham and Women's Hospital, Harvard Medical School, Boston, MA

Disclosures: Natalie Rizzo: None; Lynette Sholl: *Grant or Research Support*, Genentech; Muhammad Idrees: None; John Cheville: None; Kristine Cornejo: None; Sounak Gupta: None; Hiroshi Miyamoto: None; Michelle Hirsch: None; Andres Acosta: None

Background: Testicular Leydig cell tumors (tLCTs) represent 1-2% of testicular neoplasms overall. Although most are benign, < 5% show an aggressive biology (a-tLCTs). Given the rarity of a-tLCTs, their genetic alterations and molecular differences with indolent tLCTs remain unclear. This study compared the genetic alterations present in a-tLCTs and non-aggressive tLCTs, including mitotically active (ma-tLCT) cases that did not fully meet criteria for malignancy.

Design: Primary tumors were classified as tLCT-not otherwise specified if they had 0-1 mitoses/10 hpf, ma-tLCT if they had ≥2 mitoses/10 hpf, and a-tLCT if they met criteria for malignancy as described in the literature. Next generation sequencing (447 gene solid tumor panel) was performed. Immunohistochemistry for FH and beta-catenin was also done in a subset of cases.

Results: The cohort comprised 22 tumors from 18 patients collected between 1975-2019, including 10 a-tLCT (6 primaries, 4 metastases), 5 ma-tLCTs and 3 tLCTs (table). Twenty samples from 16 cases (8 a-tLCTs, 5 ma-tLCTs, 3 tLCTs) underwent successful sequencing (figure). Overall, the findings were as follows: 3/16 cases harbored FH mutations, 7/16 cases harbored *CTNNB1* mutations (with or without copy number variants [CNV]), 2 cases harbored only CNVs and 4 cases had no molecular alterations. CNVs, including recurrent 22q loss (4/16) and chromosome 7 gain (4/16), were only seen in a-tLCTs (6/8) and ma-tLCT (3/5). Similarly, biallelic inactivation of *FH* was only seen in a-tLCTs (2/8) and ma-tLCTs (1/5). Although the *FH*-mutated ma-tLCT did not formally meet criteria for malignancy, it measured 4 cm, had 12 mitoses/10hpf and harbored an activating *BRAF* G469V co-mutation and multiple CNVs. Activating *CTNNB1* variants were identified in 4/8 a-tLCTs, 2/5 ma-tLCTs and 1/3 tLCTs. The 2 a-tLCTs with *CTNNB1* mutations but no CNVs had <3 mitoses/10 hpf but met additional criteria for malignancy. Two a-tLCTs showed only CNVs, including *MDM2/CDK4* co-amplification, without concurrent mutations. Four cases (2/5 ma-tLCTs, 2/3 tLCTs) did not harbor any variants. Loss of FH expression (2/2 tested) and nuclear beta-catenin (6/6 tested) was confirmed by immunohistochemistry.

Case	Age	Primary	Met	a-tLCT	ma-tLCT	tLCT-NOS	Mitoses/10hpf	Genomic type
1	56		x	x			25	FH-mutated
2	27	x		x			6	FH-mutated
3	71	x		x			10	CTNNB1-mutated
4	77		x	x			14	CTNNB1-mutated
5	38	x		x			1	CTNNB1-mutated
6	69	x		x			2	CTNNB1-mutated
7	59		x	x			5	CNV only
8	70		x	x			15	CNV only
9	76	x			x		12	FH-mutated
10	65	x			x		2	CTNNB1-mutated
11	36	x			x		4	CTNNB1-mutated
12	46	x			x		4	No alterations
13	21	x			x		3	No alterations
14	39	x				x	1	CTNNB1-mutated
15	31	x				x	1	No alterations
16	21	x				x	0	No alterations
17*	80	x		x			2	N/A
18*	71	x		x			1	N/A

a-tLCT: Aggressive Leydig cell tumor
ma-tLCT: Non-aggressive and ≥2 mitoses/10hpf
tLCT-NOS: Non-aggressive and <2 mitoses/10hpf

Met: metastatic
*Failed NGS

Figure 1 - 499

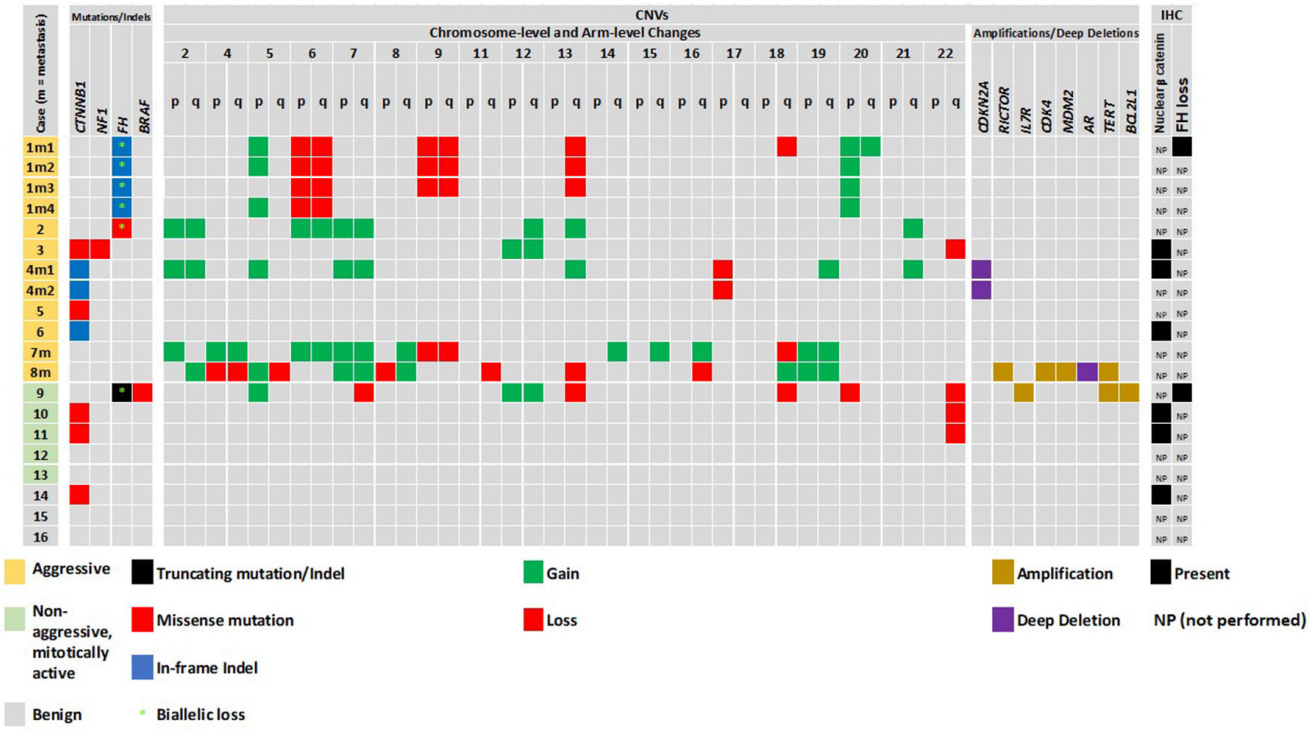

Conclusions: Three distinct subsets of a-LCTs harbor *CTNNB1* mutations, *FH* mutations and only CNVs, respectively. *CTNNB1* activation appears to be an early event that occurs across the entire biologic spectrum and is usually found with additional genetic changes in ma-tLCTs and a-tLCTs. Analysis of additional a-tLCTs is ongoing.

500 Testicular Germ Cell Tumors with Spermatic Cord Involvement: A Retrospective International Multi-Institutional Experience

Maria Del Carmen Rodriguez Pena[1], Ali Amin[2], Manju Aron[3], Piergiuseppe Colombo[4], Roni Cox[5], Dilek Baydar[6], Ivan Gallegos[7], Francesca Khani[8], Kvetoslava Michalova[9], Roberta Lucianò[10], Hiroshi Miyamoto[11], Adeboye O. Osunkoya[12], Sofía Canete-Portillo[1], Maria Rosaria Raspollini[13], Diego F Sanchez[14], Federico Scarfò[15], Jeffrey So[16], Debra Zynger[17], Shi Wei[1], George Netto[1], Cristina Magi-Galluzzi[1]
[1]The University of Alabama at Birmingham, Birmingham, AL, [2]Alpert Medical School of Brown University, Providence, RI, [3]Keck School of Medicine of USC, Los Angeles, CA, [4]Humanitas Clinical and Research Center, IRCCS, Rozzano, Italy, [5]Cleveland Clinic, Cleveland, OH, [6]Koç University, Istanbul, Turkey, [7]Hospital Clínico Universidad de Chile, Santiago, Chile, [8]Weill Cornell Medicine, New York, NY, [9]Biopticka laborator s.r.o., Plzen, Czech Republic, [10]IRCCS San Raffaele Scientific Institute, Italy, [11]University of Rochester Medical Center, Rochester, NY, [12]Emory University, Atlanta, GA, [13]University Hospital Careggi, Firenze, Italy, [14]Instituto de Patologia e Investigacion, Asuncion, Paraguay, [15]Ospedale San Raffaele, Italy, [16]St. Luke's Medical Center, Quezon City, Philippines, [17]The Ohio State University Wexner Medical Center, Columbus, OH

Disclosures: Maria Del Carmen Rodriguez Pena: None; Ali Amin: None; Manju Aron: None; Piergiuseppe Colombo: None; Roni Cox: None; Dilek Baydar: None; Ivan Gallegos: None; Francesca Khani: None; Roberta Lucianò: None; Hiroshi Miyamoto: None; Adeboye O. Osunkoya: None; Sofía Canete-Portillo: None; Maria Rosaria Raspollini: None; Federico Scarfò: None; Jeffrey So: None; Debra Zynger: None; Shi Wei: None; George Netto: None; Cristina Magi-Galluzzi: None

Background: The 8th Edition AJCC Cancer Staging Manual designates discontinuous involvement of spermatic cord soft tissue (DISC) by testicular germ cell tumors (GCT) as a metastatic deposit, upstaging the patient to clinical stage (CS) III. We conducted a retrospective international multi-institutional review to validate the current recommendations.

Design: GCT with spermatic cord involvement were collected from 15 institutions in America, Europe, and the Philippines. Demographic, clinical, pathologic, and follow-up data was obtained.

Results: Forty-six cases were included in the study. Thirty-three (72%) cases were non-seminomatous (NSGCT) and 13 (27%) seminomatous (SGCT) tumors. Twenty-seven (81%) NSGCT harbored embryonal carcinoma (EC), ranging from 10% to 100%; 8 cases were pure EC. Testicular tumor size ranged from 1.3 to 18.0 cm (mean: 6.0). After review, cases were classified as DISC (n=26; 20 NSGCT, 6 SGCT), continuous cord involvement (CCI) (n=17; 10 NSGCT, 7 SGCT) or cord lymphovascular invasion (cLVI) (n=3 NSGCT). Mean size of spermatic tumor nodule for DISC was 1.0 cm (range: 0.1-4.5); mean size of tumor extending beyond the hilum and involving spermatic cord for CCI was 1.6 cm (range: 0.2-2.5).

CS at presentation was available for 43 and follow-up (FU) for 30 patients. Mean FU was 39 months (range: 2-144). CS for DISC patients was: CS I (local disease) in 1 (4%), CS II (regional disease) in 7 (30%), and CS III (distant disease) in 15 (65%) cases. Twelve (86%) DISC were M1a (involvement of lung or lymph nodes other than retroperitoneal); 2 (14%) M1b (*tumor* spread to organs other than lung). CS for CCI patients was: CS I in 8 (47%), CS II in 4 (24%), and CS III in 5 (29%). Four (66%) CCI were M1a; 2 (33%) M1b. cLVI cases were distributed 1 per stage; one cLVI was M1a. On FU, 12/15 (80%) DISC, 11/14 (78%) CCI and 1 cLVI patients had no evidence of disease (NED) or stable disease; 3 (20%) DISC and 3 (21%) CCI showed disease progression or relapse.

Despite comparable disease progression/relapse and M1a/b status, there was a significant difference in individual CS (CS I vs. CS II vs. CS III) (p=0.0047, Fisher test) and between non-advanced (CS I) and advanced CS (CS II & CS III) (p=0.0021, Fisher test) when comparing DISC and CCI (Table 1). After adjusting for age, race, histologic tumor type and %EC, DISC remained significant as an independent factor for advanced CS (p = 0.029).

Table 1. Demographic, pathologic, and outcome features of DISC and CCI patients.

Cases	Mean age, years	Mean tumor size, cm	SGCT	NSGCT	Mean %EC	CS I	CS II	CS III	Non-advanced CS (I)	Advanced CS (II, III)	NED/ stable disease	Disease progression/relapse	M1a	M1b
DISC 26 (60%)	37.5	5.9	6 (23%)	20 (77%)	30.6	1 (4%)	7 (30%)	15 (65%)	1 (4%)	22 (96%)	12 (80%)	3 (20%)	12 (86%)	2 (14%)
CCI 17 (40%)	41	7.1	7 (41%)	10 (59%)	43.8	*8 (47%)*	*4 (24%)*	*5 (29%)*	*8 (47%)*	9 (53%)	11 (79%)	3 (21%)	4 (66%)	2 (33%)
p	0.237	0.209	0.309		0.341	***0.0047***			***0.0021***		1.000		0.200	

Conclusions: Our findings contribute evidence to the role of DISC by testicular GCT as a marker of aggressive disease and support assigning a higher pathologic stage to DISC compared to CCI.

501 Assessment and Comparison of Microsatellite Stability on a Multi-Racial Cohort of High Grade Prostate Cancer Using Idylla MSI Test® and Immunohistochemistry

Maria Del Carmen Rodriguez Pena[1], Gina DeFrank[1], Carlos Prieto Granada[1], Sofía Canete-Portillo[1], Shuko Harada[1], Alexander Mackinnon[1], George Netto[1]
[1]*The University of Alabama at Birmingham, Birmingham, AL*

Disclosures: Maria Del Carmen Rodriguez Pena: None; Gina DeFrank: None; Carlos Prieto Granada: None; Sofía Canete-Portillo: None; Shuko Harada: None; Alexander Mackinnon: None; George Netto: None

Background: High risk prostate cancer (PCa) has been shown to be associated with somatic mismatch repair pathway defect and rarely with Lynch syndrome. African-American (AA) patients and those with PCa cribriform morphology or intraductal component have a worse outcome. We set out to determine and compare microsatellite instability (MSI) status in a cohort of AA and Caucasian patients with high grade PCa with cribriform pattern and/or intraductal component.

Design: Tissue curls from radical prostatectomies with high grade PCa with intraductal component, cribriform and/or ductal morphology were obtained and analyzed for MSI status utilizing the Idylla® MSI test. The automated, real-time PCR-based system performs melting curve analysis on amplified DNA and evaluates seven biomarkers located in the *ACVR2A, BTBD7, DIDO1, MRE11, RYR3, SEC31A and SULF2* genes. A score is assigned to each biomarker and an overall MSI score between 0.00 and 1.00 is obtained. A tumor is microsatellite unstable if the MSI score is high (MSI-H). MSI-H is defined as ≥2/7 positive markers or overall MSI Score ≥0.15. Tumors with ≤1/7 positive markers or MSI Score <0.15 are considered microsatellite stable (MSS).

A TMA was constructed with the same specimens, each represented by 4 tumor and 2 benign tissue spots. Immunohistochemical staining (IHC) for MSI was performed: MLH1, MSH2, MSH6 and PMS2. Retained expression was defined as presence of nuclear staining and loss of expression as absence of nuclear staining within tumor cells. Benign prostatic tissue, stromal cells and infiltrating lymphocytes were used as internal controls.

Results: A total of 59 samples were analyzed by Idylla MSI Test and IHC MSI panel, including 28 African-American and 31 Caucasian patients. Fifty six (95%) cases had 0/7 positive markers. Three (5%) cases had 1/7 positive markers. Biomarker DIDO1 was positive in 3 / 28 (11%) AA patients: MSI scores were as follows: DIDO1 0.72, overall 0.13; DIDO1 0.87, overall 0.10; DIDO1 0.89, overall 0.12 (Figure 1). All cases had <2/7 positive markers and <0.15 MSI score thus were classified as MSS. All cases evaluated with IHC MSI panel retained expression of MLH1, MSH2, MSH6, PMS2 and were classified as MSS (Figure 2).

Figure 1 - 501

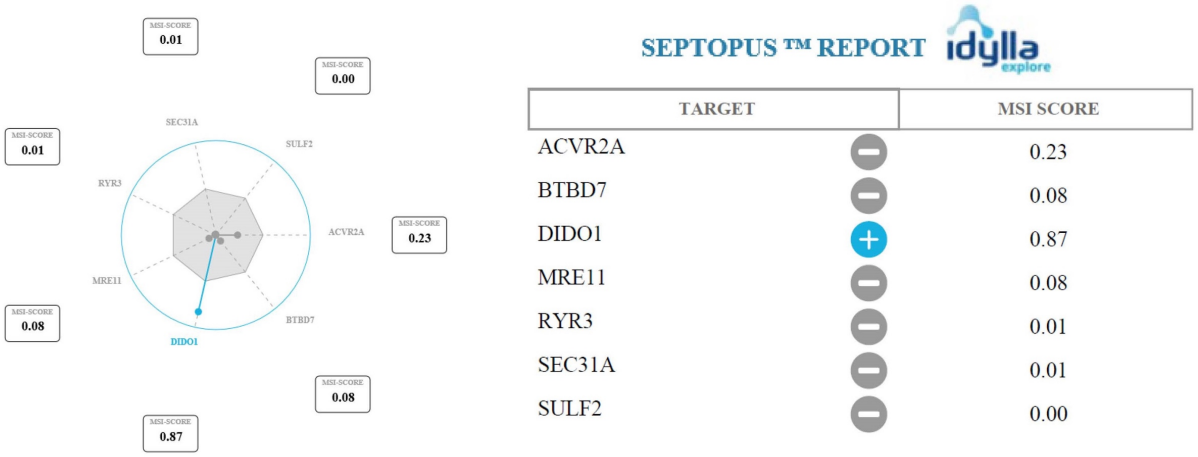

Figure 1. Septopus™ report for case #27. DIDO1 surpassed the cut-off value to be classified as positive; however, the overall MSI score was <0.15 (MSS).

Figure 2 - 501

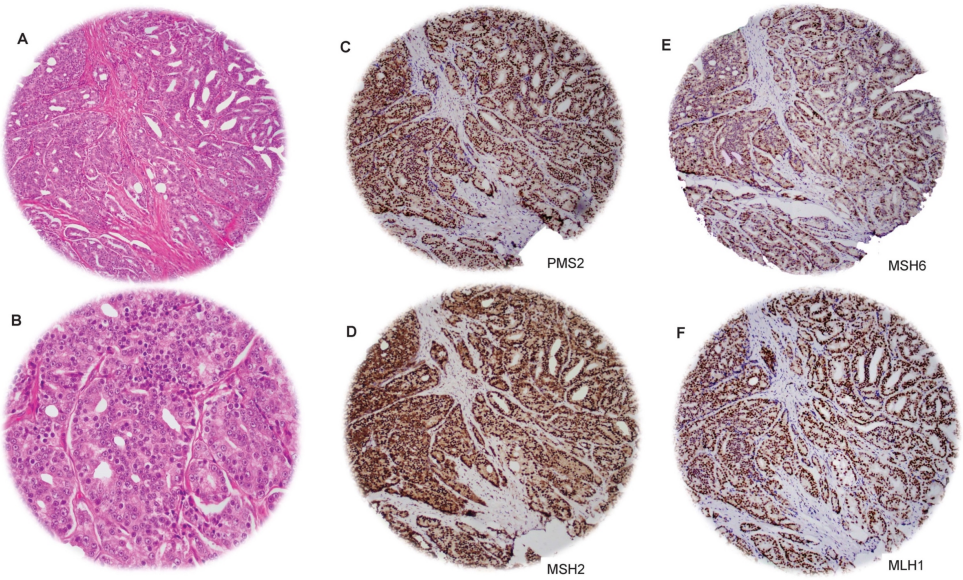

Figure 2. (A 20x, B 40x) H&E stained sections of case #27. The tumor has cribriform architecture characterized by solid nests with "punched-out" rigid lumen and atypical nuclei. (C - F 20x) Retained nuclear expression for each IHC marker component of the MSI panel.

Conclusions: This is the largest reported cohort of high grade PCa with intraductal component, cribriform and/or ductal morphology evaluated by both Idylla MSI Test and MSI IHC panel. There was 100% concordance between Idylla® MSI Test and IHC MSI panel. The Idylla MSI® test is a reliable, fully automated, easy to use option for MSI testing.

502 Genomic and Clinicopathologic Significance of BRCA2 Deletions versus BRCA2 Short Variant Mutations in Clinically Advanced Castrate Resistant Prostate Cancer (mCRPC)

Jeffrey Ross[1], Russell Madison[2], Ethan Sokol[2], Brennan Decker[2], Douglas Mata[2], Tyler Janovitz[2], Douglas Lin[2], J. Keith Killian[2], Natalie Danziger[2], Shakti Ramkissoon[3], Kimberly McGregor[2], Jeffery Venstrom[4], Alexa Schrock[2]

[1]Upstate Medical University, Syracuse, NY, [2]Foundation Medicine, Inc., Cambridge, MA, [3]Foundation Medicine, Inc., Morrisville, NC, [4]Foundation Medicine, Inc., San Francisco, CA

Disclosures: Jeffrey Ross: *Employee*, Foundation Medicine; Russell Madison: *Employee*, Foundation Medicine Inc.; *Stock Ownership*, Roche; Ethan Sokol: *Employee*, Foundation Medicine, Inc.; *Stock Ownership*, Roche; Brennan Decker: *Employee*, Foundation Medicine; Douglas Mata: *Employee*, Foundation Medicine, Inc.; Tyler Janovitz: *Employee*, Foundation Medicine; Douglas Lin: *Employee*, Foundation Medicine, Inc.; *Stock Ownership*, Roche; J. Keith Killian: *Employee*, Foundation Medicine; Natalie Danziger: *Employee*, Foundation Medicine Inc.; Shakti Ramkissoon: *Employee*, Foundation Medicine; Kimberly McGregor: *Employee*, Foundation Medicine; *Stock Ownership*, ROCHE; Jeffery Venstrom: *Employee*, Foundation Medicine; Alexa Schrock: *Employee*, Foundation Medicine; *Stock Ownership*, Roche

Background: The detection of BRCA2 genomic alterations (GA) by approved companion diagnostics is used to guide PARP inhibitor (PARPi) treatment of patients (pts) with mCRPC. Although rare, we recently showed that median time to PARPi treatment discontinuation (TTD) was significantly longer among mCRPC pts with a *BRCA1/2* deletion (del) vs other *BRCA1/2* alteration, and a trend for longer TTD among *BRCA2* vs. *BRCA1* patients (Antonarakis et al. ASCO 2020, Abstract 5527). Whether there are differences in clinical background or co-occurring alterations potentially contributing to these clinical differences remains unknown.

Design: 5,836 primarily mCRPC were sequenced using a hybrid capture-based FDA-approved comprehensive genomic profiling assay. Tumor mutational burden (TMB) was determined on up to 1.1 Mbp of sequenced DNA and microsatellite instability (MSI) was determined on 114 loci. Of these, a subset of 1,075 unique mCRPC pts were

treated in the Flatiron Health network, and thus included in a de-identified clinico-genomic database (CGDB). Clinical characteristics and PARPi treatment history were obtained via technology-enabled abstraction of electronic health records.

Results: Of 5,836 mCRPC cases, *BRCA2*del and *BRCA2* short variant (SV) GA were detected in 150 (2.6%) and 300 (5.1%) cases, respectively The *BRCA2*del pts were significantly older (P=.0004). GA in *TP53* (P=.04), *CDK12* (P=.02), *ATM* (P=.0003), *PIK3CA* (P=.01) and *BRAF* (P=.01) were significantly more frequent in *BRCA2* SV vs *BRCA*del pts. GA in *RAD21* were more frequent in *BRCA2*del pts (P=.01). Biomarkers favoring greater response to immune checkpoint inhibitors (ICPI) were more frequent in the *BRCA2* SV vs *BRCA2*del pts including MSI-high status (P.004), mean TMB (P=.002), TMB > 10 mut/Mb (P=.006) and TMB > 20 mut/Mb (P=.004).

Among mCRPC pts included in the CGDB with a *BRCA2*del (n = 6), unadjusted TTD on PARPi was 19 mos vs. 10 mos for pts with BRCA2 SV (n = 16). Statistical comparisons of TTD between the groups were not performed.

	*BRCA2*del mCRPC	*BRCA2*SV mCRPC	Significance
Number of Cases	150	300	
Median age (range) years	68 (39-89+)	65 (45-89+)	
Mean age	68.4	65.8	P=.004
GA/tumor	4.27	4.92	NS
TMPRSS2:ERG	39%	33%	NS
AR	15%	16%	NS
TP53	32%	42%	P=.04
PTEN	29%	32%	NS
MYC	17%	14%	NS
BRCA1	1%	1%	NS
CDK12	1%	6%	P=.02
ATM	0%	6%	P=.0003
RAD21	20%	11%	P=.01
PIK3CA	1%	7%	P=.01
RB1	8%	6%	NS
APC	11%	9%	NS
CCND1	1%	4%	NS
BRAF	0%	4%	P=.01
ERBB2	0%	1%	NS
MDM2	1%	1%	NS
MDM4	1%	2%	NS
PIK3C2B	1%	2%	NS
CDK4	0%	1%	NS
CDK6	2%	1%	NS
MSI High	0%	5.1%	P=.004
Median TMB	3.8	3.8	NS
Mean TMB	4.0	9.0	P=.002
TMB>10 mut/Mb	3%	11%	P=.006
TMB>20 mut/Mb	0%	5%	P=.004
PD-L1 Low Positive	7% (42 cases)	12% (109 cases)	NS
PD-L1 High Positive	0%	0%	NS

Conclusions: *BRCA2*del mCRPC differs significantly from *BRCA2* SV associated mCRPC in genomic signatures and likely propensity to benefit from ICPI based on *CDK12* mutation, MSI and TMB findings. However, in contrast with *BRCA2* SV mCRPC, the likely inability of *BRCA2*del mCRPC to produce *BRCA2* reversion mutations when treated with PARPi appears to be associated with longer TTD with these recently approved drugs.

503 Ductal Adenocarcinoma of the Prostate Confined to Prostatic Ducts (Intraductal Carcinoma with Ductal Cytology): A Series of 15 Cases Including 13 Cases Without Concurrent Invasive Cancer

Daniel Russell[1], Jonathan Epstein[2]
[1]Johns Hopkins Hospital, Baltimore, MD, [2]Johns Hopkins Medical Institutions, Baltimore, MD

Disclosures: Daniel Russell: None; Jonathan Epstein: None

Background: In the past, all prostatic duct adenocarcinomas were considered high-grade invasive carcinoma, regardless of the presence of a basal cell layer, based on the assumption that pre-existing ducts were colonized by invasive cancer. The current study investigates rare cases of IDCP with ductal cytology (IDCP-ductal) without invasive cancer or only associated low-grade cancer to determine whether they are always retrograde extension of high grade cancer or in some cases could represent a precursor lesion.

Design: The consultation files of the senior author (J.I.E.) were searched for cases of IDCP-ductal diagnosed between May 2017-April 2020, all of which had PIN4 performed, with clinical follow-up (3-36 months).

Results: 15 cases (13 patients) were identified. 13 patients lacked concurrent cancer and 2 had Gleason score (GS) 6. Of the 13 cases without concurrent cancer, follow-up was available on 11, with 4 cases of subsequent invasive cancer (1 GS 4+4=8; 1 GS 3+4=7 in 8 cores; 1 GS 4+5=9 pT3b pN1; 1 pT2 GS 6 on resection), 1 extensive IDCP-ductal, 1 extensive atypical intraductal proliferation-acinar on biopsy, and 1 benign TUR. The radical prostatectomy of the patient with GS6 with IDCP-ductal was totally embedded and serially sectioned with extensive basal immunohistochemistry performed documenting the lack of invasive high-grade cancer. 3/4 clinically managed patients had hormonal and radiation therapy, all with no evidence of disease to date, and 1 had radiation therapy only and now has biochemical recurrence. Of 12 cases available for re-review, all 12 contained papillary architecture, while 4 contained cribriform architecture (3 focally, 1 as the predominant pattern). Cytologically, cases were low (n=6) or moderate (n=6) nuclear grade.

Figure 1 - 503

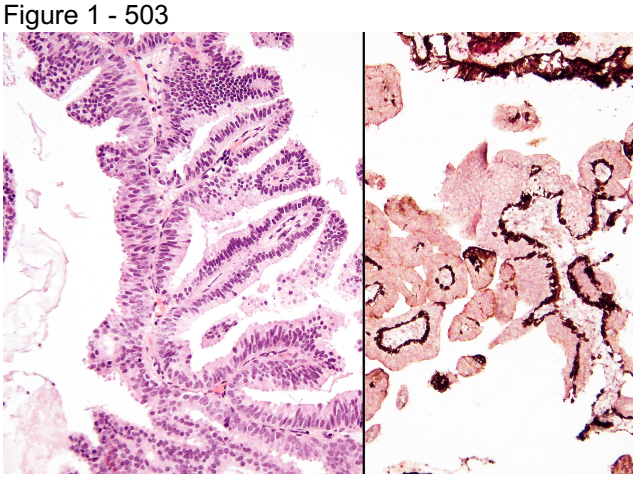

Conclusions: The current study documents the entity of IDC-ductal and characterizes its morphology. Analogous to usual acinar prostate adenocarcinoma, most cases of IDCP-ductal appear to represent retrograde invasion into pre-existing ducts by high-grade invasive carcinoma. However, rarely IDCP-ductal, similar to IDCP-acinar can exist as a precursor and not associated with invasive high-grade cancer. Our study supports reporting IDCP for ductal adenocarcinomas in an analogous manner to usual acinar prostate cancer, and not assuming that all cases of ductal adenocarcinoma that are growing with prostatic ducts (ie. surrounded by a basal cell layer) are high grade invasive tumor.

504 Verrucous Squamous Hyperplasia (VSH) of the Bladder: A Series of 23 Cases

Daniel Russell[1], Jonathan Epstein[2]
[1]Johns Hopkins Hospital, Baltimore, MD, [2]Johns Hopkins Medical Institutions, Baltimore, MD

Disclosures: Daniel Russell: None; Jonathan Epstein: None

Background: There is very scant data in the literature on VSH and its relation to carcinoma of the urinary bladder.

Design: The consultation files of the senior author (J.I.E.) were searched for cases containing VSH, with or without concurrent carcinoma diagnosed between August 2010-2019. For patients without concurrent carcinoma, clinical follow-up was obtained (median 47 mos.) and High Risk RNA HPV-in situ hybridization (ISH) was performed.

Results: Of 23 cases, 11/23 had concurrent carcinoma (mean 73.6 yrs, range 41-96). Of the 12 cases without concurrent carcinoma, clinical follow up was available for 9/12. 1/12 had clinical features highly suggestive of carcinoma and was scheduled for cystectomy (patient cancelled and was lost to follow up), 1/12 had features of fungal cystitis, 1/12 developed a benign ulcer, 4/12 were dead not from disease, and 2/12 were lost to follow-up. Of patients with concurrent carcinoma: 4/11 had extensive VSH with at least in situ squamous cell carcinoma/cannot rule out superficial invasion; 2/11 had mixed sarcomatoid urothelial carcinoma with squamous cell carcinoma; 2/11 had well-differentiated squamous cell carcinoma with 1/2 associated with longstanding schistosomiasis; 1/11 had poorly-differentiated squamous cell carcinoma; and 1/11 showed invasive urothelial carcinoma with lymphoepithelioma-like features. High Risk HPV RNA-ISH was negative in all cases with carcinoma (0/11).

Figure 1 - 504

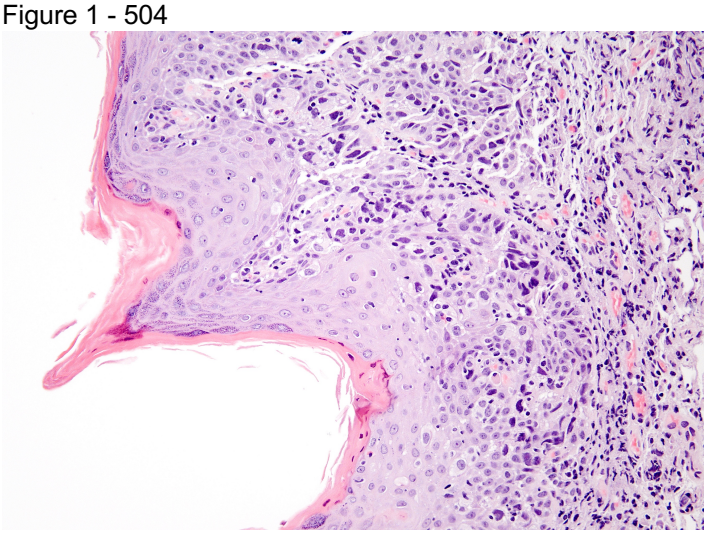

Conclusions: The current study, the largest series to date investigating VSH, supports its association with concurrent squamous cell carcinoma. What is still unclear, given the small number of patients with limited clinical follow-up, is the risk of subsequent carcinoma following isolated VSH without other concurrent high-risk findings. Until more data is accumulated, it appears prudent to recommend close clinical follow-up. In our series, HR HPV was unassociated with VSH-associated carcinoma. This is consistent with the literature that HPV-associated bladder cancers, including squamous cell carcinoma, are exceptionally rare.

505 Assessment of MYC/PTEN Status by Gene-Protein Assay in Grade Group 2 Prostate Biopsies

Daniela Salles[1], Thiago Vidotto[1], Farzana Faisal[2], Jeffrey Tosoian[3], Liana Benevides Guedes[4], Andrea Muranyi[5], Isaac Bai[6], Shalini Singh[7], Dongyao Yan[8], Kandavel Shanmugam[8], Tamara Lotan[2]
[1]Johns Hopkins Medical Institutions, Baltimore, MD, [2]Johns Hopkins University School of Medicine, Baltimore, MD, [3]University of Michigan, Ann Arbor, MI, [4]Johns Hopkins University, Baltimore, MD, [5]Roche, Indianapolis, IN, [6]Ventana Medical Systems, Inc., Oro Valley, [7]Roche Diagnostics Corporation, Tucson, AZ, [8]Roche, Oro Valley, AZ

Disclosures: Daniela Salles: None; Thiago Vidotto: None; Farzana Faisal: None; Jeffrey Tosoian: None; Liana Benevides Guedes: None; Andrea Muranyi: *Employee*, Roche Diagnostics; *Stock Ownership*, Roche Diagnostics; Isaac Bai: None; Shalini Singh: *Employee*, Roche Diagnostics; Dongyao Yan: *Employee*, Roche; Kandavel Shanmugam: *Employee*, Roche; *Employee*, Roche; Tamara Lotan: *Grant or Research Support*, Roche; *Grant or Research Support*, DeepBio

Background: Men with Grade Group 2 (Gleason 3+4=7) prostate cancer on needle biopsy have variable oncologic outcomes and genomic markers may identify patients at risk of progression. We tested a gene-protein assay to assess *MYC* and PTEN status in a cohort of Grade Group 2 patients.

Design: We leveraged a previously characterized cohort of 277 patients with Grade Group 2 diagnostic needle biopsies followed by radical prostatectomy at Johns Hopkins from 2000-2014. We annotated the maximal size of cribriform Gleason pattern 4 carcinoma and the presence of intraductal carcinoma (via p63) in each case. The biopsy block with the highest tumor volume was selected for an automated gene-protein chromogenic assay performed on a BenchMark IHC/ISH platform to simultaneously assess *MYC* gain by chromogenic *in situ* hybridization and PTEN loss by immunohistochemistry.

Results: *MYC* gain or PTEN loss alone were present in 19% and 18% of biopsies, respectively, while both alterations were present in 9%. Tumors with one or both molecular alterations were significantly more likely to show non-organ confined disease at prostatectomy. In logistic regression models including clinical stage, tumor volume on biopsy, presence of large cribriform Gleason pattern 4 foci or intraductal carcinoma, cases with *MYC* gain and PTEN loss remained at higher risk for non-organ confined disease (OR: 5.84; 95% CI: 1.60-23.15; p=0.008). The area under the curve (AUC) for a baseline model using pre-operative variables from the CAPRA score was increased from 0.64 to 0.71 upon adding *MYC*/PTEN status and to 0.74 upon inclusion of intraductal/large cribriform carcinoma status.

Conclusions: Dual *MYC*/PTEN genomic status can be assessed in a single slide using a novel, automated gene-protein assay and is independently associated with increased risk of non-organ confined disease for Grade Group 2 biopsies, adding to pre-operative parameters commonly used to predict adverse pathology at prostatectomy.

506 PTEN and ERG Status is Associated with Biochemical Recurrence after Radical Prostatectomy with Positive Surgical Margins

Daniela Salles[1], Adrianna Mendes[1], Misop Han[2], Alan Partin[2], Bruce Trock[3], Tamara Lotan[4]
[1]Johns Hopkins Medical Institutions, Baltimore, MD, [2]Johns Hopkins Hospital School of Medicine, Baltimore, MD, [3]The Johns Hopkins Medical Institutions, Baltimore, MD, [4]Johns Hopkins University School of Medicine, Baltimore, MD

Disclosures: Daniela Salles: None; Adrianna Mendes: None; Misop Han: None; Alan Partin: None; Bruce Trock: *Grant or Research Support*, Myriad Genetics, Inc; *Grant or Research Support*, MDxHealth, Inc.; Tamara Lotan: *Grant or Research Support*, Roche; *Grant or Research Support*, Myriad Genetics; *Grant or Research Support*, DeepBio

Background: Positive surgical margins at prostatectomy (RP) are associated with increased risk of biochemical recurrence (BCR), metastatic progression, and cancer-specific mortality. However, there is considerable variability in outcomes among men with positive margins, and clinicians must decide whether adjuvant radiation and hormonal therapy are needed. Accordingly, there is interest in determining whether risk of progression can be more finely stratified by evaluating genomic biomarkers in the tissue at the site of the positive margin.

Design: We used a case-cohort design for the outcome of BCR, selecting 215 patients from a cohort of 813 RP patients treated at Johns Hopkins Hospital from 2008-2017 with positive surgical margins and available clinical data. Tissue microarrays (TMA) with quadruplicate sampling were created from the tumor at the surgical margin and stained for PTEN, ERG and Ki-67. Cases were scored dichotomously (PTEN, ERG) or by Ki-67 staining index, using previously validated protocols. Analysis employed conditional logistic regression weighted for case-cohort design.

Results: Overall, 19.2% (37/193) of evaluable cases had PTEN loss and 36.9% (73/198) of evaluable cases had ERG expression. The median Ki-67 index was 0.42%. In univariable analysis, PTEN, ERG and Ki-67 were all significantly associated with BCR. In multivariable analysis adjusting for adjuvant radiation, CAPRA-S score (which includes preoperative prostate specific antigen levels, RP Grade Group, surgical margins status, extraprostatic extension, seminal vesicle invasion, and lymph node invasion) and the 4 categories of combined PTEN/ERG status, PTEN/ERG status remained significantly associated with risk of BCR, though Ki-67 was no longer significant. ERG positive tumors with intact PTEN (HR=3.04; 95% CI:1.13-8.16), p<0.0001, and ERG positive tumors with PTEN loss (HR=6.01; 95% CI: 2.58-13.99) , p=0.027,were both significantly associated with a higher risk of BCR compared to those that were ERG negative with PTEN intact.

Conclusions: ERG positive tumors with or without PTEN loss at the positive surgical margin at RP are associated with a significantly higher risk of BCR, even when controlling for clinical-pathologic variables and adjuvant treatment. If validated, ERG/PTEN status may be useful in decision-making surrounding adjuvant treatment after RP.

507 Role of Hexokinase-1 and LAMP-1 Immunohistochemistry to Differentiate Oncocytoma and Chromophobe Renal Cell Carcinoma from Other Renal Neoplasms

Swati Satturwar[1], Dimitrios Korentzelos[1], Susana Jorge[2], Gabriela Quiroga-Garza[1], Sheldon Bastacky[1], Hugo Santos[3], Jose-Luis Capelo-Martínez[4], Rajiv Dhir[5]
[1]University of Pittsburgh Medical Center, Pittsburgh, PA, [2]Lisbon, Portugal, [3]LAQV-REQUIMTE, Caparica, Portugal, [4]Caparica, Portugal, [5]UPMC Shadyside Hospital, Pittsburgh, PA

Disclosures: Swati Satturwar: None; Dimitrios Korentzelos: None; Susana Jorge: None; Gabriela Quiroga-Garza: None; Sheldon Bastacky: None; Hugo Santos: None; Jose-Luis Capelo-Martínez: None; Rajiv Dhir: None

Background: Renal oncocytomas (RO) are benign and chromophobe renal cell carcinomas (chRCC) are malignant neoplasms of the kidney, respectively with overlapping histomorphology. In an effort to design new diagnostic modalities for kidney tumors, a proteomics-based approach was utilized to study differential protein expression on biopsies of 5 RO, 5 chRCC, 7 clear cell renal carcinoma (ccRCC), 5 papillary renal cell carcinoma (p RCC) and 5 normal adjacent tissue (NAT) samples. Top differentially expressed proteins were identified as potential novel biomarkers. Of these biomarkers, hexokinase (HK-1) is involved in the glycolysis pathway and lysosomal associated membrane protein -1 (LAMP-1) presents carbohydrate ligand to selectins and shuttles between endosome-lysosome membrane and plasma membrane. The aim of this study was to validate these biomarkers by using immunohistochemistry (IHC).

Design: Tissue micro-arrays (TMAs) were constructed using 4 cores of RO (n=30), chRCC (n=12), ccRCC (n=40), p RCC (n=26) and 1 core of NAT (n=20). IHC was performed using rabbit monoclonal antibodies for proteins: HK-1 [EPR10134(B), Abcam] and LAMP-1 (EPR4204, Abcam). Granular cytoplasmic staining of any intensity was considered as positive. Granules were scored as (0=negative, 1=focal, 2=moderate, 3=abundant) for HK-1 and (0=negative; D=diffuse, A=apical, F=focal) for LAMP-1. Percent positivity of the cells was also recorded.

Results: Figures 1 and 2 summarizes HK-1 and LAMP-1 IHC results. HK-1 showed diffuse positivity in most ROs. With a cut-off of 2 or above score and >90% cells positivity; HK-1 has a sensitivity of 96.7% and a specificity of 98.7% to distinguish ROs from other renal neoplasms. LAMP-1 shows diffuse positivity in chRCCs and apical or focal positivity in ROs. Diffuse LAMP-1 staining has a sensitivity of 91.7% and specificity of 100% to distinguish Chromophobe RCC from other renal neoplasms. Both markers showed variable positivity in normal kidney tissue and were negative in most ccRCCs and pRCCs.

Figure 1 - 507

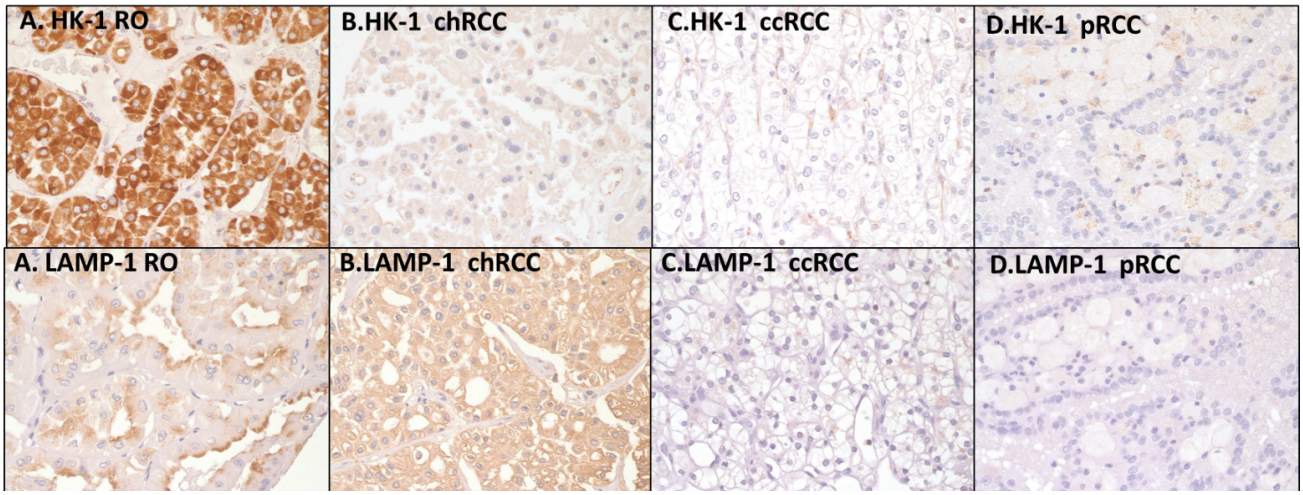

Figure 2 - 507

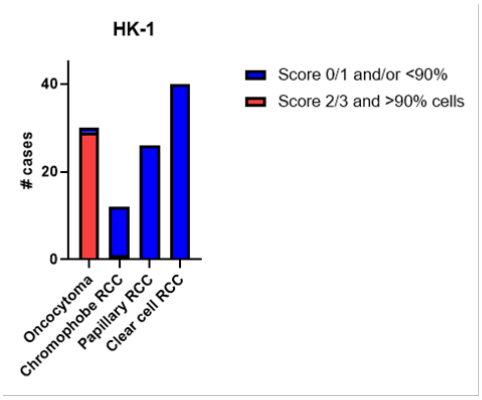

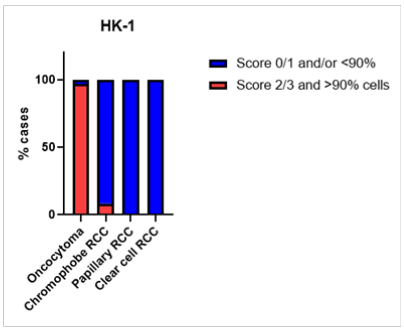

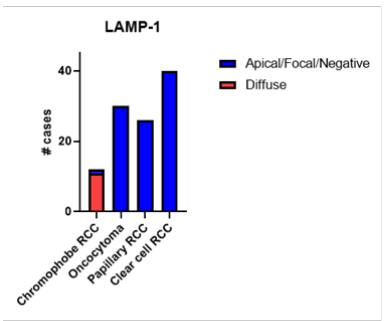

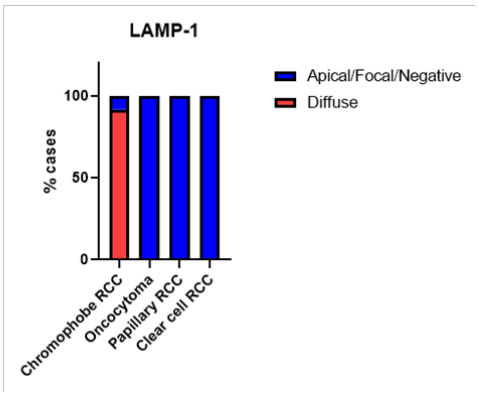

Conclusions: Novel biomarkers identified using proteomic profiling can discriminate renal neoplasm subtypes. Our preliminary data shows that HK-1 and LAMP-1 may emerge as sensitive and specific biomarkers for ROs and chRCCs respectively that would be useful to differentiate them from other renal neoplasms.

508 Mullerian Serous Borderline Tumors of the Paratestis: A Clinicopathologic Study with Novel Histologic Findings

Ali Shahabi[1], Ondrej Hes[2], Ankur Sangoi[3], Aleksei Konstantinov[4], Sean Williamson[1], Liang Cheng[5], Christopher Przybycin[1]
[1]Cleveland Clinic, Cleveland, OH, [2]Biopticka laborator s.r.o., Plzen, Czech Republic, [3]El Camino Hospital, Mountain View, CA, [4]St. Petersburg Clinical and Research Oncological Center, St. Petersburg, Russia, [5]Indiana University, Indianapolis, IN

Disclosures: Ali Shahabi: None; Ondrej Hes: None; Ankur Sangoi: None; Aleksei Konstantinov: None; Sean Williamson: None; Liang Cheng: None; Christopher Przybycin: None

Background: All cellular subtypes of ovarian-type epithelial tumors have been described in the paratestis, with serous borderline tumor (SBT) as the most commonly reported. However, information about the morphologic spectrum, immunophenotype, and natural history of these lesions is limited, particularly with regard to comparison with their ovarian counterparts. Such information is important, as these lesions are rare and the differential diagnosis includes highly aggressive epithelial tumors such as malignant mesothelioma of the tunica vaginalis.

Design: We collected SBTs involving the paratestis from multiple institutions, characterized the morphologic findings, performed an immunohistochemical panel including PAX8, ER, PR, calretinin, and D2-40, and obtained clinical follow up information.

Results: Five SBT were identified. Mean patient age was 51 years (range 25–78). All cases presented as a testicular mass and ranged in size from 0.4 to 10.5 cm. Four tumors (80%) arose from the tunica albuginea, 2 of which extended into the testicular parenchyma. One tumor involved the tunica vaginalis. Associated pre-existing Müllerian lesions were identified in 3 cases (60%), and included a serous cystadenofibroma (1 case) and endosalpingiosis (2 cases). The classic features of ovarian SBT (papillae lined by atypical serous cells with hierarchical branching and "detached" cellular tufts) were identified in 4 cases (80%). The remaining case had features of primary peritoneal serous borderline tumor (micropapillary clusters of cells resembling a non-invasive epithelial implant of SBT). Autoimplants and microinvasion, seen in ovarian SBT but to our knowledge not described in paratesticular SBT, were each present in 2 cases (40%). Immunohistochemistry, performed in 4 cases and summarized in the table, supported the diagnosis of Müllerian SBT in all cases stained. Clinical follow up, available in 4 cases, showed no adverse events (metastasis, death) related to SBT.

Serous borderline tumors of the paratestis: Immunohistochemical findings

	PAX-8	ER	PR	Calretinin	D2-40
Case 1	Positive	Positive	Positive	Negative	Negative
Case 2	Positive	Positive	Positive	Negative	Negative
Case 3	Positive	Positive	Negative	Negative	Negative
Case 4	Positive	Positive	Negative	Negative	Negative

Conclusions: We present a series of paratesticular SBT with features not previously reported (primary peritoneal SBT-like pattern, autoimplants, microinvasion) and further support the indolent behavior of these neoplasms.

509 Survival Analysis Using Cancer and Gleason Pattern Area Ratios Obtained With Deep Learning-Based AI

Ha-Young Shin[1], Joonyoung Cho[2], Sun Woo Kim[2], Hyeyoon Chang[2], Tae-Yeong Kwak[3]
[1]Deep Bio Inc., South Korea, [2]Deep Bio Inc., Seoul, South Korea, [3]Deep Bio Inc., Guro-gu, South Korea

Disclosures: Ha-Young Shin: *Employee*, Deep Bio Inc.; Joonyoung Cho: *Employee*, Deep Bio Inc.; Sun Woo Kim: *Stock Ownership*, Deep Bio Inc.; Hyeyoon Chang: *Employee*, DeepBio Inc; Tae-Yeong Kwak: *Employee*, Deep Bio Inc.

Background: The Gleason grading system is a widely used rubric for the prognosis of prostate cancer that uses the prevalence of so-called ‘Gleason patterns’ in prostate tissue sections to assign scores. The goal of this study is

to determine whether the inclusion of cancer and Gleason pattern area ratios of tissue samples along with the Gleason grades can improve the prediction of time to biochemical recurrence in prostate cancer patients.

Design: The data analyzed in this study come from The Cancer Genome Atlas program's prostate data set (TCGA-PRAD). However, the cancer and Gleason pattern 3, 4, and 5 area ratios were obtained by analyzing the patients' resection slide images with a deep learning-based AI trained on prostate core needle biopsy images. Specifically, we obtained four ratios, here called the cancer rate, 3 rate, 4 rate, and 5 rate. The cancer rate is the proportion of the tissue specimen that is cancerous, while the 3, 4, and 5 rates indicate the proportions of that cancerous tissue composed of Gleason patterns 3, 4, and 5, respectively. Because the latter three will add to 1, the 5 rate was excluded in the model to avoid multicollinearity. The original data set contains 500 subjects, but only 336 remain after removing those without diagnostic slides or survival times. 49 patients, or 14.58%, experienced failure.

Features missing more than 5% of the data were removed, leaving a total of 14 features. Missing data were imputed using Bayesian ridge regression by chained equations. We performed survival analysis using the Cox proportional hazards model with elastic net regularization and models were evaluated using the concordance, or C-index. We used nested cross-validation for model selection and assessment, with 5 inner and outer folds. This entire process was done twice, with and without the three ratios as features (the Gleason scores were included both times).

Results: The C-index was 0.708 with the ratios and 0.675 without the ratios, yielding a difference of 0.033. The respective 95% confidence intervals, obtained by bootstrapping, are [0.638, 0.809], [0.588, 0.773], and [-0.032, 0.119]. The p-value for the hypothesis that the ratios offer no improvement in C-index is 0.125. The standardized 3 and 4 rates had the most significant hazard ratios. Standardized features and their corresponding hazard ratios are shown in the table below. The features are ordered by importance as measured by the absolute value of their coefficients in the Cox model.

Feature	Hazard ratio
3 rate	0.88487
4 rate	1.09287
Primary Gleason grade	1.09224
Pathologic T stage	1.07519
Secondary Gleason grade	1.04676
Race (Asian)	1.01533
Tertiary Gleason grade	1.00702
Histologic diagnosis	1.00000
Race (black or African-American)	1.00000
Laterality (left)	1.00000
Cancer rate	1.00000
Laterality (right)	1.00000
Race (white)	1.00000
Age at initial pathologic diagnosis	1.00000

Conclusions: Gleason scores are powerful tools for evaluating prostate cancer. Our analysis suggests that using cancer and Gleason pattern area ratios, as determined by an AI, in addition to Gleason scores can improve the C-index. Unfortunately, the data set is too small and has too few failures to draw definitive conclusions. Further investigation with a larger data set is required, but the results seem promising.

510 Morphologic Patterns in Primary Tumor Determines Overall Survival in a Cohort of Patients with Clear Cell Renal Cell Carcinoma

Deepika Sirohi[1], Jonathan Chipman[1], Beatrice Knudsen[2], Evan Raps[3], Marc Barry[2], Daniel Albertson[4], Jonathon Mahlow[2], Ting Liu[5], Prayushi Sharma[6], Andrew Hahn[7], Neeraj Agarwal[8]
[1]The University of Utah, Salt Lake City, UT, [2]The University of Utah/ARUP Laboratories, Salt Lake City, UT, [3]The University of Utah/ARUP Laboratories, [4]The University of Utah, [5]ARUP Laboratories, University of Utah, Salt Lake City, UT, [6]Huntsman Cancer Institute, Salt Lake City, WA, [7]The University of Texas MD Anderson Cancer Center, Houston, TX, [8]Huntsman Cancer Institute, Salt Lake City, UT

Disclosures: Deepika Sirohi: None; Jonathan Chipman: None; Beatrice Knudsen: None; Evan Raps: None; Marc Barry: None; Daniel Albertson: None; Jonathon Mahlow: None; Ting Liu: None; Prayushi Sharma: None; Andrew Hahn: None; Neeraj Agarwal: *Consultant*, Astellas, Astra Zeneca, Bayer, Bristol Myers Squibb, Clovis, Eisai, Eli Lilly, EMD Serono, Exelixis, Foundation Medicine, Genentech, Janssen, Merck, Nektar, Novartis, Pfizer, Pharmacyclics, and Seattle Genetics.

Background: The grading of clear cell renal cell carcinoma (CCRCC) has prognostic implications and is based on a combination of nuclear features and histologic growth patterns (HGP). Amongst HGPs, thus far, only sarcomatoid and rhabdoid HGPs are used for grading and confer the worst prognosis after nephrectomy. Many different HGPs are observed in CCRCC, but their prognostic significance is unclear. To discover other HGPs that predict clinical outcomes, we analyzed 24 HGPs in surgically resected CCRCC.

Design: We systematically recorded 24 HGPs and histologic features, necrosis and WHO/ISUP nuclear grade in a retrospective cohort of primary CCRCC comprised of 134 patients with metastatic CCRCC (mCCRCC), and 40 patients with localized CCRCC. We determined the association between each HGP and overall survival (OS) from a cox model adjusting for age, sex, race and International Metastatic Disease Consortium category (none, favorable, intermediate, or poor). Co-occurrence of patterns were assessed using a heatmap of spearman's correlation.

Results: Surprisingly, nuclear grade 2 was the highest grade in 38% (n=51) of primary CCRCCs that progressed to metastasis, while nuclear grade 3 was present in 43% (n=57) of mCCRCC and in 15% of non-mCCRCC (n = 6). We identified 4/24 HGPs (low-grade spindle, fused nests/sheets, sarcomatoid, and rhabdoid) in the primary tumors of patients, that were associated with shorter OS (respective Hazard Ratio (HR): 1.97, 2.09, 2.63, 3.24; $p < 0.05$ for each), in contrast to the well-formed nested HGP that was associated with longer OS (HR = 0.58; $p = 0.016$) (Figure-1). Importantly, low-grade spindle and/or fused nests were identified in 12 (14%) primary CCRCC with nuclear grade 2 in the metastatic group. We frequently observed co-occurrence of HGPs in the same tumor (Figure 2).

Figure 1 - 510

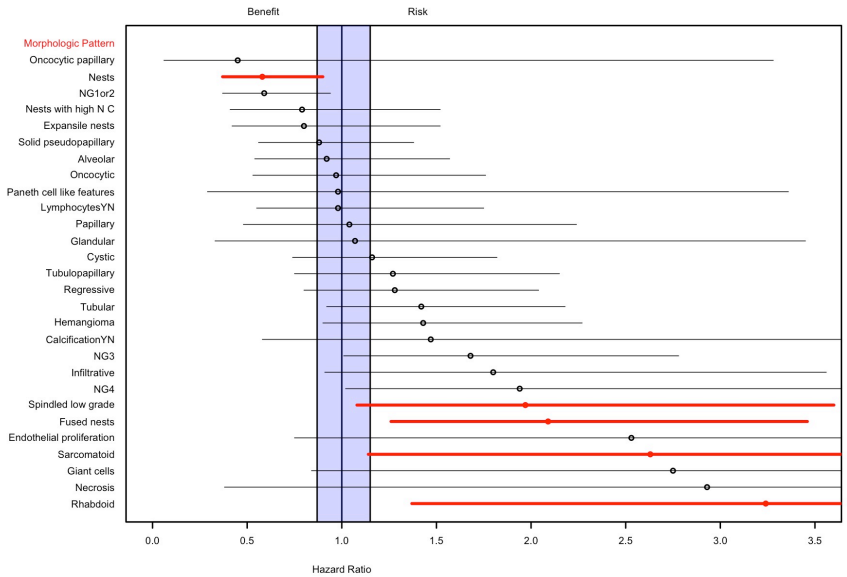

Figure 2 - 510

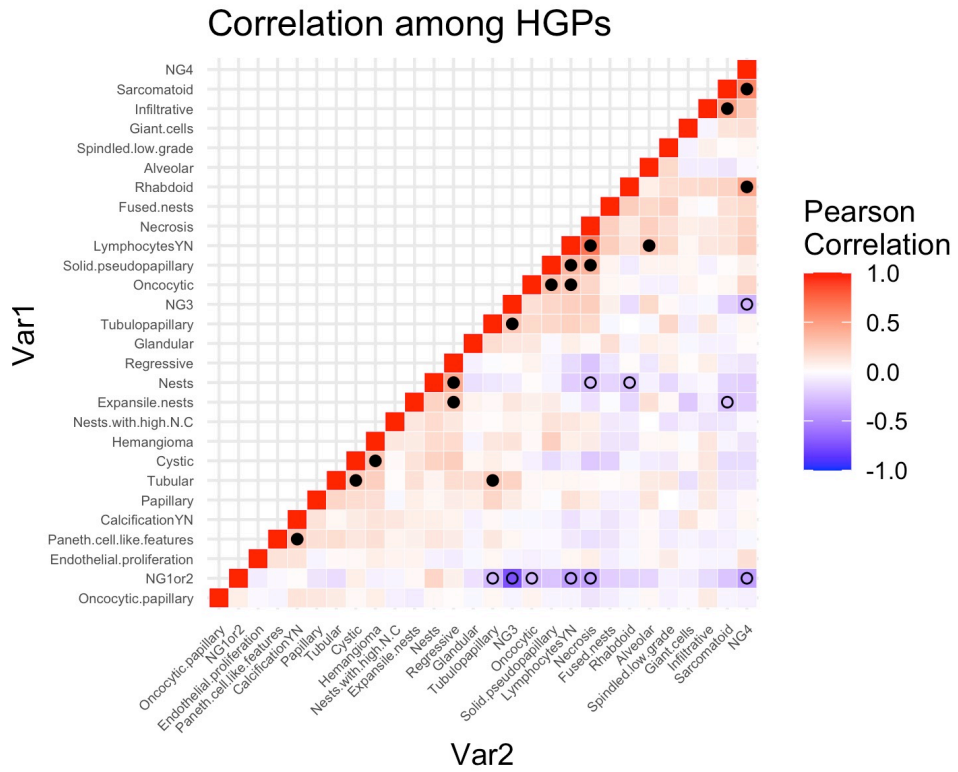

Conclusions: We identified 5 HGPs in primary CCRCCs that predict OS of CCRCC patients; two of which included the well-established prognostic sarcomatoid and rhabdoid HGP. Our data support the novel concept of an association between HGP in the primary tumor and patient survival among patients with localized and metastatic CCRCC. Thus, HGPs may harbor salient biomarkers predictive of OS. HGPs may form based on intrinsic mechanisms of cancer cells leading to aggressive behavior in primary and metastatic CCRCC.

511 Hyper-Activation of Neddylation Pathway in Bladder Cancer

Sami Souccar[1], Beverly Wang[1], Ahmad Charifa[1], Xiaolin Zi[1], Ramy Yaacoub[1], Robert Edwards[2]
[1]UCI Medical Center, Orange, CA, [2]UC Irvine Health, Orange, CA

Disclosures: Sami Souccar: None; Beverly Wang: None; Ahmad Charifa: None; Robert Edwards: None

Background: Neddylation is a multistep process similar to ubiquitination, wherein NEDD8 is passed down a stepwise enzymatic cascade (NAE1/UBA3, then UBE2M or UBE2F, then RBX or E3 ligases), which is conjugated to lysine residues of a substrate. The substrates include Cullin ring ligases and a family of non-Cullin proteins the tumor suppressors p53 and VHL, RTKs including EGFR and TGFBR2, and transcriptional regulators like HIF1a. Over expression of components of the neddylation pathway has been linked to alterations in regulation of cell growth, viability, differentiation and various cancers, specifically esophageal adenocarcinoma (adenoca) and lung squamous cell carcinoma (SCC) and adenoca. Neddylation inhibitors have been used to induce apoptosis in cancer cells. This study aims to evaluate the presence and/or overactivity of the neddylation pathway in bladder cancer, to investigate its potential utility as a prognostic or therapeutic target.

Design: Nine Tissue microarrays (TMAs) containing 315 patients' bladder carcinomas were utilized, with histologic subtypes as follows: 151 SCC, 143 urothelial carcinoma (UC), and 21 adenoca. 1 mm diameter core samples were collected from the tumor area in triplicated and embedded in the TMA blocks. Eight bladder biopsies with no pathologic alteration were selected to serve as negative contro DCUN1D5 ls. All TMA slides and controls were stained with anti-Nedd8 , anti-UBA3, UBE2F and DCNL5 polyclonal antibodies to evaluate expression levels of the

neddylation pathway enzymes from each step of the cascade. Staining intensity was scored semiquantitatively from 0-3, 0 = negative, 1 = low, 2 = moderate, and 3 = high.

Results: The majority of carcinomas showed moderate to high intensity staining in NEDD8 compared to normal bladder tissues ?(table 1). UBA3 and UBE2F staining were variable but the majority were low to moderate intensity in both normal and tumor cells. DCUN1D5 staining was mostly negative in carcinomas and of low intensity in normal tissues. Tumor grade is not associated with average staining intensity, as some higher grade carcinomas had low intensity and some had high intensity. Data stratification by clinical features including age, sex, overall survival, tumor stage and lymph node involvement did not correlate with staining positivity or intensity.

Urothelial Carcinoma				
Intensity	NEDD8	UBA3	UBEF2	DCUN1D5
0	1%	4%	68%	58%
1	3%	53%	24%	34%
2	33%	39%	8%	7%
3	63%	4%	0%	1%
Squamous Cell Carcinoma				
Intensity	NEDD8	UBA3	UBEF2	DCUN1D5
0	2%	40%	60%	68%
1	5%	50%	40%	20%
2	41%	9%	0%	11%
3	52%	1%	0%	1%
Adenocarcinoma				
Intensity	NEDD8	UBA3	UBEF2	DCUN1D5
0	0%	14%	65%	76%
1	24%	50%	35%	24%
2	50%	29%	0%	0%
3	26%	7%	0%	0%
Normal urothelium				
Intensity	NEDD8	UBA3	UBEF2	DCUN1D5
0	100%	12%	25%	50%
1	0%	51%	50%	50%
2	0%	37%	25%	0%
3	0%	0%	0%	0%

Figure 1 – 511

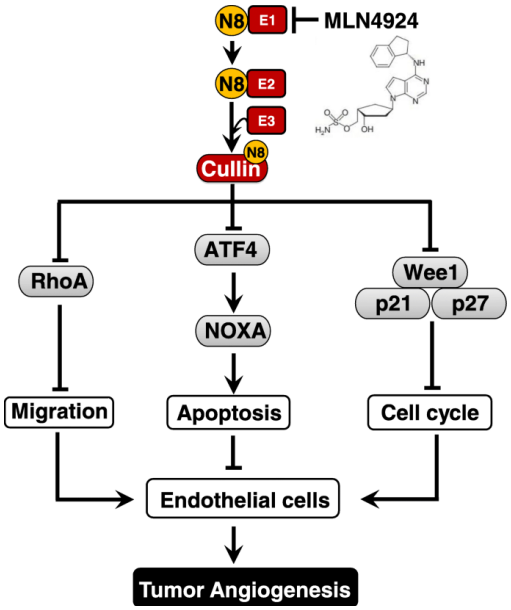

Figure 2 – 511

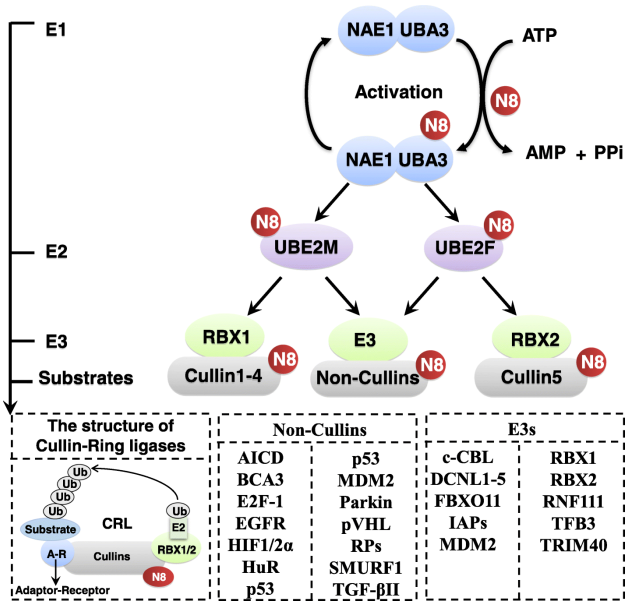

Conclusions: Our results show overexpression of NEDD8 in carcinoma but no significant difference in expression of UBA3, UBE2F and DCUN1D5 between normal bladder, SCC, urothelial carcinoma, or adenocarcinoma. Future investigations will include additional immunohistochemical staining for down-stream components (cullins) of the Neddylation pathway that control different cellular functions such as hypoxia, survival and proliferation, oxidative stresses and DNA repairs.

512 Presence of Corpora Amylacea Among Prostate Cancer Cells: An Unrecognized Feature of Intraductal Carcinoma of the Prostate

Miho Sugie[1], Taishi Takahara[2], Akiko Ohashi[2], Sassa Naoto[2], Toyonori Tsuzuki[2]
[1]Nagoya, Japan, [2]Aichi Medical University Hospital, Nagakute, Japan

Disclosures: Miho Sugie: None; Akiko Ohashi: None; Toyonori Tsuzuki: None

Background: Corpora amylacea (CA) is present in benign prostatic ducts and acini, and its presence is considered suggestive of negative or low-risk prostate cancer. The clinicopathological definition of CA among prostate cancer cells (CAPCCs)—described as CA entirely surrounded by invasive cancer cells—has not been discussed. As intraductal carcinoma of the prostate (IDC-P) is a well-known adverse prognostic factor in prostate cancer, this study aimed to elucidate the relationship between CAPCC and IDC-P.

Design: We enrolled 366 patients who underwent robotic-assisted radical prostatectomies between 2012 and 2018 at Aichi Medical University Hospital. All surgical specimens were independently reviewed by two genitourinary pathologists.

Results: The median age of the patients was 68.5 years; the median serum prostate-specific antigen was 6.49 ng/ml. IDC-P was observed in 143 (39.1%) patients, while the presence of CAPCC was observed in 47 cases (12.8%). Patients with CAPCC were associated with more advanced clinical and pathological T stages, as well as Gleason scores, than those without CAPCC (p=0.018, p<0.001, p=0.036). Notably, the presence of CAPCC was significantly associated with the presence of IDC-P (39 cases) and a high Gleason score compared with the absence of CAPCC (12 cases) (p<0.001 and p=0.036, respectively).

		All (n=366)	CAPCC		p-value
			Absent (n=319)	Present (n=47)	
Age	Median [range]	68.5 [49-83]	68.5 [49-82]	68.5 [57-83]	0.171
cT	cT1c	190 (51.9%)	172 (53.9%)	18 (38.2%)	0.018
	cT2a	78 (21.3%)	65 (20.3%)	14 (29.7%)	
	cT2b	10 (2.7%)	9 (2.8%)	1 (2.1%)	
	cT2c	57 (15.6%)	52 (16.3%)	5 (10.6%)	
	cT3a	24 (6.6%)	16 (5%)	8 (17%)	
	cT3b	6 (1.6%)	5 (1.6%)	1 (2.1%)	
PSA	Median [range]	6.485 [3.054-72]	6.274 [3.052-72]	7.494 [4.07-65]	0.145
pT	pT2	250 (68.3%)	230 (72.1%)	21 (44.7%)	<0.001
	pT3a	90 (25.4%)	74 (23.1%)	16 (34%)	
	pT3b	24 (6.6%)	14 (4.4%)	10 (21.2%)	
	pT4	1 (0.3%)	1 (0.3%)		
IDC-P	Absent	223 (60.9%)	215 (67.4%)	8 (17%)	<0.001
	Present	143 (39.1%)	104 (32.6%)	39 (83%)	
Grade Group	1	45 (12.3%)	44 (13.8%)	1 (2.1%)	0.036
	2	138 (37.7%)	124 (38.8%)	14 (29.8%)	
	3	101 (27.6%)	87 (27.3%)	14 (29.8%)	
	4	27 (7.4%)	23 (7.2%)	4 (8.5%)	
	5	55 (15%)	41 (12.9%)	14 (29.8%)	
Gleason pattern 5	Absent	201 (54.9%)	185 (58%)	16 (34%)	0.003
	Present				

Figure 1 - 512

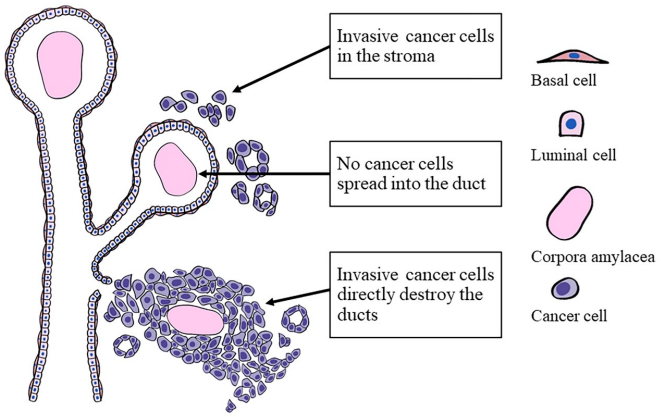

Figure 2 - 512

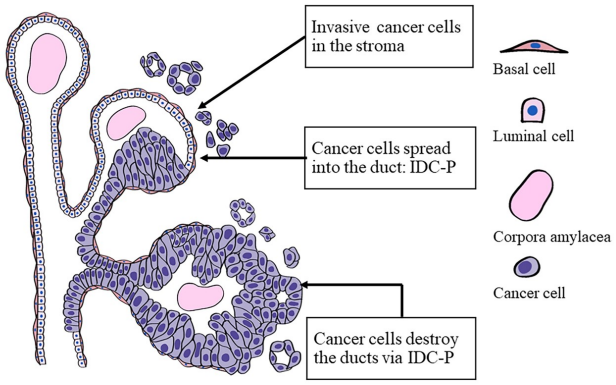

Conclusions: The presence of CAPCC is an adverse pathological feature, often closely related to IDC-P. CAPCC may, therefore, be a surrogate finding to detect IDC-P via hematoxylin and eosin staining.

513 Radical Prostatectomy Findings and Oncologic Outcomes in Patients with Prostate Cancer Detected on Systematic Sextant Biopsy Only, MRI-targeted Biopsy Only, or Both

Nivedita Suresh[1], Ying Wang[1], Hiroshi Miyamoto[1]
[1]University of Rochester Medical Center, Rochester, NY

Disclosures: Nivedita Suresh: None; Ying Wang: None; Hiroshi Miyamoto: None

Background: MRI-targeted biopsy (T-Bx) has been shown to more accurately detect prostate cancer. However, the clinical significance of prostate cancer detection on T-Bx needs to be further investigated. In the present study, we compare radical prostatectomy findings and oncologic outcomes in patients with prostate cancer detected on sextant biopsy (S-Bx) and/or T-Bx.

Design: We assessed consecutive patients who had undergone T-Bx in addition to systematic S-Bx (6 parts, ≥12 cores), followed by radical prostatectomy at our institution between 2015 and 2019. Within our Surgical Pathology database, we identified a total of 193 men who met the inclusion criteria for prostatic adenocarcinoma on S-Bx and/or T-Bx (see Table). Cases undergoing neoadjuvant therapy prior to radical prostatectomy were excluded from analysis.

Results: Prostate cancer was detected on S-Bx only (n=24), T-Bx only (n=34), or both S-Bx and T-Bx (B-Bx; n=135). In B-Bx cases, Grade Group (GG) on T-Bx was the same as the highest GG on S-Bx (n=65) and higher (n=37) or lower (n=33) than that on S-Bx. Compared to cases with prostate cancer detected on S-Bx only, those on T-Bx only or B-Bx showed significantly higher tumor grade on biopsy [*e.g.* GG2-5: S-Bx 50% vs. T-Bx 88% (P=0.001) or B-Bx 84% (P<0.001)] or radical prostatectomy [*e.g.* GG2-5: S-Bx 83% vs. T-Bx 100% (P=0.025) or B-Bx 100% (P<0.001)] and significantly larger estimated tumor volume. There were no significant differences in pT or pN stage, surgical margin status, or preoperative prostate-specific antigen level between cancers detected on S-Bx only vs. T-Bx only or B-Bx. There were also no significant differences in any of these clinicopathologic features between cancers detected on T-Bx only vs. B-Bx. Meanwhile, Kaplan-Meier analysis coupled with log-rank test revealed no significant differences in the risk of biochemical recurrence after radical prostatectomy between cancers detected on S-Bx only vs. T-Bx only (P=0.146), S-Bx only vs. B-Bx (P=0.269), or T-Bx only vs. B-Bx (P=0.366).

	S-Bx (n=24)	T-Bx (n=34)	B-Bx (n=135)	*P* (S-Bx vs T-Bx)	*P* (S-Bx vs B-Bx)	*P* (T-Bx vs B-Bx)
Age (mean, year)	64.7	65.3	65.8	0.658	0.397	0.626
PSA (mean, ng/mL)	10.20	10.02	9.05	0.933	0.550	0.439
Bx Grade Group				0.011[a]	0.001[a]	0.593[a]
1	12 (50%)	4 (12%)	21 (16%)			
2	8 (33%)	19 (56%)	64 (47%)			
3	2 (8%)	7 (21%)	25 (18%)			
4	1 (4%)	4 (12%)	18 (13%)			
5	1 (4%)	0 (0%)	7 (5%)			
RP Grade Group				0.007[a]	<0.001[a]	0.575[a]
1	4 (17%)	0 (0%)	0 (0%)			
2	13 (54%)	22 (65%)	70 (52%)			
3	7 (29%)	9 (26%)	45 (33%)			
4	0 (0%)	0 (0%)	3 (2%)			
5	0 (0%)	3 (9%)	17 (13%)			
pT stage				0.652[b]	0.277[b]	0.267[b]
2/2+	15 (63%)	21 (62%)	64 (47%)			
3a	8 (33%)	13 (38%)	65 (48%)			
3b	1 (4%)	0 (0%)	6 (4%)			
pN stage				0.377[c]	1.000[c]	0.212[c]
0	19 (79%)	33 (97%)	124 (92%)			
1	1 (4%)	0 (0%)	8 (6%)			
X	4 (17%)	1 (3%)	3 (2%)			
Surgical margin				0.467	1.000	0.477
Negative	19 (79%)	30 (88%)	106 (79%)			
Positive	5 (21%)	4 (12%)	29 (21%)			
Tumor volume (mean, cc)	4.33	6.83	7.31	0.020	<0.001	0.631

[a] GG1 vs GG2-3 vs GG4-5; [b] pT2/2+ vs pT3a vs pT3b; [c] pN0 vs pN1

Conclusions: Detection of prostate cancer on T-Bx was found to strongly associate with higher tumor grade and larger tumor volume, but not with other adverse pathology in radical prostatectomy specimens such as pT3 disease, lymph node metastasis, and positive surgical margin, as well as the risk of disease recurrence following radical prostatectomy.

514 The Clinical Significance of Perineural Invasion by Prostate Cancer on MRI-Targeted Biopsy

Nivedita Suresh[1], Yuki Teramoto[1], Takuro Goto[1], Ying Wang[1], Hiroshi Miyamoto[1]
[1]University of Rochester Medical Center, Rochester, NY

Disclosures: Nivedita Suresh: None; Yuki Teramoto: None; Takuro Goto: None; Ying Wang: None; Hiroshi Miyamoto: None

Background: MRI-targeted biopsy (T-Bx) has been shown to more accurately detect prostate cancer. Meanwhile, perineural invasion (PNI) by prostate cancer detected on sextant biopsy (S-Bx) has been implicated in adverse pathologic features, including extraprostatic extension, and resultant poor patient outcomes. In the present study, we compare radical prostatectomy findings and oncologic outcomes in patients with prostate cancer (with or without PNI) detected on T-Bx.

Design: We assessed consecutive patients who had undergone T-Bx in addition to systematic S-Bx (6 parts, ≥12 cores), followed by radical prostatectomy in 2015-2019. Within our Surgical Pathology database, we identified a total of 169 men who met the inclusion criteria for prostatic adenocarcinoma on T-Bx. Cases undergoing neoadjuvant therapy prior to prostatectomy were excluded.

Results: In all cases where prostate cancer was detected on T-Bx only (n=34) or both S-Bx and T-Bx (B-Bx; n=135), PNI was found in 33 (19.5%) T-Bxs. Compared with no PNI cases on T-Bx, T-Bx PNI was associated with higher Grade Group (GG) on biopsy (*e.g.* GG3-5: 39.7% vs. 72.7%, *P*<0.001) or prostatectomy (*e.g.* GG3-5: 41.2% vs. 63.6%, *P*=0.020), higher pT stage (*e.g.* pT3: 42.6% vs. 78.8%, *P*<0.001), and lymph node metastasis (pN1: 1.5% vs. 18.2%, *P*<0.001). There were no significant differences in surgical margin status or estimated tumor volume. Meanwhile, the presence of PNI on T-Bx was significantly (*P*<0.001) correlated with that on S-Bx. Kaplan-Meier analysis coupled with log-rank test revealed no significant difference in the risk of biochemical recurrence after radical prostatectomy between cases with vs. without PNI on T-Bx (*P*=0.294). Next, in the 135 B-Bx cases, PNI was found on S-Bx only (n=31), T-Bx only (n=15), or B-Bx (n=16). The presence of PNI on T-Bx was associated with higher biopsy GG (S-Bx vs. T-Bx: *P*=0.006; S-Bx vs. B-Bx: *P*=0.020), higher pT stage (S-Bx vs. T-Bx: *P*=0.025; S-Bx vs. B-Bx: *P*=0.019), pN1 disease (S-Bx vs. T-Bx: *P*=0.095), and larger tumor volume (S-Bx vs. B-Bx: *P*=0.049), but not with prostatectomy GG. There were no significant differences in all of these clinicopathologic features between cases with PNI on T-Bx only vs. B-Bx, except marginally (*P*=0.081) larger tumor volume in B-Bx PNI cases. Outcome analysis further showed a significantly higher risk of biochemical recurrence in patients with PNI on B-Bx, compared to those with PNI on S-Bx (*P*=0.002) or T-Bx (*P*=0.028) only. In multivariate analysis with Cox regression model, PNI on B-Bx showed significance for recurrence (hazard ratio 25.91, 95% confidence interval 1.195-561.8, *P*=0.038).

Conclusions: The presence of PNI on T-Bx was found to associate with worse histopathologic features in radical prostatectomy specimens. In addition, B-Bx was associated with poorer prognosis as an independent predictor, compared to cases with PNI on S-Bx or T-Bx only. Pathologists may thus need to specify PNI, if present, on S-Bx, T-Bx, or both.

515 Institutional Review of Kidney Tumors by Size: Are We Under Staging Renal Tumors 7 cm and Greater?

Georges Tabet[1], Aileen Grace Arriola[1]
[1]*Temple University Hospital, Philadelphia, PA*

Disclosures: Georges Tabet: None; Aileen Grace Arriola: None

Background: The management of kidney tumors is ever evolving toward nephron-sparing surgery (partial nephrectomy [PN]). Surgeons are pushing the limit of performing PN on large kidney tumors due to improved post-operative renal function. This trend may present challenges for pathologists to properly stage kidney tumors. The purpose of this study is to examine whether kidney tumors larger than 7 cm are being adequately staged at our institution.

Design: Nephrectomy cases between 2010-2020 were identified. Procedure type, tumor size, tumor type, pathological staging, and follow up was collected from the electronic medical records. Cases were divided into two main groups, one for PN and another for radical/total nephrectomy (RN). Fisher's exact test was used to test for associations; a p-value less than 0.05 was considered statistically significant.

Results: For PN cases, there were 28 (6%) that were ≥7 cm in size (7.3-15.5cm) and n=429 (94%) that were <7 cm in size (0.6-6.9 cm). Although larger tumors were more likely to be staged as pT3 or pT4 as compared to tumors <7cm, the majority of them were still staged as being confined to the kidney (see Table). For RN, there were 83 (44%) that were ≥7 cm in size (7.0-21.6 cm) and 107 (56%) that were <7 cm in size (0.6-6.9 cm). Larger tumors were more likely to be staged as pT3 and pT4 as compared to tumors <7 cm. This association is stronger as compared to PN. Overall, among tumors ≥7 cm, 39% and 86% of RN and PN, respectively, are still being staged as confined to the kidney (pT1 and pT2). Follow-up data was available on 21/24 ≥7cm PN and 294/412 <7cm PN cases staged as limited to the kidney. Among ≥7cm PN cases, only one patient (5%) developed recurrence and metastasis (chromophobe renal cell carcinoma [RCC]), while 26 (9%) patients demonstrated recurrence or metastasis in the <7cm PN group (clear cell RCC=14, chromophobe RCC=4, papillary RCC type 1=3, papillary RCC type 2=3, and RCC unclassified=2) (p-value=1). There was available follow-up information on 26/32 ≥7 cm RN and 62/76 <7cm RN cases staged as limited to the kidney. Among ≥7 cm RN cases, 31% (n=8) developed recurrence or metastasis (clear cell RCC=4, papillary RCC type 2=4), while only 11% (n=7) of <7 cm RN cases developed recurrence and/or metastasis (clear cell RCC=2, papillary RCC type 1=2, papillary RCC type 2=2, and RCC unclassified=1) (p=0.0583).

Partial Nephrectomy			
	Tumor Size <7 cm **(n=429)**	**Tumor Size ≥7cm** **(n=28)**	**p-value**
Tumor Extent pT1 & pT2 pT3 & pT4	412 (96%) 17 (4%)	24 (86%) 4 (14%)	**0.0328**
Radical/Total Nephrectomy			
	Tumor Size <7 cm **(n=107)**	**Tumor Size ≥7cm** **(n=83)**	**p-value**
Tumor Extent pT1 & pT2 pT3 & pT4	76 (71%) 31 (29%)	32 (39%) 51 (61%)	**<0.00001**

Conclusions: Our findings show that the association between tumor size and tumor extent is stronger in radical nephrectomies in comparison to partial nephrectomy. This highlights that larger tumors are potentially understaged in the partial nephrectomy group at our institution. Re-review of such cases might provide more insight as to the reasons for potential understaging.

516 Immune Checkpoint Inhibitor (ICPI) Biomarkers in Clinically Advanced Castrate Resistant Prostate Cancer (mCRPC): A Comparative Comprehensive Genomic Profiling (CGP) Study

Michel Tawil[1], Natalie Danziger[2], Brennan Decker[2], Tyler Janovitz[2], Douglas Lin[2], Richard Huang[3], J. Keith Killian[2], Shakti Ramkissoon[4], Ole Gjoerup[2], Kimberly McGregor[2], Jeffery Venstrom[5], Jeffrey Ross[6]
[1]SUNY Upstate Medical University, Syracuse, NY, [2]Foundation Medicine, Inc., Cambridge, MA, [3]Foundation Medicine, Inc., Cary, NC, [4]Foundation Medicine, Inc., Morrisville, NC, [5]Foundation Medicine, Inc., San Francisco, CA, [6]Upstate Medical University, Syracuse, NY

Disclosures: Michel Tawil: None; Natalie Danziger: *Employee*, Foundation Medicine Inc.; Brennan Decker: *Employee*, Foundation Medicine; Tyler Janovitz: *Employee*, Foundation Medicine; Douglas Lin: *Employee*, Foundation Medicine, Inc.; *Stock Ownership*, Roche; Richard Huang: *Employee*, Foundation medicine; J. Keith Killian: *Employee*, Foundation Medicine; Shakti Ramkissoon: *Employee*, Foundation Medicine; Ole Gjoerup: None; Kimberly McGregor: *Employee*, Foundation Medicine; *Stock Ownership*, ROCHE; Jeffery Venstrom: *Employee*, Foundation Medicine; Jeffrey Ross: *Employee*, Foundation Medicine

Background: Unlike lung adenocarcinoma (LAC) and skin melanoma (Mel), ICPI therapy is not currently standard of care treatment, and its usage is not guided by biomarkers in mCRPC patients. This study evaluated the landscape of biomarkers associated with ICPI therapy response in mCRPC in comparison with these well-studied disease types.

Design: 5617 clinically advanced mCRPC, 16,271 LAC and 2,232 Mel were sequenced to evaluate all classes of GA using a hybrid capture-based CGP assay. Tumor mutational burden (TMB) was determined on up to 1.1 Mbp and microsatellite instability (MSI) was determined on 114 loci. PD-L1 expression was determined by IHC (Dako 22C3) with low positive tumor cell expression at 1-49% and high at ≥50%.

Results: mCRPC had lower frequencies of biomarkers predictive of favorable ICPI response including GA/tumor, high TMB and PD-L1 expression than LAC or Mel. *CDK12* GA which have been linked to favorable ICPI response were significantly greater in mCRPC. Frequencies of GA linked to ICPI resistance including inactivation of *STK11*, *ARID1A*, *KEAP1* and amplification of *MDM2* were lower in mCRPC than LAC or Mel. At 4%, MSI High status was significantly more frequent in mCRPC than LAC or Mel. Of mCRPC patients with TMB≥ 10mut/Mb and determinable MSI status, 62% (n=142) were MSI-H and mutation signatures associated with tobacco use or UV exposure were extremely rare (n=1, tobacco). Compared to mCRPC with TMB<10mut/Mb, mCRPC patients with

TMB≥ 10mut/Mb harbored more frequent alterations in *TP53* (52 v 41%), *MSH2* (42 vs <1%), *AR* (35 v 15%), *BRCA2* (15 v 8%), *PIK3CA* (20 v 6%), *ARID1A* (17 v 1%) and *ATM* (12 v 5%) (all p<0.01); had similar frequencies of *PTEN, RAD21, MYC,* and *CDK12;* and had fewer *TMPRSS2:ERG* fusions (19 v 34%, p<0.001).

	mCRPC	Lung AC	Melanoma	Significance	
				mCRPC vs LAC	mCRPC vs Mel
Cases	5,617	16,271	2,232		
Age (range in years)	67 (38-89+)	68 (17-89+)	66 (9-89+)	NS	NS
GA/tumor	4.0	5.3	6.1	P<.0001	P<.0001
AR	16%	<1%	<1%	P<.0001	P<.0001
CDK12	6%	1%	1%	P<.0001	P<.0001
PBRM1	1%	2%	3%	NS	P=.01
STK11	<1%	19%	1%	P<.0001	NS
KEAP1	<1%	7%	<1%	P<.0001	NS
ARID1A	2%	6%	4%	P<.0001	P=.02
MDM2 amp	1%	5%	3%	P<.0001	NS
CD274 (*PD-L1*) amp	<1%	1%	1%	NS	NS
MSI High	4%	<1%	<1%	P<.0001	P<.0001
Median TMB mut/Mb	2.5	6.3	11.3		
Mean TMB	4.0	8.7	24.2	P<.0001	P<.0001
TMB > 10 mut/Mb	5%	32%	55%	P<.0001	P<.0001
TMB > 20 mut/Mb	3%	10%	34%	P<.0001	P<.0001
PD-L1 IHC low	9% (1703 cases)	27% (8810 cases)	39% (780 cases)	P<.0001	P<.0001
PD-L1 IHC high	1%	32%	9%	P<.0001	P<.0001

Conclusions: When compared with LAC and Mel, other than a higher frequency of MSI high status, mCRPC features lower frequencies of positive ICPI predictive biomarkers, including high TMB and PD-L1 expression. A significant potential opportunity to increase ICPI therapy use in mCRPC is the relatively high frequency of *CDK12* mutations, which deserves further investigation.

517 Do Ki67 Proliferation Rates Correlate with Molecular Genomic Prognostication Results: A Low-Cost Alternative

Arnel Urbiztondo[1], Shivanshu Awasthi[1], Kosj Yamoah[1], Aram Vosoughi[2], Julio Pow-Sang[1], Jasreman Dhillon[1]
[1]H. Lee Moffitt Cancer Center & Research Institute, Tampa, FL, [2]Yale School of Medicine, New Haven, CT

Disclosures: Arnel Urbiztondo: None; Shivanshu Awasthi: None; Kosj Yamoah: None; Jasreman Dhillon: None

Background: Commercially available genomic signature tests help prognosticate metastatic potential of localized prostatic adenocarcinoma (PA). One tests uses a panel of 22 mRNA genes for the same and generates a genomic score between 0 and 1 with 0.1 increments, representing a 10% increase in the risk of metastasis. Immunohistochemical labeling with Ki-67 reflects nuclear proliferative rate (PR) and may be a prognostic predictor of the metastatic potential of PA.

Design: 30 cases (28 needle cores and 2 prostatectomies) of PA, Gleason score (GS) of 6(3+3) and 7(3+4) for studied. All these cases were tested for molecular genomic test and a section from the same block was stained for Ki-67. Ki67 PR was counted under 20X using an Olympus microscope and the Cellsens Digital imaging software program. Maximum of 10 fields of highest staining fields were selected and counted. In 13 cases due to small size of PA, there were <10 HPFs (4-9 HPFs) counted. Total number of tumor cells range from 842-3686. Corresponding H&E slides were reviewed for GMS and % of pattern 4. Pearson correlation coefficient was used to assess the correlation and two-sample T test was used to assess the differences in the distribution pneumaric variables.

Results: 18 cases had GS 7(3+4) and 12 had GS 6(3+3). Ki67 PR ranged from 1.4 to 10.3% (GS6 - 2.2% to 8.8%; GS7 - 1.4% to 13.3%). Correlation between molecular risk classifier and Ki67 was positively correlated (Pearson correlation (*r*) = 0.38, p = 0.03). When grouped by GS, 6(3+3) were clustered within the lower molecular prognostication score and low Ki67 expression. Ki67 PR was lower in GS 6(3+3) compared to 7(3+4), ($Ki67_{mean}$ 4.12 vs 6.30, p = 0.03). Ki67 PR positively correlated with the molecular risk classifier within GS 6 cases but due to small number of cases, it was not significant (r = 0.18, p = 0.58). % pattern 4 in GS 7(3+4) ranged from 2-40 and a positive correlation was observed between Ki67 expression and pattern component 4 (*r* = 0.22, p = 0.3).

Figure 1 - 517

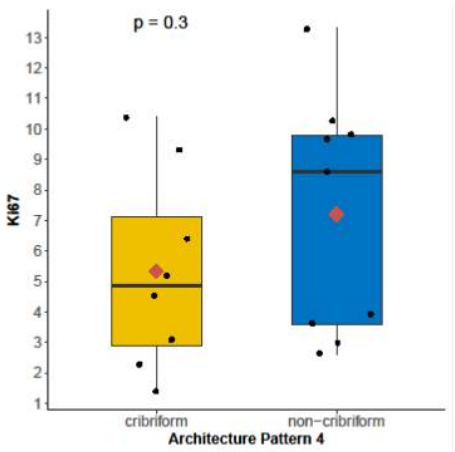

Figure 2 - 517

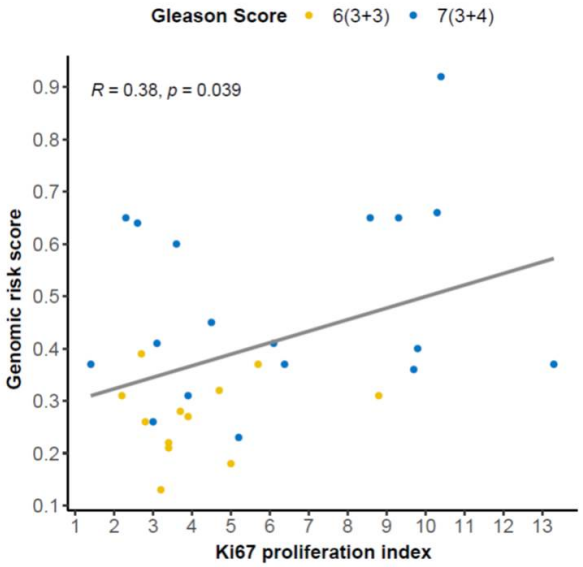

Conclusions:

1. Ki67 proliferation rates correlate with the results of more expensive prognostic molecular test
2. Ki67 immunohistochemical stain can be used as a cheap alternative to the more expensive molecular tests
3. Ki67 results can add value in the decision making for active surveillance
4. Ki67 results correlate with the GS and the % of pattern 4 present in GS 7(3+4)

518 Prognostic Significance of Perinephric Fat Invasion in Renal Cell Carcinoma

Aida Valencia Guerrero[1], Esther Oliva[2], Chin-Lee Wu[3], Peter Sadow[2], Shulin Wu[4], Kristine Cornejo[4]
[1]Vanderbilt Medical Center, Nashville, TN, [2]Massachusetts General Hospital, Harvard Medical School, Boston, MA, [3]Massachusetts General Hospital, Newton Center, MA, [4]Massachusetts General Hospital, Boston, MA

Disclosures: Aida Valencia: None; Esther Oliva: None; Chin-Lee Wu: None; Peter Sadow: None; Shulin Wu: None; Kristine Cornejo: None

Background: Perirenal fat invasion (PFI) is a key component of renal cell carcinoma (RCC) staging. However, its prognostic significance when compared to other patterns of pT3 extrarenal extension such as sinus fat (SFI) and renal vein (RVI) invasion remains controversial. The aim of the study is to analyze the prognostic significance of PFI in comparison to other forms of invasion in patients with pT3 RCCs

Design: We searched the pathology files from 2005-2015 and identified 1236 nephrectomies for RCC. Patients with pT3 tumors (n=306) were grouped based upon patterns of invasion and compared to survival outcomes using the Kaplan-Meier method. Univariate and multivariate cox proportional-hazards regression methods were used to evaluate impacts of clinicopathologic parameters on survival

Results: Of the 306 patients with pT3 RCC, 52 (17%) had tumors with PFI as the only pattern of invasion. Among 42/52 patients with follow-up: 26 (61%) had no evidence of disease (NED) with a mean follow-up of 99.6 months, 8 (19%) were alive with disease (AWD), 4 (9.5%) died of disease (DOD), and 4 (9.5%) died of other disease (DOOD). Kaplan-Meier survival curves revealed the cancer specific survival (CSS) and overall survival (OS) to be significantly better in patients with PFI alone, than in those with other isolated forms of extrarenal invasion (e.g. SFI, RVI, pelvicalyceal system (PCS)) or in varying combinations of invasion (p=<0.001) (Figure 1). Additionally, the presence of multiple patterns of extrarenal extension, particularly those in combination with PFI are associated with a poorer prognosis (p<0.001)

Multivariable analysis showed ISUP/WHO Grade 4 (p=0.034; p=0.021) and a combination of PFI + other forms of invasion (p=0.009; p=0.002) are independent predictors of CSS and OS, respectively. Additionally, tumor size >7 cm (p=0.022), ISUP/WHO Grade 4 (p<0.001) and the combination of PFI + other forms of invasion (p=0.002) are significantly associated with disease progression defined as local recurrence or metastases

Figure 1 - 518

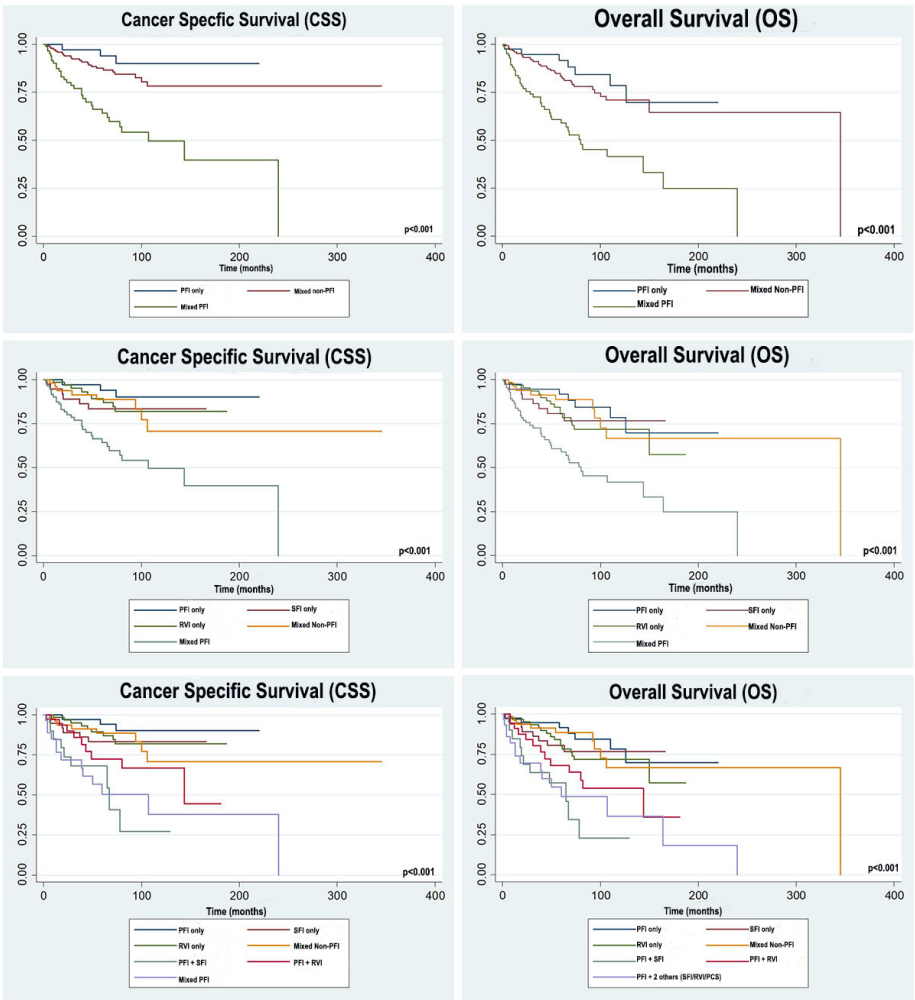

Conclusions: Our results show patients with PFI alone to have significantly better outcomes than those with other forms of invasion. The presence of multiple patterns, particularly including PFI are associated with a poorer prognosis. Therefore, identifying isolated and multiple patterns of extrarenal extension may aid in improving risk stratification of patients with pT3 RCCs. Additional studies are needed to corroborate our observations

519 Comparison of Discontinuous Foci of Tumor in Prostate Biopsies with Subsequent Radical Prostatectomies

Ramya Krishna Velagapudi[1], Shobha Parajuli[1]
[1]*University of Cincinnati Medical Center, Cincinnati, OH*

Disclosures: Ramya Krishna Velagapudi: None; Shobha Parajuli: None

Background: Prostate adenocarcinoma is one of the top three leading causes of cancer in men worldwide. Needle biopsy remains one of the important modalities in guiding patient management. Discontinuous tumor foci with intervening benign prostate tissue in needle core biopsies are commonly encountered, but there is no consensus on optimal method of reporting. We evaluated biopsies with discontinuous foci and compared with subsequent radical prostatectomy (RP) to determine the optimal method of reporting.

Design: Retrospective review of cases with discontinuous tumor foci in prostate biopsy was performed over a period of three years (01/2017–12/2019). Biopsy slides were reviewed and both additive and end-to-end length of discontinuous tumor foci was measured. Subsequent RP slides were reviewed to assess the tumor for focality (single or multiple), margin positivity, extra-prostatic extension (EPE) and bilateral disease.

Results: Thirty nine patients with prostate biopsies had discontinuous tumor foci. Of these, 19 patients underwent RP. The patients are divided into two groups: Group A (Gr A) includes patients with single large focus of tumor at RP while Group B (Gr B) includes patient with multiple foci of tumor at RP. 14/19 (74%) patients had single large focus of tumor at RP while 5/19 (26%) patients had multiple foci of tumor at RP. The greatest dimension of tumor in RP (Table 1) ranged from 14 – 36 mm in Gr A and 7 – 11 mm in Gr B. In Gr A: 6/14 (43%) had positive margins, 8/14 (57%) had EPE and 9/14 (64%) had bilateral disease. In Gr B: 1/5 (20%) had positive margins, 3/5 (60%) had EPE and 4/5 (80%) had bilateral disease. The prostatectomy in Gr B were found to have multiple biopsy cores with discontinuous foci 80% (4/5) compared to only 28% (4/14) cases in Gr A. Bilateral disease were more common in Gr B (80%). In 5 cases of RP with margin positivity, the additive length ranged from 1 – 7 mm, end-to-end length from 6 – 16 mm and greatest dimension of tumor on RP from 7 – 39 mm, indicating end-to-end length corresponds better with tumor size and margin positivity.

		Single focus at prostatectomy (Group 1) (14/19 = 74%)	Multiple foci of tumor at prostatectomy (Group 2) (5/19 = 26%)
BIOPSY MEASUREMENTS			
Grade Group	1 (3+3)	4 (29%)	1 (20%)
	Combined 1&2	2 (14%)	1 (20%)
	2 (3+4)	4 (29%)	2 (40%)
	3 (4+3)	3 (21%)	1 (20%)
	4 and 5	1 (7%)	0
Additive length (mean ± SD)		3.3 ± 1.9 mm	3.33 ± 1.6 mm
End-to-End length (mean ± SD)		8.7 ± 2.8 mm	8.5 ± 1.7 mm
Intervening benign tissue (mean ± SD)		4.9 ± 2.5 mm	5.2 ± 1.8 mm
PROSTATECTOMY MEASUREMENTS			
Size of tumor on prostatectomy (mean ± SD)		22.6 ± 9.5 mm	13.8 ± 5.1 mm
Margin positivity (p=0.36)		6/14 (43%)	1/5 (20%)
Extra prostatic extension		8/14 (57%)	3/5 (60%)
Bilateral disease		9/14 (64%)	4/5 (80%)
Multiple cores with discontinuous foci in same biopsy set		4/14 (28%)	4/5 (80%)

Conclusions: Our study concludes that majority of cases with discontinuous foci at prostate biopsy will show a single large tumor focus at RP. Multiple biopsy cores with discontinuous tumor foci correlates with multiple foci of tumor at RP. Although the cases are limited in this study, end to end measurement appears to correlate better with greatest size of the tumor and margin positivity at RP.

520 Evaluation of VSTM2a Expression in Various Renal and Urothelial Tumors by mRNA In Situ Hybridization

Stephen Wall[1], Jianhui Shi[1], Haiyan Liu[1], Fan Lin[1]
[1]*Geisinger Medical Center, Danville, PA*

Disclosures: Stephen Wall: None; Jianhui Shi: None; Haiyan Liu: None; Fan Lin: None

Background: Mucinous and tubular spindle cell carcinoma (MTSCC) of kidney are generally considered a low-grade (LG) neoplasm with rare exceptions. Papillary renal cell carcinoma (PRCC) of the low-grade is often a differential of MTSCC due to substantial overlapping in morphology and immunophenotype. Recent studies have shown V-set and transmembrane domain containing 2A (VSTM2A) to be a novel cancer specific biomarker in MTSCC (*Wang et al. 2018*). In this study, we investigated the diagnostic utility of VSTM2a expression in various renal and urothelial tumors by mRNA in-situ hybridization (ISH).

Design: Detection of VSTM2a mRNA expression by RNA ISH was performed using the Leica Bond III automated staining platform on tissue microarrays (TMA) of 208 cases of various renal and urothelial tumors including high-grade (HG) clear cell renal cell carcinoma (CCRCC) (N=38), LG CCRCC (N=40), urothelial carcinoma (N=47), PRCC (N=53), chromophobe renal cell carcinoma (chRCC) and oncocytoma (N=30). In addition, MTSCC (N=5) and LG PRCC (N=2) on small biopsies and surgical specimens were also studied. The VSTM2a RNA probe was provided by Advanced Cell Diagnostics. The staining results were recorded as negative (<5% of tumor cells stained with < 2 dots per tumor cell), low-level expression (>5% of tumor cells stained with ≥ 2 dots per tumor cell), or high-level expression (>5% of tumor cells stained with clusters of signal).

Results: The staining results are summarized in Table 1. High level expression was seen in 100% (5 of 5) MTSCCs (Fig.1a-b). Low level expression was noted in 2 cases of LG PRCC on surgical/small biopsy cases (Fig. 2a-b). The other tumors on TMAs including PRCCs exhibited no expression of VSTM2a

Table 1. Summary of VSTM2a Expression in Tumors from Various Organs

Diagnosis (N)	VSTM2a Positive Cases, N (%)
TMA, PRCC (N= 53)	0
TMA, CCRCC, LG (N= 40)	0
TMA, CCRCC, HG (N= 38)	0
TMA, ChRCC and oncocytoma (N= 30)	0
TMA, Urothelial carcinoma (N= 47)	0
Surgical/Small biopsy, PRCC, LG (N= 2)	2 (100%), low-level
Surgical/Small biopsy, MTSCC (N=5)	5 (100%), high-level

Figure 1 - 520

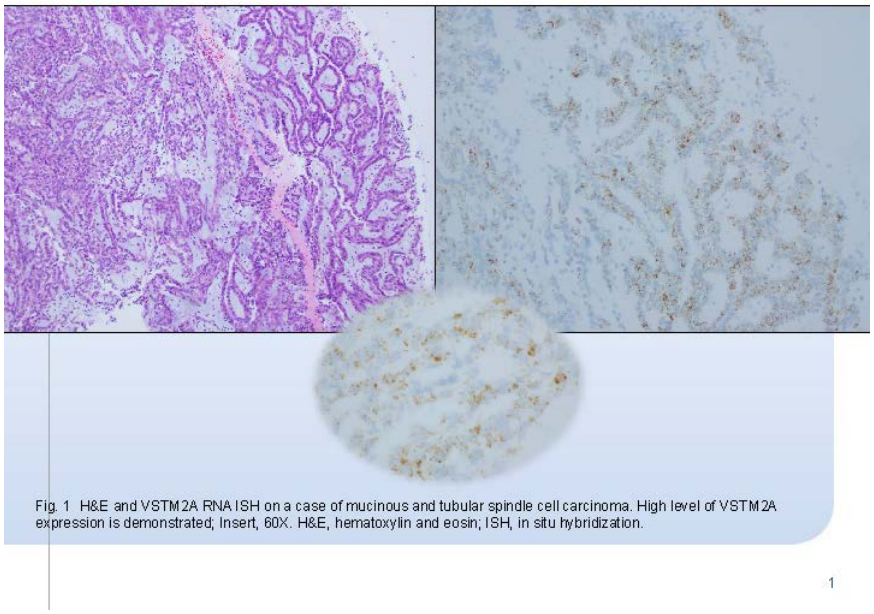

Fig. 1 H&E and VSTM2A RNA ISH on a case of mucinous and tubular spindle cell carcinoma. High level of VSTM2A expression is demonstrated; Insert, 60X. H&E, hematoxylin and eosin; ISH, in situ hybridization.

Figure 2 - 520

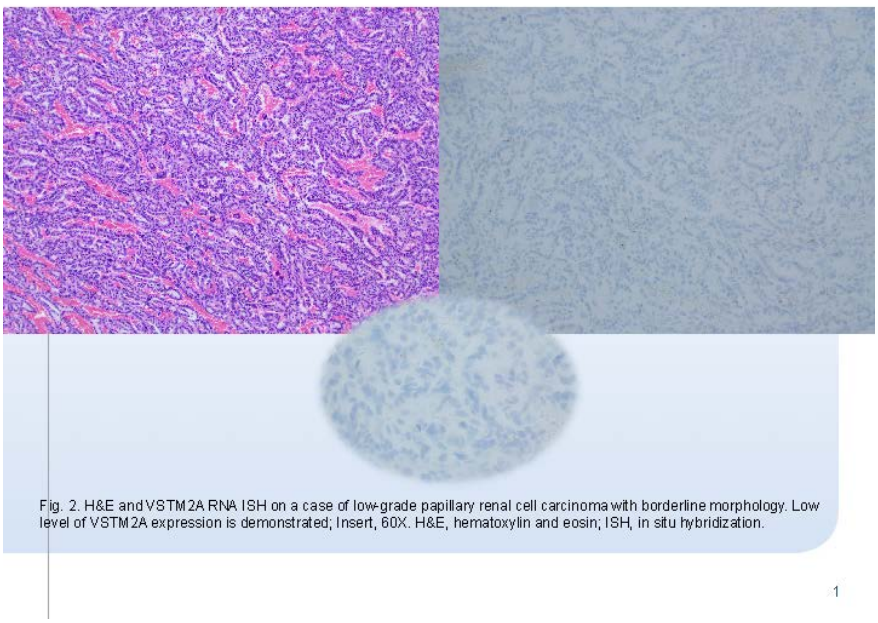

Fig. 2. H&E and VSTM2A RNA ISH on a case of low-grade papillary renal cell carcinoma with borderline morphology. Low level of VSTM2A expression is demonstrated; Insert, 60X. H&E, hematoxylin and eosin; ISH, in situ hybridization.

Conclusions: Our data demonstrate that mRNA ISH is an effective technology in detecting VSTM2a expression in MTSCCs. In contrast, the majority of PRCCs were negative for VSTM2a, although, two cases of LG PRCC on surgical/small biopsies showed low level expression, which may suggest the tumors displaying a mixture of PRCC and MTSCC or being borderline MTSCCs. Regardless, our data support that VSTM2a expression by mRNA ISH is sensitive and specific for MTSCC and can be a great adjunct to the pathologist when dealing with small biopsy specimens where PRCC and MTSCC are in the differential considerations.

521 Identification of Known and Novel MicroRNAs from Urine Exosomes in Non-Muscle Invasive Bladder

Beatriz Walter Rodriguez[1], Vladimir Valera[2], Maria Merino[3]
[1]National Cancer Institute, National Institutes of Health, Bethesda, MD, [2]National Institutes of Health, Bethesda, MD, [3]National Cancer Institute, Bethesda, MD

Disclosures: Beatriz Walter Rodriguez: None; Maria Merino: None

Background: Exosomes are small secreted vesicles containing protein and genetic material that reflect their cell of origin. They participate in intercellular communication by delivering proteins, mRNA, miRNA, and lncRNA to recipient cells and have been found in different biological fluids including blood and urine. Investigation of miRNA in exosomes content may generate a bladder cancer-specific exosome profile that could serve potentially as non-invasive biomarkers for diagnosis, prognosis, and treatment response.

Design: Exosomes were isolated from cell-free urine samples obtained from patients with high grade and or CIS non-muscle invasive bladder cancer and normal controls, followed by microRNA extraction. Next-generation deep sequencing was used for the identification of microRNAs in these samples. Corresponding bladder biopsies were also analyzed.

Results: Significant and highly expressed mature microRNAs, confirmed in miRbase were detected by miRDeep2 score and selected for further analysis. From the total of MicroRNAs obtained, 274 were known microRNAs and 334 were novel predicted microRNAs. MicroRNAs commonly dysregulated in urine bladder cancer samples included hsa-423-5p (100%), hsa-30da-5p (71%), hsa-Let-7b (42%), hsa-148a-5p (42%), and hsa-125b-5p (28%). Patients with CIS showed similar expression profile (hsa-let7b-5p, hsa-423-5p, hsa-200-a). Invasive high grade urothelial carcinoma showed a specific hsa-16-5p and hsa-191-5p expression. Similar profile was also shared by patients who had responded to intravesical BCG versus those who were unresponsive to intravesical treatment.

Conclusions: Our study demonstrates the potential of exosomal microRNAs as a non-invasive biomarker for non-muscle invasive bladder urothelial carcinoma. The biomarkers have great potential not only for diagnosis, but also for early detection, detection of tumor recurrence and progression, and treatment response.

522 The Clinical Impact of Comedonecrosis within Intraductal Carcinoma of the Prostate

Ying Wang[1], Yuki Teramoto[1], Takuro Goto[1], Hiroshi Miyamoto[1]
[1]University of Rochester Medical Center, Rochester, NY

Disclosures: Ying Wang: None; Yuki Teramoto: None; Takuro Goto: None; Hiroshi Miyamoto: None

Background: Intraductal carcinoma of the prostate (IDC-P) in which comedonecrosis is occasionally present is a distinct entity of aggressive prostate cancer. Meanwhile, assigning a Gleason grade to IDC-P is not recommended, although necrosis in conventional prostatic adenocarcinoma is considered a grade 5 pattern. Nonetheless, the clinical significance of necrosis associated with IDC-P remains poorly understood. In the present study, we compare radical prostatectomy findings and oncologic outcomes in patients with prostate cancer showing IDC-P with vs. without necrosis.

Design: We studied consecutive patients who had undergone radical prostatectomy at our institution during the entire year of 2010. Within our Surgical Pathology database, we identified a total of 272 cases with Grade Group (GG) 2 or higher cancer. We then histologically re-reviewed if there were IDC-P and necrosis within IDC-P in these prostatectomy specimens. Cases that had undergone short-term neoadjuvant therapy prior to prostatectomy (n=4), as well as those where the histology slides had been unavailable for review (n=3), were excluded from analysis.

Results: Of the 265 cases examined, 88 (33.2%) exhibited IDC-P, including 19 (21.6%) with necrosis (IDC-P/N+) and 69 (78.4%) without necrosis (IDC-P/N-) within IDC-P (see Table). When compared between IDC-P/N- vs. IDC-P/N+ cases, the presence of necrosis was significantly associated with higher tumor grade (*e.g.* GG2 vs. GG3-5, p<0.001; GG2-3 vs. GG 4-5, p<0.001; GG2-4 vs. GG5, p=0.019), higher pT stage (*e.g.* pT2/pT3a vs. pT3b, p=0.046), and larger estimated tumor volume (p<0.001). There were no significant differences in preoperative

prostate-specific antigen level and pN or surgical margin status. Kaplan-Meier analysis coupled with log-rank test revealed a significantly (p=0.0003) higher risk of biochemical recurrence after radical prostatectomy in IDC-P/N+ patients, compared to those with IDC-P/N-. In multivariate analysis with Cox regression model, IDC-P/N+ showed significance for recurrence, compared with IDC-P/N- (hazard ratio 4.42, 95% confidence interval 1.90-10.28, p=0.0006). Meanwhile, as expected, IDC-P was strongly associated with all of the adverse clinicopathologic features described above, as well as the increased risk of biochemical recurrence in a univariate analysis, compared to those without IDC-P.

	IDC-P(-) (n=177)	**IDC-P(+)** (n=88)	**P value**	**IDC-P(+)/N(-)** (n=69)	**IDC-P(+)/N(+)** (n=19)	**P value**
PSA (mean ± SEM, ng/mL)	6.52 ± 0.32	8.03 ± 0.57	0.0124	8.23 ± 0.66	7.31 ± 1.04	0.5082
Grade Group			<0.0001			0.0004
2	149 (84.2%)	33 (37.5%)		32 (46.4%)	1 (5.3%)	
3	20 (11.3%)	35 (39.8%)		27 (39.1%)	8 (42.1%)	
4	4 (2.3%)	8 (9.1%)		4 (5.8%)	4 (21.1%)	
5	4 (2.3%)	12 (13.6%)		6 (8.7%)	6 (31.6%)	
pT stage			<0.0001			0.0936
2/2+	119 (67.2%)	22 (25.0%)		19 (27.5%)	3 (15.8%)	
3a	54 (30.5%)	49 (55.7%)		40 (58.0%)	9 (47.4%)	
3b	4 (2.3%)	17 (19.3%)		10 (14.5%)	7 (36.8%)	
pN stage			0.0024[a]			0.4782[a]
0	133 (75.1%)	71 (80.7%)		56 (81.2%)	15 (78.9%)	
1	5 (2.8%)	13 (14.8%)		9 (13.0%)	4 (21.1%)	
X	39 (22.0%)	4 (4.5%)		4 (5.8%)	0 (0%)	
Surgical margin			0.0020			0.3436
Negative	163 (92.1%)	69 (78.4%)		56 (81.2%)	13 (68.4%)	
Positive	14 (7.9%)	19 (21.6%)		13 (18.8%)	6 (31.6%)	
Tumor volume (mean ± SEM, cc)	5.76 ± 0.39	10.21 ± 0.93	<0.0001	8.28 ± 0.72	17.22 ± 2.97	<0.0001
10-year RFS	82.5%	50.9%	<0.0001	62.8%	19.6%	0.0003

N, necrosis; PSA, prostate-specific antigen, RFS, recurrence-free survival

[a] pN0 vs. pN1

Conclusions: Compared with IDC-P/N-, IDC-P/N+ was found to associate with worse histopathologic features on radical prostatectomy as well as poorer prognosis as an independent predictor. Pathologists may thus need to report the presence or absence of not only IDC-P but also necrosis within IDC-P.

523 Downregulation of Epithelial Protein Lost in Neoplasm (EPLIN) is Associated with Aggressive Prostate Cancer at the Protein and Transcriptomic Levels

Daqing Wu[1], Alira Danaher[1], Adeboye O. Osunkoya[2]
[1]Atlanta, GA, [2]Emory University, Atlanta, GA

Disclosures: Daqing Wu: None; Adeboye O. Osunkoya: None

Background: Experimental models have demonstrated that epithelial protein lost in neoplasm (EPLIN) is a putative suppressor of tumor metastasis via the suppression of epithelial-mesenchymal transition and stemness in prostate cancer (PCa) cells. However, the expression profile of EPLIN in human specimens has not be well characterized, and may reveal a potential prognostic biomarker indicative of PCa progression.

Design: Immunohistochemical stain (IHC) for EPLIN was performed to evaluate its expression in a prostate tissue microarray composed of 69 primary PCa cases with variable Gleason scores (Grade groups) and 10 cases composed of benign prostatic glands and stroma. In addition, the expression profile of EPLIN transcripts was

analyzed using Prostate Cancer Transcriptome Atlas (PCTA) database that includes 1,321 clinical specimens from 38 PCa cohorts.

Results: EPLIN protein was highly expressed in all the examined benign prostate tissues (60.0% 3+, 40.0% 2+). The overall positive rate of EPLIN was 94.2% in PCa tissues (43.5% 3+, 23.2% 2+, 27.5% 1+). The IHC score for EPLIN expression in high-grade PCa (Gleason scores 8-10/Grade groups 4-5; 1.82 +- 0.15) was significantly lower that than in benign prostatic glands (2.6 +- 0.16; p = 0.02) or low-grade PCa (Gleason score <= 7/Grade groups1-2; 2.43 +- 0.19; p = 0.01). There was no statistically significant difference between EPLIN expression in benign prostatic glands and low-grade PCa (p = 0.59) (Figure 1). In addition, at the transcriptomic level, EPLIN expression in primary PCa was significantly reduced when compared with that of benign prostatic glands (fold change = -0.142; p < 0.001), and further reduced in metastatic castration-resistant PCa (fold change = -0.357; p < 0.001) (Figure 2).

Figure 1 - 523

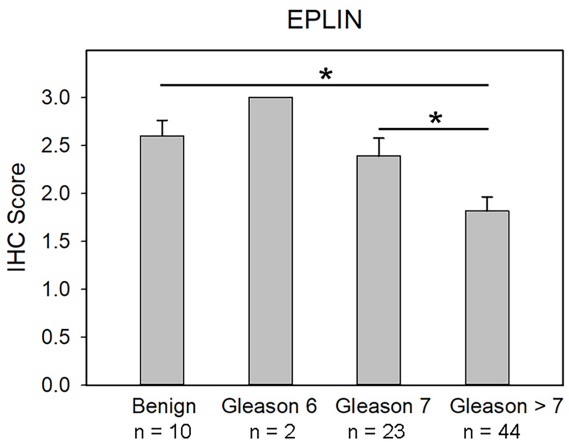

Figure 2 - 523

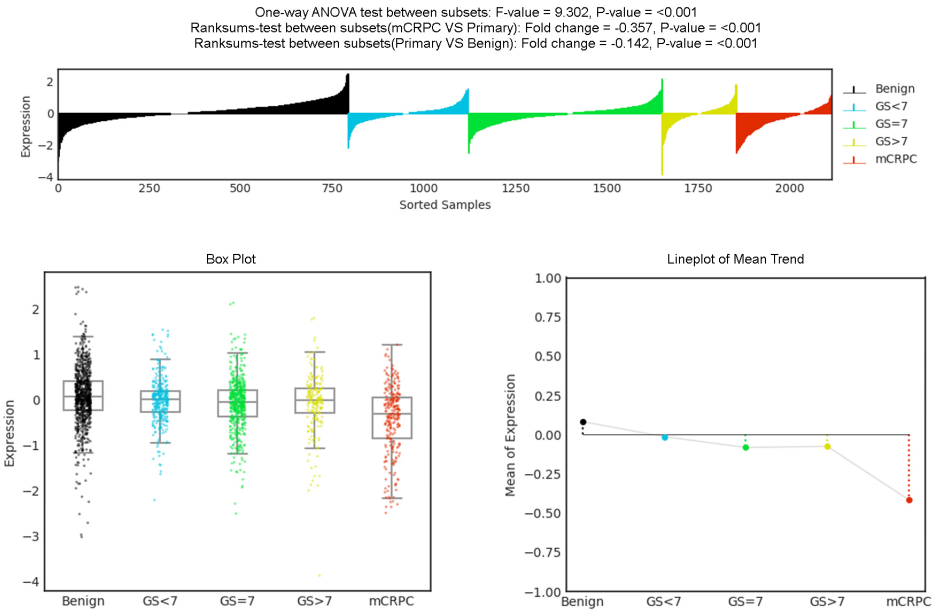

Conclusions: EPLIN expression at both RNA and protein levels is downregulated in PCa, and its reduction is further associated with high-grade and metastatic, castration-resistant PCa. These results suggest that EPLIN downregulation may serve as a predictor of tumor aggressiveness and poor prognosis in PCa patients.

524 Development and Validation of a Multiplex Immuno-Oncology Predictive Biomarker and Digital Pathology Workflow for Assessment of Urothelial Carcinoma

Henry Xie[1], Ekaterina Olkhov-Mitsel[2], Samira Alminawi[2], Elzbieta Slodkowska[3], Michelle Downes[2]
[1]University of Toronto, Toronto, Canada, [2]Sunnybrook Health Sciences Centre, Toronto, Canada, [3]Sunnybrook Health Sciences Centre, University of Toronto, Toronto, Canada

Disclosures: Henry Xie: None; Ekaterina Olkhov-Mitsel: None; Samira Alminawi: None; Elzbieta Slodkowska: None; Michelle Downes: None

Background: Immune checkpoint inhibitors (ICI) therapies have demonstrated significant benefit in the treatment of many tumors including high grade urothelial cancer (HGUC) of the bladder. However, high variability in patients' clinical responses highlights the need for biomarkers to aid patient stratification. ICI relies on an intact host immune response. In this context, we hypothesize that markers of activated cytotoxic T lymphocytes (CD8, granzyme-B) and immune suppression (FOXP3) might provide sufficient stratification metrics to improve patient selection for ICI therapy. A major obstacle for deployment of such a strategy is the limited quantities of tumor-derived biopsy material. Therefore, in this work, we develop a multiplex biomarker and explore its concordance with conventional single stain results using digital image analysis.

Design: Triplicate core tissue microarrays of 207 muscle invasive, HGUC of bladder had sequential 4 micron sections cut and stained with CD8, FOXP3 and granzyme-B. An inhouse developed tri-chromogen multiplex immunohistochemistry (m-IHC) assay consisting of CD8 (green), granzyme B (brown), and FOXP3 (red) was used to stain the next sequential tissue section. All slides were scanned using Aperio ScanScope AT Digital Scanner at 40X. Quantitative digital image analysis was performed using QuPath version 0.2.3 open-source software. Scores from triplicate cores were averaged for each HGUC specimen for each marker. Intraclass correlation coefficients (ICC) were used to compare percent positive cells between the single- and multi-plex assays.

Results: Comparison among Single and Multiplex immunostain using correlation coefficient (ICC) to compare percent positive cells (please see Table 1)

Table 1:

	ICC	95% confidence interval	P value
CD8			
Single vs. Multiplex	0.688	0.588-0.764	<0.001
FOXP3			
Single vs. Multiplex	0.694	0.585-0.772	<0.001
Granzyme			
Single vs. Multiplex	0.641	0.352-0.781	<0.001

Conclusions: m-IHC offers significant advantages in characterizing the host immune microenvironment particularly in limited biopsy tissue material. Utilizing a digital image workflow resulted in significant concordance between m-IHC and individual single stains ($p<0.001$ for all assessments). This suggests that a multiplex marker may be of use in assessing the host immune status and could be used in conjunction with PD-L1 as a predictor of response to ICI therapy.

525 Clinicopathologic Features of Post-Neoadjuvant Chemotherapy High-Grade Urothelial Carcinoma with Complete Pathologic Response

Chen Yang, Lakeridge Health Oshawa, Oshawa, Canada

Disclosures: Chen Yang: None

Background: Neoadjuvant chemotherapy before cystectomy is the standard of care for bladder high-grade urothelial carcinoma, particularly in cases with muscularis propria (detrusor muscle) invasion. In our practice, we have encountered numerous cases where complete pathologic response was achieved (no residual carcinoma). Objective of this study was to identify the clinicopathologic features of cases of post-neoadjuvant chemotherapy high-grade urothelial carcinoma with complete pathologic response.

Design: We retrospective searched our archives for cases of cystectomy or cystoprostatectomy cases with a prior diagnosis of high-grade urothelial carcinoma with slides available for review and clinical history of neo-adjuvant chemotherapy. All cases were reviewed to confirm the diagnosis and identify the presence of any histologic variants. Cases with no clinical follow-up were excluded from our study.

Results: A total of 35 cases (2 cases Ta; 7 cases T1; and 26 cases T2 on biopsy) with complete response and 29 cases (2 cases Tis; 6 cases T1; and 21 cases T2 on biopsy) with partial response were identified. In review of the histology, 34.3% (12/35) of patients with complete response had histologic variants (4 micropapillary, 3 glandular, 2 squamous, 2 plasmacytoid, and 2 sarcomatoid). In comparison, 37.9% (11/29) with partial response had histologic variants (4 squamous, 3 micropapillary, 2 plasmacytoid, 1 neuroendocrine, 1 enteric). In cases with residual carcinoma, 7 cases showed urothelial carcinoma in-situ only, 2 cases showed Ta disease, 8 cases showed T1 disease, 8 cases showed T2 disease, and 4 cases showed T3 or T4 disease. On follow-up (mean 38 months, range 1 to 100 months), one patient (2.9%) with complete response died related to disease, compared to 8 patients (27.6%) with partial response ($p = 0.0084$). Two patients (5.7%) with complete response had metastatic disease, compared to 8 patients (27.6%) with partial response ($p = 0.034$).

Conclusions: Pathologic complete responders fare much better than patients with only partial response. Presence of histologic variants of urothelial carcinoma do not predict response to chemotherapy. Additional studies to examine the molecular features to identify patients who respond better to chemotherapy.

526 Molecular Characterization of Sporadic Renal Hybrid Oncocytic Chromophobe Tumors with Uninformative Karyotype

Jing Yang[1], Anthony Sisk[2], Fabiola Quintero-Rivera[3], Brian Cone[4]
[1]University of California, Los Angeles, Los Angeles, CA, [2]The Regents of the University of California, Los Angeles, Los Angeles, CA, [3]University of California, Irvine, Orange, CA, [4]Affiliated Pathologist Medical Group, Los Angeles, CA

Disclosures: Jing Yang: None; Anthony Sisk: None; Fabiola Quintero-Rivera: None; Brian Cone: None

Background: Renal hybrid oncocytic/chromophobe tumors (HOCT) are rare neoplasms with mixed morphologic features resembling chromophobe renal cell carcinoma (ChRCC) and oncocytoma (RO). Distinguishing HOCT from ChRCC is important as the latter represents a malignant neoplasm, while HOCTs are generally indolent. Our study focuses on sporadic cases not associated with Birt-Hogg-Dube syndrome. The goal of this study is to review the pathologic and molecular cytogenetics features of HOCT.

Design: Nineteen cases from 2003 to 2018 diagnosed as HOCT, atypical oncocytoma and oncocytic renal epithelial neoplasm with hybrid features were identified. After histologic review, thirteen were found to be morphologically compatible with HOCT. In addition to review of clinicopathologic features, an immunohistochemical panel (Table 1) and G-karyotype analysis were performed. Subsequently, tissue cores were obtained and studied by chromosomal microarray analysis (CMA) using the Oncoscan chip (Affymetrix) to detect copy number variants (CNV).

Results: The majority of the tumors showed a subtle admixture of ChRCC and RO features while one tumor showed completely distinct areas resembling ChRCC and RO. Normal karyotype findings were seen in 2/3 of the available cases and deemed uninformative, compatible with age related abnormalities or an incomplete study. Microarray data was compared to the results of a previous study on HOCT (Luis-Cordero et al. Modern Pathology (2019) 32:1698-1707) and the major findings are summarized in Figure 1.

Clinicopathologic Features	HOCT (n=13)
Age, years	
median (range)	62 (22)
Sex, no. (%)	
male	4/13 (31%)
female	9/13 (69%)
Tumor Size (cm)	
median (range)	4.3 (9.4)

Immunohistochemistry, positive (%)	
CK7	9/12 (75%)
CD10	2/10 (20%)
Racemase	12/12 (100%)
C-KIT	7/12 (58%)
PAX8	10/10 (100%)
Pankeratin	7/10 (70%)
E-cadherin	3/10 (30%)
S100	4/10 (40%)
EMA	10/10 (100%)
Cyclin D1	12/12 (100%)

Figure 1 - 526

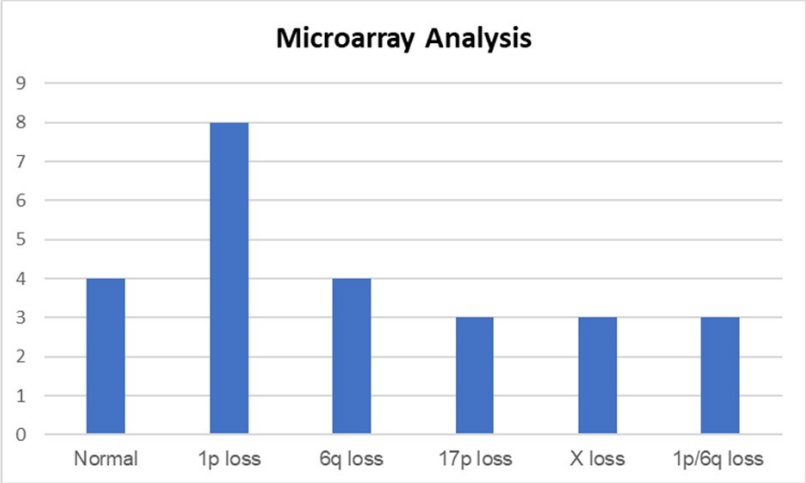

Conclusions: In a cytogenetic analysis of HOCT, we show that while karyotype is often un-informative (failed, incomplete study, or normal), tissue CMA may provide additional information. In our study, the tissue CMA provided diagnostically useful data in 9 of 13 cases. Four of 13 had normal results. Of the remaining 9 cases, 8 had loss of 1p, 4 had loss of 6q, 3 showed a loss of 17p and 3 showed loss of chromosome X. Only 3 of 9 had the previously reported loss of both 1p and 6q. Two cases had more complex karyotypes overlapping with ChRCC, while three others had findings that overlapped with oncocytoma. Other less common aberrations in less than 3 samples included loss of 22, 3p, 18q, 2 and 2q. Additionally, CMA is likely superior to standard karyotype analysis for the classification of HOCT and should be considered the first tier-test for genetic/CNV evaluation of tumors exhibiting overlapping features.

527 Identifying Patients with CKD Risk At The Time of Nephrectomy Procedure; When to Initiate Nephrology Consult

Yihe Yang[1], Zachary Kozel[2], Purva Sharma[2], Oksana Yaskiv[3], Jose Torres[2], Shashank Pandya[2], Kenar Jhaveri[4], Madhu Bhaskaran[5], Manish Vira[6], Vanesa Bijol[6]
[1]Donald and Barbara Zucker School of Medicine at Hofstra/Northwell, Riverhead, NY, [2]Donald and Barbara Zucker School of Medicine at Hofstra/Northwell, Lake Success, NY, [3]Northwell Health System, New York, NY, [4]Donald and Barbara Zucker School of Medicine at Hofstra/Northwell, Great Neck, NY, [5]Hofstra Northwell School of Medicine, Lake Success, NY, [6]Donald and Barbara Zucker School of Medicine at Hofstra/Northwell, Manhasset, NY

Disclosures: Yihe Yang: None; Zachary Kozel: None; Purva Sharma: None; Oksana Yaskiv: None; Jose Torres: None; Shashank Pandya: None; Kenar Jhaveri: *Consultant*, Astex Pharmaceuticals; *Consultant*, Natera; Madhu Bhaskaran: None; Manish Vira: None; Vanesa Bijol: None

Background: The prevalence of chronic kidney disease (CKD) is high among kidney neoplasm patients because of the overlapping risk factors. Our purpose is to identify CKD risk factors in kidney cancer survivors.

Design: Clinicopathologic correlations were analyzed in a retrospective cohort including 361 nephrectomy patients with kidney tumor (Department of Pathology at Northwell Health between July 2018 and May 2020). We performed a two-stage analysis to identify the risk factors associated with decreased eGFR during follow-up. 1. Exploration stage: Confounder stratification was used. Correlations between risk factors and kidney function during follow-up were analyzed. 2. Confirmation stage: Multivariate linear mixed model was performed to identify the independent risk factors of decreased kidney function post nephrectomy.

Results: Independent risk factors of decreased eGFR at baseline and during follow up were female gender (p=0.024), older age (p=0.012), BMI ³ 25 kg/m^2 (p<0.001), established diagnosis of CKD (p<0.001), eGFR £ 60 ml/min/1.73m^2 at the time of nephrectomy (p<0.001), radical nephrectomy (p<0.001), interstitial fibrosis and tubular atrophy>25% (p=0.005), and severe arteriolar sclerosis (p=0.013), table 1. BMI ³ 25 kg/m^2 and radical nephrectomy were independently associated with steeper slope of eGFR decrease (Figures1-2). All patients showed decrease of eGFR within 3 months post nephrectomy. In baseline eGFR>90ml/min/1.73m^2 group, the eGFR rebounded during extended follow-up, while the ones with baseline eGFR£60ml/min/1.73m^2 showed gradual kidney function decrease. The overall average eGFR is 62.0±2.9ml/min/1.73m^2 in IFTA≤25% cases and 54.0±2.0 ml/min/1.73m^2 in IFTA>25% cases. 10% patients with eGFR ≤60 mL/min/1.73 m² had <10% GS, while >60% of patients with eGFR < 60 mL/min/1.73 m² showed >25% GS. The overall average eGFR is 59.6 ± 2.1 ml/min/1.73m^2 and 56.5 ± 2.1 ml/min/1.73m^2 in cases without severe AAS and with severe AAS, respectively. In the patients with follow-up>3 months, 84% of them were identified retrospectively to fulfill criteria for CKD diagnosis, while only 15% had documented CKD diagnosis. The established CKD diagnosis percentage in different CKD stages were: 0% in CKD stage 1; 10.7% in CKD stage 2; 15.3% in CKD stage 3; 12.5% in CKD stage 4; and 95.0% in CKD stage 5.

Table: Multivariate linear mixed model

Risk Factor	Numerator df	Denominator df	F	Sig.
Intercept	1	321.099	723.632	0.000
Gender * time	2	165.995	1.213	0.300
Age (Quantile) * time	6	180.668	1.906	0.082
eGFR at nephrectomy (semiquantitative) * time	4	168.486	24.213	0.000
GS% * IFTA%	1	281.778	2.360	0.126
NxType * time	2	165.872	37.380	0.000
Tumor size (in partial nephrectomy)	2	303.833	2.411	0.091
Gender	1	280.109	5.187	0.024
Age (Quantile)	3	288.869	3.709	0.012
History of hypertension	1	311.272	0.773	0.380
History of DM	1	310.209	0.768	0.381
History of CKD	1	297.127	54.088	0.000
Overweight	1	275.958	12.642	0.000
eGFR at nephrectomy (semiquantitative)	2	294.997	167.253	0.000
GS% > 25%	1	284.966	0.075	0.784
IFTA% > 25%	1	282.023	7.910	0.005
AAS	1	310.513	6.296	0.013
NxType	1	348.175	36.142	0.000
Tumor Type	8	308.499	0.866	0.545
time	2	185.122	112.704	0.000
Overweight * time	2	181.043	5.020	0.008

Figure 1 - 527

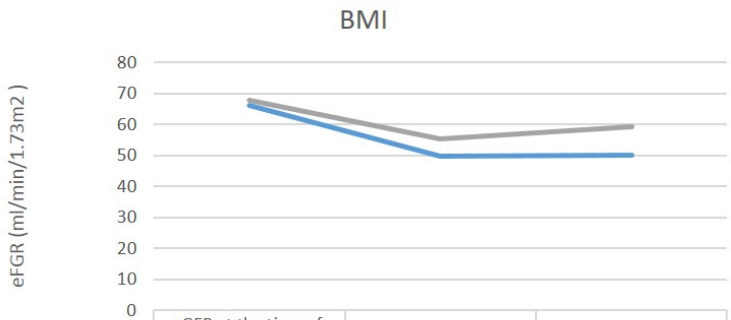

	eGFR at the time of nephrectomy	eGFR at FU1	eGFR at FU2
BMI <25.0	65.991	49.601	50.163
BMI>=25.0	67.747	55.429	59.191

Figure 2 - 527

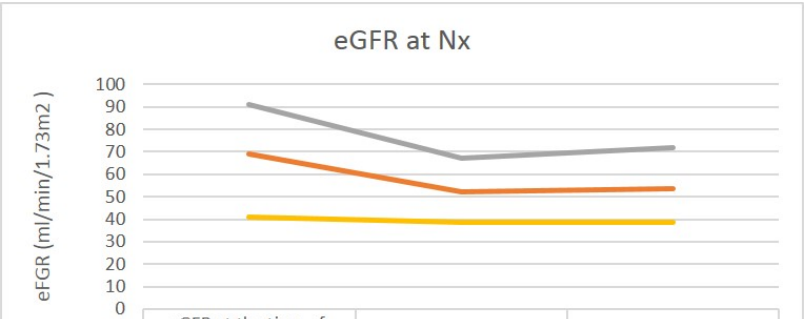

	eGFR at the time of nephrectomy	eGFR at FU1	eGFR at FU2
>=90	90.937	67.041	71.73
60-89	68.922	51.974	53.726
<=59	40.748	38.531	38.576

Conclusions: We propose a minimum workup for all patients undergoing nephrectomy to include SCr, eGFR, and urinalysis. Non-neoplastic pathology evaluation of nephrectomy specimens should include an estimate of % global sclerosis and IFTA to help identify patients at risk of CKD progression. Patients with any proteinuria and/or eGFR ≤ 60 at the time of nephrectomy or in follow-up with Urology, and/or >25% GS or IFTA, should be referred for early nephrology consultation.

528 The Prognostic Impact of Combining Cribriform Architecture Prostatic Adenocarcinoma with CAPRA Score on Patient Outcome

Yan Hong (Shirley) Yu[1], Theodorus Van Der Kwast[2], Michelle Downes[3]
[1]Sunnybrook Health Sciences Centre, University of Toronto, Toronto, Canada, [2]University Health Network, Toronto, Canada, [3]Sunnybrook Health Sciences Centre, Toronto, Canada

Disclosures: Yan Hong (Shirley) Yu: None; Theodorus Van Der Kwast: None; Michelle Downes: None

Background: The Cancer of the Prostate Risk Assessment (CAPRA) score has been widely utilized in predicting prostate cancer (PCa) metastasis and mortality. Intraductal carcinoma (IDC) and cribriform carcinoma (CC) are morphologic features associated with worse prognosis and are frequently found in nodal metastases in PCa patients. The present study aims to determine the prognostic significance of CAPRA score in conjunction with the presence of cribriform architecture (IDC or CC) on biopsies on patient outcome.

Design: Matched prostate biopsies positive for prostatic adenocarcinoma and subsequent prostatectomy specimens were retrospectively reviewed. The presence of IDC/CC on biopsy was documented. The CAPRA score was tabulated using patient age, PSA at diagnosis, Gleason score of the biopsy, percentage of biopsy cores positive for adenocarcinoma, and clinical stage (T-stage). The outcome variables measured were pathological stage (pT) at the time of surgery and biochemical recurrence (BCR) at follow up. Statistical analyses were performed using SPSS.

Results: Two hundred and sixty eight cases were identified and IDC or CC was found in 62 (23%) needle biopsies. Fifteen patients had BCR on follow up. In terms of pT, 146 patients were pT2 and 122 patients were pT3 at prostatectomy. On univariate analysis, CAPRA score had a statistically significant association with BCR ($p < 0.05$) and pT ($p < 0.001$). However the effect of CAPRA score on BCR was weak (HR 1.34). IDC/CC correlated with pT ($p < 0.001$) and not BCR. Multivariate analysis showed that CAPRA score and IDC/CC were independent predictors of pT. When considered as the main predictor, CAPRA score had a statistically significant association with pT ($p < 0.001$, OR = 1.65, 95% CI = 1.37 – 2.01). The addition of IDC/CC did not alter its effect or significance. IDC/CC had a stronger influence on pT ($p < 0.05$, OR = 2.18, 95% CI = 1.14 – 4.21) compared to the CAPRA score.

Conclusions: Combining CAPRA score with IDC/CC on biopsy does not significantly alter its prognostic value, suggesting that these are independent predictors. IDC/CC is a stronger predictor of pT3 at prostatectomy than CAPRA score.

529 Immune Landscape of Bladder Cancer and Its Aggressive Highly Lethal Variants

Michael Zaleski[1], Ziqiao Wang[1], Jolanta Bondaruk[1], David Cogdell[1], Sangkyou Lee[1], Marek Kimmel[2], Peng Wei[1], Charles Guo[1], Bogdan Czerniak[1]
[1]The University of Texas MD Anderson Cancer Center, Houston, TX, [2]Rice University, Houston, TX

Disclosures: Michael Zaleski: None; Ziqiao Wang: None; Jolanta Bondaruk: None; David Cogdell: None; Sangkyou Lee: None; Marek Kimmel: None; Peng Wei: None; Charles Guo: None; Bogdan Czerniak: None

Background: The immunological composition of the tumor microenvironment is complex and poorly understood but holds great significance in light of advancements in immunotherapy. Bladder carcinoma is diverse with many aggressive morphologic variants. We aim to elucidate the immune infiltrate of these neoplasms.

Design: Gene expression profiling with Illumina's DASL platform was performed on paraffin-embedded samples of the MD Anderson cohort of conventional urothelial carcinoma (n=84: luminal-43, basal-28, double negative-13), micropapillary (n=43), sarcomatoid (n=28), small cell (n=22), and plasmacytoid (n=12) variants. A cohort of 408 (luminal-212, basal-179, double negative-17) muscle-invasive bladder cancers in The Cancer Genome Atlas (TCGA) was used as a reference. The immune profile of genes identified through DAVID was used to analyze the immune infiltrate of B, T, CD8, MacTH1, and dendritic cell clusters. Additional analysis was performed by CIBERSORT using the expression profile of 547 genes to assess 22 immune cell types. These analyses were complemented by the expression profiles of 78 regulatory genes of the immune system.

Results: The stratification of conventional urothelial carcinomas into luminal, basal, and double negative subtypes disclosed that progression to sarcomatoid and small cell variants was through the basal subtype while micropapillary and plasmacytoid variants were uniformly luminal. Conventional basal and double negative subtypes in the TCGA and MD Anderson cohorts were enriched for immune infiltrates (54.1 and 76.4% in the TCGA and 64.2 and 76.9% in the MD Anderson cohorts). There was enrichment for immune infiltrate in sarcomatoid variant and 81.2% were immune hot. In contrast, small cell carcinomas were depleted of immune infiltrate and 86.4% were immune cold. In the luminal category 39.5% of micropapillary and 75% of plasmacytoid variants were immune hot. Bladder cancer variants had unique expression profile of immune regulatory proteins which included overexpression of ADORA2A, a T cell inhibitor in small cell carcinoma. PDCD1LG2, program cell death 1 ligand 2, was overexpressed in sarcomatoid carcinoma while VTCN1, T cell inhibitor was overexpressed in micropapillary variant. SELP, a regulator of innate immunity was overexpressed in plasmacytoid variant.

Conclusions: Bladder cancer and its variants demonstrate potentially therapeutically important immune microenvironment which can be exploited for targeted therapies.

530 Next-Generation Sequencing Analyses of Gene Mutations in Urachal Carcinoma

Michael Zaleski[1], Hui Chen[1], Bogdan Czerniak[1], Charles Guo[1]
[1]*The University of Texas MD Anderson Cancer Center, Houston, TX*

Disclosures: Michael Zaleski: None; Hui Chen: None; Bogdan Czerniak: None; Charles Guo: None

Background: Urachal carcinoma is a rare disease that has not been well studied regarding the characteristic molecular alterations. Herein we analyzed gene mutations in a large cohort of patients with urachal carcinoma from a single institution, which were correlated with their clinical and pathologic features.

Design: We retrospectively studied 30 patients with urachal carcinoma who had Next-Generation Sequencing (NGS) tests on formalin-fixed, paraffin-embedded tumor tissues. The targeted NGS gene panels ranged from 50 to 409 genes. Histologic slides were reviewed for pathologic features, and clinical data were collected from medical records.

Results: The patients included 21 men and 9 women with a mean age of 53 years (range 24-75 years). The urachal tumors were composed of mucinous adenocarcinoma (n=19), enteric adenocarcinoma (n=10), and high-grade neuroendocrine carcinoma (n=1). Additionally, 8 cases of mucinous-type adenocarcinoma showed focal signet ring cells features. The Sheldon system was used for cancer stage. At initial presentation, 17 patients had metastatic disease at Stage 4, and 13 patient were presented at Stage 3. Subsequently, 10 patients in the latter group developed metastatic disease in a mean time of 2.8 years (range 1.2-10.4 years). Targeted NGS tests were performed on primary urachal tumors (n=13) and metastases (n=17) (Fig. 1). All the tumors showed gene mutations with a mean of 3 mutations (range 1-6) per tumor. *TP53* was the most frequently mutated gene (n=25), followed by *KRAS* (n=9), *GNAS* (n=8), *SMAD4* (n=7), *KIT* (n=3), *MAP2K1* (n=3), *ARID1A* (n=3), *PIK3CA* (n=3), *NOTCH1* (n=2), *ATM* (n=2), and *NF1* (n=2). GNAS mutation was significantly associated with mucinous histology (p=0.043). *KRAS* mutation was significantly associated with Stage 4 disease (p=0.02) and younger age (under the age of 53 years, the mean age of our cohort) (p=0.046). Furthermore, Kaplan-Meier survival curve and log rank analysis showed a significant association of *KRAS* mutation with poor patient survival (p=0.006) (Fig. 2).

Figure 1 - 530

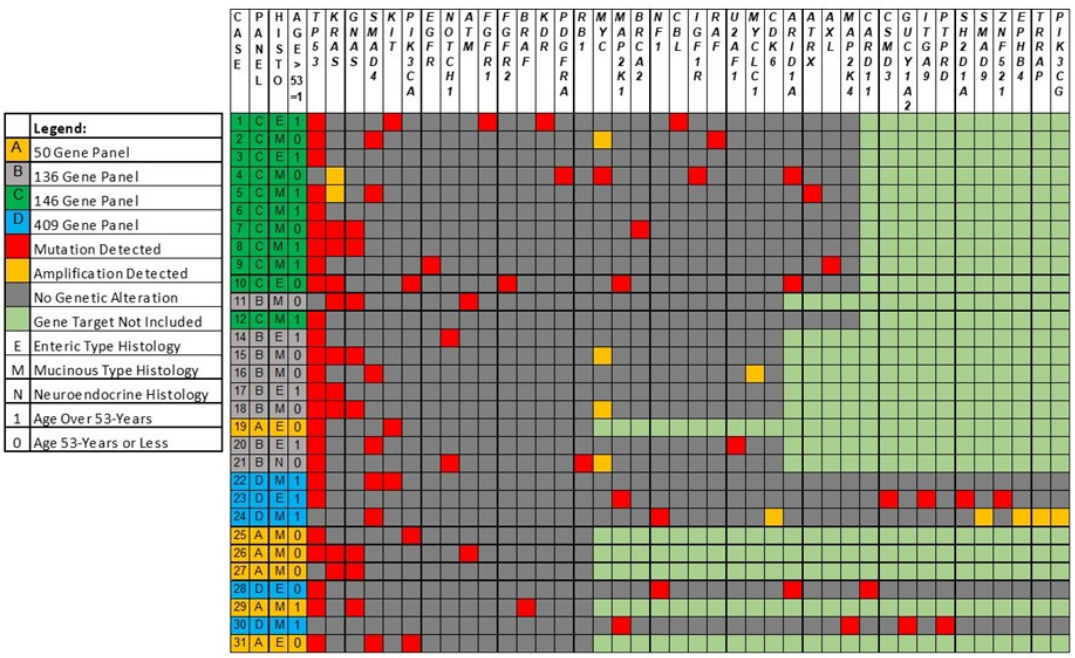

Figure 1. Next-Generation Sequencing analysis showed distinct gene mutations in urachal carcinoma in association with clinicopathologic features.

Figure 2 - 530

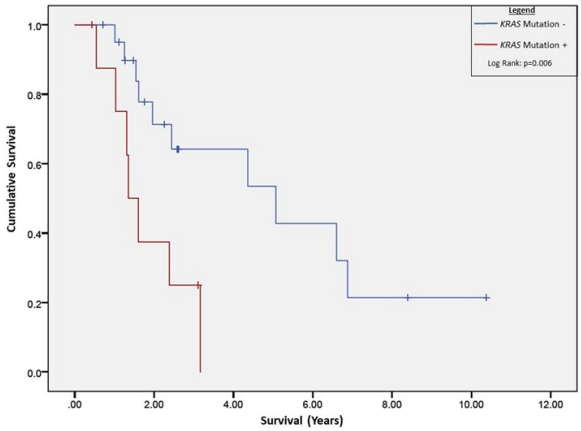

Figure 2. Kaplan-Meier survival curve and log rank analysis showed *KRAS* mutation was associated with a significantly poorer survival in patients with urachal carcinoma (p=0.006).

Conclusions: Urachal carcinoma shows distinct gene mutations in oncogenes and tumor suppressor genes, which may underlie the development and progression of this aggressive disease. The presence of KRAS mutation in urachal carcinoma is significantly associated with advanced stage, young patient age, and poor outcome.

531 FAP is a Potential Theranostic Target for PSMA-negative Castration Resistant Prostate Cancer

Chunlai Zuo[1], RongRong Huang[1], Christine Mona[2], Tamara Lotan[3], Lawrence True[4], Colm Morrissey[5], Johannes Czernin[2], Jeremie Calais[2], Clara Magyar[1], Huihui Ye[6]
[1]David Geffen School of Medicine at UCLA, Los Angeles, CA, [2]UCLA Center for the Health Sciences, Los Angeles, CA, [3]Johns Hopkins University School of Medicine, Baltimore, MD, [4]University of Washington Medical Center, Seattle, WA, [5]University of Washington, Seattle, WA, [6]University of California, Los Angeles, Los Angeles, CA

Disclosures: Chunlai Zuo: None; RongRong Huang: None; Christine Mona: None; Tamara Lotan: *Grant or Research Support*, Roche; *Grant or Research Support*, Myriad Genetics; *Grant or Research Support*, DeepBio; Lawrence True: None; Colm Morrissey: None; Johannes Czernin: *Stock Ownership*, Sofie Bioscience; *Stock Ownership*, Trethera Corporation; Jeremie Calais: None; Clara Magyar: None; Huihui Ye: None

Background: Prostate-specific membrane antigen (PSMA) is a relevant target for PET-CT imaging and radionuclide therapy of metastatic prostate cancer (PCa). However, metastatic castration resistant PCa (mCRPC) frequently loses PSMA expression after patients are heavily treated with intense androgen deprivation therapy (IADT). Fibroblast activation protein (FAP) is expressed by carcinoma-associated fibroblasts in many cancer types. We hypothesized that FAP can be used as a theranostics target for PSMA-negative CRPC. In this study, we aimed to evaluate expression of FAP and PSMA in CRPC.

Design: We queried 210 tissue microarray (TMA) cores of CRPC (70 tumors), including locally advanced CRPC (N=14) from Johns Hopkins Hospital and mCRPC (N=56) from University of Washington rapid autopsy TMA. The entire cohort is composed of 43 adenocarcinoma, 15 small cell carcinoma (SmCC), and 12 “anaplastic carcinoma”. Immunohistochemistry (IHC) for PSMA and FAP was performed. For manual scoring, IHC score was calculated as immunopercentage (0-100%) x immunointensity (0-3). Definiens quantitative imagine analysis were performed in parallel, in which we used % of positive areas for FAP and H-score for PSMA, respectively.

Results: FAP expression showed no significant difference among adenocarcinoma (medium 12.7; IGR=5.0-27.5), anaplastic carcinoma (medium 30.0; IGR=10.0-40.0), and SmCC (medium 10.0; IGR=2.3-40.0). In comparison to adenocarcinoma (medium 98.3; IGR=25.0-220.0), anaplastic carcinoma demonstrated comparable PSMA expression (medium 187.5; IGR=28.5-275.0) while SmCC showed significantly reduced, near-zero PSMA

expression (medium 1.0; IGR=0-1.0; p=0.000). Algorithms of Definiens quantitative image analysis were established, with results in good agreement with manual scoring (Table 1).

Table 1. Expression Levels of FAP and PSMA in Histologic Subtypes of mCRPC

	Manual Scoring			
	Median FAP (IQR)	p Value	Median PSMA (IQR)	p Value
Adenocarcinoma	12.7 (5.0, 27.5)		98.3 (25.0, 220.0)	
Anaplastic carcinoma	30.0 (10.0, 40.0)	0.199	187.5 (28.5, 275.0)	0.328
Small cell carcinoma	10.0 (2.3, 40.0)	0.865	1.0 (0, 1.0)	0.000
	Computational Scoring			
	Median FAP (IQR)	p Value	Median PSMA (IQR)	p Value
Adenocarcinoma	0.5 (0.1, 1.2)		152.6 (58.2, 269.6)	
Anaplastic carcinoma	1.1 (0.2, 2.8)	0.21	249.0 (27.6, 283.8)	0.641
Small cell carcinoma	1.0 (0.3, 1.1)	0.45	1.7 (0.4, 2.6)	0.009

Conclusions: In our study, FAP shows similar levels of expression in all above histologic subtypes of heavily treated mCRPC. FAP is a promising novel target to diagnose or treat PSMA-negative mCRPC.